STATISTICAL INFERENCE IN HIGH-DIMENSIONAL MODELS

A Dissertation

by

SANGYOON YI

Submitted to the Office of Graduate and Professional Studies of
Texas A&M University
in partial fulfillment of the requirements for the degree of

DOCTOR OF PHILOSOPHY

Chair of Committee,	Xianyang Zhang
Committee Members,	Mohsen Pourahmadi
	Irina Gaynanova
	Yong Chen
Head of Department,	Daren B.H. Cline

August 2020

Major Subject: Statistics

ABSTRACT

This dissertation consists of the two independent studies on statistical inference in high-dimensional models. The first study considers high-dimensional linear model where the number of predictors is greater than the sample size. The second study covers high-dimensional association tests in genomics where the number of features exceeds the sample size.

In the first study, we develop a new method to estimate the projection direction in the debiased Lasso estimator. The basic idea is to decompose the overall bias into two terms corresponding to strong and weak signals respectively. We propose to estimate the projection direction by balancing the squared biases associated with the strong and weak signals as well as the variance of the projection-based estimator. Standard quadratic programming solver can efficiently solve the resulting optimization problem. In theory, we show that the unknown set of strong signals can be consistently estimated and the projection-based estimator enjoys the asymptotic normality under suitable assumptions. A slight modification of our procedure leads to an estimator with a potentially smaller order of bias comparing to the original debiased Lasso. We further generalize our method to conduct inference for a sparse linear combination of the regression coefficients. Numerical studies demonstrate the advantage of the proposed approach concerning coverage accuracy over some existing alternatives.

The second study presents a novel two-stage approach for more powerful confounder adjustment in large-scale multiple testing to strike a balance between the Type I error and power. Specifically, we use the unadjusted z-statistics to enrich signals in the first stage and then use the adjusted z-statistics to remove the false signals due to confounders in the second stage. We develop a new way of simultaneously choosing the two cutoffs in both steps. This is based on our estimates for the false rejections by using nonparametric empirical Bayes approach. We show that our proposed method provides asymptotic false discovery rate control and delivers more power than the traditional one-stage approach. Promising finite sample performance is demonstrated via simulations and real data illustration in comparison with existing competitors.

DEDICATION

To my parents.

ACKNOWLEDGMENTS

First and foremost, I would like to express my utmost appreciation to my advisor Dr. Xianyang Zhang for his continuous support and patience during my graduate study. It will be remembered as my best luck in my life to have the opportunity to work with such a great mentor. He has consistently provided me with tremendous assistance including a lot of academic advice with his expertise and his kind encouragement. I could be inspired by him not only with statistical insights but also with the attitude what researcher must have. A million of words is not enough for his wonderful supervision.

I wish to extend my deep gratitude to the committee members, Drs. Mohsen Pourahmadi, Irina Gaynanova and Yong Chen for their willingness to serve on my committee and their guidance. I am also grateful for Drs. Jun Chen and Lu Yang at Mayo Clinic. It has been a great pleasure to work with Dr. Chen and Dr. Yang has kindly answered all of my questions to help my understanding about the real data set analyzed in Chapter 3. Special thanks have to go to my friends in the department. Rakheon Kim, Myeongjong Kang and Hyunwoong Chang have been extremely encouraging. It has been really enjoyable and refreshing me to spend time with them.

Most importantly, I want to dedicate this dissertation to my family. My parents and sister have supported me with their unconditional love and inspiration. Without them, none of the works in this dissertation would have been possible. I would lastly like to acknowledge Siyeon Kim. Her warmhearted encouragement deserves to take the credit for the completion of this work.

CONTRIBUTORS AND FUNDING SOURCES

Contributors

This work was supported by a dissertation committee consisting of Professors Xianyang Zhang (chair), Mohsen Pourahmadi and Irina Gaynanova of the Department of Statistics and Professor Yong Chen of the Department of Finance.

The project in Chapter 3 was also guided by Dr. Jun Chen of the Division of Biostatistics and Informatics at Mayo Clinic. The numerical studies therein were conducted by Drs. Jun Chen and Lu Yang. All other work conducted for the dissertation was completed by the student independently.

Funding Sources

Graduate study was supported by graduate assistantships from the Department of Statistics at Texas A&M University and partially supported by NSF grants DMS-1607320, DMS-1811747 and DMS-1830392.

TABLE OF CONTENTS

Page

LIST OF FIGURES

FIGURE Page

LIST OF TABLES

TABLE Page

1. INTRODUCTION

This dissertation consists of the two independent studies on statistical inference in high-dimensional models where the number of predictors (or features) exceeds the sample size. The first study focus on high-dimensional linear model in Chapter 2. The second study considers high-dimensional association tests in genomic association analysis in Chapter 3.

Chapter 2 : Projection-based Inference for High-dimensional Linear Models

Though the statistical properties of Lasso have been extensively studied, relatively little is known about its statistical inference. It is a challenging problem because the Lasso does not have a tractable asymptotic limit. To tackle this problem, the debiased Lasso is recently introduced in the seminal works such as Zhang and Zhang (2014), van de Geer et al. (2014) and Javanmard and Montanari (2014). Zhang and Zhang (2014) introduced the idea of regularized projection, which is designed to remove the bias in the Lasso. The resulting debiased Lasso is shown to have an asymptotic normal limit. However, its empirical performance often turns out to be relatively unstable and can be very undesirable in some numerical experiments.

Chapter 2 is motivated by an attempt to more directly taking into account the bias term. As the asymptotic normality depends on the bias term, the debiased Lasso would have performed well if it had fully removed the bias term. However, the original debiased Lasso often showed the larger bias for some finite samples. Also, it could be numerically observed that the bias term associated with the strong signals contributes more to the overall bias.

The main contribution of the project is to propose an alternative way to find the projection direction for the debiased Lasso estimator. Specifically, taking into account different contribution of signal strengths to the overall bias, we formulate an optimization problem which appropriately balances the squared biases associated with the strong and weak signals as well as the variance of the projection-based estimator for efficiency. For a more adaptive estimation, we assign different weights to the squared bias terms associated with the strong and weak signals in the objective function. The resulting optimization problem can be cast into a quadratic programming problem

which can be efficiently solved using a standard quadratic programming solver.

For the method to be self-contained, we further address the following two points: (1) the estimation of the set of strong signals and (2) the selection of the weights to the squared bias terms. For (1), we develop a new method to obtain a surrogate set, which is shown to estimate the set of strong signals consistently. For (2), we employ the residual bootstrap approach to estimate the coverage probabilities associated with different choices of weights and select the one that delivers the shortest interval width while ensuring that the bootstrap estimate of the coverage probability is close to the nominal level.

In theory, under suitable assumptions, we show that the newly obtained projection-based estimator enjoys the asymptotic normality. Also, a slight modification of our procedure leads to an estimator with a potentially smaller order of bias compared to the original debiased Lasso. We further generalize our method to conduct statistical inference for a sparse linear combination of the regression coefficients under a suitable assumption on a loading vector. By extensive simulations, it could be verified that the proposed approach shows promising performance and smaller bias than some alternatives do.

Chapter 3 : Two-Stage Large-Scale Multiple Testing with Confounding Factors

In genome-wide association studies, it is important to identify genomic features that are associated with a variable of interest such as disease status. However, due to the constraint of clinical sample collection, potential confounding factors exist. While failing to adjust for confounding factors may lead to inflated type I error, adjustment for confounding effects can exacerbate the already low statistical power in genome-scale association tests.

Thus, to strike a balance between type I error and power, we propose a novel two-stage approach for more powerful confounder adjustment in large-scale multiple testing. Given m features and thresholds $t_1, t_2 \geq 0$, the two-stage procedure can be described as follows:

Step 1. Use the unadjusted statistics to determine a preliminary set of features $\mathcal{D}_1 = \big\{1 \leq i \leq m : |Z_i^U| \geq t_1\big\}$,

Step 2. Reject the null hypothesis for the i-th feature $H_{0,i}$ when $|Z_i^A| \geq t_2$ and $i \in \mathcal{D}_1$. As a

result, the final set of discoveries is given by $\mathcal{D}_2 = \big\{1 \le i \le m : |Z_i^U| \ge t_1, |Z_i^A| \ge t_2\big\}$,

where Z_i^U, Z_i^A denote the unadjusted and adjusted z-statistics associated with the i-th feature, respectively. In the first step, we try to enrich the signals by using the unadjusted statistics. In the second step, we then remove the false signals due to confounders and try to control the FDR at the desired level. Since we use a more lenient p-value cutoff in the second step due to a much less multiple testing burden, the two-stage procedure achieves a way better power than the commonly used adjusted procedure. We also propose an approach of simultaneously selecting both cutoffs. Specifically, the thresholds are chosen to control the estimate for the FDR while maximizing the number of rejections.

The main difficulty here is to estimate the expected number of false rejections, which depends on the effects of the confounding factors on each feature. As the number of features could be in the thousands, it thus requires estimating a large number of nuisance parameters. To tackle this difficulty, we adopt an empirical Bayes approach by assuming that the nuisance parameters are generated from a common prior distribution, which allows us to express the expected number of false rejections as a functional of the prior distribution. Therefore, we can translate the task into estimating the prior distribution instead of direct estimation of a large number of nuisance parameters. The prior distribution is estimated via the general maximum likelihood empirical Bayes estimation, as in Jiang and Zhang (2009) and Koenker and Mizera (2014), which can be cast into a convex optimization problem. Under suitable assumptions, we show that our estimate for the expected number of false rejections is consistent, and the proposed method provides asymptotic FDR control. Through extensive numerical studies, we demonstrate that the recommended two-stage procedure outperforms the commonly used approaches in a wide range of settings.

2. PROJECTION-BASED INFERENCE FOR HIGH-DIMENSIONAL LINEAR MODELS

2.1 Introduction

Uncertainty quantification after model selection has been an active field of research in statistics for the past few years. The problem is challenging as the Lasso type estimator does not admit a tractable asymptotic limit due to its non-continuity at zero. Standard bootstrap and subsampling techniques cannot capture such non-continuity and thus fail for the Lasso estimator even in the low-dimensional regime. Several attempts have been made in the recent literature to tackle this challenge. For example, (Multi) sample-splitting and subsequent statistical inference procedures have been developed in Wasserman and Roeder (2009) and Meinshausen et al. (2009). Meinshausen and Bühlmann (2010) proposed the so-called stability selection method based on subsampling in combination with selection algorithms. Chatterjee and Lahiri (2011, 2013) have considered the bootstrap methods that can provide valid approximation to the limiting distributions of the Lasso and adaptive Lasso estimators, respectively.

For statistical inference after model selection, Berk et al. (2013) developed a post-selection inference procedure by reducing the problem to one of simultaneous inference. Lockhart et al. (2014) constructed a statistic from the Lasso solution path and showed that it converges to a standard exponential distribution. To account for the effects of the selection, Lee et al. (2016) developed an exact post-selection inference procedure by characterizing the distribution of a post-selection estimator conditioned on the selection event. By leveraging the same core of statistical framework, Tibshirani et al. (2016) proposed a general scheme to derive post-selection hypothesis tests at any step of forward stepwise and least angle regression, or any step along the Lasso regularization path. Barber and Candès (2015) proposed an inferential procedure by adding knockoff variables to create certain symmetry among the original variables and their knockoff copies. By exploring such symmetry, they showed that the method provides finite sample false discovery rate control. The knockoff procedure has been extended to the high dimensional linear model in Barber and

Candès (2019) and the settings in which the conditional distribution of the response is completely unknown in Candès et al. (2018).

Along with a different line that is more closely related to the current work, Zhang and Zhang (2014) first introduced the idea of regularized projection, which has been further explored and extended in van de Geer et al. (2014) and Javanmard and Montanari (2014). The common idea is to find a projection direction designed to remove the bias term in the Lasso estimator. The resulting debiased Lasso estimator which is no longer sparse was shown to admit an asymptotic normal limit. To find the projection direction, the nodewise Lasso regression by Meinshausen and Bühlmann (2006) was adopted in both Zhang and Zhang (2014) and van de Geer et al. (2014), while Javanmard and Montanari (2014) considered a convex optimization problem to approximate the precision matrix of the design. Zhang and Cheng (2017) and Dezeure et al. (2017) proposed boostrap-assisted procedures to conduct simultaneous inference based on the debiased Lasso estimators. Belloni et al. (2014) developed a two-stage procedure with the so-called post-double-selection as first and least squares estimation as second stage. Ning and Liu (2017) proposed a decorrelated score test in a likelihood based framework. Zhu and Bradic (2018a,b) developed projection-based methods that are robust to the lack of sparsity in the model parameter. More recent advances along this direction include Neykov et al. (2018) and Chang et al. (2019). Focusing on the theoretical aspects of debiased Lasso, Javanmard and Montanari (2018) studied the optimal sample size for debiased Lasso and Cai and Guo (2017) showed that the debiased estimator achieves the minimax rate. Although the methodology and theory for the debiased Lasso estimator are elegant, its empirical performance could be undesirable. For instance, the average coverage rate for active variables could be far lower than the nominal levels in finite sample [see, e.g., van de Geer et al. (2014)].

A natural question to ask is whether there exist alternative projection directions that can improve the finite sample performance in the original debiased Lasso estimator. In this paper, we propose a new method to estimate the projection direction and construct a novel Bias Reducing Projection (BRP) estimator, which is designed to further reduce the bias of the original debiased

Lasso estimator. Different from the nodewise Lasso adopted in both Zhang and Zhang (2014) and van de Geer et al. (2014), we propose a direct approach to estimate the projection direction. Our method is related to the procedure in Javanmard and Montanari (2014) but differs in the following aspects. (i) We formulate a different objective function which appropriately balances the squared bias and the variance of the BRP estimator; (ii) We decompose the bias term into two parts according to a preliminary estimate of the signal strength: one associated with the strong signals and the other one related to the weak signals and noise; (iii) We develop new methods to estimate the set of strong signals and to select the tuning parameters involved in the objective function.

Our approach relies crucially on the following observation in finite sample: the bias term associated with the strong signals contributes more to the overall bias. Motivated by this fact, we estimate the projection direction by minimizing an objective function that assigns different weights to the squared bias terms associated with the strong and weak signals. The set of strong signals is unknown but can be consistently estimated based on a preliminary debiased Lasso estimator. The resulting optimization problem can be cast into a quadratic programming problem which can be efficiently solved using a standard quadratic programming solver. We use residual bootstrap to estimate the coverage probabilities associated with different choices of weights and select the one that delivers the shortest interval width while ensuring that the bootstrap estimate of the coverage probability is close to the nominal level.

In theory, we show that the unknown set of strong signals can be consistently estimated by a surrogate set based on a preliminary projection-based Lasso estimator, where the projection direction is obtained using a novel formulation. The BRP estimator is shown to enjoy the asymptotic normality under suitable assumptions. As one of the main contributions, we prove that a slight modification of our BRP estimator leads to an estimator with a potentially smaller order of bias comparing to the original debiased Lasso. We further generalize our BRP estimator to conduct statistical inference for a sparse linear combination of the regression coefficients under suitable assumptions on a loading vector. We demonstrate the usefulness of the proposed approach by comparing it with the state-of-the-art approaches in simulations.

The rest of Chapter 2 is organized as follows. We introduce the projection-based estimator and develop a new formulation to find the projection direction in Section 2.2. We propose a method to estimate the set of strong signals and show its consistency in Section 2.3.1. We establish the asymptotic normality of the BRP estimator in Section 2.3.2 and the modified BRP estimator which could result in a potentially smaller order of bias compared to the original debiased Lasso is proposed in Section 2.3.3. Section 2.4 generalizes the method to conduct inference for a sparse linear combination of the regression coefficients. In Section 2.5, we discuss several details about the implementation of our new method including a bootstrap-assisted procedure for choosing the tuning parameters. Section 2.6 presents some numerical results. Technical details and additional numerical results are gathered in Section A.1 and A.2, respectively.

Throughout Chapter 2, we use the following notations: For a matrix $\mathbf{A} \in \mathbb{R}^{d\times d}$ and two sets $I, J \subseteq [d] := \{1, 2, \ldots, d\}$, denote by $\mathbf{A}_{I,J}$ ($\mathbf{A}_{-I,-J}$) the submatrix of $\mathbf{A}$ with (without) the rows in I and columns in J. Write $\mathbf{A}_{[d],-I} = \mathbf{A}_{-I}$. Similarly for a vector $a \in \mathbb{R}^q$, write a_I (a_{-I}) the subvector of a with (without) the components in I. Let $\|a\|_q$ with $0 \le q \le \infty$ be the l_q norm of a and write $\|a\| = \|a\|_2$. For two sets $\mathcal{S}_1, \mathcal{S}_2$, let $\mathcal{S}_1 \setminus \mathcal{S}_2$ be the set of elements in $\mathcal{S}_1$ but not in $\mathcal{S}_2$. Denote by $|\mathcal{S}_1|$ the cardinality of $\mathcal{S}_1$. For a square matrix $\mathbf{A}$, let $\lambda_{\max}(\mathbf{A})$ and $\lambda_{\min}(\mathbf{A})$ be its largest and smallest eigenvalues respectively. Define $\|\mathbf{A}\| = \|\mathbf{A}\|_{\text{op}} = \sup_{a\in\mathcal{S}^{d-1}} \|\mathbf{A}a\|$ as the operator norm of $\mathbf{A}$, where $\mathcal{S}^{d-1}$ is the unit sphere in $\mathbb{R}^d$. The sub-gaussian norm of a random variable X which we denote by $\|X\|_{\psi_2}$ is defined as $\|X\|_{\psi_2} = \sup_{q\ge 1} q^{-1/2}(E|X|^q)^{1/q}$. For a random vector $X \in \mathbb{R}^d$, its sub-gaussian norm can be defined as $\|X\|_{\psi_2} = \sup_{a\in\mathcal{S}^{d-1}} \|a^\top X\|_{\psi_2}$. The sub-exponential norm of a random variable X which we denote by $\|X\|_{\psi_1}$ is defined as $\|X\|_{\psi_1} = \sup_{q\ge 1} q^{-1}(E|X|^q)^{1/q}$. For a random vector $X \in \mathbb{R}^d$, its sub-exponential norm can be defined as $\|X\|_{\psi_1} = \sup_{a\in\mathcal{S}^{d-1}} \|a^\top X\|_{\psi_1}$. Let $(\mathcal{M}, \rho)$ be a metric space and let $\varepsilon > 0$. A subset $\mathcal{N}_\varepsilon$ of $\mathcal{M}$ is called an ε-net of $\mathcal{M}$ if every point $x \in \mathcal{M}$ can be approximated within ε by some point $y \in \mathcal{N}_\varepsilon$, i.e., $\rho(x, y) \le \varepsilon$. The minimal cardinality of an ε-net of $\mathcal{M}$ is called the covering number of $\mathcal{M}$.

2.2 Projection-based estimator

To illustrate the idea, we shall focus on the high-dimensional linear model:

$$Y = \mathbf{X}\beta + \epsilon, \tag{2.1}$$

where $Y = (y_1, \ldots, y_n)^\top \in \mathbb{R}^{n\times 1}$ is the response vector, $\mathbf{X} = (X_1, \ldots, X_p) \in \mathbb{R}^{n\times p}$ is the design matrix, $\beta = (\beta_1, \ldots, \beta_p)^\top \in \mathbb{R}^{p\times 1}$ is the vector of unknown regression coefficients with $\|\beta\|_0 = s_0$ and $\epsilon = (\epsilon_1, \ldots, \epsilon_n)^\top$ is the vector of independent errors with the common variance σ^2.

2.2.1 Motivation

Suppose we are interested in conducting inference for a single regression coefficient β_j for $1 \le j \le p$. We first rewrite model (2.1) as

$$\eta_j := Y - \mathbf{X}_{-j}\beta_{-j} = X_j\beta_j + \epsilon. \tag{2.2}$$

If the value of η_j is known, the problem would reduce to the inference about β_j in a simple linear regression model. As η_j is not directly observable, a natural idea is to replace η_j by a suitable estimator defined as

$$\hat{\eta}_j = Y - \mathbf{X}_{-j}\hat{\beta}_{-j} = X_j\beta_j + \epsilon + \mathbf{X}_{-j}(\beta_{-j} - \hat{\beta}_{-j}), \tag{2.3}$$

where $\hat{\beta}$ is a preliminary estimator for β. Here (2.3) is an approximation to (2.2) with the extra term $\mathbf{X}_{-j}(\beta_{-j} - \hat{\beta}_{-j})$ due to the estimation effect by replacing β_{-j} with $\hat{\beta}_{-j}$. In this paper, we focus on the Lasso estimator given by

$$\hat{\beta} = \underset{\tilde{\beta}\in\mathbb{R}^p}{\operatorname{argmin}} \left\{ \frac{1}{2n}\|Y - \mathbf{X}\tilde{\beta}\|^2 + \lambda\|\tilde{\beta}\|_1 \right\}$$

whose properties have now been well understood [see e.g. Bühlmann and van de Geer (2011); Hastie et al. (2015)]. We also try the alternative Lasso formulation without penalizing β_j in our

numerical studies and find that it does not improve the finite sample performance. Now given a projection vector $v_j = (v_{j,1}, \ldots, v_{j,n})^\top \in \mathbb{R}^{n\times 1}$ such that $v_j^\top X_j = n$, we define the projection-based estimator for β_j as

$$\tilde{\beta}_j(v_j) := \frac{1}{n} v_j^\top \hat{\eta}_j = \beta_j + \frac{1}{n} v_j^\top \epsilon + R(v_j, \beta_{-j}), \tag{2.4}$$

where $R(v_j, \beta_{-j}) = n^{-1} v_j^\top \mathbf{X}_{-j}(\beta_{-j} - \hat{\beta}_{-j})$ is the bias term caused by the estimation effect. (2.4) implies that

$$\sqrt{n}(\tilde{\beta}_j(v_j) - \beta_j) = \frac{1}{\sqrt{n}} v_j^\top \epsilon + \sqrt{n} R(v_j, \beta_{-j}).$$

To ensure that $\tilde{\beta}_j(v_j)$ has asymptotically tractable limiting distribution, we require the bias term $\sqrt{n}R(v_j, \beta_{-j})$ to be dominated by the leading term $n^{-1/2} v_j^\top \epsilon$, which converges to a normal limit under suitable assumptions. In other words, the bias term $\sqrt{n}R(v_j, \beta_{-j})$ controls the non-Gaussianity of $\tilde{\beta}_j(v_j)$. A practical challenge here is that the bias $\sqrt{n}R(v_j, \beta_{-j})$ can be hardly estimated directly from the data. It is common in the literature to replace $|\sqrt{n}R(v_j, \beta_{-j})|$ by a conservative estimator using the $l_1 - l_\infty$ bound, i.e.,

$$\|\sqrt{n}(\beta_{-j} - \hat{\beta}_{-j})\|_1 \|n^{-1} v_j^\top \mathbf{X}_{-j}\|_\infty. \tag{2.5}$$

See Zhang and Zhang (2014), van de Geer et al. (2014), Javanmard and Montanari (2014). We note that the variance of $n^{-1/2} v_j^\top \epsilon$ is equal to $\sigma^2 n^{-1} \|v_j\|^2$. To achieve efficiency, we shall also try to minimize $\sigma^2 n^{-1} \|v_j\|^2$ given that the bias $\sqrt{n}R(v_j, \beta_{-j})$ is properly controlled. Because the first term in (2.5) is independent of v_j, we can seek a projection direction to minimize a linear combination of $\|n^{-1} v_j^\top \mathbf{X}_{-j}\|_\infty^2$ and the variance $\sigma^2 n^{-1} \|v_j\|^2$. However, the $l_1 - l_\infty$ bound on the whole bias term could be conservative as it does not take into account the specific form of the bias

term. We note that the bias term can be written as

$$\begin{aligned}
&\sqrt{n}R(v_j, \beta_{-j}) = \frac{1}{\sqrt{n}} \sum_{k \neq j} v_j^\top X_k (\beta_k - \hat{\beta}_k) \\
=&\frac{1}{\sqrt{n}} \sum_{k \in \mathcal{S}_j^{(1)}(\nu)} v_j^\top X_k (\beta_k - \hat{\beta}_k) + \frac{1}{\sqrt{n}} \sum_{k \in \mathcal{S}_j^{(2)}(\nu)} v_j^\top X_k (\beta_k - \hat{\beta}_k) \qquad (2.6) \\
=&\sqrt{n}R_{(1)}(v_j, \beta_{-j}) + \sqrt{n}R_{(2)}(v_j, \beta_{-j}),
\end{aligned}$$

where $\mathcal{S}_j^{(1)}(\nu) := \mathcal{S}(\nu) \setminus \{j\}$ and $\mathcal{S}_j^{(2)}(\nu) := \mathcal{S}(\nu)^{\complement} \setminus \{j\}$ denote the index sets (except j) associated with the strong and weak signals respectively for $\mathcal{S}(\nu) := \{k : |\beta_k| \geq \nu\}$ and both $R_{(1)}(v_j, \beta_{-j})$ and $R_{(2)}(v_j, \beta_{-j})$ are defined accordingly. Here ν is a threshold that separates the coefficients into two-groups namely the group with strong signals and the group with weak or zero signal. For example, one can set $\nu = c_0\sqrt{\log(p)/n}$ for some large enough constant c_0, which is the minimax rate for support recovery.

The formulation (2.6) using the decomposition associated with signal strengths can be empirically motivated. Specifically, it generally provides a smaller bias than the one without such decomposition with the simulated data. Figure 2.1 illustrates one such representative case where we make a comparison of the biases for projection vectors calculated based on two different methods: the one solves (2.8) by using the estimated set of strong signals as in Section 2.3.1 (denoted by "With Decomposition") and the other one solves the same problem but with $\mathcal{A}_j^{(1)} = \emptyset$ (denoted by "Without Decomposition"). It can be seen that "With Decomposition" shows a smaller bias than "Without Decomposition." Similar results could be observed in various simulation settings.

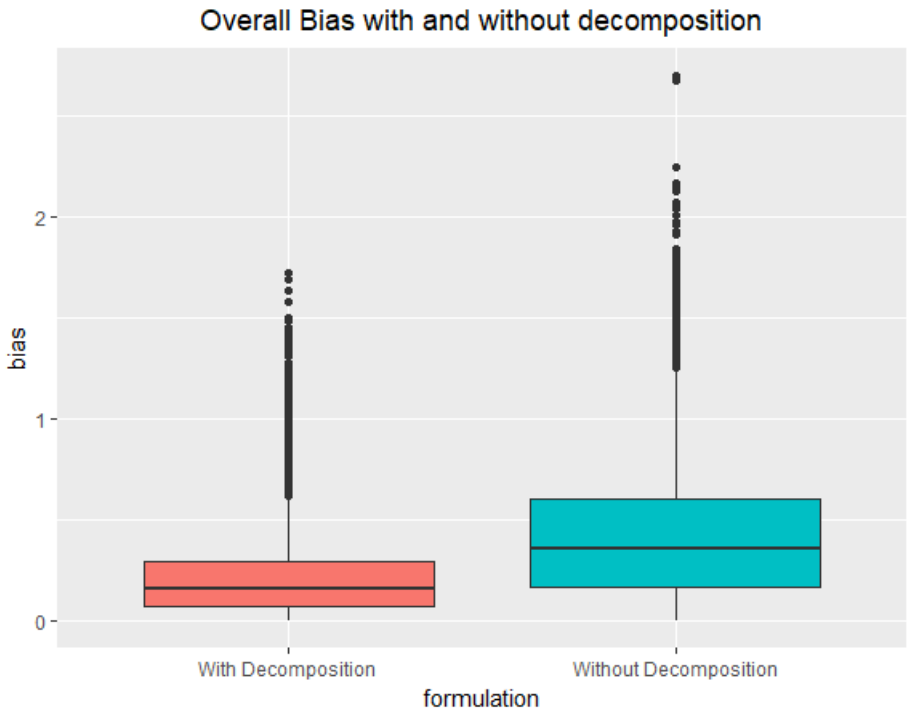

Figure 2.1: Boxplots of the absolute values of the normalized bias terms defined in (2.25) by "With Decomposition" and "Without Decomposition." The non-zero β_j's are independently generated from $U(0,4)$ with $s_0 = 10$. All the simulation settings are the same as the case with the Toeplitz covariance structure and standard normal error in Section 2.6. The results are based on 100 simulation runs.

2.2.2 A new projection direction

In this subsection, we propose a novel formulation to find the projection direction. When $|\mathcal{S}_j^{(1)}(\nu)| \leq n$, we have the freedom to choose v_j to make the term $\|n^{-1}v_j^\top \mathbf{X}_{\mathcal{S}_j^{(1)}(\nu)}\|_\infty$ arbitrarily small. In fact, we can always choose v_j such that it is orthogonal to all X_k with $k \in \mathcal{S}_j^{(1)}(\nu)$. The basic idea here is to find a projection direction v_j such that it is "more orthogonal" to the space spanned by $\{X_k\}_{k\in\mathcal{S}_j^{(1)}(\nu)}$ as compared to the space spanned by $\{X_k\}_{k\in\mathcal{S}_j^{(2)}(\nu)}$. With this intuition in our mind and the goal to balance the squared bias with the variance, we formulate the following

optimization problem

$$\min_{v_j} \left(\gamma_1 \max_{k \in S_j^{(1)}(\nu)} |n^{-1} v_j^\top X_k|^2 + \gamma_2 \max_{k \in \mathcal{S}_j^{(2)}(\nu)} |n^{-1} v_j^\top X_k|^2 + \sigma^2 n^{-1} \|v_j\|^2 \right),$$
$$\text{s.t.} \quad v_j^\top X_j = n, \tag{2.7}$$

where $\gamma_1, \gamma_2 > 0$ are tuning parameters which control the trade-off between the squared bias and the variance. The term $\gamma_1 \max_{k \in S_j^{(1)}(\nu)} |n^{-1} v_j^\top X_k|^2$ ($\gamma_2 \max_{k \in S_j^{(2)}(\nu)} |n^{-1} v_j^\top X_k|^2$) corresponds to the $l_1 - l_\infty$ bound for $R^2_{(1)}$ ($R^2_{(2)}$). By introducing two ancillary variables u_{j1}, u_{j2}, (2.7) can be cast into the following quadratic programming problem

$$\begin{aligned}
&\min_{u_{j1}, u_{j2}, v_j} \quad (\gamma_1 u_{j1}^2 + \gamma_2 u_{j2}^2 + \sigma^2 n^{-1} \|v_j\|^2), \\
&\text{s.t.} \ \ v_j^\top X_j = n, \\
&-u_{j1} \le n^{-1} v_j^\top X_k \le u_{j1}, \quad k \in \mathcal{S}_j^{(1)}(\nu), \\
&-u_{j2} \le n^{-1} v_j^\top X_k \le u_{j2}, \quad k \in \mathcal{S}_j^{(2)}(\nu),
\end{aligned}$$

which can be solved efficiently using existing quadratic programming solver.

The set $\mathcal{S}_j^{(1)}(\nu)$ is generally unknown and needs to be replaced by a surrogate set $\mathcal{A}_j^{(1)}$ with $|\mathcal{A}_j^{(1)}| \le n$. In Section 2.3.1, we describe a method to select $\mathcal{A}_j^{(1)}$ based on a preliminary projection-based estimators. We show that $\mathcal{A}_j^{(1)}$ converges asymptotically to a nonrandom limit, i.e.,

$$P\left(\mathcal{A}_j^{(1)} = \mathcal{B}_j^{(1)}\right) \to 1,$$

for a nonrandom subset $\mathcal{B}_j^{(1)}$ of $[p]$. We remark that $\mathcal{B}_j^{(1)}$ does not need to agree with $\mathcal{S}_j^{(1)}(\nu)$ for our procedure to be valid. To ensure that the remainder term is negligible, the theoretical analysis in Section 2.3.2 suggests that γ_1 and γ_2 should both be of the order $O(\sigma^2 n / \log p)$. Combining the above discussions, we now state the optimization problem for obtaining the optimal projection

direction

$$\begin{aligned}
&\min_{u_{j1},u_{j2},v_j} \quad \left(C_1\frac{n}{\log p}u_{j1}^2 + C_2\frac{n}{\log p}u_{j2}^2 + n^{-1}\|v_j\|^2\right), \\
&\text{s.t. } v_j^\top X_j = n, \\
&-u_{j1} \le n^{-1}v_j^\top X_k \le u_{j1}, \quad k \in \mathcal{A}_j^{(1)}, \\
&-u_{j2} \le n^{-1}v_j^\top X_k \le u_{j2}, \quad k \in \mathcal{A}_j^{(2)},
\end{aligned} \tag{2.8}$$

where $\mathcal{A}_j^{(2)} := \left(\mathcal{A}_j^{(1)}\right)^{\complement} \setminus \{j\}$ and $C_1, C_2 > 0$ are tuning parameters whose choice will be discussed in Section 2.5.1.

Remark 2.1. A related method is the refitted Lasso by Liu and Yu (2013). The idea is to refit the model selected by the Lasso and conduct inference based on the refitted least squares estimator. Such an estimator fits into the framework of the projection-based estimators. To see this, let $\hat{S}$ be the set of active variables selected by the Lasso and note that $\hat{\beta}_k = 0$ for $k \notin \hat{S}$. For each $j \in \hat{S}$, let $\hat{w}_j$ be the projection of X_j onto the orthogonal space of $\mathbf{X}_{\hat{S}\setminus\{j\}}$. Then the refitted least squares estimator is given by $\hat{w}_j^\top(Y - X_{-j}\hat{\beta}_{-j})/(\hat{w}_j^\top X_j)$. It is easy to see that the bias for the refitted least squares estimator is proportional to $\sum_{k\notin\hat{S}} \hat{w}_j^\top X_k\beta_k$, which disappears when the selected model contains all significant variables. However, when the model selection consistency fails, such a procedure is no longer valid due to the nonnegligible bias.

2.3 Methodology

2.3.1 Surrogate set

We describe a procedure to estimate the set of strong signals based on a preliminary projection-based estimator. It should be noted that the estimator here is different from the original debiased Lasso because it is based on the novel formulation (2.8). Specifically, for some $\tau > 0$, we define our estimate for the set of strong signals as

$$\mathcal{A}(\tau) := \{l : |T_l| > \sqrt{\tau \log p}\} \quad \text{where} \quad T_l = \frac{\sqrt{n}\tilde{\beta}_l(\hat{v}_l)}{\hat{\sigma}n^{-1/2}||\hat{v}_l||} \tag{2.9}$$

where $\hat{\sigma}$ is an estimator of the noise level σ and $\tilde{\beta}_l(\hat{v}_l)$ is a projection-based estimator with $\hat{v}_l$ being the solution to the following optimization problem

$$\begin{aligned} &\min_{u_l, v_l} \quad \left(C_0 \frac{n}{\log p} u_l^2 + n^{-1} \|v_l\|^2 \right), \\ &\text{s.t. } \; v_l^\top X_l = n, \\ &-u_l \le n^{-1} v_l^\top X_k \le u_l, \quad k \neq l. \end{aligned} \tag{2.10}$$

In practice, both C_0 and τ need to be appropriately chosen. The details for the selection are discussed in Section 2.5.2. Note that (2.10) is a special case of (2.8) when we have no knowledge about the set of strong signals, that is, $\mathcal{A}_l^{(1)} = \emptyset$. We define the surrogate sets to be

$$\mathcal{A}_j^{(1)}(\tau) := \mathcal{A}(\tau) \setminus \{j\}, \quad \mathcal{A}_j^{(2)}(\tau) := \mathcal{A}(\tau)^{\complement} \setminus \{j\}. \tag{2.11}$$

Throughout the paper, we consider the variance estimator

$$\hat{\sigma}^2 = \frac{1}{n} \|Y - \mathbf{X}\hat{\beta}\|^2 \tag{2.12}$$

which appears to outperform an alternative estimator $\|Y - \mathbf{X}\hat{\beta}\|^2/(n - \|\hat{\beta}\|_0)$ studied in Reid et al. (2016), see Figure A.11 in the supplementary material for a comparison. Before presenting the main result of this subsection, we introduce some assumptions.

Assumption 2.1. *There exist a set $\mathcal{B} \subseteq [p] = \{1, 2, \ldots, p\}$ and $0 \le d_0 < d_1$ such that*

$$\begin{aligned} \max_{l \in \mathcal{B}^{\complement}} \frac{|\sqrt{n}\beta_l|}{\sigma} &\le \sqrt{d_0 \log p}, \\ \min_{l \in \mathcal{B}} \frac{|\sqrt{n}\beta_l|}{\sigma} &\ge \sqrt{d_1 \log p}. \end{aligned}$$

Assumption 2.2. *The error ϵ is a mean-zero sub-gaussian random vector with the sub-gaussian norm κ_ϵ.*

Assumption 2.3. *The preliminary estimator satisfies that*

$$\sqrt{n}\|\hat{\beta} - \beta\|_1 = O_p(s_0\sqrt{\log(p)}).$$

Assumption 2.4. *The variance estimator $\hat{\sigma}^2$ is consistent in the sense that $\hat{\sigma}/\sigma \xrightarrow{p} 1$.*

Assumption 2.5. *Suppose the design matrix $\mathbf{X} \in \mathbb{R}^{n\times p}$ has i.i.d. rows with zero population mean and covariance matrix $\mathbf{\Sigma} = (\Sigma_{i,j})_{i,j=1}^p$. Assume that*

1. $\max_j \Sigma_{j,j} < \infty$;
2. $\lambda_{\min}(\mathbf{\Sigma}) \geq \Lambda_{\min} > 0$;
3. *The rows of $\mathbf{X}$ are sub-gaussian with the sub-gaussian norm $\kappa < \infty$.*

Assumption 2.6. *n, p and s_0 satisfy the rate condition $s_0 \log p/\sqrt{n} = o(1)$.*

Assumption 2.1 allows the strengths of strong and weak signals to be the same order and thus is much weaker than the "beta-min" condition which requires the weak signals to be of smaller order. Assumptions 2.3 and 2.4 are satisfied for the Lasso estimator and the variance estimator $\hat{\sigma}$ in (2.12) under suitable regularity conditions [Bühlmann and van de Geer (2011)]. Assumptions 2.2 and 2.5 require the error and design to be sub-gaussian. Similar assumptions have been made in van de Geer et al. (2014). Like Javanmard and Montanari (2014), the validity of our method does not rely on the sparsity of the precision matrix of the design, which is required in the nodewise Lasso regression for the original debiased Lasso. In view of Cai and Guo (2017), the rate condition in Assumption 2.6 cannot be relaxed without extra information. Zhu and Bradic (2018a,b) proposed testing procedures in high-dimensional linear models which impose much weaker restrictions on model sparsity or the loading vector representing the hypothesis. However, their methods require certain auxiliary sparse models, which are not needed for our procedure.

Define $\mathbf{\Sigma}_{j\backslash -j} = \mathbf{\Sigma}_{j,j} - \mathbf{\Sigma}_{j,-j}\mathbf{\Sigma}_{-j,-j}^{-1}\mathbf{\Sigma}_{-j,j}$ and $\kappa_{0j} = 2\left(1 + \sqrt{\Lambda_{\min}^{-1}\mathbf{\Sigma}_{j,j}}\right)\kappa^2$ for $1 \leq j \leq p$. The following proposition shows that the surrogate set $\mathcal{A}_j^{(1)}(\tau)$ with a properly chosen τ converges to $\mathcal{B} \setminus \{j\}$.

Proposition 2.1. Define $\mathcal{A}_j^{(1)}(\tau)$ and $\mathcal{A}_j^{(2)}(\tau)$ as in (2.11) and let $\hat{v}_l$ be the solution to (2.10) for $l \neq j$. Suppose d_0, d_1 and τ satisfy

$$\frac{\sigma^2}{32e\kappa_\epsilon^2}(\sqrt{\tau} - \sqrt{d_0 \max_l \mathbf{\Sigma}_{l,l}})^2 > 1$$

and $\sqrt{d_1/M} - \sqrt{\tau} > 0$ where

$$M = \left(\min_{1\le l\le p} \mathbf{\Sigma}_{l\backslash -l}\right)^2 \left(2C_0 \left(\min_{1\le l\le p} \frac{1}{8e^2}\frac{1}{(\kappa_{0l})^2}\right)^{-1} + \max_{1\le l\le p} \mathbf{\Sigma}_{l\backslash -l}\right).$$

Then under Assumptions 2.1-2.6, we have

$$\mathbb{P}\left(\max_{l\in\mathcal{B}_j^{(2)}} |T_l| \le \sqrt{\tau \log p}\right) \to 1,$$
$$\mathbb{P}\left(\min_{l\in\mathcal{B}_j^{(1)}} |T_l| > \sqrt{\tau \log p}\right) \to 1,$$

where $\mathcal{B}_j^{(1)} := \mathcal{B} \setminus \{j\}$ and $\mathcal{B}_j^{(2)} := \left(\mathcal{B}_j^{(1)}\right)^{\complement} \setminus \{j\}$. As a consequence, $\mathbb{P}\left(\mathcal{A}_j^{(1)}(\tau) = \mathcal{B}_j^{(1)}\right) \to 1$.

Remark 2.2. As shown in Proposition 2.1, the surrogate set in (2.11) has an asymptotic (nonrandom) limit, which implies that the projection direction obtained in (2.8) is asymptotically independent of the random error ϵ. This fact is useful in the proof of Theorem 2.1 later. To ensure the independence between the projection direction and the random error, we can also employ the sample splitting strategy, i.e., we split the samples into two subsamples, estimate the set of strong signals based on the first subsample and construct the projection-based estimator based on another subsample. As we use all samples in building the projection-based estimator, our method is more efficient than the sample splitting strategy.

Remark 2.3. When $d_0 = 0$, $\mathcal{B}$ coincides with the support of β. Proposition 2.1 suggests that one can consistently recover the support of β by thresholding the projection-based estimator.

2.3.2 Bias reducing projection (BRP) estimator

In this subsection, we introduce the bias reducing projection (BRP) estimator and study its asymptotic behavior. Let $\tilde{v}_j$ be the solution to (2.8) based the surrogate sets in (2.11). Then the BRP estimator $\tilde{\beta}_j(\tilde{v}_j)$ is defined as

$$\tilde{\beta}_j(\tilde{v}_j) = \frac{1}{n}\tilde{v}_j^\top \hat{\eta}_j = \frac{1}{n}\tilde{v}_j^\top (Y - \mathbf{X}_{-j}\hat{\beta}_{-j}).$$

In the following, we introduce the two asymptotic results depending on whether the surrogate set is estimated from the same data set used to find the projection direction. We first state the following theorem on the asymptotic normality when the surrogate set is estimated via (2.11).

Theorem 2.1. Denote by $\tilde{v}_j$ the solution to (2.8) with $\mathcal{A}_j^{(1)}(\tau)$ and $\mathcal{A}_j^{(2)}(\tau)$ in (2.11). Suppose the assumptions in Proposition 2.1 hold and further assume that for some $\delta > 0$,

$$\|\tilde{v}_j\|_{2+\delta} = o_{a.s.}(\|\tilde{v}_j\|). \tag{2.13}$$

Then we have

$$\frac{\sqrt{n}\left(\tilde{\beta}_j(\tilde{v}_j) - \beta_j\right)}{\hat{\sigma} n^{-1/2}\|\tilde{v}_j\|} \xrightarrow{d} N(0,1). \tag{2.14}$$

Thus an asymptotic $100(1-\alpha)\%$ confidence interval for β_j is given by

$$\text{CI}(1-\alpha) = \left\{ b \in \mathbb{R} : \left| \frac{\sqrt{n}(\tilde{\beta}_j(\tilde{v}_j) - b)}{\hat{\sigma} n^{-1/2}\|\tilde{v}_j\|} \right| \leq z_{1-\alpha/2} \right\}, \tag{2.15}$$

where $z_{1-\alpha/2}$ is the $1-\alpha/2$ quantile of $N(0,1)$.

(2.13) is a Lyapunov type condition which implies the central limit theorem. This type of assumption regarding the projection direction has also been imposed in Dezeure et al. (2017). It can be dropped under the Gaussian assumption on the errors. If the surrogate set is chosen based on prior knowledge or estimated from an independent data set (e.g., based on sample splitting), then Assumptions 2.1-2.2 can be relaxed and we have the following result.

Corollary 2.1. Suppose the surrogate set $\mathcal{A}_j^{(1)}$ is independent of the data. Under Assumptions 2.3-2.6 and further assuming that for some $\delta > 0$, $E[|\epsilon_i|^{2+\delta}] < \infty$ and $\|\tilde{v}_j\|_{2+\delta} = o_{a.s.}(\|\tilde{v}_j\|)$, then (2.14) still holds.

2.3.3 Modified bias reducing projection (MBRP) estimator

We introduce a modified bias reducing projection (MBRP) estimator which is motivated by Proposition 2.1 and the refitted Lasso idea. This new estimator would lead to a potentially smaller order of bias compared to that of the original debiased Lasso estimator under suitable assumptions as shown in Proposition 2.2. Thus, it is expected to provide better empirical coverage probability. See more details in Section 2.6. To motivate the MBRP estimator, we note that the bias associated with the BRP estimator based on some estimator $\check{\beta}$ for β can be written as

$$\begin{aligned}\sqrt{n}R(v_j, \beta_{-j}) &= \frac{1}{\sqrt{n}} \sum_{k \neq j} v_j^\top X_k (\beta_k - \check{\beta}_k) \\ &= \frac{1}{\sqrt{n}} \sum_{k \in \mathcal{B}_j^{(1)}} v_j^\top X_k (\beta_k - \check{\beta}_k) + \frac{1}{\sqrt{n}} \sum_{k \in \mathcal{B}_j^{(2)}} v_j^\top X_k (\beta_k - \check{\beta}_k)\end{aligned}$$

where $\mathcal{B}_j^{(1)}, \mathcal{B}_j^{(2)}$ are the same as in Proposition 2.1. When $|\mathcal{B}_j^{(1)}| \leq n$, we can always require v_j to be exactly orthogonal to $\mathbf{X}_{\mathcal{B}_j^{(1)}}$. So, the bias associated with the set of strong signals becomes zero. Thus it suffices to control the bias term associated with $\mathcal{B}_j^{(2)}$ by properly choosing v_j and $\check{\beta}$, which will be clarified below.

To find the projection direction for the MBRP estimator, we consider the optimization problem

$$\begin{aligned}&\min_{u_{j2}, v_j} \quad \left(C_2 \frac{n}{\log p} u_{j2}^2 + n^{-1} \|v_j\|^2 \right), \\ &\text{s.t. } v_j^\top X_j = n, \\ &n^{-1} v_j^\top X_k = 0, \quad k \in \mathcal{A}_j^{(1)}, \\ &-u_{j2} \leq n^{-1} v_j^\top X_k \leq u_{j2}, \quad k \in \mathcal{A}_j^{(2)}.\end{aligned} \tag{2.16}$$

Different from (2.8), we require the projection direction to be orthogonal to the column space of

$\mathbf{X}_{\mathcal{A}_j^{(1)}}$ in (2.16). Instead of using the Lasso estimator $\hat{\beta}$, we shall adopt the refitted least squares estimator $\check{\beta}$ as our preliminary estimator, i.e.,

$$\check{\beta}_{\mathcal{A}_j^{(1)}} = \underset{\tilde{\beta}}{\operatorname{argmin}} \frac{1}{2n}\|Y - \mathbf{X}_{\mathcal{A}_j^{(1)}}\tilde{\beta}\|^2, \quad \check{\beta}_{\mathcal{A}_j^{(2)}} = 0. \tag{2.17}$$

The MBRP estimator is then defined as

$$\tilde{\beta}_j(\bar{v}_j) = \frac{1}{n}\bar{v}_j^\top(Y - \mathbf{X}_{-j}\check{\beta}_{-j}) = \beta_j + \frac{1}{n}\bar{v}_j^\top\epsilon + R(\bar{v}_j, \beta_{-j}) \tag{2.18}$$

where $R(\bar{v}_j, \beta_{-j}) = n^{-1}\bar{v}_j^\top\mathbf{X}_{-j}(\beta_{-j} - \check{\beta}_{-j})$ and $\bar{v}_j$ is the solution to problem (2.16). The MBRP estimator can be viewed as an intermediate estimator between the refitted Lasso and the BRP estimator based on (2.8). While (2.16) is a variant of (2.8) seeking for a projection direction that is exactly orthogonal to the column space of $\mathbf{X}_{\mathcal{A}_j^{(1)}}$, the modified procedure uses the refitted estimator for β as the refitted Lasso does as noted in Remark 2.1.

We argue that the bias term $\sqrt{n}R(\bar{v}_j, \beta_{-j})$ which controls non-Gaussianity could have a potnetially smaller order compared to that of the original debiased Lasso estimator in the following.

Proposition 2.2. Denote by $\bar{v}_j$ the solution to (2.16) with $\mathcal{A}_j^{(1)}(\tau)$ and $\mathcal{A}_j^{(2)}(\tau)$ defined in (2.11). Let $\check{\beta}$ be the refitted least square estimator in (2.17). Conditional on the event $\{\mathcal{A}_j^{(2)} = \mathcal{B}_j^{(2)}\}$, we have

$$|\sqrt{n}R(\bar{v}_j, \beta_{-j})| \leq O_p\left(\sqrt{d_0}\|\beta_{\mathcal{B}_j^{(2)}}\|_0\frac{\log p}{\sqrt{n}}\right) \tag{2.19}$$

under Assumptions 1 and 5. If we further assume that

$$\sqrt{d_0}\|\beta_{\mathcal{B}_j^{(2)}}\|_0 = o(s_0), \tag{2.20}$$

the bias $\sqrt{n}R(\bar{v}_j, \beta_{-j})$ is asymptotically negligible with smaller order than that of the original debiased Lasso given by $O_p(s_0 \log p/\sqrt{n})$.

In particular, (2.20) holds if $d_0 = o(1)$ and $d_1 = O(1)$, i.e., the strength of weak signals is

of smaller order compared to the strong signals. It is more stringent than Assumption 2.1 where the magnitudes of the set of strong signals and weak signals are allowed to be of the same order. However, it should be mentioned that Proposition 2.2 is not necessary for the asymptotic normality in Corollary 2.2 to be achieved. The following result shows the asymptotic normality of (2.18) which can be proved by using similar arguments as those for Theorem 2.1.

Corollary 2.2. Under the assumptions in Theorem 2.1, we have

$$\frac{\sqrt{n}\left(\tilde{\beta}_j(\bar{v}_j) - \beta_j\right)}{\hat{\sigma} n^{-1/2} \|\bar{v}_j\|} \xrightarrow{d} N(0,1),$$

where $\tilde{\beta}_j(\bar{v}_j)$ is defined in (2.18) and $\bar{v}_j$ is the solution to (2.16).

2.4 Inference on a sparse linear combination of parameters

In some applications, one may be interested in conducting inference on $a^\top \beta$ for a (sparse) loading vector $a = (a_1, \ldots, a_p)^\top \in \mathbb{R}^p$ with $\|a\|_0 = s \ll n$. Denote by $S = S(a) = \{1 \le j \le p : a_j \neq 0\}$ the support set of a. Our method can be generalized to construct estimator and conduct inference for $a^\top \beta = a_S^\top \beta_S$. Recall that $\hat{\beta}$ is the preliminary estimator of β. Define

$$\eta_S = Y - \mathbf{X}_{-S}\beta_{-S} = \mathbf{X}_S \beta_S + \epsilon$$

and

$$\hat{\eta}_S = Y - \mathbf{X}_{-S}\hat{\beta}_{-S} = \mathbf{X}_S \beta_S + \epsilon + \mathbf{X}_{-S}(\beta_{-S} - \hat{\beta}_{-S}).$$

We construct an estimator for $a^\top \beta$ in the form of $n^{-1} v_a^\top \hat{\eta}_S$, where $v_a = (v_{a,1}, \ldots, v_{a,n})^\top$ is a projection direction such that $n^{-1} v_a^\top \hat{\eta}_S$ has tractable asymptotic limit. Notice that

$$\begin{aligned} n^{-1} v_a^\top \hat{\eta}_S =& n^{-1} v_a^\top \mathbf{X}_S \beta_S + n^{-1} v_a^\top \epsilon + n^{-1} v_a^\top \mathbf{X}_{-S}(\beta_{-S} - \hat{\beta}_{-S}) \\ =& a_S^\top \beta_S + (n^{-1} v_a^\top \mathbf{X}_S - a_S^\top)\beta_S + n^{-1} v_a^\top \epsilon + n^{-1} v_a^\top \mathbf{X}_{-S}(\beta_{-S} - \hat{\beta}_{-S}). \end{aligned}$$

Under the equality constraint that $n^{-1}v_a^\top \mathbf{X}_S - a_S^\top = 0$ and by rearranging the above terms, we have

$$\sqrt{n}(n^{-1}v_a^\top \hat{\eta}_S - a_S^\top \beta_S) = n^{-1/2}v_a^\top \epsilon + \sqrt{n}R(v_a, \beta_{-S}), \tag{2.21}$$

where $R(v_a, \beta_{-S}) = n^{-1}v_a^\top \mathbf{X}_{-S}(\beta_{-S} - \hat{\beta}_{-S})$. Similar to (2.6), the bias term can be decomposed into two parts corresponding to different strengths of the signals. Let $\mathcal{A}_S^{(1)}$ be the surrogate set for the set of strong signals (excluding the elements in S), which can be obtained in a similar way as described in Section 2.3.1. Following the derivations in Section 2.2, we can formulate the following optimization problem to find v_a

$$\begin{aligned}
&\min_{u_{a1}, u_{a2}, v_a} \quad \left(C_1 \frac{n}{\log p} u_{a1}^2 + C_2 \frac{n}{\log p} u_{a2}^2 + n^{-1}\|v_a\|^2 \right), \\
&\text{s.t. } \; v_a^\top X_S = n a_S^\top, \\
&-u_{a1} \le n^{-1}v_a^\top X_k \le u_{a1}, \quad k \in \mathcal{A}_S^{(1)}, \\
&-u_{a2} \le n^{-1}v_a^\top X_k \le u_{a2}, \quad k \in \mathcal{A}_S^{(2)},
\end{aligned} \tag{2.22}$$

where $\mathcal{A}_S^{(2)} := \left(\mathcal{A}_S^{(1)} \cup S\right)^{\complement}$. Denote by $(\tilde{u}_{a1}, \tilde{u}_{a2}, \tilde{v}_a)$ the solution to (2.22). Our estimator for $a^\top \beta$ is thus given by $n^{-1}\tilde{v}_a^\top \hat{\eta}_S$ whose asymptotic normality is established in the following theorem.

Theorem 2.2. With $\|a\|_0 = s \ll n$, suppose the assumptions in Proposition 2.1 hold and $\|\tilde{v}_a\|_{2+\delta} = o_{a.s.}(\|\tilde{v}_a\|)$ for some $\delta > 0$. Then, we have

$$\frac{\sqrt{n}\left(n^{-1}\tilde{v}_a^\top \hat{\eta}_S - a^\top \beta\right)}{\hat{\sigma} n^{-1/2}\|\tilde{v}_a\|} \xrightarrow{d} N(0,1). \tag{2.23}$$

Thus an asymptotic $100(1-\alpha)\%$ confidence interval for $a^\top \beta$ is given by

$$\mathbf{CI}(1-\alpha) = \left\{ b \in \mathbb{R} : \left| \frac{\sqrt{n}\left(n^{-1}\tilde{v}_a^\top \hat{\eta}_S - b\right)}{\hat{\sigma} n^{-1/2}\|\tilde{v}_a\|} \right| \le z_{1-\alpha/2} \right\},$$

where $z_{1-\alpha/2}$ is the $1-\alpha/2$ quantile of $N(0,1)$.

We mention some existing works for inference on linear combinations of β. When the sparsity level s_0 is known, Cai and Guo (2017) obtained the minimax expected length of confidence intervals for $a^\top\beta$ in both the sparse and dense loading regions. They further showed that without the knowledge of s_0, rate-optimal adaptation in the sparse loading regime is only possible under Assumption 2.6 and in the dense loading regime, adaptation to s_0 is impossible. In Zhu and Bradic (2018b), the authors proposed a test for linear hypothesis, which does not impose restriction on model sparsity or the loading vector representing the hypothesis. Nevertheless, compared to our method, the method by Zhu and Bradic (2018b) requires an additional sparse model to account for the dependence between the so-called synthesized feature and the stabilized feature.

Parallel to Corollary 2.1, if the surrogate set is estimated based on prior information or an independent data set, Assumptions 2.1-2.2 can be dropped and the asymptotic normality can be established as follows.

Corollary 2.3. Suppose the surrogate set $\mathcal{A}_j^{(1)}$ is independent of the data. Under Assumptions 2.3-2.6 and further assuming that for some $\delta > 0$, $E[|\epsilon_i|^{2+\delta}] < \infty$ and $\|\tilde{v}_a\|_{2+\delta} = o_{a.s.}(\|\tilde{v}_a\|)$, then (2.23) still holds.

2.5 Implementation details

2.5.1 Selecting the tuning parameters

Bootstrap for debiased Lasso has been recently studied in both Zhang and Cheng (2017) and Dezeure et al. (2017) to approximate the sampling distribution of the debiased Lasso estimator. Here we propose a bootstrap-assisted approach for choosing the tuning parameters in (2.8), (2.10) and (2.16). Specifically, the residual bootstrap is used to obtain the empirical coverage rate and its standard error for selecting the optimal tuning parameters. We focus our discussions on (2.8) and remark that the procedure is applicable to (2.10) and (2.16) as well. Let

$$\varepsilon = (\varepsilon_1, \ldots, \varepsilon_n)^\top = Y - \mathbf{X}\hat{\beta}$$

and $\bar{\varepsilon}_i = \varepsilon_i - n^{-1}\sum_{j=1}^n \varepsilon_j$ be the centered residual where $\hat{\beta}$ denotes the cross-validated Lasso estimator. Given a sequence of tuning parameters $\left\{\left(c_{1,j,(k)}, c_{2,j,(k)}\right)\right\}_{k=1}^K$, we first calculate $\tilde{v}_j\left(c_{1,j,(k)}, c_{2,j,(k)}\right)$ which is the solution to (2.8) given $\left(c_{1,j,(k)}, c_{2,j,(k)}\right)$. Note that the projection direction $\tilde{v}_j$ only needs to be calculated once for each pair of tuning parameters. Given $\left\{\tilde{v}_j\left(c_{1,j,(k)}, c_{2,j,(k)}\right)\right\}_{k=1}^K$, we do the following.

1. To generate the b-th bootstrap sample, we sample n residuals with replacement from $\{\bar{\varepsilon}_i\}_{i=1}^n$ and denote the corresponding samples by $\varepsilon_b^* = (\varepsilon_{b,1}^*, \ldots, \varepsilon_{b,n}^*)^\top$. Then, generate Y_b^* such that $Y_b^* = \mathbf{X}\hat{\beta} + \varepsilon_b^*$.

2. With (X, Y_b^*), calculate the cross-validated Lasso estimator $\hat{\beta}_b^*$ as well as the projection-based estimator

$$\tilde{\beta}_j(\tilde{v}_j(c_{1,j,(k)}, c_{2,j,(k)})) = \frac{\tilde{v}_j(c_{1,j,(k)}, c_{2,j,(k)})^\top (Y_b^* - \mathbf{X}_{-j}\hat{\beta}_{b,-j}^*)}{n},$$

   where $\hat{\beta}_{b,-j}^*$ denotes $\hat{\beta}_b^*$ without the j-th component. We then calculate the $100(1-\alpha)\%$ confidence interval $\text{CI}_{b,j,(k)}^*$ by using (2.15). For each j, calculate $I(\hat{\beta}_j \in \text{CI}_{b,j,(k)}^*)$ which is 1 if $\hat{\beta}_j$ is covered by $\text{CI}_{b,j,(k)}^*$ and 0 otherwise. Also, calculate the length of $\text{CI}_{b,j,(k)}^*$ and denote it as $\text{Len}_{b,j,(k)}^*$.

3. Repeat the above steps for B bootstrap samples. We then obtain the bootstrap coverage rate for each $\hat{\beta}_j$ as

$$\widehat{\text{Cover}}_{j,(k)} = \frac{\sum_{b=1}^B I(\hat{\beta}_j \in \text{CI}_{b,j,(k)}^*)}{B},$$

   and its standard error

$$\text{SE}(\widehat{\text{Cover}}_{j,(k)}) = \sqrt{\frac{\widehat{\text{Cover}}_{j,(k)}(1 - \widehat{\text{Cover}}_{j,(k)})}{B}},$$

   and its average length

$$\text{AvgLen}_{j,(k)} = \frac{\sum_{b=1}^B \text{Len}_{b,j,(k)}^*}{B}.$$

4. We choose the tuning parameters for β_j as

$$(c^*_{1,j,(k)}, c^*_{2,j,(k)}) = \underset{k}{\text{argmin}}\, \text{AvgLen}_{j,(k)}$$
$$\text{s.t. } \widehat{\text{Cover}}_{j,(k)} + \text{SE}(\widehat{\text{Cover}}_{j,(k)}) \geq 1 - \alpha.$$

In words, the optimal pair of tuning parameters is selected with the minimum average interval length among all the pairs whose empirical coverage rate increased by one standard error is at least the nominal level $1 - \alpha$.

2.5.2 Empirical analysis of the effect of tuning parameters

We empirically investigate the sensitiveness of our method to the choice of tuning parameters. Throughout this subsection, we suppose the rows of $\mathbf{X} \in \mathbb{R}^{100\times 500}$ are i.i.d realizations from $N(0, \mathbf{\Sigma})$ with $\Sigma_{j,k} = 0.9^{|j-k|}$ (Toeplitz) or $\Sigma_{j,k} = 0.8$ (Equicorrelation) for $j \neq k$ and $\Sigma_{jj} = 1$. Regression coefficients β_j's are generated by either Case 1 with $s_0 = 10$ or Case 2 with $s_0 = 4$ as described in Section 2.6. The errors are independently generated from the standard normal distribution. The nominal level is 95% and results are based on 100 independent simulation runs.

We first explore the effect of C_0 on the estimation of the surrogate set and the impact of C_1 and C_2 on the coverage rate and interval width of the BRP-based confidence interval. The results for β_j generated from Case 2 with $s_0 = 4$ and Toeplitz covariance $\mathbf{\Sigma}$ are summarized in Figure 2.2. As seen from Panel A, the surrogate set $\mathcal{A}(\tau)$ with $\tau = 2$ correctly identifies the large coefficients when $C_0 \geq 2$. Panels B-D provide the average coverage rate, bias and length of the BRP-based confidence intervals for the active set over a prespecified set of grid points for (C_1, C_2). The coverage probability and interval width both tend to increase with the values of C_1 and C_2. These results appear to suggest that fixing one parameter at a reasonably large value while choosing the other parameter to balance the coverage probability and interval width would generally deliver similar results as simultaneously selecting the two parameters.

To confirm this intuition, we set $C_0 = 2$, $C_1 = 8$ and use the procedure in Section 2.5.1 to

select C_2 over the following prespecified grid points

$$\left\{c_{2,j,(k)}\right\}_{k=1}^{K} = \{0.3, 0.6, \cdots, 14.7, 15.0\}. \tag{2.24}$$

We denote the corresponding procedures by "Fix-BRP" and "Fix-MBRP" and compare their performance with the procedures that select all tuning parameters automatically using the method in Section 2.5.1. Notice that fixing C_0 and C_1 would significantly ease the computational burden. Figure 2.3 presents the empirical coverage probabilities and lengths of the 95% confidence intervals and the normalized overall bias as in (2.25). Fix-BRP and Fix-MBRP perform equally well in terms of the coverage accuracy and bias as compared to BRP and MBRP but with a much lower computational cost. Indeed similar results are observed for the other simulation setups in Section 2.6.1. For the rest of the paper, we shall adopt the above procedure by fixing C_0 and C_1 to implement the proposed method.

Finally, we study the impact of B and τ. Figure 2.4 summarizes the performance of the BRP and MBRP-based confidence intervals with different values of B and τ. The results are not sensitive to the bootstrap sample size B. We also observe that a larger τ tends to deliver higher coverage for MBRP in the equicorrelation case. Unreported numerical studies show that similar phenomenon can be observed for the other simulation setups. In Section 2.6 below, we shall fix $B = 200$ and $\tau = 2$.

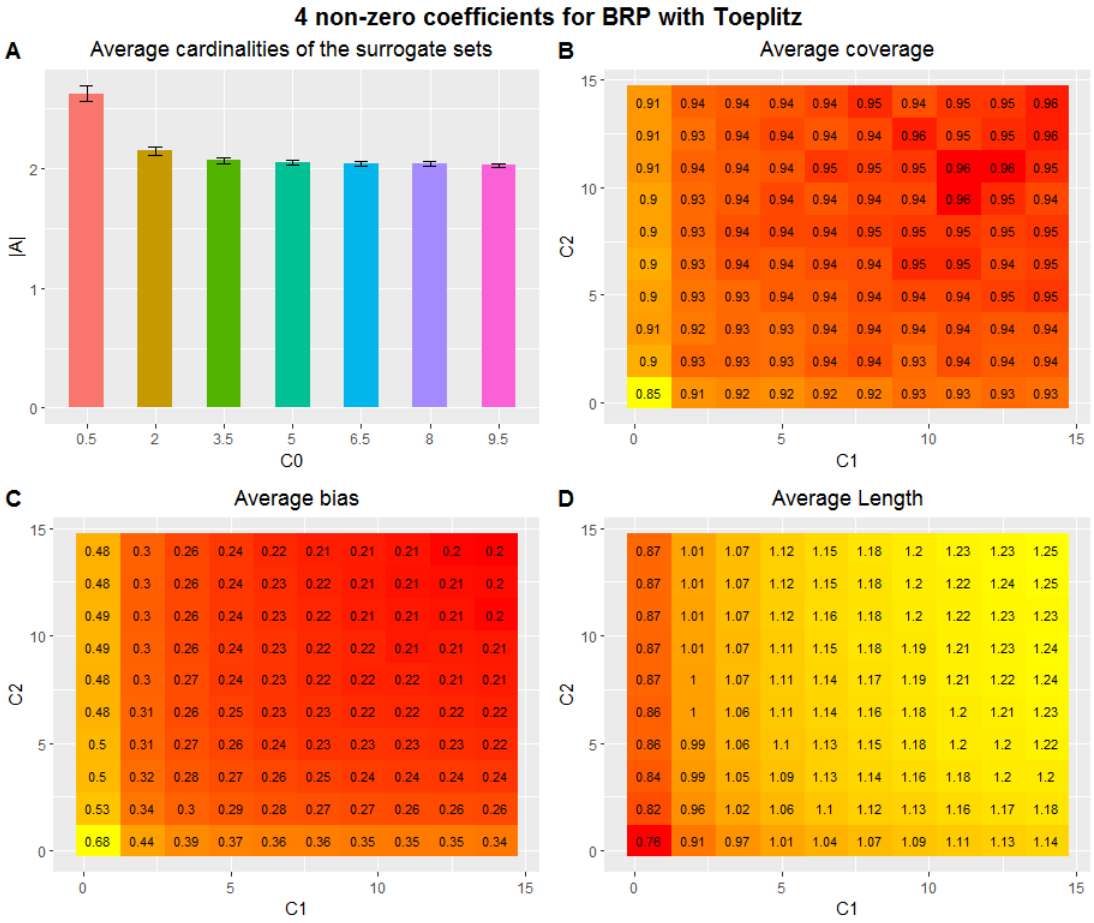

Figure 2.2: The first set of figures on empirical analysis of the effect of tuning parameters for BRP. Panel A shows the barplots of the average cardinality of $\mathcal{A}(\tau)$ against C_0. Error bars in the barplots represent the interval within one standard error of the average value. Panel B (C or D) shows the heatmap of the average coverage rates (bias or length) by the BRP estimator over a prespecified grid points for (C_1, C_2). The number represents the average coverage probability (bias or length) of the 95% confidence intervals for the active set.

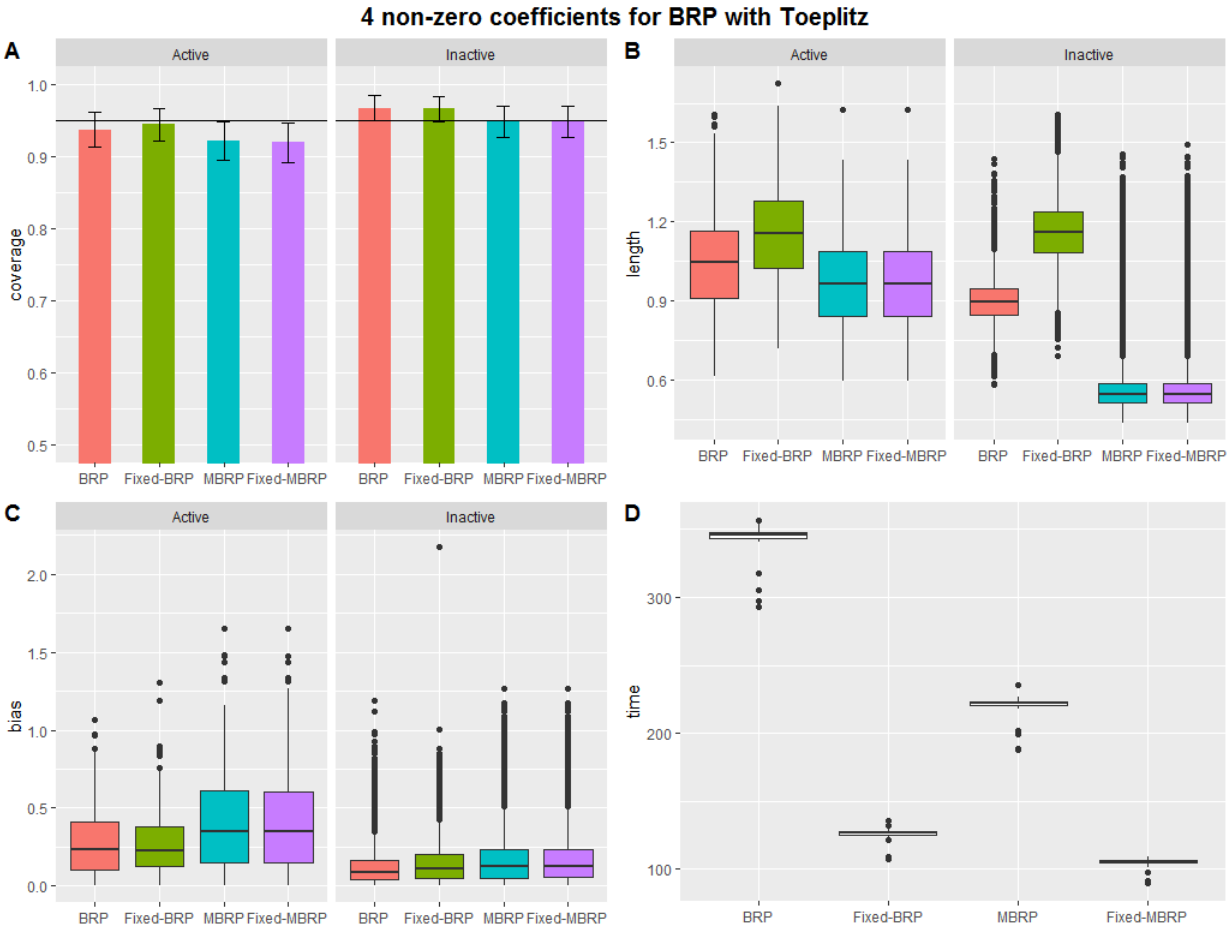

Figure 2.3: The second set of figures on empirical analysis of the effect of tuning parameters for BRP. Panel A shows the barplots of the empirical coverage and Panels B-C display the boxplots for the length and bias of the 95% confidence intervals of each method. In Panel A, the horizontal line indicates the nominal level and error bars represent the interval within one standard deviation of the empirical coverage. Panel D shows the boxplots of the computation time (in seconds) for each method.

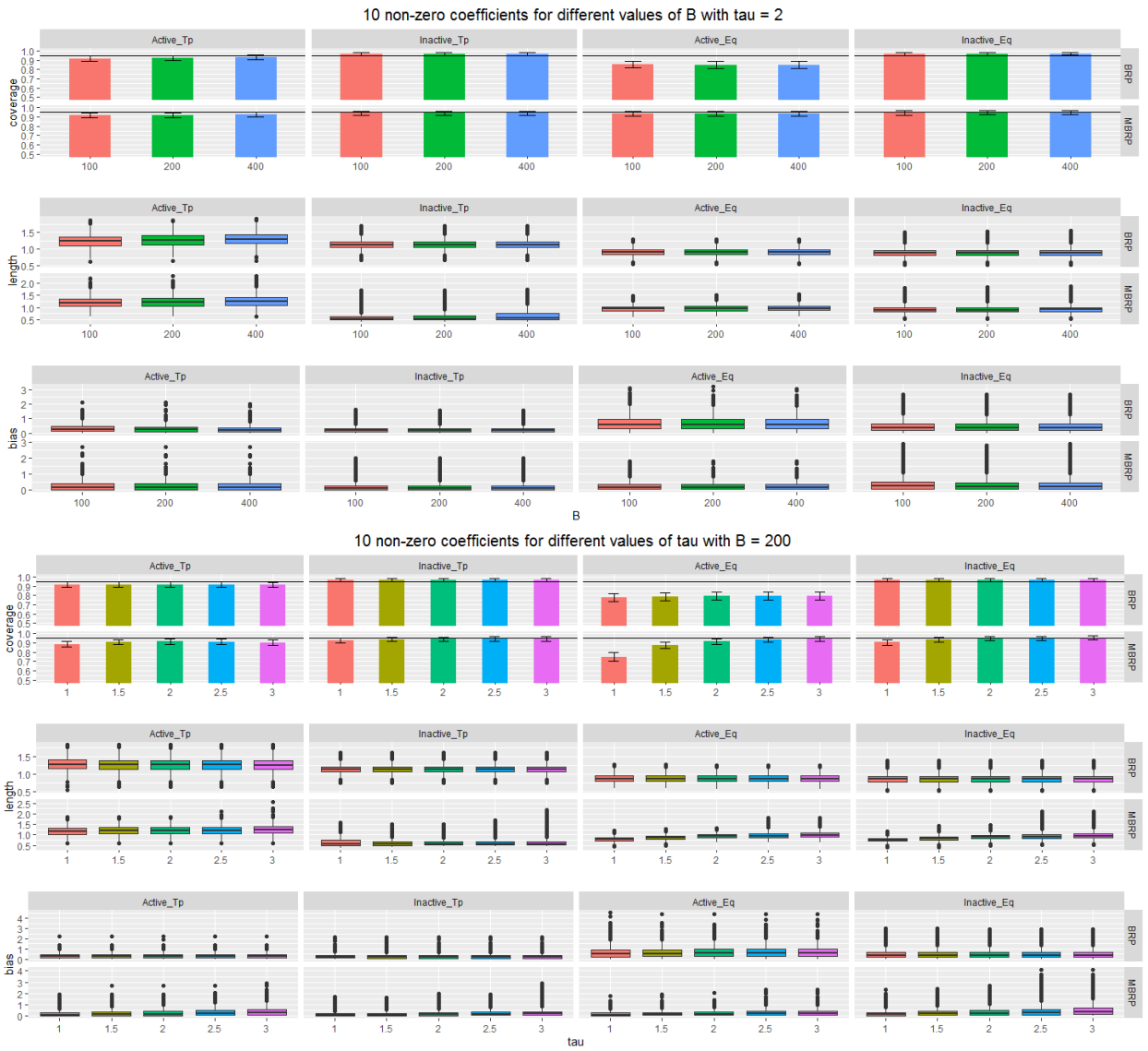

Figure 2.4: Set of figures on empirical analysis of the effect of tuning parameters B and τ. Barplots for the empirical coverage and boxplots for the length and bias of the 95% confidence intervals for both the active and inactive sets with different values of B and τ. The horizontal line in the barplots indicates the nominal level. Error bars in the barplots represent the interval within one standard deviation of the empirical coverage. The data are independently generated from Case 1 with $s_0 = 10$ and standard normal error as in Section 2.6.

2.6 Numerical results

2.6.1 Confidence interval for a single regression coefficient

We conduct simulations to evaluate the finite sample performance of the proposed BRP and MBRP estimators. We use the R package `quadprog` to solve the quadratic programming problems involved in our methods and the R package `doMC` with 5 cores for parallel computation. All the other implementation details are the same as described in Section 2.5. For comparison, we implement the debiased Lasso in van de Geer et al. (2014) (denoted by DB) using the R package `hdi` and the method in Javanmard and Montanari (2014) (denoted by JM) using the code posted on the authors' website. As we encounter some numerical issue when implementing JM's code for the equicorrelation covariance structure of $\mathbf{X}$ in (ii). Therefore, we only report the results of JM for the toeplitz covariance structure of $\mathbf{X}$. In addition, we present the results of the double selection approach in Belloni et al. (2014) (denoted by BCH) using the R package `hdm`. Due to the high computational cost of BCH in the case of equicorrelation covariance, we only report the result for the active set. We also implement the method in Zhu and Bradic (2018b) (denoted by "ZB" and "ZB2"). The only difference between ZB and ZB2 lies on the choice of the constant c in the tuning parameter $\eta = \sqrt{c(\log p)/n}$ in (12) of their paper. In ZB, we set $c = 2$ as suggested by the authors while in ZB2, we let $c = 10^{-3}$.

In (2.1), the rows of $\mathbf{X}$ are considered to be i.i.d realizations from $N(0, \mathbf{\Sigma})$ with $\Sigma_{jj} = 1$ under two scenarios: (i) $\Sigma_{j,k} = 0.9^{|j-k|}$ (denoted as Tp); (ii) $\Sigma_{j,k} = 0.8$ for all $j \neq k$ (denoted as Eq). To generate β, we consider the following two cases,

> Case 1: $\beta_j \overset{i.i.d.}{\sim} U(0, 4)$ with $s_0 = 3, 5, 10, 15$.
>
> Case 2: Half of the non-zero β_j's are independently generated from $U(0, 0.5)$ and the rest are generated from $U(2.5, 3)$ with $s_0 = 4, 8, 12, 16$.

The errors are independently generated from (a) the standard normal distribution; (b) the studentized $t(4)$ distribution, i.e., $t(4)/\sqrt{2}$; (c) the centralized and studentized Gamma(4,1) distribution,

i.e., $(\text{Gamma}(4,1)-4)/2$. The simulation results for (b) and (c) are summarized in the supplementary material. To save space, we only included the results of BCH, ZB and ZB2 for case (a). Throughout the simulations, we set $n = 100$, $p = 500$ and the nominal level $1 - \alpha = 0.95$. All the simulation results are based on 100 independent simulation runs.

We summarize the empirical coverage probabilities, the corresponding confidence interval lengths and the absolute value of the overall normalized bias defined as

$$\text{Bias} = \frac{|\sqrt{n}R(v_j, \beta_{-j})|}{\sqrt{\hat{\sigma}^2 n^{-1}\|v_j\|^2}} \tag{2.25}$$

for both the active set and the inactive set in Figures 2.5-2.8. The R code of Javanmard and Montanari (2014) makes a finite sample adjustment. To avoid unfair comparison, we do not include their method in the bias comparison. As inverting the test statistic in Zhu and Bradic (2018b) doesn't provide a closed form of confidence interval, the interval lengths of ZB and ZB2 are numerically calculated by using the bisection-type method. To avoid computational burden therein, we only calculate the lengths of 5 confidence intervals of ZB and ZB2 for inactive set in each simulation runs.

We observe that (i) BRP and MBRP generally provide more accurate coverage for the active set in comparison to DB and JM. The coverage probability for the active set based on DB can be significantly lower than the nominal level. While BCH shows similar or slightly higher coverage rate than BRP for the Toeplitz covariance structure, its coverage rate is lower than the nominal level in the equicorrelation case; (ii) The interval length of BCH is generally similar or wider than the lengths of BRP and MBRP, which is in turn wider than that of DB for the active set. Both ZB and ZB2 tend to provide wider confidence intervals compared to the other methods. (iii) For the equicorrelation covariance structure and $s_0 \geq 10$, ZB2 delivers the most accurate coverage rate followed by MBRP. In contrast, the other methods significantly undercover in these cases. (iv) The better coverage of the active set for our method is closely related to the smaller bias. Interestingly, the coverage rate for the inactive set seems not sensitive to the bias; (v) The computation time of

our method is between those of DB and ZB as shown in Table 2.1; (vi) The bias associated with the active set tends to be larger than that with the inactive set especially in the case of Toeplitz covariance. BRP seems to overally reduce the bias associated with both the active and inactive sets in such case; (vii) The coverage rate for the inactive set is usually close or above the nominal level for all methods except for ZB. According to our extensive simulations, the over-coverage is partly caused by the overestimation of the noise level as illustrated in Figure A.11 in the supplementary material. Overall, our proposed method appears to outperform DB, JM, BCH and ZB in terms of coverage accuracy.

	Min	Q1	Median	Q3	Max
BRP	107.60	125.30	126.70	127.80	135.20
MBRP	89.65	104.34	105.21	106.35	109.03
DB	26.29	33.45	34.41	35.66	38.20
ZB	457.90	471.30	476.50	483.20	499.50

Table 2.1: Computation time (in seconds) of each method for constructing 500 confidence intervals calculated by the R package `microbenchmark`. The five number summaries are obtained based on 100 independent simulation runs.

Figures 2.9-2.10 plot the bias and length of BRP and MBRP against C_2 selected by the procedure in Section 2.5.1. It is interesting to note that for BRP, the interval width generally increases while the bias decreases with C_2. The pattern is less obvious for MBRP with most of the values of C_2 concentrate around the lower end of the grid points in (2.24).

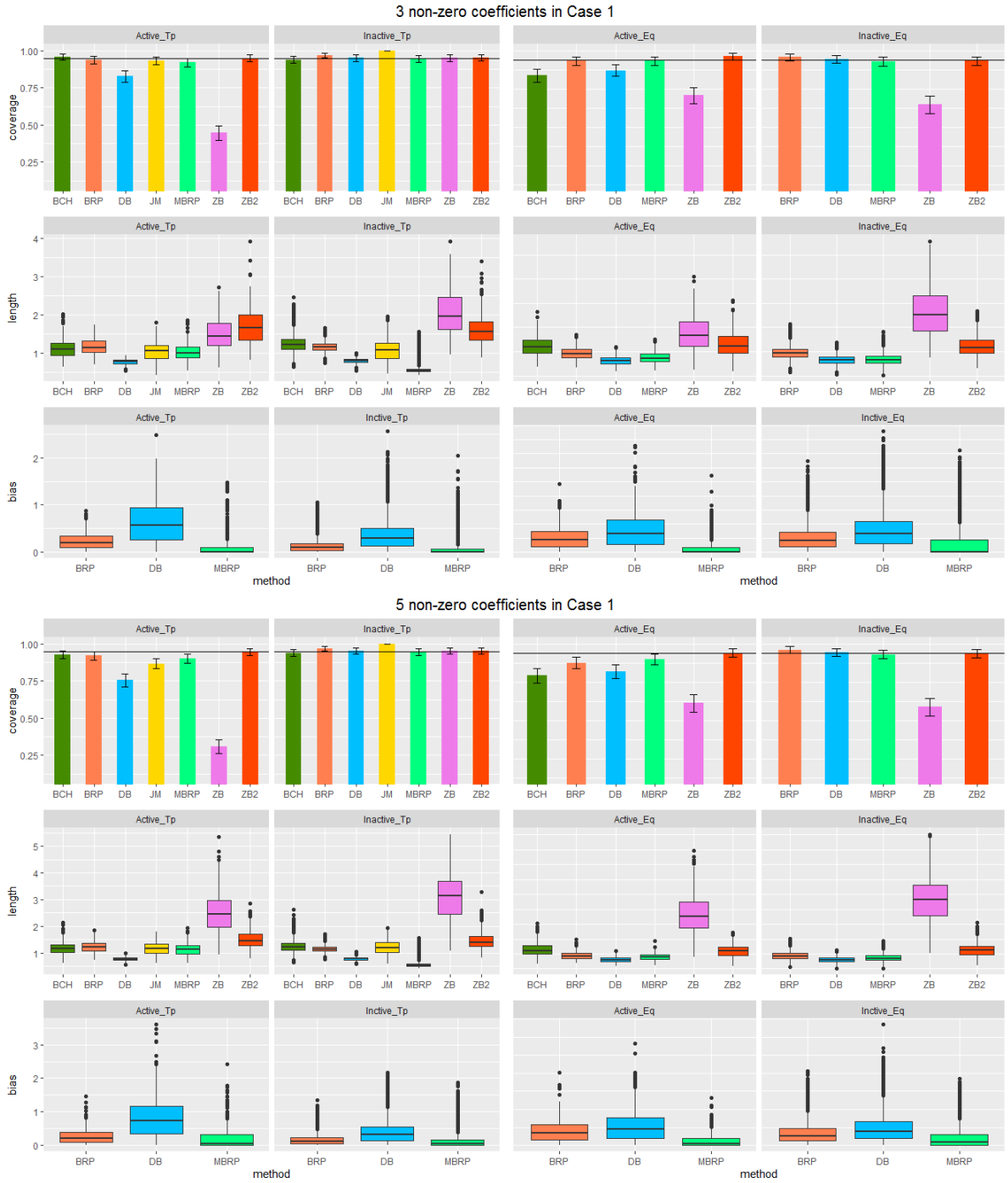

Figure 2.5: Simulation results for Case 1 with $s_0 = 3, 5$ and standard normal random error. Barplots for the empirical coverage and boxplots for the length and bias of the 95% confidence intervals. The horizontal line in the barplots indicates the nominal level. Error bars in the barplots represent the interval within one standard deviation of the empirical coverage.

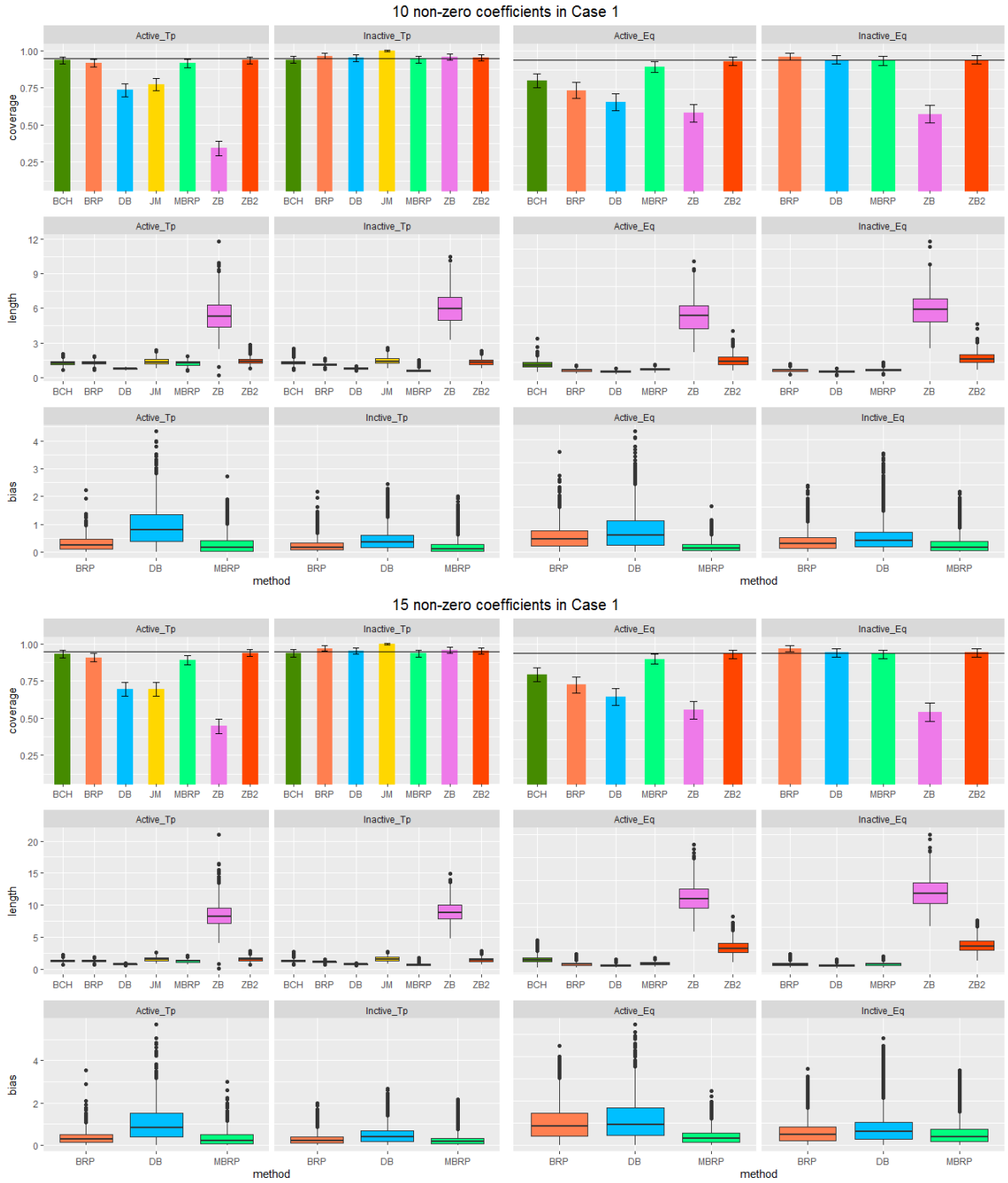

Figure 2.6: Simulation results for Case 1 with $s_0 = 10, 15$ and standard normal random error. Barplots for the empirical coverage and boxplots for the length and bias of the 95% confidence intervals. The horizontal line in the barplots indicates the nominal level. Error bars in the barplots represent the interval within one standard deviation of the empirical coverage.

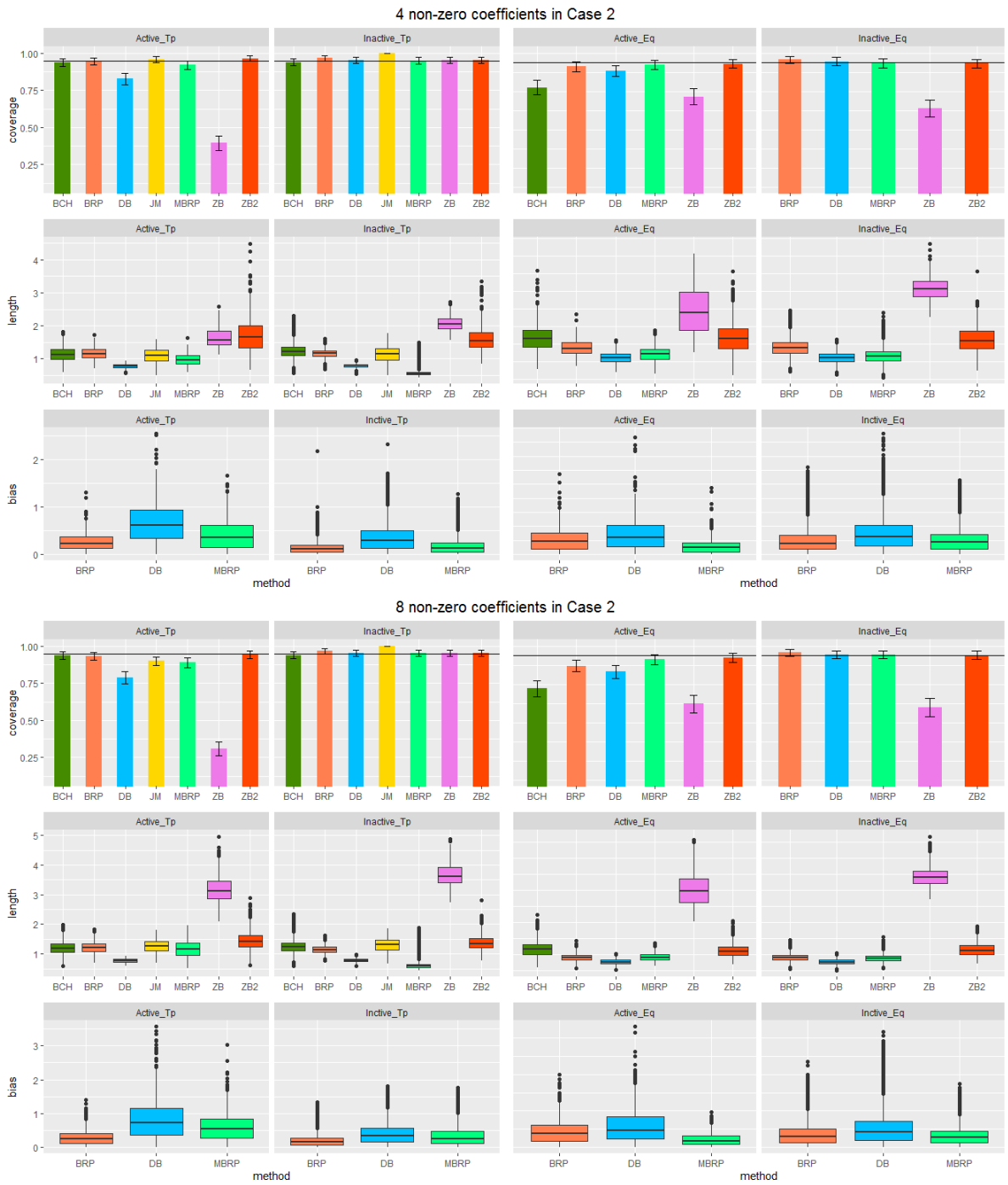

Figure 2.7: Simulation results for Case 2 with $s_0 = 4, 8$ and standard normal random error. Barplots for the empirical coverage and boxplots for the length and bias of the 95% confidence intervals. The horizontal line in the barplots indicates the nominal level. Error bars in the barplots represent the interval within one standard deviation of the empirical coverage.

Figure 2.8: Simulation results for Case 2 with $s_0 = 12, 16$ and standard normal random error. Barplots for the empirical coverage and boxplots for the length and bias of the 95% confidence intervals. The horizontal line in the barplots indicates the nominal level. Error bars in the barplots represent the interval within one standard deviation of the empirical coverage.

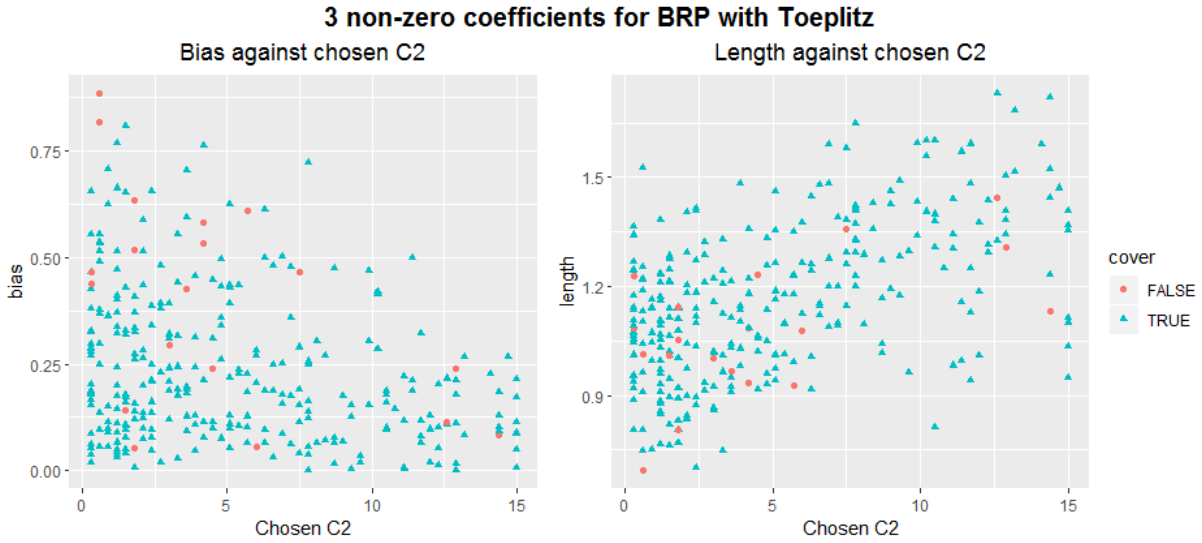

Figure 2.9: Scatterplots of the bias and length of the BRP-based confidence interval for the active set with $s_0 = 3$ and Toeplitz covariance structure for $\mathbf{X}$ against the selected C_2. The point shapes and colors indicate whether the constructed confidence intervals include the true parameter or not.

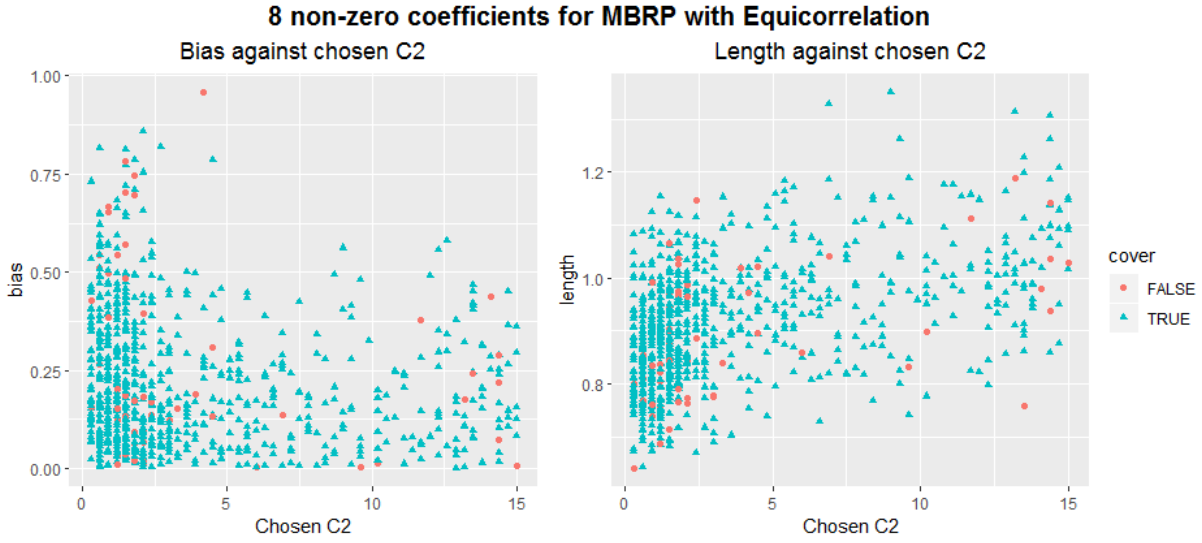

Figure 2.10: Scatterplots of the bias and length of the MBRP-based confidence interval for the active set with $s_0 = 8$ and equicorrelation covariance structure for $\mathbf{X}$ against the selected C_2. The point shapes and colors indicate whether the constructed confidence intervals include the true parameter or not.

2.6.2 Confidence interval for a sparse linear combination of regression coefficients

In this subsection, we investigate the finite sample performance of the method in Section 2.4. We consider the case where a linear contrast for two coefficients is of interest. We set the true regression coefficient $\beta = (b_1, b_1, b_2, b_3, 0, \cdots, 0)^\top$, where b_1, b_2, b_3 are drawn independently from $U(0, 4)$. Depending on a, we consider the following two cases:

1. Contrast 1: $a = (1, -1, 0, \cdots, 0)^\top$ and $a^\top \beta = b_1 - b_1 = 0$;

2. Contrast 2: $a = (0, 0, 1, -1, , 0, \cdots, 0)^\top$ and $a^\top \beta = b_2 - b_3 \neq 0$.

We adopt the same procedures as before for choosing the surrogate set and the tuning parameters but the results are based on 300 independent simulation runs. The configuration for ϵ is the same as in the previous subsection. The results for t-distributed and gamma errors are presented in the supplementary material.

Figure 2.11 shows the empirical coverage rates, the corresponding confidence interval widths as well as the bias for each contrast. For the Toeplitz covariance structure, BRP and MBRP provide closer coverage rate to the nominal level but with wider interval length than DB does. In particular, MBRP delivers the smallest bias. Thus, the better coverage for our method is again closely related to the smaller bias in the finite sample. For the equicorrelation covariance structure, the coverage rates of all the methods are close to the nominal level. We also note that ZB2 provides satisfactory coverage probabilities while ZB significantly undercovers in the case of Toeplitz covariance structure. Similar to the case for a single regression coefficient, the lengths of ZB and ZB2 are generally wider than those of the other methods.

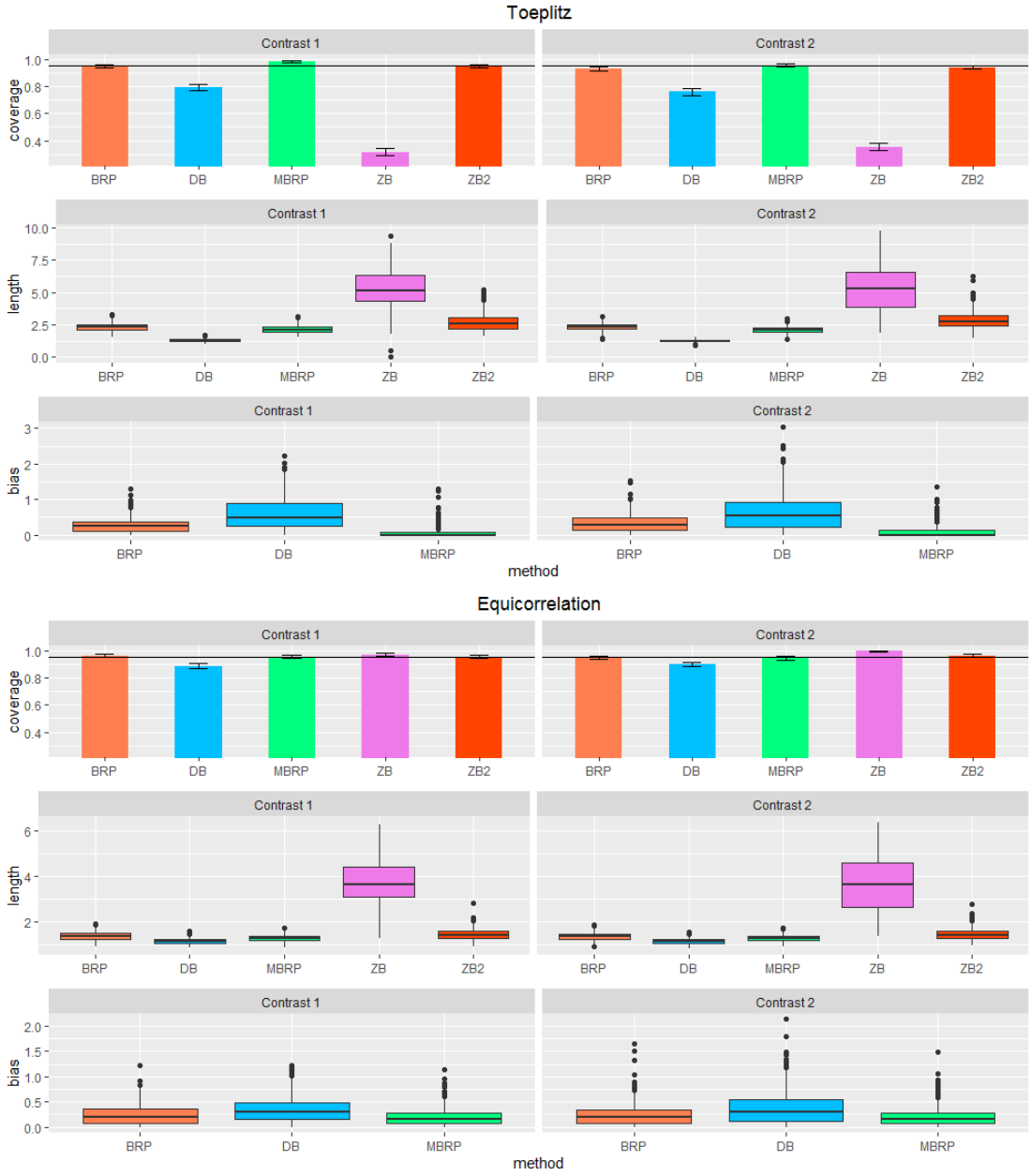

Figure 2.11: Simulation results for a sparse linear combination of β and standard normal random error. Barplots for the empirical coverage and boxplots for the length and bias of the 95% confidence intervals for each contrast. The horizontal line in the barplots indicates the nominal level. Error bars in the barplots represent the interval within one standard deviation of the empirical coverage.

2.6.3 Real data analysis

As a real data application, we consider a dataset of riboflavin (vitamin B_2) production by Bacillus subtilis. The dataset is available in the R package `hdi` and has also been analyzed in van de Geer et al. (2014) and Javanmard and Montanari (2014). It contains $n = 71$ observations of $p = 4088$ covariates of gene expressions and a response of riboflavin production. We model the data using (2.1) and consider the following multiple hypothesis testing for the significance of each gene:

$$H_{j,0} : \beta_j = 0 \quad \text{for} \quad j = 1, \cdots, 4088.$$

We use Theorem 2.1 and Corollary 2.2 to calculate the p-values based on BRP and MBRP respectively. The Holm procedure is adopted for multiplicity adjustment with the 5% significance level. Neither of our methods finds any significant predictors, which is also the case for DB while there turn out to be two significant genes YXLD-at and YXLE-at identified by JM.

3. TWO-STAGE FALSE DISCOVERY RATE CONTROL FOR CONFOUNDER ADJUSTMENT IN GENOMICS STUDIES

3.1 Introduction

One central theme of genomic data analysis is to identify genomic features that are associated with a variable of interest such as disease status. The associated features are subject to further replication and validation, and the validated features could then be followed up for more in-depth mechanistic study or be used as biomarkers for disease presentation, diagnosis, and prognosis if they have sufficient predictive power. Due to the constraint of clinical sample collection, the variable of interest is often correlated with other variables, which may potentially confound the associations of interest. One example is the identification of microbiome biomarkers for endometrial cancer based on a comparison between benign and malignant tumor samples. Patients with benign tumors are usually much younger than those with malignant tumors since the progression to malignancy requires multiple genomic events. Age has also been known to be associated with the female genital microbiome. Therefore, age is a confounding factor, and we need to control it if the aim is to identify cancer-related microbiome biomarkers reliably. Controlling the confounders could significantly increase the rate of successful validation, reduce the overall cost and shorten the time from discovery to clinical tests. However, confounder adjustment exacerbates the already low statistical power for genome-scale association tests due to a substantial multiple testing burden. If no confounder adjustment is performed, we are faced with a severely inflated type I error, with the extent of inflation depending on the number and strength of associations with the confounder. Increasing the statistical power for a confounded association study while controlling for the false positives is a statistical topic of critical importance. Surprisingly, few statistical efforts have been made for this important topic. Some recent contributions include Price et al. (2006), Leek and Storey (2008), Sun et al. (2012) and Wang et al. (2017).

The traditional way of confounder adjustment for high-dimensional association tests is to adjust

for confounders for each genomic feature and further correct the individual association p-values for multiple testing using false discovery rate (FDR) control. This procedure seems a standard statistical practice for genomic association analysis with the aim to maintain the correct type I error rate level. Here we show that such a method is subject to lower statistical power and we propose a novel two-stage FDR procedure for more powerful confounder adjustment. In the first stage, we use the unadjusted z-statistics to enrich signals (for both false and real signals). We then remove the false signals in the second stage due to confounders by using the adjusted z-statistics and control the FDR at the desired level. Since in the second step we use a more lenient p-value cutoff due to a much less multiple testing burden, we could achieve a way better power than the commonly used adjusted procedure. A particular challenge is the choice of the cutoff values in the two stages. Our main contribution is to propose a new way of simultaneously selecting both cutoffs. By choosing two thresholds simultaneously, we automatically take into consideration the selection effect caused by the first stage. The proposed method can be viewed as a two-dimensional generalization of the classical Benjamini-Hochberg (BH) procedure, where we search for the cutoff values in a two-dimensional region. In the BH procedure, one replaces the number of false rejections by its expectation under the null to come up with a (conservative) estimate for the FDR. The threshold is chosen to control the estimate for the FDR while maximizing the number of rejections. An intrinsic difficulty in our case is that the expected number of false rejections depends on the effects of the confounding factors on each feature. As the number of features could be in the thousands, it thus requires estimating a large number of nuisance parameters. To tackle this challenge, we adopt an empirical Bayesian viewpoint by assuming that the nuisance parameters are generated from a common prior distribution. The Bayesian viewpoint allows us to express the expected number of false rejections as a functional of the prior distribution. Therefore, we can translate the task into estimating the prior distribution instead of a direction estimation of a large number of nuisance parameters. It is worth mentioning that the problem we are facing is in a similar spirit to the g-factor of intelligence of Spearman (1904). The prior distribution is estimated via the general maximum likelihood empirical Bayes estimation [Jiang and Zhang (2009); Koenker and Mizera

(2014)], which can be cast into a convex optimization problem. Under suitable assumptions, we show that the empirical Bayes estimate of the expected number of false rejections is consistent and the proposed method provides asymptotic FDR control. Through extensive numerical studies, we demonstrate that the recommended two-stage procedure outperforms the commonly used one-stage approach in a wide range of settings.

The rest of this chapter proceeds as follows. We introduce the two-stage FDR controlling procedure in Section 3.2. Section 3.3 justifies the asymptotic validity of the proposed procedure. We conduct asymptotic power analysis in Section 3.4. Section 3.5 presents numerical results from both simulations and real data analysis. As modern genomics data are generated based on sequencing, the response Y_i in (3.1) would not be necessarily continuous. For such case, we extend the proposed two-step procedure to generalized linear model in Section B.2. The technical details are gathered in Section B.3.

In Chapter 3, we use the following notations: For $x, y \in \mathbb{R}$, let $x \vee y = \max(x, y)$ and $x \wedge y = \min(x, y)$. Let $d_H(f, g) = (1/2)\int(\sqrt{f(x)} - \sqrt{g(x)})^2 dx$ be the Hellinger distance between two densities f and g. For a matrix $\mathbf{C}$, denote by $P_{\mathbf{C}} = \mathbf{C}(\mathbf{C}^\top\mathbf{C})^{-1}\mathbf{C}^\top$ the projection matrix associated with the column space of $\mathbf{C}$ and define $P_{\mathbf{C}}^\perp = \mathbf{I} - P_{\mathbf{C}}$. Let $\|\mathbf{C}\|_2$ and $\|\mathbf{C}\|_{\max}$ be the spectral norm and the elementwise maximum norm of $\mathbf{C}$, respectively. Denote by $\lambda_{\min}(\mathbf{C})$ and $\lambda_{\max}(\mathbf{C})$ the minimum and maximum eigenvalues of $\mathbf{C}$. Let $\phi(\cdot)$ and $\Phi(\cdot)$ be the probability density function and cumulative distribution function of the standard normal distribution. Denote by χ^2_k the chi-square distribution with k degrees of freedom.

3.2 Methodology

3.2.1 Basic setup

Consider the following linear models:

$$Y_i = \mathbf{1}_{n\times 1} b + X\alpha_i + \mathbf{Z}\boldsymbol{\beta}_i + e_i, \quad e_i \overset{\text{i.i.d.}}{\sim} N(0, \sigma_i^2 \mathbf{I}_n), \quad 1 \le i \le m, \tag{3.1}$$

where $Y_i \in \mathbb{R}^{n\times 1}$ is the response vector, $X = (X_1, \ldots, X_n)^\top \in \mathbb{R}^{n\times 1}$ is the covariate of interest, $\mathbf{Z} = (z_1, \ldots, z_n)^\top \in \mathbb{R}^{n\times d}$ is the design matrix associated with the confounding factors, and $\alpha_i \in \mathbb{R}$ and $\boldsymbol{\beta}_i = (\beta_{i1}, \ldots, \beta_{id})^\top \in \mathbb{R}^{d\times 1}$ are the parameters associated with the covariate and confounding factors respectively. By centering the response, covariate and confounding factors, we can assume without loss of generality that $b = 0$ throughout the following discussions.

Under (3.1), there are four different categories to consider

A. Solely associated with the variable of interest: $\alpha_i \neq 0, \boldsymbol{\beta}_i = 0$;

B. Solely associated with the confounder: $\alpha_i = 0, \boldsymbol{\beta}_i \neq 0$;

C. Associated with both the variable of interest and confounder: $\alpha_i \neq 0, \boldsymbol{\beta}_i \neq 0$;

D. Not associated with either the variable of interest or confounder: $\alpha_i = 0, \boldsymbol{\beta}_i = 0$.

The goal of this work is to develop a multiple testing procedure for simultaneously testing m hypotheses

$$H_{0,i} : \alpha_i = 0 \quad \text{versus} \quad H_{a,i} : \alpha_i \neq 0, \quad i = 1, 2, \ldots, m,$$

while adjusting for the confounding effects. We let $\hat{\alpha}_i^A$ be the estimator of α_i after adjusting for the confounding effect, and $\hat{\alpha}_i^U$ be the unadjusted version without taking into account the confounding factors. Specifically, we have

$$\begin{aligned}
\hat{\alpha}_i^A &= (X^\top P_{\mathbf{Z}}^\perp X)^{-1} X^\top P_{\mathbf{Z}}^\perp Y_i = \alpha_i + (X^\top P_{\mathbf{Z}}^\perp X)^{-1} X^\top P_{\mathbf{Z}}^\perp e_i, \\
\hat{\alpha}_i^U &= (X^\top X)^{-1} X^\top Y_i = \alpha_i + (X^\top X)^{-1} X^\top \mathbf{Z}\boldsymbol{\beta}_i + (X^\top X)^{-1} X^\top e_i.
\end{aligned}$$

Under (3.1), the estimator of the noise level σ_i^2 is given by

$$\hat{\sigma}_i^2 = \frac{1}{n-d-1}(Y_i - X\hat{\alpha}_i^A - \mathbf{Z}\hat{\boldsymbol{\beta}}_i)^\top (Y_i - X\hat{\alpha}_i^A - \mathbf{Z}\hat{\boldsymbol{\beta}}_i) = \frac{1}{n-d-1} Y_i^\top P_{\mathbf{W}}^\perp Y_i,$$

where $\hat{\boldsymbol{\beta}}_i = (\mathbf{Z}^\top P_X^\perp \mathbf{Z})^{-1} \mathbf{Z}^\top P_X^\perp Y_i$ and $\mathbf{W} = (X, \mathbf{Z})$. Let $\Omega = X^\top X/n$, $\Gamma = X^\top \mathbf{Z}/n$, $\Omega_{X|\mathbf{Z}} = X^\top P_{\mathbf{Z}}^\perp X/n$ and $\Omega_{\mathbf{Z}|X} = \mathbf{Z}^\top P_X^\perp \mathbf{Z}/n$. The adjusted and unadjusted z-statistics for testing $H_{0,i}$ can

be defined as

$$Z_i^A = \sqrt{n}\Omega_{X|\mathbf{Z}}^{1/2}\hat{\alpha}_i^A/\hat{\sigma}_i = \sqrt{n}\Omega_{X|\mathbf{Z}}^{1/2}\alpha_i/\hat{\sigma}_i + \Omega_{X|\mathbf{Z}}^{-1/2}X^\top P_{\mathbf{Z}}^\perp e_i/(\sqrt{n}\hat{\sigma}_i),$$
$$Z_i^U = \sqrt{n}\Omega^{1/2}\hat{\alpha}_i^U/\hat{\sigma}_i = \sqrt{n}\Omega^{1/2}\alpha_i/\hat{\sigma}_i + \sqrt{n}\Omega^{-1/2}\Gamma\boldsymbol{\beta}_i/\hat{\sigma}_i + \Omega^{-1/2}X^\top e_i/(\sqrt{n}\hat{\sigma}_i),$$

where we have used the variance estimator under model (3.1) for both statistics.

Figure 3.1 shows that the average power of the traditional approach only using the adjusted statistics decreases as the confounding effect gets stronger. Motivated by this fact, we propose a novel two-stage procedure which can be described as follows: given the thresholds $t_1, t_2 \geq 0$,

Step 1. Use the unadjusted statistics to determine a preliminary set of features $\mathcal{D}_1 = \big\{1 \leq i \leq m : |Z_i^U| \geq t_1\big\}$.

Step 2. Reject $H_{0,i}$ for $|Z_i^A| \geq t_2$ and $i \in \mathcal{D}_1$. As a result, the final set of discoveries is given by $\mathcal{D}_2 = \big\{1 \leq i \leq m : |Z_i^U| \geq t_1, |Z_i^A| \geq t_2\big\}$.

The first two plots in Figure 3.2 illustrates the above procedure step by step. The basic idea of this procedure is to find the threshold for the unadjusted statistics in step 1 to screen out a large number of noises in Category D. This step enriches both true and false signals. Then, the second step tries to find out another threshold for the adjusted statistics to separate true signals in Categories A and C from false signals in Category B. Although the unadjusted statistics are unable to distinguish the noise in Category B from the signals, they can preserve or even increase the signal strength. To see this, we note that

$$|\Omega^{1/2}\alpha_i| \geq |\Omega_{X|Z}^{1/2}\alpha_i|.$$

When $\boldsymbol{\beta}_i = 0$, the unadjusted statistics can better preserve the signal strength comparing to the adjusted one.

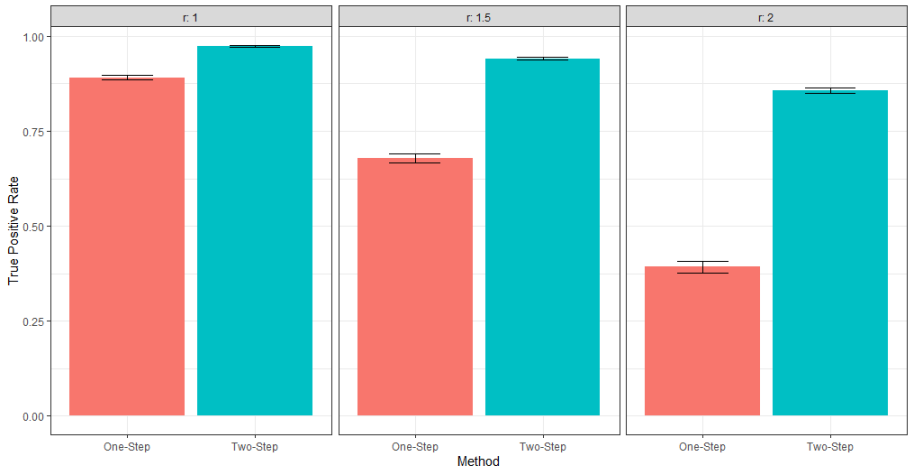

Figure 3.1: Barplots of the true positive rates for the different values of r in (B.1). Here r is proportional to the correlation between X and $\mathbf{Z}$ which thus represent the magnitude of the confounding effect. The data generation scheme is shown in Section B.1. Error bars in the bar plots represent the interval within two standard devation of the true positive rate.

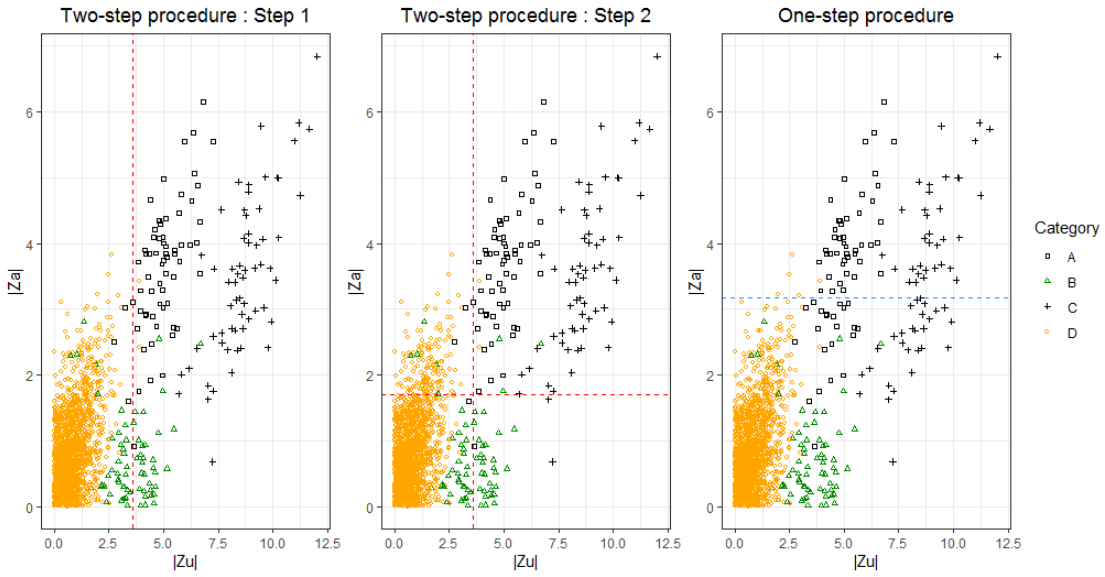

Figure 3.2: Scatter plots of $|Z_i^U|$ against $|Z_i^A|$ to illustrate the traditional one-step method and two-step procedure. The figures are based on a single dataset generated as described in Section B.1 with $r = 2$. While the first two plots describes the two-step procedure where the red vertical and horizontal lines denote the chosen cutoff. The plot on the far right shows the traditional one-step method where the horizontal line denotes the cutoff found by the Storey's procedure.

3.2.2 Approximation of the false discovery proportion

Recall that t_i is the threshold in Step i for $i = 1, 2$. We propose a method to simultaneously select the two thresholds. Note that the ith hypothesis will be rejected if and only if

$$|Z_i^U| \geq t_1 \quad \text{and} \quad |Z_i^A| \geq t_2.$$

In Step 2, all rejections from Categories B and D ($\alpha_i = 0$) will be considered as false rejections/discoveries. Therefore, the false discovery proportion (FDP) is defined as

$$\begin{aligned}
&\text{FDP}(t_1, t_2) \\
=&\frac{\sum_{i:\alpha_i=0} \mathbf{1}\{|Z_i^U| \geq t_1, |Z_i^A| \geq t_2\}}{\sum_{i=1}^m \mathbf{1}\{|Z_i^U| \geq t_1, |Z_i^A| \geq t_2\}} \\
=&\frac{\sum_{i:\alpha_i=0} \mathbf{1}\{|\sqrt{n}\Omega^{-1/2}\Gamma\boldsymbol{\beta}_i/\hat{\sigma}_i + \Omega^{-1/2}X^\top e_i/(\sqrt{n}\hat{\sigma}_i)| \geq t_1, |\Omega_{X|\mathbf{Z}}^{-1/2}X^\top P_{\mathbf{Z}}^\perp e_i/(\sqrt{n}\hat{\sigma}_i)| \geq t_2\}}{\sum_{i=1}^m \mathbf{1}\{|Z_i^U| \geq t_1, |Z_i^A| \geq t_2\}}.
\end{aligned} \tag{3.2}$$

Let (V_1, V_2) be the bivariate normal random variables such that

$$\begin{pmatrix} V_1 \\ V_2 \end{pmatrix} \sim N_2 \left(\begin{pmatrix} 0 \\ 0 \end{pmatrix}, \begin{pmatrix} 1 & \Omega^{-1/2}\Omega_{X|\mathbf{Z}}^{1/2} \\ \Omega_{X|\mathbf{Z}}^{1/2}\Omega^{-1/2} & 1 \end{pmatrix} \right).$$

Replacing the numerator by the corresponding expectation (conditional on $X, \mathbf{Z}$ and $\boldsymbol{\beta}_i$'s) and $\hat{\sigma}_i$ by σ_i in (3.2), we obtain

$$\text{FDP}(t_1, t_2) \approx \frac{\sum_{i:\alpha_i=0} L(\mu_i, t_1, t_2)}{\sum_{i=1}^m \mathbf{1}\{|Z_i^U| \geq t_1, |Z_i^A| \geq t_2\}} \leq \frac{\sum_{i=1}^m L(\mu_i, t_1, t_2)}{\sum_{i=1}^m \mathbf{1}\{|Z_i^U| \geq t_1, |Z_i^A| \geq t_2\}}, \tag{3.3}$$

where $\mu_i = \mu_{i,n} := \sqrt{n}\Omega^{-1/2}\Gamma\boldsymbol{\beta}_i/\sigma_i$ and $L(\mu, t_1, t_2) = P\left(|\mu + V_1| \geq t_1, |V_2| \geq t_2 | \mu\right)$.

The major challenge here is the estimation of the expected number of false rejections given by $\sum_{i=1}^m L(\mu_i, t_1, t_2)$, which involves a large number of nuisance parameters μ_i's. A natural strategy is to estimate each μ_i separately by $\hat{\mu}_i$, and replace $L(\mu_i, t_1, t_2)$ by the plug-in estimate $L(\hat{\mu}_i, t_1, t_2)$. It seems natural to use the least squares estimator given by $\hat{\mu}_i = \sqrt{n}\Omega^{-1/2}\Gamma\hat{\boldsymbol{\beta}}_i/\hat{\sigma}_i$. However,

this method does not lead to a consistent estimation of the number of false rejections when there is non-negligible proportion of weak confounding factors.[1] To see this, we note that $\hat{\mu}_i$ approximately follows a normal distribution with mean μ_i and variance $A^2 = \Omega^{-1/2}\Gamma\Omega^{-1}_{\mathbf{Z}|X}\Gamma^T\Omega^{-1/2}$. Some algebra shows that

$$L(\hat{\mu}_i, t_1, t_2) \approx P(|\mu_i + \tilde{V}_1| \geq t_1, |\tilde{V}_2| \geq t_2 | \mu_i) \neq L(\mu_i, t_1, t_2),$$

where

$$\begin{pmatrix} \tilde{V}_1 \\ \tilde{V}_2 \end{pmatrix} \sim N_2 \left(\begin{pmatrix} 0 \\ 0 \end{pmatrix}, \begin{pmatrix} 1 + A^2 & \Omega^{-1/2}\Omega^{1/2}_{X|\mathbf{Z}} \\ \Omega^{1/2}_{X|\mathbf{Z}}\Omega^{-1/2} & 1 \end{pmatrix} \right).$$

Compared to the joint distribution of (V_1, V_2), we see that the least squares estimator introduces extra variation to the first component of the bivariate normal distribution. We have also considered soft and hard thresholding estimators for μ_i. The consistency of these regularized estimators requires a minimum signal assumption which again rules out the case of weak confounding factors. To overcome the difficulty, we shall adopt a Bayesian viewpoint by assuming that μ_i's are generated from a common prior distribution. The Bayesian viewpoint allows us to borrow cross-sectional information (from different linear models) to estimate the number of false rejections without estimating individual μ_i's respectively.

3.2.3 Nonparametric empirical Bayes

In this subsection, we propose a nonparametric empirical Bayes approach to estimate the number of false rejections. Define

$$\hat{\mathbf{a}} = \frac{\Omega^{-1/2}\Gamma}{\sqrt{\Omega^{-1/2}\Gamma\Omega^{-1}_{\mathbf{Z}|X}\Gamma^\top\Omega^{-1/2}}}, \quad \hat{\boldsymbol{\xi}}_i = \sqrt{n}\hat{\boldsymbol{\beta}}_i/\sigma_i, \quad \boldsymbol{\xi}_i = \sqrt{n}\boldsymbol{\beta}_i/\sigma_i.$$

[1] A confounding factor is said to be weak if its coefficient $\boldsymbol{\beta}_i$ decays to zero at the rate $n^{-1/2}$ or faster. In this case, $\limsup_{n\to+\infty} |\mu_{i,n}| = \delta_i \in [0, +\infty)$.

Under (3.1) and conditional on $\mathbf{W} = (X, \mathbf{Z})$, we have the Gaussian location model,

$$\hat{\eta}_i = \eta_i + \epsilon_i \tag{3.4}$$

where $\hat{\eta}_i = \hat{\mathbf{a}}^\top \hat{\boldsymbol{\xi}}_i$ is an estimator for $\eta_i = \hat{\mathbf{a}}^\top \boldsymbol{\xi}_i$ and $\epsilon_i \overset{i.i.d.}{\sim} N(0,1)$.

Suppose $\boldsymbol{\xi}_i$'s are independently generated from some distribution, see Assumption 3.5. Under suitable assumptions detailed in Section 3.3, we can show $\hat{\mathbf{a}} \overset{a.s.}{\to} \mathbf{a}$ for $\mathbf{a}$ defined in (3.9). Denote by G_0 the (prior) distribution for $\mathbf{a}^\top \boldsymbol{\xi}_i$. The goal here is to estimate G_0 based on $\{\hat{\eta}_i\}$. It will become clear later that how the estimate of G_0 is useful in estimating the expected number of false rejections. Following Kiefer and Wolfowitz (1956) and Jiang and Zhang (2009), we consider the general maximum likelihood estimator (GMLE) $\widehat{G}_{m,n}$ for G_n defined as

$$\widehat{G}_{m,n} = \underset{G \in \mathcal{G}}{\operatorname{argmax}} \sum_{i=1}^{m} \log f_G(\hat{\eta}_i) \tag{3.5}$$

where $\mathcal{G}$ denotes the set of all probability distributions on $\mathbb{R}$ and $f_G(x) = \int \phi(x-u) dG(u)$ is the convolution between G and ϕ. As σ_i's are generally unknown in practice, however, $\widehat{G}_{m,n}$ is not obtainable. To obtain a feasible estimator, we consider the GMLE $\widetilde{G}_{m,n}$ defined as

$$\widetilde{G}_{m,n} = \underset{G \in \mathcal{G}}{\operatorname{argmax}} \sum_{i=1}^{m} \log f_G(\tilde{\eta}_i) \tag{3.6}$$

where $\tilde{\eta}_i = \hat{\mathbf{a}}^\top \tilde{\boldsymbol{\xi}}_i$ for $\tilde{\boldsymbol{\xi}}_i = \sqrt{n}\hat{\boldsymbol{\beta}}_i / \hat{\sigma}_i$. By the Carathéodory's theorem, there exist discrete solutions to (3.5) and (3.6) with no more than $m+1$ support points . Thus we can write the solutions as

$$\widehat{G}_{m,n}(u) = \sum_{j=1}^{m} \hat{\pi}_j \mathbf{1}\left\{\hat{s}_j \le u\right\}, \quad \widetilde{G}_{m,n}(u) = \sum_{j=1}^{m} \tilde{\pi}_j \mathbf{1}\left\{\tilde{s}_j \le u\right\}$$

where $\sum_{j=1}^{m} \hat{\pi}_j = \sum_{j=1}^{m} \tilde{\pi}_j = 1$ for $\hat{\pi}_j, \tilde{\pi}_j \ge 0$, $\{\hat{s}_1, \cdots, \hat{s}_m\}$ and $\{\tilde{s}_1, \cdots, \tilde{s}_m\}$ are two sets of support points for $\widehat{G}_{m,n}$ and $\widetilde{G}_{m,n}$, respectively. From the definition of $\widehat{G}_{m,n}$ and $f_{\widehat{G}_{m,n}}$, the support of $\widehat{G}_{m,n}(u)$ is always within the range of $\hat{\eta}_i$ due to the monotonicity of $\phi(x-u)$ in $|x-u|$. Similarly,

the support of $\widetilde{G}_{m,n}(u)$ is always within the range of $\tilde{\eta}_i$. These observations would be useful for our theoretical analysis, see Section B.3. It is also worth noting that the optimization in (3.6) can be cast as convex optimization problem that can be efficiently solved by modern interior point methods. The readers are referred to Koenker and Mizera (2014) for more detailed discussions.

3.2.4 Two-stage Benjamini-Hochberg procedure

Given the feasible estimator $\widetilde{G}_{m,n}$ of the prior distribution and in view of (3.3), we consider an approximate upper bound for $\text{FDP}(t_1, t_2)$ defined as

$$\widetilde{\text{FDP}}(t_1, t_2) := \frac{\sum_{i=1}^m \int L(Ax, t_1, t_2) d\widetilde{G}_{m,n}(x)}{\sum_{i=1}^m \mathbf{1}\left\{|Z_i^U| \geq t_1, |Z_i^A| \geq t_2\right\}} = \frac{m \int L(Ax, t_1, t_2) d\widetilde{G}_{m,n}(x)}{\sum_{i=1}^m \mathbf{1}\left\{|Z_i^U| \geq t_1, |Z_i^A| \geq t_2\right\}}.$$

For a desired FDR level $q \in (0, 1)$, we choose the optimal threshold such that

$$(T_1^*, T_2^*) = \underset{(t_1,t_2)\in\mathcal{F}_q}{\text{argmax}} \sum_{i=1}^m \mathbf{1}\left\{|Z_i^U| \geq t_1, |Z_i^A| \geq t_2\right\} \tag{3.7}$$

where $\mathcal{F}_q = \{(t_1, t_2) \in \mathbb{R}^+ \times \mathbb{R}^+ : \widetilde{\text{FDP}}(t_1, t_2) \leq q\}$ with $\mathbb{R}^+ = (0, +\infty)$. This procedure can be viewed as a variant of the Benjamini-Hochberg (BH) procedure adapted to the two-stage approach introduced in Section 3.2.1.

Remark 3.1. The rejection region we consider is of the form

$$\{(z^U, z^A) : |z^U| \geq t_1, |z^A| \geq t_2\}.$$

In particular, if $t_1 = 0$, it reduces to the usual rejection region $\{z^A : |z^A| \geq t_2\}$ from the one-stage approach based on the adjusted statistics. Therefore, our approach produces at least as many rejections as the one-stage approach as we are searching over a larger class of rejection regions to maximize the number of discoveries.

It is well known that when the number of signals is a substantial proportion of the total number of hypotheses, the BH procedure will be overly conservative. To adapt to the proportion of signals,

we develop a modification of John Storey's approach [Storey (2002)] in our setting. To illustrate the idea, we assume that Z_i^A approximately follows the mixture model:

$$\pi_{0i}N(0,1) + (1-\pi_{0i})N(\mu_i^A, 1)$$

where $\mu_i^A = \sqrt{n}\Omega_{X|\mathbf{Z}}^{1/2}\alpha_i/\sigma_i$ and π_{0i} denotes the probability that $\alpha_i = 0$.[2] Notice that

$$P(|Z_i^A| \le \lambda) = \pi_{0i}(1-2\Phi(-\lambda)) + (1-\pi_{0i})P(|N(\mu_i^A,1)| \le \lambda) \approx \pi_{0i}(1-2\Phi(-\lambda)),$$

provided that $P(|N(\mu_i^A,1)| \le \lambda) \approx 0$. Thus $\mathbf{1}\left\{|Z_i^A| \le \lambda\right\}/\{1-2\Phi(-\lambda)\}$ can be viewed as a conservative estimator for the mixing probability π_{0i}. We note

$$\begin{aligned}
\frac{1}{m}\sum_{i:\alpha_i=0} L(\mu_i, t_1, t_2) =& \frac{1}{m}\sum_{i=1}^m \mathbf{1}\{\alpha_i = 0\} L(\mu_i, t_1, t_2) \\
&\approx \int L(Ax, t_1, t_2) d\widetilde{G}_{m,n}(x) \frac{1}{m}\sum_{i=1}^m \pi_{0i} \\
&\le \int L(Ax, t_1, t_2) d\widetilde{G}_{m,n}(x) \frac{1}{m}\sum_{i=1}^m \frac{P(|Z_i^A| \le \lambda)}{1-2\Phi(-\lambda)} \\
&\approx \int L(Ax, t_1, t_2) d\widetilde{G}_{m,n}(x) \frac{1}{m}\sum_{i=1}^m \frac{\mathbf{1}\left\{|Z_i^A| \le \lambda\right\}}{1-2\Phi(-\lambda)}.
\end{aligned}$$

In view of the above derivation, we consider the FDR estimate given by

$$\widetilde{\mathrm{FDP}}_\lambda(t_1,t_2) = \frac{\int L(Ax,t_1,t_2) d\widetilde{G}_{m,n}(x) \sum_{i=1}^m \mathbf{1}\left\{|Z_i^A| \le \lambda\right\}}{(1-2\Phi(-\lambda)) \sum_{i=1}^m \mathbf{1}\left\{|Z_i^U| \ge t_1, |Z_i^A| \ge t_2\right\}},$$

where λ is a prespecified number as in John Storey's approach. With this modification, for a desired FDR level $q \in (0,1)$, we choose the optimal threshold such that

$$(\widetilde{T}_1^*, \widetilde{T}_2^*) = \underset{(t_1,t_2)\in\mathcal{F}_{q,\lambda}}{\mathrm{argmax}} \sum_{i=1}^m \mathbf{1}\left\{|Z_i^U| \ge t_1, |Z_i^A| \ge t_2\right\}, \tag{3.8}$$

[2]We emphasize that the validity of our procedure does not rely on the mixture model assumption which is merely used to motivate John Storey's procedure.

where

$$\mathcal{F}_{q,\lambda} := \left\{(t_1, t_2) \in \mathbb{R}^+ \times \mathbb{R}^+ : \widetilde{\text{FDP}}_\lambda(t_1, t_2) \leq q\right\}.$$

3.3 Asymptotic FDR control

The two-stage procedure is shown to provide asymptotic FDR control under suitable assumptions. Denote by m_0 and m_1 the number of null and alternative hypotheses among the m hypotheses respectively. Let $\breve{Z}_i^U$ and $\breve{Z}_i^A$ be the z-statistics by replacing $\hat{\sigma}_i$ with σ_i in Z_i^U and Z_i^A, respectively. Define $L_0(\mu, t_1, t_2) = \mathbb{P}(|\mu + \breve{V}_1| \geq t_1, |\breve{V}_2| \geq t_2|\mu)$ where

$$\begin{pmatrix} \breve{V}_1 \\ \breve{V}_2 \end{pmatrix} \sim N_2 \left(\begin{pmatrix} 0 \\ 0 \end{pmatrix}, \begin{pmatrix} 1 & \mathbb{E}[\Omega]^{-1/2} C_{X|\mathbf{Z}}^{1/2} \\ C_{X|\mathbf{Z}}^{1/2} \mathbb{E}[\Omega]^{-1/2} & 1 \end{pmatrix} \right)$$

with $C_{X|\mathbf{Z}} = \mathbb{E}[\Omega] - \mathbb{E}[\Gamma]\mathbb{E}[\Psi]^{-1}\mathbb{E}[\Gamma]^\top$ for $\Psi = \mathbf{Z}^\top\mathbf{Z}/n$. We also let $A_0^2 = \mathbb{E}[\Omega]^{-1/2}\mathbb{E}[\Gamma]C_{\mathbf{Z}|X}^{-1}\mathbb{E}[\Gamma]^\top\mathbb{E}[\Omega]^{-1/2}$ and

$$\mathbf{a}^\top = \frac{\mathbb{E}[\Omega]^{-1/2}\mathbb{E}[\Gamma]}{\sqrt{\mathbb{E}[\Omega]^{-1/2}\mathbb{E}[\Gamma]C_{\mathbf{Z}|X}^{-1}\mathbb{E}[\Gamma]^\top\mathbb{E}[\Omega]^{-1/2}}} \tag{3.9}$$

where $C_{\mathbf{Z}|X} = \mathbb{E}[\Psi] - \mathbb{E}[\Omega]^{-1}\mathbb{E}[\Gamma]^\top\mathbb{E}[\Gamma]$. We first introduce the following definitions and assumptions.

Definition 3.1. *A random variable $X \in \mathbb{R}$ is said to be sub-gaussian with the variance proxy σ^2 if $\mathbb{E}[X] = 0$ and its moment generating function satisfies*

$$\mathbb{E}[\exp(tX)] \leq \exp\left(\frac{\sigma^2 t^2}{2}\right) \quad \textit{for any } t \in \mathbb{R}.$$

Definition 3.2. *A random variable $X \in \mathbb{R}$ is said to be sub-exponential with the parameter θ if*

$\mathbb{E}[X] = 0$ *and its moment generating function satisfies*

$$\mathbb{E}[\exp(tX)] \leq \exp\left(\frac{\theta^2 t^2}{2}\right) \quad \textit{for any } |t| \leq \frac{1}{\theta}.$$

Assumption 3.1. *Suppose* $m_0/m \to \pi_0 \in (0,1)$.

Assumption 3.2. *Assume that*

$$\frac{\sum_{i:\alpha_i=0} \mathbf{1}\left\{|\breve{Z}_i^U| \geq t_1, |\breve{Z}_i^A| \geq t_2\right\}}{m_0} \xrightarrow{a.s.} K_0(t_1,t_2),$$
$$\frac{\sum_{i:\alpha_i\neq 0} \mathbf{1}\left\{|\breve{Z}_i^U| \geq t_1, |\breve{Z}_i^A| \geq t_2\right\}}{m_1} \xrightarrow{a.s.} K_1(t_1,t_2),$$

for every $(t_1,t_2) \in \mathbb{R}^+ \times \mathbb{R}^+$*, where*

$$K_0(t_1,t_2) = \mathbb{E}_{\mathbf{a}^\top \boldsymbol{\xi}}[L_0(A_0 \mathbf{a}^\top \boldsymbol{\xi}, t_1, t_2)] \ \textit{for} \ \mathbf{a}^\top \boldsymbol{\xi} \sim G_0 \tag{3.10}$$

and $K_0(t_1,t_2), K_1(t_1,t_2)$ *are both non-negative continuous functions of the arguments* (t_1,t_2).

Assumption 3.3. *Assume that*

$$\lambda_{\min}(C_{\mathbf{Z}|X}) > 0, \quad \lambda_{\min}(\mathbb{E}[\Psi]) > 0, \quad \mathbb{E}[X_1^2] > 0,$$
$$0 < \min_{1\leq i\leq m} \sigma_i \leq \max_{1\leq i\leq m} \sigma_i < \infty.$$

Assumption 3.4. *Assume that the components of* $\mathbf{Z}$ *and* X *are both sub-gaussian.*

Assumption 3.5. *Assume* $\{\boldsymbol{\xi}_i\}_{i=1}^d$ *is a sequence of i.i.d. continuous random vectors with the density* h *whose support set is given by* $\left\{x \in \mathbb{R}^d : \|x\|_{\max} \leq B(\log m)^b\right\}$ *for some* $B, b \geq 0$.

Assumption 3.6. *Assume* $m = m(n)$ *such that* $m(n) \to +\infty$ *as* $n \to +\infty$ *and* $\limsup_{n\to+\infty} \frac{m(n)}{n^{p_0}} < \infty$ *for some* $p_0 > 0$.

Assumption 3.1 requires the asymptotic null proportion to be strictly between zero and one. Assumption 3.2 allows certain forms of dependence, such as m-dependence, ergodic dependence

and certain mixing type dependence. Assumption 3.3 implies that $C_{\mathbf{Z}|X}^{-1}$ exists and the noise level is uniformly bounded from below and above. Assumption 3.4 allows us to use concentration inequalities for sub-gaussian and sub-exponential random variables. Assumption 3.5 implies that G_0 has a bounded support that expands slowly with m. From Assumption 3.6, the number of features m is some function of n and m is allowed to be polynomially larger than the sample size n.

Remark 3.2. *The assumption that $\boldsymbol{\xi}_i$ has a density is merely used to simplify the presentation of the proof of Lemma B.7. When $\boldsymbol{\xi}_i$ has a discrete distribution, the similar arguments in the proof of Lemma B.7 can be modified to obtain a similar result. We omit the details here to conserve the space.*

Before stating the main result, we introduce the following lemma which establishes the uniform convergence of $\int L(Ax, t_1, t_2) d\widetilde{G}_{m,n}(x)$.

Lemma 3.1. *Let $\widetilde{G}_{m,n}$ be the estimator of G_0 as defined in (3.6). Under Assumptions 3.3-3.6, for any $t_1', t_2' > 0$, we have*

$$\sup_{t_1 \le t_1', t_2 \le t_2'} \left| \int L(Ax, t_1, t_2) d\widetilde{G}_{m,n}(x) - \int L_0(A_0 x, t_1, t_2) dG_0(x) \right| \xrightarrow{a.s.} 0.$$

Let

$$V_m(t_1, t_2) = \sum_{i:\alpha_i = 0} \mathbf{1}\left\{ |Z_i^U| \ge t_1, |Z_i^A| \ge t_2 \right\}, \quad S_m(t_1, t_2) = \sum_{i:\alpha_i \ne 0} \mathbf{1}\left\{ |Z_i^U| \ge t_1, |Z_i^A| \ge t_2 \right\},$$
$$F_m(\lambda) = \frac{1}{m} \sum_{i=1}^{m} \mathbf{1}\left\{ |Z_i^A| \le \lambda \right\}, \quad F(\lambda) = \pi_0(1 - 2\Phi(-\lambda)) + (1 - \pi_0)(1 - K_1(0, \lambda)).$$

The following lemma shows the almost sure convergence as in Assumption 3.2 with $(\breve{Z}_i^U, \breve{Z}_i^A)$ replaced by (Z_i^U, Z_i^A).

Lemma 3.2. *Under Assumptions 3.2-3.3 and 3.6, we have*

$$\frac{1}{m_0}V_m(t_1,t_2) \overset{a.s.}{\to} K_0(t_1,t_2), \quad \frac{1}{m_1}S_m(t_1,t_2) \overset{a.s.}{\to} K_1(t_1,t_2), \quad F_m(\lambda) \overset{a.s.}{\to} F(\lambda).$$

Recall that

$$\widetilde{\text{FDP}}_\lambda(t_1,t_2) = \frac{\int L(Ax,t_1,t_2)d\widetilde{G}_{m,n}(x)\sum_{i=1}^m \mathbf{1}\left\{|Z_i^A| \le \lambda\right\}}{(1-2\Phi(-\lambda))\sum_{i=1}^m \mathbf{1}\left\{|Z_i^U| \ge t_1, |Z_i^A| \ge t_2\right\}}$$

and $(\widetilde{T}_1^*, \widetilde{T}_2^*)$ is the optimal threshold as defined in (3.8). By Lemmas 3.1-3.2, under Assumptions 3.1-3.2, it then follows that

$$\widetilde{\text{FDP}}_\lambda(t_1,t_2) \overset{a.s.}{\to} \text{FDP}_\lambda^\infty(t_1,t_2)$$

where

$$\text{FDP}_\lambda^\infty(t_1,t_2) := \frac{\mathbb{E}_{\boldsymbol{a}^\top\boldsymbol{\xi}}[L_0(A_0\boldsymbol{a}^\top\boldsymbol{\xi},t_1,t_2)]\left\{\pi_0(1-2\Phi(-\lambda)) + (1-\pi_0)(1-K_1(0,\lambda))\right\}}{(1-2\Phi(-\lambda))K(t_1,t_2)}$$

and $K(t_1,t_2) = \pi_0 K_0(t_1,t_2) + (1-\pi_0)K_1(t_1,t_2)$. We impose the following assumption to reduce the searching region for (t_1,t_2) to a rectangle of the form $[0,t_1^*] \times [0,t_2^*]$.

Assumption 3.7. *Assume that there exist t_1^* and t_2^* such that FDP$_\lambda^\infty(t_1^*,0) < q$, FDP$_\lambda^\infty(0,t_2^*) < q$ and $K(t_1^*,t_2^*) > 0$.*

Let

$$\widetilde{\text{FDR}}_m = \mathbb{E}\left[\frac{V_m(\widetilde{T}_1^*,\widetilde{T}_2^*)}{V_m(\widetilde{T}_1^*,\widetilde{T}_2^*) + S_m(\widetilde{T}_1^*,\widetilde{T}_2^*)}\right].$$

We show the asymptotic FDR control in the following theorem.

Theorem 3.1. *Under Assumptions 3.1-3.7, we have*

$$\limsup_m \widetilde{FDR}_m \le q.$$

3.4 Power analysis

In this section, we derive the asymptotic power of the two-stage John Storey procedure. Our derivation is heuristic but can be made rigorous under suitable assumptions. Define

$$(T_{1,\text{Two}}, T_{2,\text{Two}}) = \underset{(t_1,t_2)\in\mathcal{F}_{q,\text{Two}}}{\text{argmax}} \; K(t_1, t_2)$$

where

$$\mathcal{F}_{q,\text{Two}} = \left\{(t_1, t_2) \in \mathbb{R}^+ \times \mathbb{R}^+ : \text{FDP}^{\infty}_{\lambda}(t_1, t_2) \leq q\right\}.$$

Then, the asymptotic power of the two-stage procedure is given by

$$\text{Power}_{\text{Two}} = \lim_{m\to\infty} \frac{\sum_{i:\alpha_i\neq 0} \mathbf{1}\left\{|Z_i^U| \geq T_{1,\text{Two}}, |Z_i^A| \geq T_{2,\text{Two}}\right\}}{m_1} = K_1(T_{1,\text{Two}}, T_{2,\text{Two}}).$$

As a comparison the asymptotic power of the one-step procedure is equal to

$$\text{Power}_{\text{One}} = K_1(0, T_{2,\text{One}})$$

where $T_{2,\text{One}} = \text{argmax}_{t_2\in\mathcal{F}_{q,\text{One}}} K(t_1, t_2)$ with $\mathcal{F}_{q,\text{One}} = \{t_2 \in \mathbb{R}^+ : \text{FDP}^{\infty}_{\lambda}(0, t_2) \leq q\}$. Since $\mathcal{F}_{q,\text{One}} \subset \mathcal{F}_{q,\text{Two}}$, we have

$$K(T_{1,\text{Two}}, T_{2,\text{Two}}) \geq K(0, T_{2,\text{One}}),$$

that is, the two-stage procedure delivers more rejections.

Lemma 3.3. *Suppose $\text{FDP}^{\infty}_{\lambda}(t_1, t_2)$ is a continuous function of (t_1, t_2). Then, we have $\text{Power}_{\text{Two}} \geq \text{Power}_{\text{One}}$.*

Proof of Lemma 3.3. Let $M(\lambda) = (1 - 2\Phi(-\lambda))^{-1}(1 - \pi_0)(1 - K_1(0, \lambda))$. Since $\text{FDP}^{\infty}_{\lambda}(t_1, t_2)$

is a continuous function of (t_1, t_2), we must have

$$\begin{aligned} \frac{\pi_0 K_0(T_{1,\text{Two}}, T_{2,\text{Two}}) + M(\lambda) K_0(T_{1,\text{Two}}, T_{2,\text{Two}})}{K(T_{1,\text{Two}}, T_{2,\text{Two}})} &= q, \\ \frac{\pi_0 K_0(0, T_{2,\text{One}}) + M(\lambda) K_0(0, T_{2,\text{One}})}{K(0, T_{2,\text{One}})} &= q. \end{aligned} \tag{3.11}$$

The fact that $K(T_{1,\text{Two}}, T_{2,\text{Two}}) \geq K(0, T_{2,\text{One}})$ implies both $K_0(T_{1,\text{Two}}, T_{2,\text{Two}}) \geq K_0(0, T_{2,\text{One}})$ from (3.11) and

$$\begin{aligned} &(1-\pi_0) K_1(T_{1,\text{Two}}, T_{2,\text{Two}}) - M(\lambda) K_0(T_{1,\text{Two}}, T_{2,\text{Two}}) \\ =&(1-q) K(T_{1,\text{Two}}, T_{2,\text{Two}}) \\ \geq&(1-q) K(0, T_{2,\text{One}}) = (1-\pi_0) K_1(0, T_{2,\text{One}}) - M(\lambda) K_0(0, T_{2,\text{One}}) \end{aligned}$$

after rearranging the terms in (3.11). As $K_0(T_{1,\text{Two}}, T_{2,\text{Two}}) \geq K_0(0, T_{2,\text{One}})$, it follows that

$$\begin{aligned} (1-\pi_0) K_1(T_{1,\text{Two}}, T_{2,\text{Two}}) &\geq (1-\pi_0) K_1(0, T_{2,\text{One}}) + M(\lambda) \left\{ K_0(T_{1,\text{Two}}, T_{2,\text{Two}}) - K_0(0, T_{2,\text{One}}) \right\} \\ &\geq (1-\pi_0) K_1(0, T_{2,\text{One}}) \end{aligned}$$

which completes the proof. ♢

3.5 Numerical studies

3.5.1 Simulation

3.5.1.1 Simulation setup

We conduct extensive simulations to evaluate the finite-sample performance of the proposed method. As the numbers of hypotheses could range from thousands to millions in genome-scale multiple testing, we set $m = 10,000$ and $n = 100$. For demonstration purpose, we consider $X, \mathbf{Z} \in \mathbb{R}^{n \times 1}$ and generate the response Y_i's by (3.1) with $\sigma_i = 1$. To have a comprehensive study of the performance of the proposed method under different scenarios, we vary the following parameter configurations for simulations:

Config 1: The correlation between X and $\mathbf{Z}$ (denoted by Corr$(X, \mathbf{Z})$).

Config 2: The density and strength of the signals of interest ($\alpha_i \neq 0$).

Config 3: The density and strength of the confounding signals ($\boldsymbol{\beta}_i \neq 0$).

Config 4: The number of co-location of the signals of interest and confounding signals.

For Config 1, we induce the correlation between X and Z by simulating

$$X_0 \sim N_n(\mathbf{0}_n, \mathbf{I}_n), \;\; X|X_0 \sim N_n(\rho X_0, \mathbf{I}_n), \;\; Z|X_0 \sim N_n(\rho X_0, \mathbf{I}_n),$$

where $\rho = 0.5, 1.25$ and 2, which correspond to Corr$(X, Z) = 0.2, 0.6$ and 0.8 (denoted as "low", "medium" and "high" in Figures 3.3-3.9), respectively. For Config 2 and Config 3,

$$\alpha_i, \beta_i \sim \frac{\pi}{2}\text{Unif}(-l-r, -l) + \frac{\pi}{2}\text{Unif}(l, l+r) + (1-\pi)\delta(0),$$

where $\delta(0)$ denotes a point mass at 0. Here, we try three levels of signal density $\pi = 0.05, 0.01$ and 0.20 (denoted as "low", "medium" and "dense" in Figures 3.3-3.9) and three levels of signal strength $l = 0.2, 0.3$ and 0.4 (denoted as "weak", "moderate" and "strong" in Figures 3.3-3.9) with $r = 0.2$. For Config 4, we consider the following two cases:

1. No co-location: $\alpha_i \boldsymbol{\beta}_i = 0$ for all i.
2. 50% co-location: $|S_{\alpha\boldsymbol{\beta}}| = 0.5 \times \min\{|S_\alpha|, |S_{\boldsymbol{\beta}}|\}$ where

$$S_{\alpha\boldsymbol{\beta}} = \{i|\alpha_i\boldsymbol{\beta}_i \neq 0\}, \;\; S_\alpha = \{i|\alpha_i \neq 0\}, \;\; S_{\boldsymbol{\beta}} = \{i|\boldsymbol{\beta}_i \neq 0\}.$$

One assumption of our method is the independence of the errors across different features. Such assumption may be violated in some real applications. We thus study the robustness of our method to the violation of the independence assumption. Specifically, we investigated the robustness of the proposed method to correlated errors by considering

1. AR(1) correlation structure with $\text{Corr}(\epsilon_{ij}, \epsilon_{ik}) = 0.6^{|j-k|}$ where ϵ_{ij} and ϵ_{ik} denote the j-th and k-th element of $\epsilon_i = (\epsilon_{i1}, \ldots, \epsilon_{in})^\top$, respectively.

2. Block correlation structure of random errors where we simulate 100 blocks with within-block correlation 0.6.

Our proposed approach is denoted by "TwoStage-T" in Figures 3.3-3.9. For comparison, we also report the results of the following methods:

(i) OneStage-U: linear regression with the covariate of interest without adjustment of the confounder.

(ii) OneStage-A: linear regression with the covariate of interest adjusting the confounder; This is the traditional procedure.

(iii) TwoStage-N: a naive two-stage procedure, which first runs "OneStage-A", and if the confounder is not significant, "OneStage-U" is applied.

All the methods (i)-(iii) use the q-value approach by Storey (2002) for multiplicity control after the computation of feature-wise p-values. We evaluate the performance based on FDR control and power with a target FDR level of 5%. Results are averaged over 100 simulation runs. Both the means and their 95% CIs are reported in the bar plots.

3.5.1.2 Simulation results

Figure 3.3 shows the performance of the proposed method under varying signal density and signal strength of X with the different degrees of $\text{Corr}(X, \mathbf{Z})$. We first note that both OneStage-A and TwoStage-T control the FDR at the target level across the settings while OneStage-U and TwoStage-N show the inflated type I error rates which gets even higher as $\text{Corr}(X, \mathbf{Z})$ increases. Thus, we make a power comparison between TwoStage-T and OneStage-A in Panel B. Clearly, our proposed method has a substantial increase in power when the confounding is strong while the power is comparable when the confounding is weak. The power improvement is more striking

when the signal is weak or moderate. Thus, TwoStage-T could be particularly useful for real applications where it is challenging to identify weak signals among many potential confounders.

Figure 3.4 shows the effect of the density and strength of the confounding signal with $\pi = 0.1$ and the moderate strength for α_i. Our proposed approach provides FDR control at the target level across settings and has the same power advantage when the confounding is not weak. However, the power difference decreases as the confounding signal becomes denser. Such phenomenon seems to be natural since the traditional OneStage-A, which adjusts the confounder for every feature, would be effective when the confounder affects every feature. The strength of the confounding signal also reduces the power difference slightly, which could be explained by the increased statistical power of OneStage-A due to significant reduction of the error variance.

Figure 3.5 summarizes the result for Case 2 where the signal of interest and the signal from the confounder have co-locations. Our proposed approach still turns out to be more powerful than the traditional approach when the signal density of the confounder is low or the confounding is strong. However, as the density of the confounding signal gets denser, the power improvement decreases. Also, TwoStage-T is slightly less powerful than OneStage-A when the confounding is weak. Therefore, our method is more advantageous when the confounding signal is not dense and the confounding signal does not tend to co-locate with the signal of interest.

The simulation results of the block and AR(1) correlation structure are shown in Figures 3.6-3.7. Under both covariance structures, the proposed method controls the FDR around the target level and its power is comparable to that of the independent error case, indicating the robustness of our method.

As our proposed method provides asymptotic FDR control for a large number of features, it would be worth to see how its finite sample performance changes under a much smaller feature size than $m = 10,000$. The results with the feature sizes of 100 and 500 are shown in Figures 3.8-3.9. We note FDR is controlled at the target level with $m = 500$, but the FDR is slightly inflated with $m = 100$, especially when Corr$(X, \mathbf{Z})$ is high. Thus, a relatively large m needs to be set for our method for FDR control while a conservative target FDR level should be used for a small m.

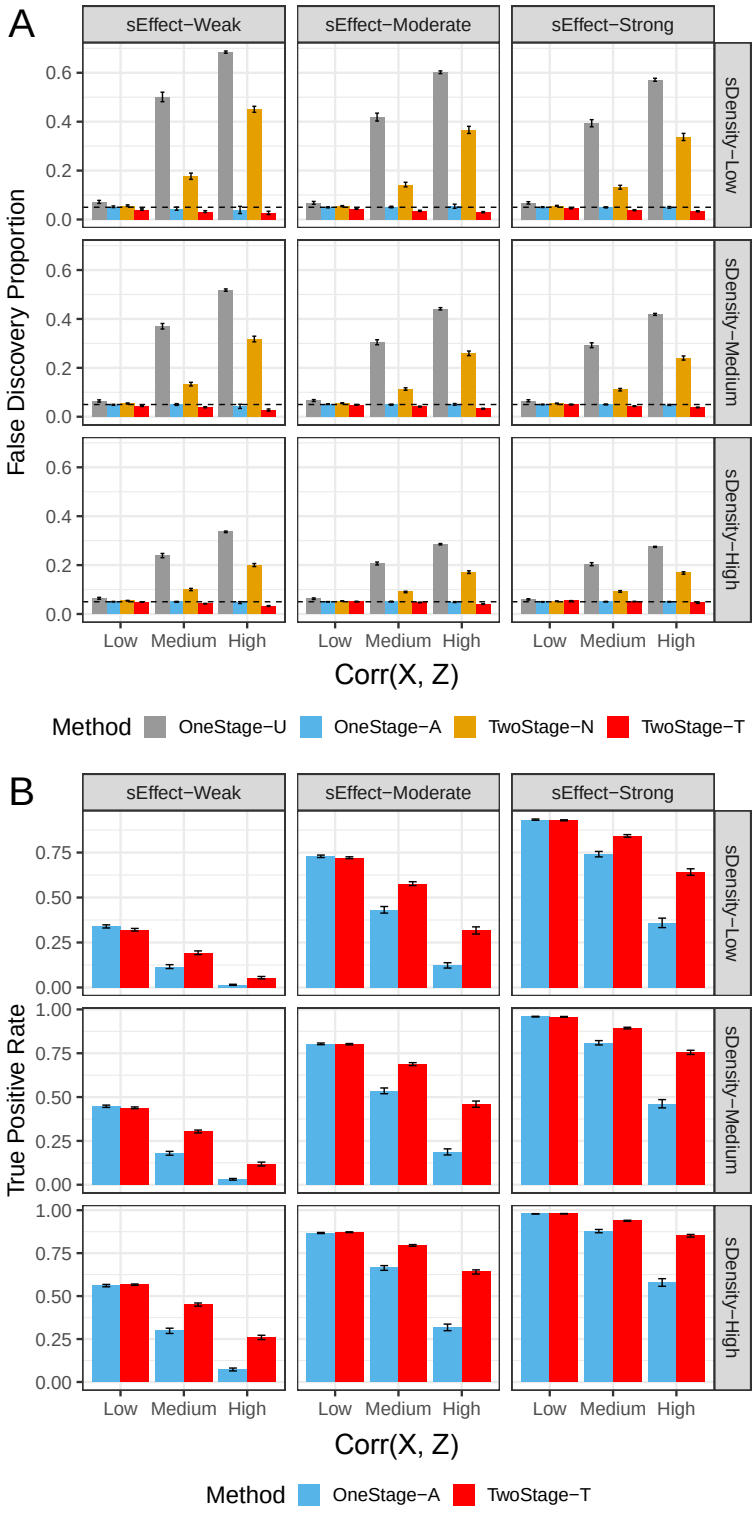

Figure 3.3: Performance comparison across different densities (sDensity) and strengths (sEffect) of the signal from the covariate of interest. The density of the confounding signal is 10% with a medium strength.

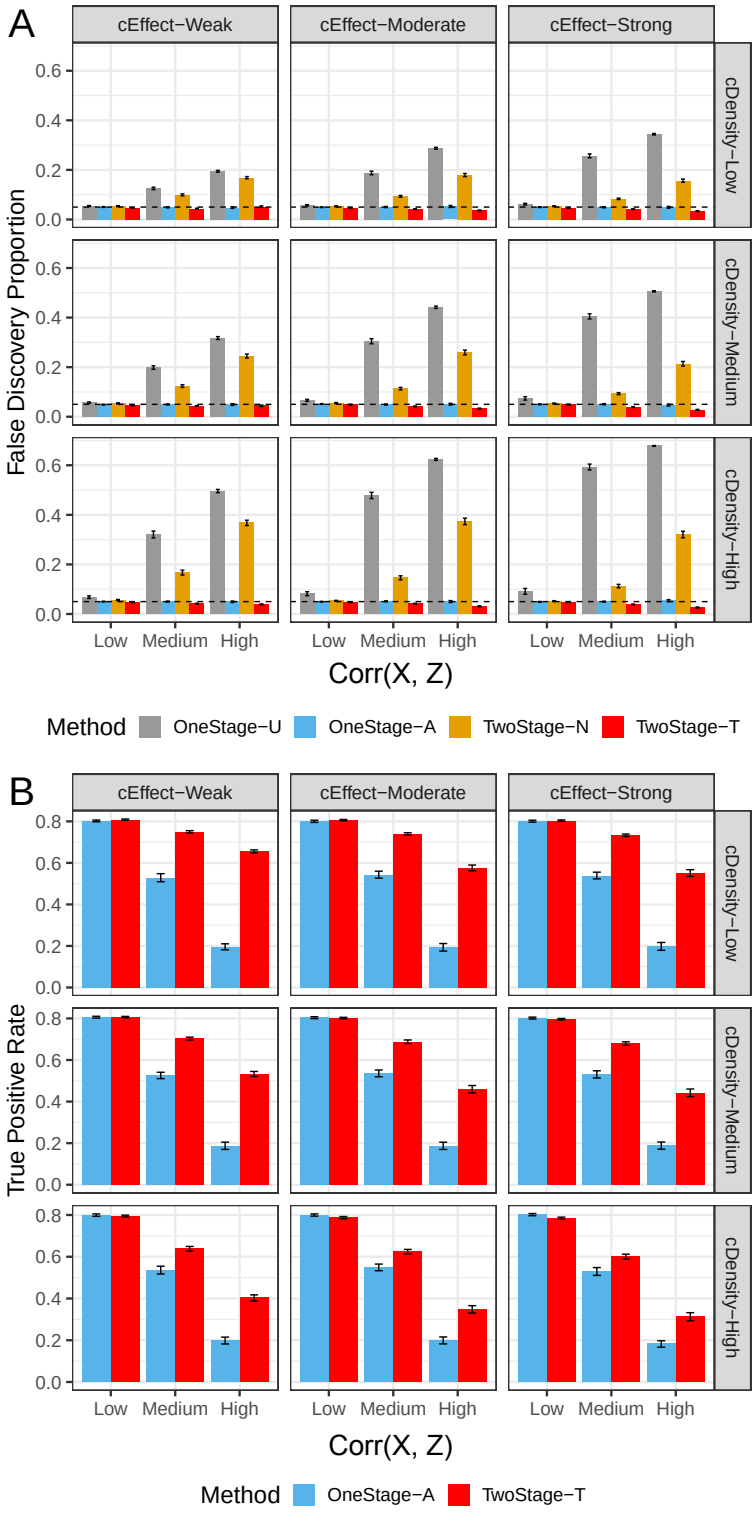

Figure 3.4: Performance comparison across different densities (cDensity) and strengths (cEffect) of the signal from the confounder. The density of the signal of interest is 10% with a medium strength.

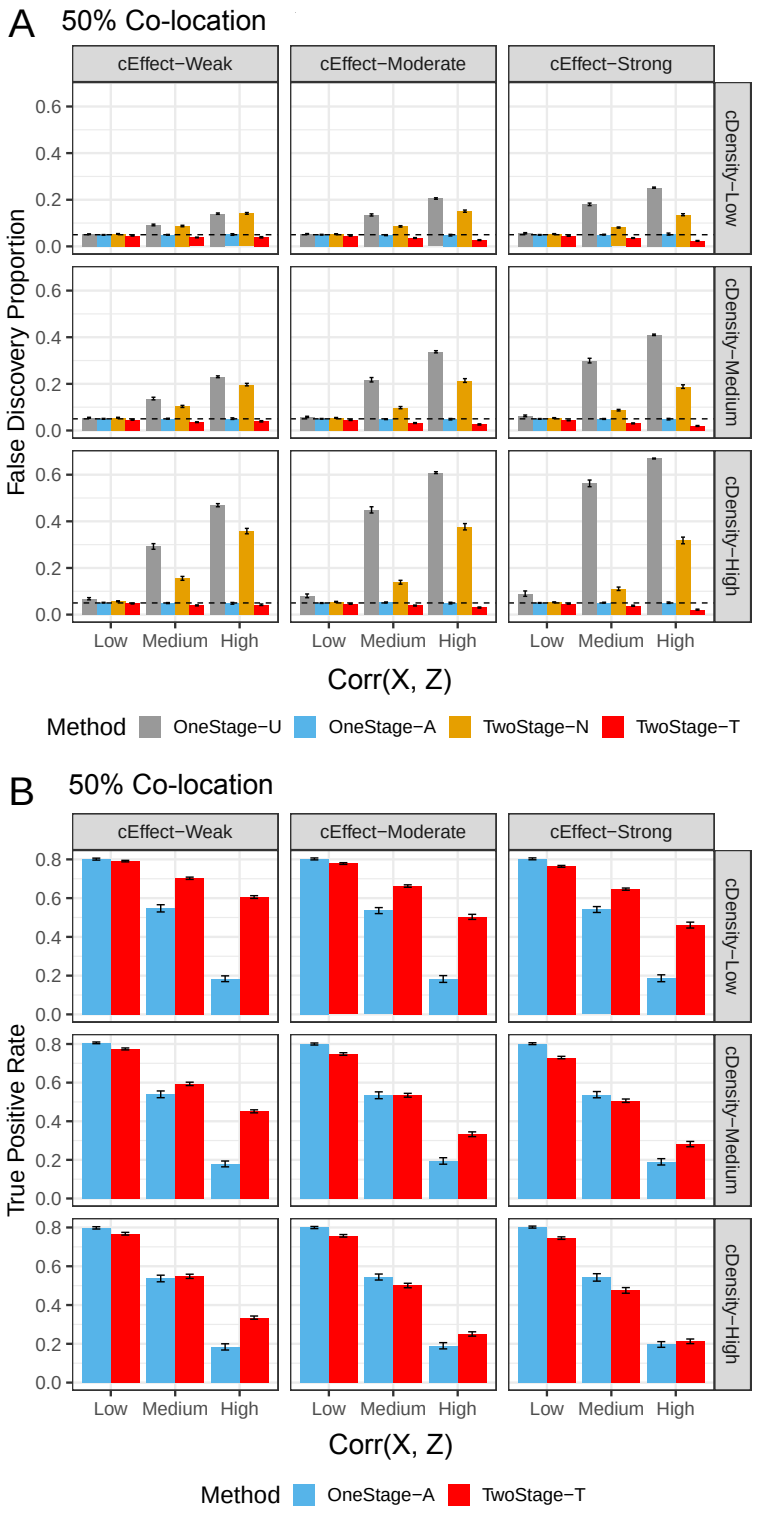

Figure 3.5: Performance comparison across different densities (cDensity) and strengths (cEffect) of the signal from the confounder when 50% of the confounding signal having co-locations with the signal of interest. The density of the signal of interest is 10% with a medium strength.

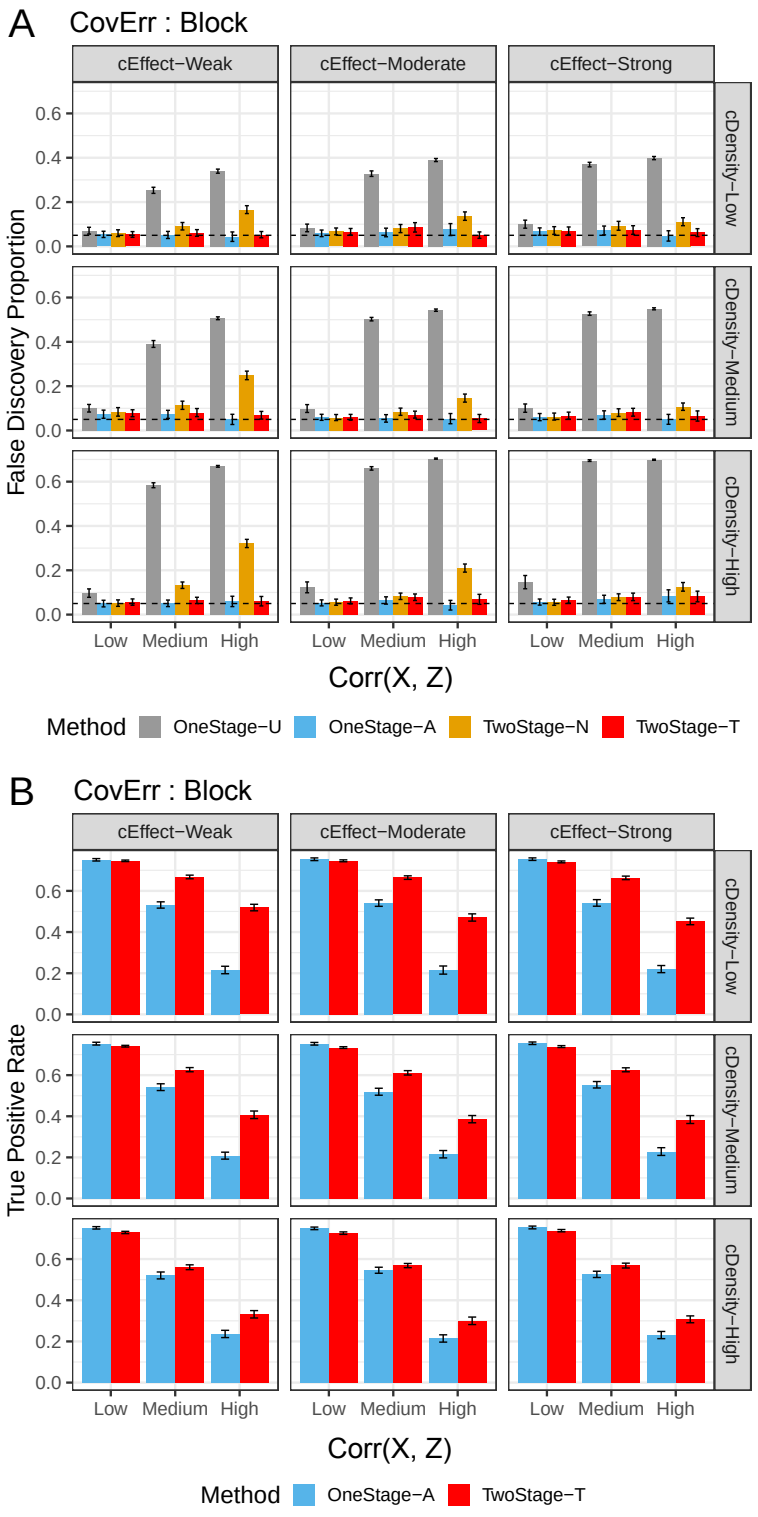

Figure 3.6: Performance comparison across different densities (cDensity) and strengths (cEffect) of the signal from the confounder when the errors from different features have a block correlation structure. The density of the signal of interest is 10% with a medium strength.

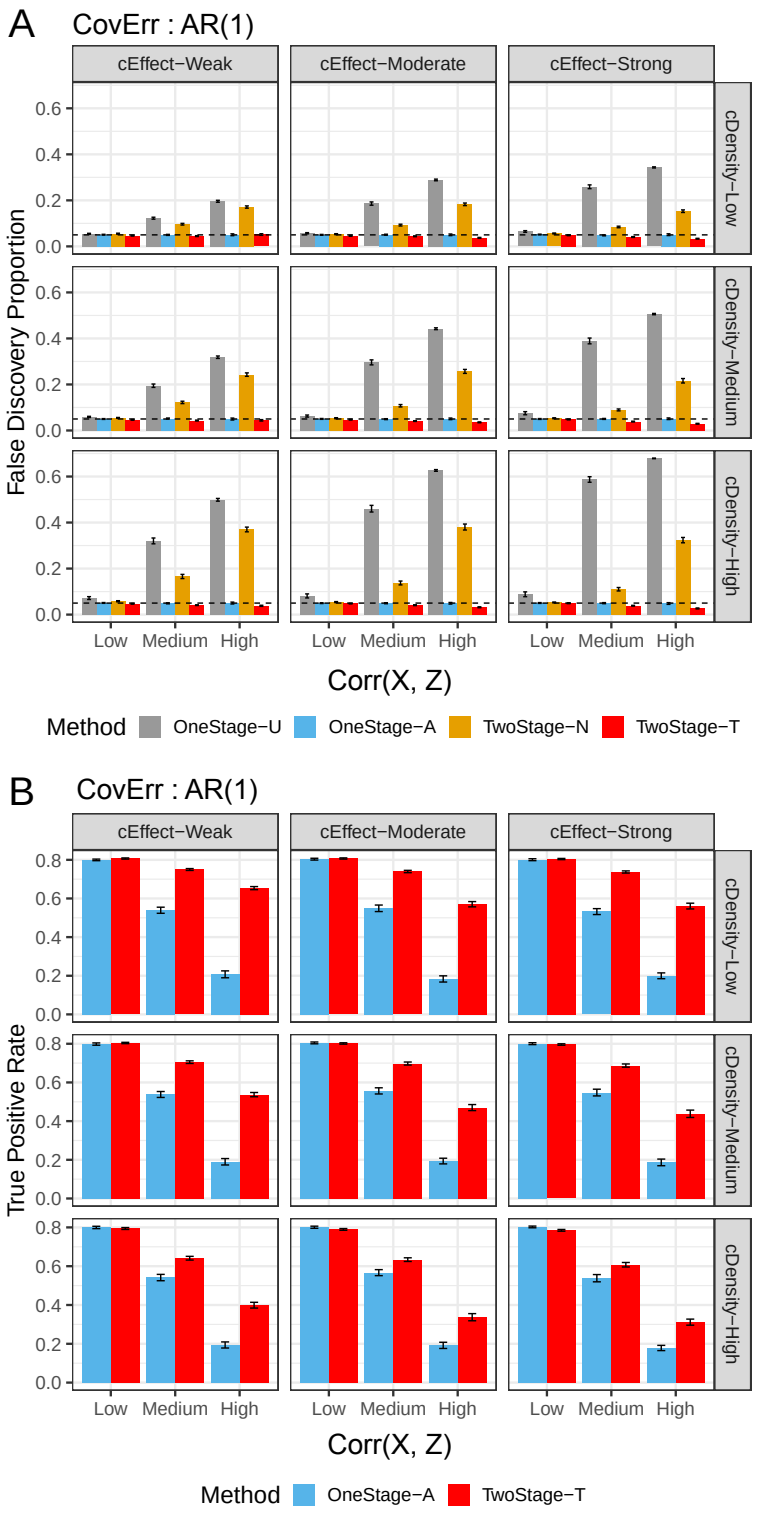

Figure 3.7: Performance comparison across different densities (cDensity) and strengths (cEffect) of the signal from the confounder when the errors from different features have an AR(1) correlation structure. The density of the signal of interest is 10% with a medium strength.

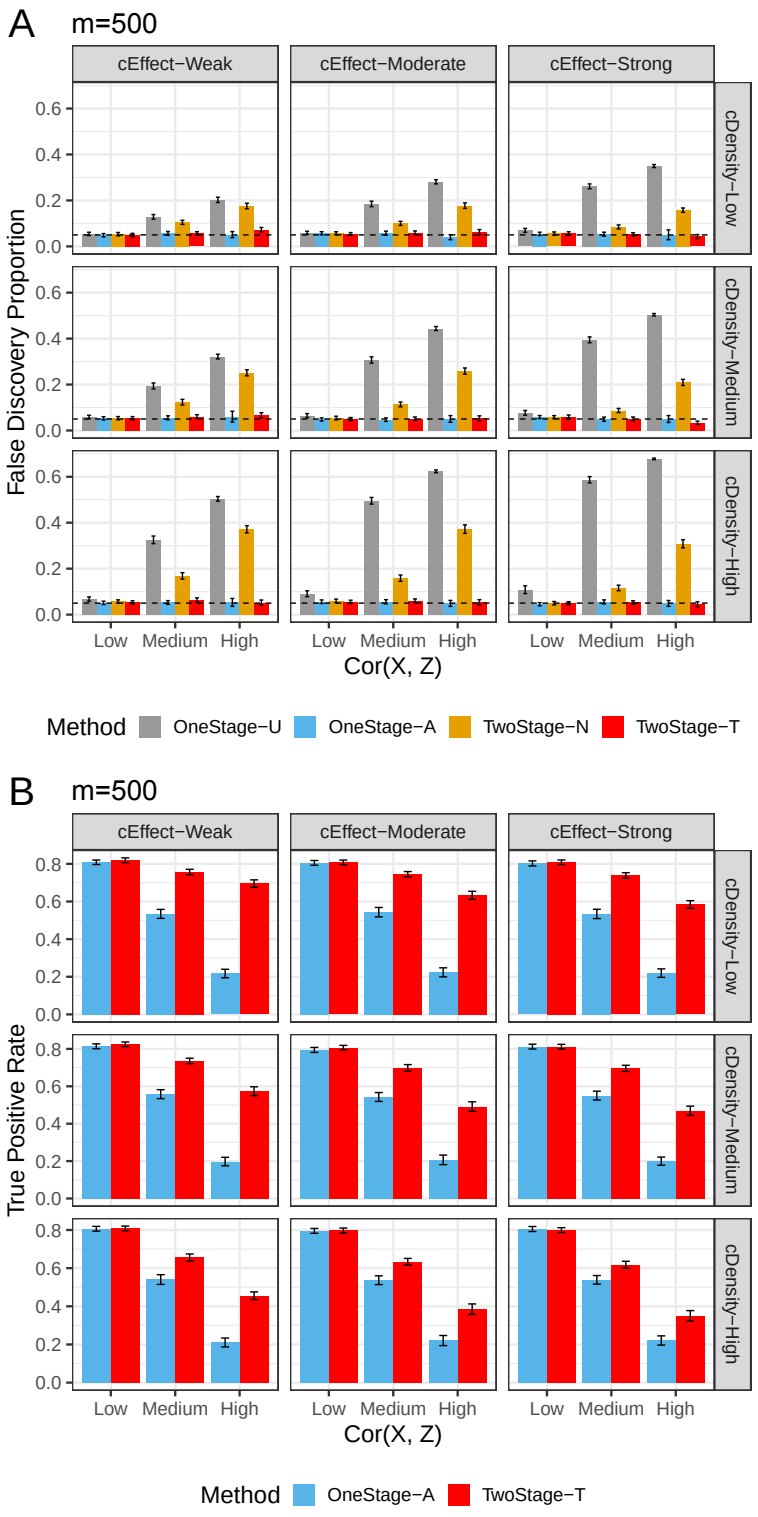

Figure 3.8: Performance comparison across different densities (cDensity) and strengths (cEffect) of the signal from the confounder at $m = 500$. The density of the signal of interest is 10% with a medium strength.

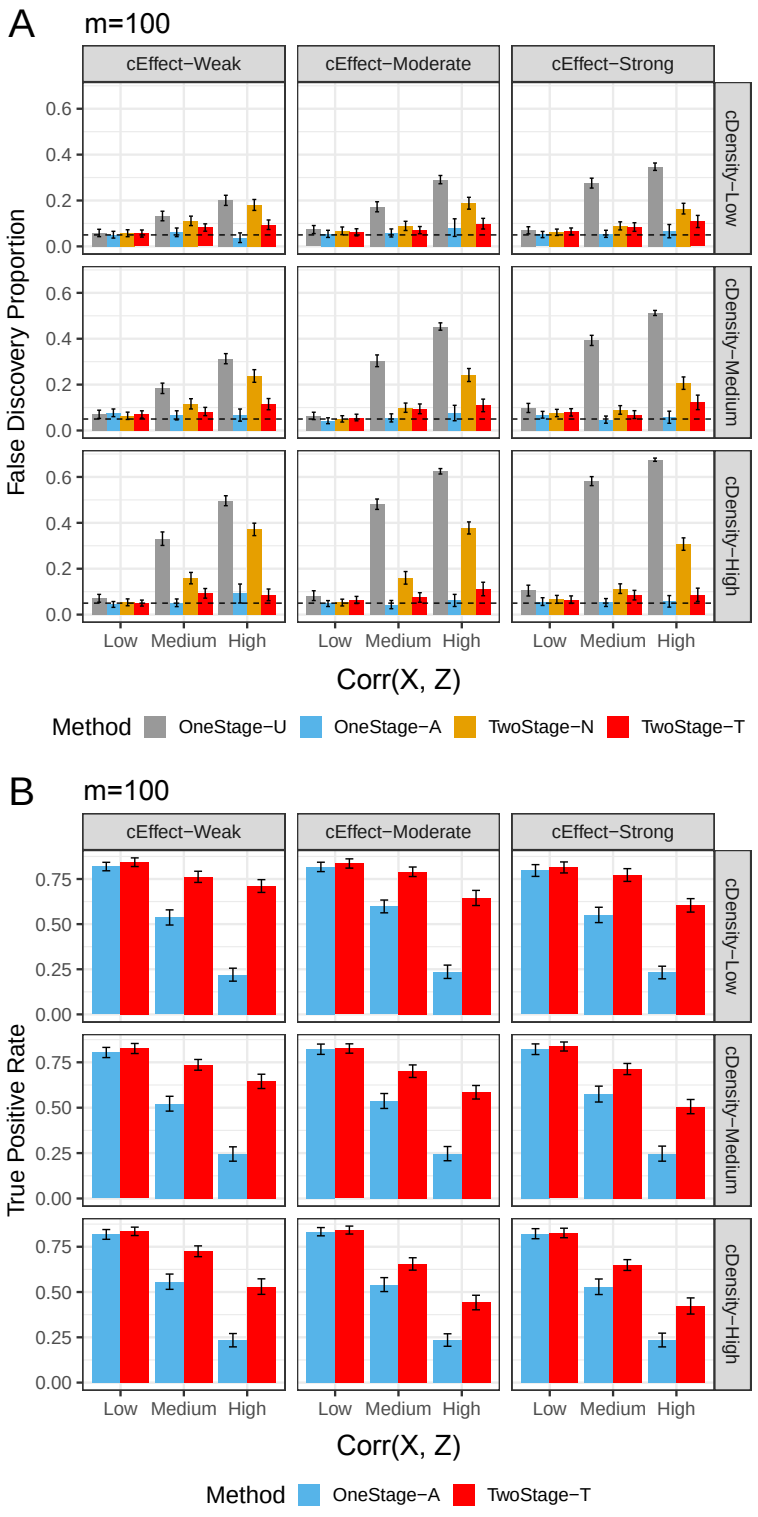

Figure 3.9: Performance comparison across different densities (cDensity) and strengths (cEffect) of the signal from the confounder at $m = 100$. The density of the signal of interest is 10% with a medium strength.

3.5.2 Real data analysis

3.5.2.1 Application to Metabolomics data

We apply OneStage-A and TwoStage-T in Section 3.5.1 to the real data in Metabolomics from the association studies of insulin resistance (IR) and serum metabolome. In this data set, IR is estimated by homeostatic model assessment (HOMA-IR) and serum metabolome profiles consist of 325 polar metabolites and 876 molecular lipids with $n = 289$. The details of the data can be found in Pedersen et al. (2016).

We fit the model (3.1) with HOMA-IR and each serum metabolome as X and Y_i, respectively. In addition, Body mass index (BMI) is included in the model as confounder $\mathbf{Z}$ because HOMA-IR is known to be largely influenced by BMI in epidemiological studies. Figure 3.10 shows that TwoStage-T discovers more metabolites/lipids significantly associated with HOMA-IR than OneStage-A does.

It is worth to explain the metabolites/lipids significantly associated with HOMA-IR in terms of Biology. Pedersen et al. (2016) introduces the notion of clusters to group a large number of serum metabolomes and biologically explains the data in view of clusters. In short, a set of polar metabolites (or that of molecular lipids) constitutes a cluster. Such cluster is referred as either IR-metabotype or insulin sensitivity (IS)-metabotype if it is positively or negatively correlated with HOMA-IR. For more details, see Pedersen et al. (2016).

Figure 3.11 implies that the number of discoveries by TwoStage-T is comparable to that by OneStage-A for IR-metabotype while TwoStage-T discovers 11 more serum metabolomes for IS-metabotype. We can briefly mention the biological insights for some illustrative discoveries by TwoStage-T.

1. IR-metabotype: Similar to the result by Pedersen et al. (2016), OneStage-A finds 4 amino acids in cluster labelled as M10. TwoStage-T not only successfully discovers those branched chain amino acids but also M_75_Hydrocinnamic acid. Importantly, hydrocinnamic acid is a known inhibitor of branched-chain α-keto acid dehydrogenase kinase, which regulates the

breakdown of branched chain amino acids by Tso et al. (2013).

2. IS-metabotype: According to Pedersen et al. (2016), IS-metabotype is solely made up with lipids, phospholipids and triacylglycerols with odd carbon number and high double bond content. TwoStage-T discovers 4 more phospholipids (L_175_PE(38:3), L_162_PE(34:0), L_300_PC(36:5), L_734_PC(30:0e)) than OneStage-A does. Interestingly, L_14_ sphingomyelin(d18:1/16:0) in cluster L14 and L_825_SM(d18:1/26:2) in cluster L20 are founded by TwoStage-T only.

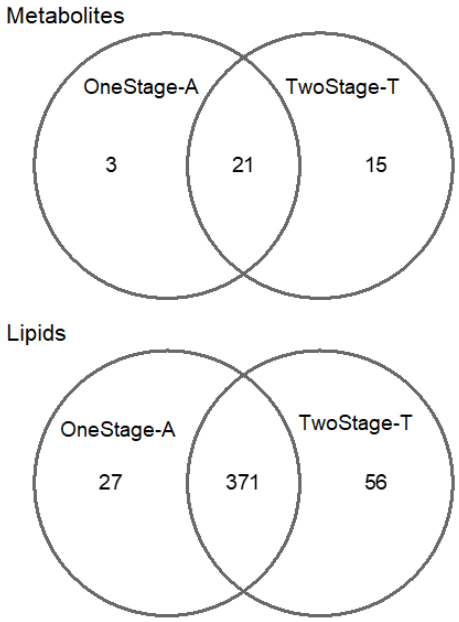

Figure 3.10: Venn diagrams of the number of polar metabolites and molecular lipids significantly associated with HOMA-IR by OneStage-A and TwoStage-T.

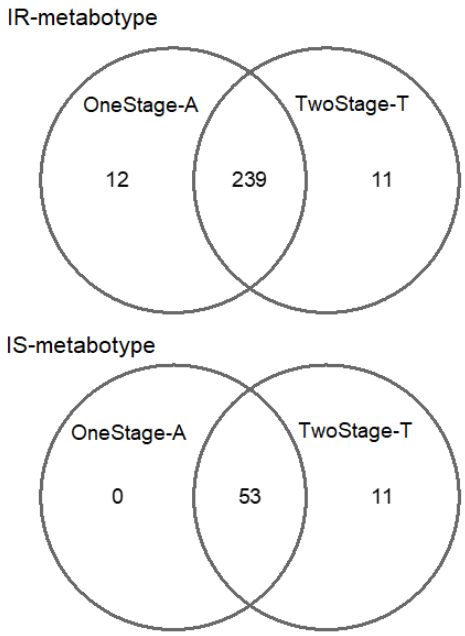

Figure 3.11: Venn diagrams of the number of polar metabolites and molecular lipids in either IR-metabotype or IS-metabotype that are significantly associated with HOMA-IR by OneStage-A and TwoStage-T.

3.5.2.2 Application to Methylation data

We also apply OneStage-A and TwoStage-T for the Methylation data in Huang et al. (2020). 54 EWAS datasets are summarized from 51 Gene Expression Omnibus (GEO) methylation datasets grouped by phenotype, tissue source and cell type. Each EWAS dataset is sequenced by Infinium Human Methylation 450K BeadChip platform and is preprocessed including data normalization, quality control for samples and quality control for probes. To capture the significant sources of variability, surrogate variable analysis is implemented by the packages `isva` and `SmartSVA` in Teschendorff et al. (2011) and Chen et al. (2017), respectively. As a measure for DNA methylation, we use M-values transformed from beta values. For more details about the data, see Huang et al. (2020).

54 EWAS data are independently analyzed each of which has its own phenotype such as disease status, smoke, etc. Specifically, for each EWAS data, we fit the model (3.1) with M-values as Y_i's,

the phenotype as X and the surrogate variables as $\mathbf{Z}$. In this context, the number of discoveries is often said to be the detected number of differentially methylated CpG positions (DMPs). Panel A in Figure 3.12 shows that $\log$ of the number of discoveries by OneStage-A and TwoStage-T. The median of detected DMPs by TwoStage-T is 55 while that by OneStage-A is 22.5. Thus, compared to OneStage-A, our proposed method provides more discoveries of genomic features.

We next conduct the down-sampling analysis with EWAS22 dataset with $n = 111$ and smoke as phenotype. The goal here is to see whether TwoStage-T finds more DMPs than OneStage-A does at a smaller sample size. We first define a list of "gold standard" fDMPs from the association p-values based on the full dataset by applying Bonferroni correction ($\alpha = 0.05$). We draw the stratified sub-sample from the full data with size 20, 40, 60, 80 and 100 as the phenotype is binary. Then, we compare the percentage of fDMPs detected by OneStage-A to that by TwoStage-T. Panel B in Figure 3.12 shows the result of down-sampling analysis with 100 independent replications. While the power gradually increases as the sub-sample size gets bigger for both methods, it is clear that our proposed method detects more fDMPs than OneStage-A at any sample sizes.

To examine whether the additional discoveries by TwoStage-T is by random or not, we perform validation analysis on the five age-associated EWAS datasets (EWAS26, EWAS27, EWAS30, EWAS39 and EWAS45). Given the exclusively identified DMPs (the phenotypes found to be not significant by TwoStage-T only) for each EWAS data, we compare the distributions of the association p-values corresponding to those discoveries in the other 4 EWAS datasets with the estimated density of the association p-values in each EWAS dataset. In Figure 3.13, the histograms in the first four columns show steep slopes while the density in the last column has relatively gentle slope for each age-associated EWAS dataset. This implies that the extra findings by TwoStage-T is not random. If those are randomly detected, the overall trend of histograms shall be similar to that of the corresponding density.

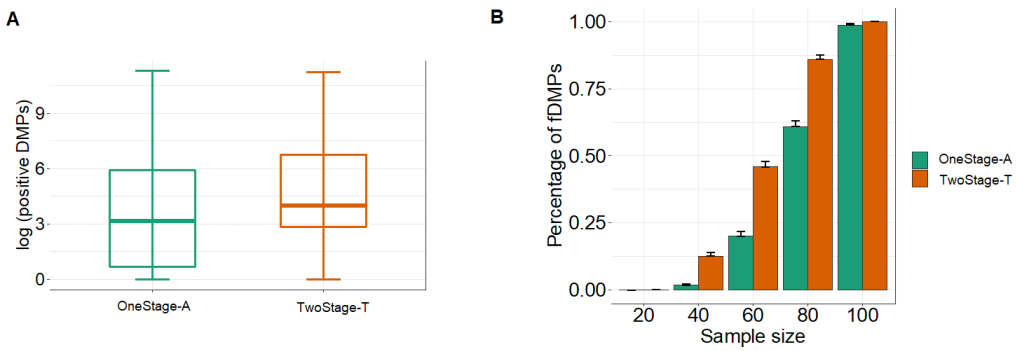

Figure 3.12: Figures for the application to Methylation data. Panel A shows boxplots of log of Positive DMPs for OneStage-A and TwoStage-T on the EWAS datasets. “Positive DMPs" simply denotes the number of DMPs plus a pseudo-count of 1 to avoid 0 in log. Panel B shows barplots of the proportion of fDMPs discovered by OneStage-A and TwoStage-T at sample size 20, 40, 60, 80 and 100. Error bar indicates the standard error of 100 iterations.

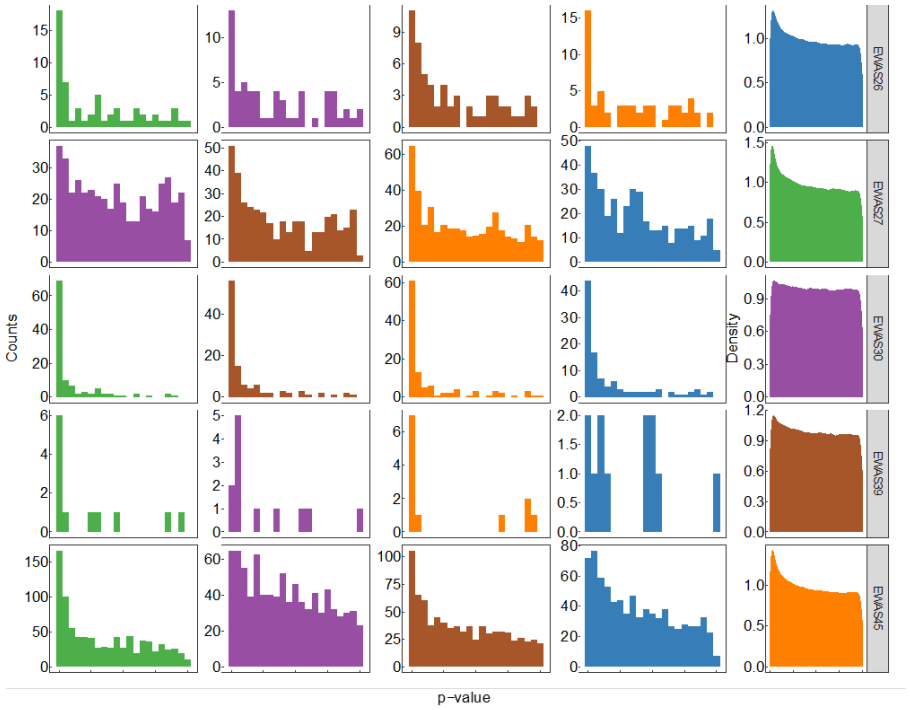

Figure 3.13: A set of figures for validation of the additional discoveries by TwoStage-T in age-associated EWAS datasets. The distributions of the association p-values corresponding to the additional discoveries by TwoStage-T are shown in the first 4 columns. The plots in the last column illustrate the density of the association p-values for each EWAS dataset. Each EWAS dataset is shown in one color.

4. SUMMARY AND CONCLUSIONS

In Chapter 2, we have proposed a new method to find the projection direction in the debiased Lasso estimator and demonstrated its advantage over the original debiased Lasso estimator in van de Geer et al. (2014) and the method in Javanmard and Montanari (2014). The main contributions of this work are summarized below.

- We propose a new formulation to estimate the projection direction by properly balancing the biases associated with the strong and weak signals respectively.
- We show that the set of strong signals can be consistently estimated and establish the asymptotic normality of the proposed estimator.
- We further propose a modified estimator which can lead to a smaller order of bias comparing to the original debiased Lasso both theoretically and empirically.
- We generalize our idea to conduct inference for a sparse linear combination of regression coefficients.

As for future research, we expect that our method can be extended to other settings such as the generalized linear models, the Cox proportional hazards model and nonparametric additive models.

In Chapter 3, a novel two-stage procedure is developed for high-dimensional association tests in genomics with the presence of confounding variables. The main contributions of this work can be summarized as follows.

- We propose a way of simultaneously selecting both cutoffs in the proposed method. Specifically, the thresholds are chosen to control the estimate for the FDR while maximizing the number of rejections.
- This estimate for the FDR is based on the nonparametric empirical Bayes approach to approximate the expected number of false rejections rather than directly estimating the nuisance parameters.

- We show that our estimate for the expected number of false rejections is consistent and the newly proposed method provides asymptotic FDR control.

For future research, it would be interesting to apply the idea of the two-step procedure to jointly analyze multiple p-values which are readily available these days from different studies.

REFERENCES

Barber, R. F. and Candès, E. J. (2015). Controlling the false discovery rate via knockoffs. *The Annals of Statistics, 43*(5), 2055-2085.

Barber, R. F. and Candès, E. J. (2019). A knockoff filter for high-dimensional selective inference. *The Annals of Statistics, 47*(5), 2504-2537.

Benjamini, Y. and Hochberg, Y. (1995). Controlling the false discovery rate: a practical and powerful approach to multiple testing. *Journal of the Royal statistical society: series B (Methodological), 57*(1), 289-300.

Belloni, A., Chernozhukov, V. and Hansen, C. (2014). Inference on treatment effects after selection among high-dimensional controls. *The Review of Economic Studies, 81*(2), 608-650.

Berk, R., Brown, L., Buja, A., Zhang, K. and Zhao, L. (2013). Valid post-selection inference. *The Annals of Statistics, 41*(2), 802-837.

Bühlmann, P. and van de Geer, S. (2011). *Statistics for high-dimensional data: methods, theory and applications*. Springer Science & Business Media.

Cai, T. T. and Guo, Z. (2017). Confidence intervals for high-dimensional linear regression: Minimax rates and adaptivity. *The Annals of Statistics, 45*(2), 615-646.

Candès, E., Fan, Y., Janson, L. and Lv, J. (2018). Panning for gold: 'model-X' knockoffs for high dimensional controlled variable selection. *Journal of the Royal Statistical Society: Series B (Statistical Methodology), 80*(3), 551-577.

Chang, J., Chen, S. X., Tang, C. Y. and Wu, T. T. (2019). High-dimensional empirical likelihood inference. *arXiv preprint arXiv:1805.10742*.

Chatterjee, A. and Lahiri, S. N. (2011). Bootstrapping lasso estimators. *Journal of the American Statistical Association, 106*(494), 608-625.

Chatterjee, A. and Lahiri, S. N. (2013). Rates of convergence of the adaptive LASSO estimators to the oracle distribution and higher order refinements by the bootstrap. *The Annals of Statistics, 41*(3), 1232-1259.

Chen, J., Behnam, E., Huang, J., Moffatt, M. F., Schaid, D. J., Liang, L. and Lin, X. (2017). Fast and robust adjustment of cell mixtures in epigenome-wide association studies with SmartSVA. *BMC genomics, 18*(1), 413.

Dezeure, R., Bühlmann, P. and Zhang, C.-H. (2017). High-dimensional simultaneous inference with the bootstrap. *Test, 26*(4), 685-719

Fahrmexr, L. (1990). Maximum likelihood estimation in misspecified generalized linear models. *Statistics, 21*(4), 487-502.

Hastie, T., Tibshirani, R. and Wainwright, M. (2015). *Statistical learning with sparsity: the lasso and generalizations*. CRC press.

Huang, J., Bai, L., Cui, B., Wu, L., Wang, L., An, Z., Ruan, S., Yu, Y., Zhang, X. and Chen, J. (2020). Leveraging biological and statistical covariates improves the detection power in epigenome-wide association testing. *Genome biology, 21*, 1-19

Javanmard, A. and Montanari, A. (2014). Confidence intervals and hypothesis testing for high-dimensional regression. *The Journal of Machine Learning Research, 15*(1), 2869-2909.

Javanmard, A. and Montanari, A. (2018). Debiasing the lasso: Optimal sample size for Gaussian designs. *The Annals of Statistics, 46*(6A), 2593-2622.

Jiang, W. and Zhang, C. H. (2009). General maximum likelihood empirical Bayes estimation of normal means. *The Annals of Statistics, 37*(4), 1647-1684

Kiefer, J. and Wolfowitz, J. (1956). Consistency of the maximum likelihood estimator in the presence of infinitely many incidental parameters. *The Annals of Mathematical Statistics*, 887-906.

Koenker, R. and Mizera, I. (2014). Convex optimization, shape constraints, compound decisions, and empirical Bayes rules. *Journal of the American Statistical Association, 109*(506), 674-685.

Laurent, B. and Massart, P. (2000). Adaptive estimation of a quadratic functional by model selection. *The Annals of Statistics, 28*(5), 1302-1338.

Lee, J. D., Sun, D. L., Sun, Y. and Taylor, J. E. (2016). Exact post-selection inference, with application to the lasso. *The Annals of Statistics, (44)*(3), 907-927.

Leek, J. T. and Storey, J. D. (2008). A general framework for multiple testing dependence. *Pro-*

ceedings of the National Academy of Sciences, 105(48), 18718-18723.

Liu, H. and Yu, B. (2013). Asymptotic properties of Lasso+mLS and Lasso+Ridge in sparse high-dimensional linear regression. *Electronic Journal of Statistics, 7*, 3124-3169.

Lockhart, R., Taylor, J., Tibshirani, R. and Tibshirani, R. (2014). A significance test for the lasso. *The Annals of Statistics, 42*(2), 413-468.

Meinshausen, N. and Bühlmann, P. (2006). High-dimensional graphs and variable selection with the lasso. *The Annals of Statistics, 34*(3), 1436-1462.

Meinshausen, N., Meier, L. and Bühlmann, P. (2009). P-values for high-dimensional regression. *Journal of the American Statistical Association, 104*(488), 1671-1681.

Meinshausen, N. and Bühlmann, P. (2010). Stability selection. *Journal of the Royal Statistical Society: Series B (Statistical Methodology), 72*(4), 417-473.

Neykov, M., Ning, Y., Liu, J. S. and Liu, H. (2018). A unified theory of confidence regions and testing for high-dimensional estimating equations. *Statistical Science, 33*(3), 427-443.

Ning, Y. and Liu, H. (2017). A general theory of hypothesis tests and confidence regions for sparse high dimensional models. *Annals of Statistics*, **45**, 158-195.

Pedersen, H. K., Gudmundsdottir, V., Nielsen, H. B., Hyotylainen, T., Nielsen, T., Jensen, B. A. H., Forslund, K., Hildebrand, F., Prifti, E., Falony, G., Chatelier, E. L., Levenez, F., Dorè, J., Mattila, I., Plichta, D. R., Pöhö, P., Hellgren, L. I., Arumugam, M., Sunagawa, S., ... and Pedersen, O. (2016). Human gut microbes impact host serum metabolome and insulin sensitivity. *Nature, 535*(7612), 376-381.

Price, A. L., Patterson, N. J., Plenge, R. M., Weinblatt, M. E., Shadick, N. A. and Reich, D. (2006). Principal components analysis corrects for stratification in genome-wide association studies. *Nature genetics, 38*(8), 904.

Reid, S., Tibshirani, R. and Friedman, J. (2016). A study of error variance estimation in lasso regression. *Statistica Sinica*, 35-67.

Rigollet, P. and Hütter, J. C. (2015). *High dimensional statistics.* Lecture notes for course 18S997, Massachusetts Institute of Technology. Available at `http://www-math.mit.`

edu/~rigollet/PDFs/RigNotes17.pdf.

Spearman, C. (1904). The proof and measurement of association between two things. *The American Journal of Psychology, 15*(1), 72-101.

Storey, J. D. (2002). A direct approach to false discovery rates. *Journal of the Royal Statistical Society: Series B (Statistical Methodology), 64*(3), 479-498.

Sun, Y., Zhang, N. R. and Owen, A. B. (2012). Multiple hypothesis testing adjusted for latent variables, with an application to the AGEMAP gene expression data. *The Annals of Applied Statistics, 6*(4), 1664-1688.

Teschendorff, A. E., Zhuang, J. and Widschwendter, M. (2011). Independent surrogate variable analysis to deconvolve confounding factors in large-scale microarray profiling studies. *Bioinformatics, 27*(11), 1496-1505.

Tibshirani, R. J., Taylor, J., Lockhart, R. and Tibshirani, R. (2016). Exact post-selection inference for sequential regression procedures. *Journal of the American Statistical Association, 111*(514), 600-620.

Tso, S. C., Qi, X., Gui, W. J., Chuang, J. L., Morlock, L. K., Wallace, A. L., Ahmed, K., Laxman, S., Campeau, P. M., Lee, B. H., Hutson, S. M., Tu, B. P., Williams, N. S., Tambar, U. K., Wynn, R. M. and Chuang D. T. (2013). Structure-based design and mechanisms of allosteric inhibitors for mitochondrial branched-chain α-ketoacid dehydrogenase kinase. *Proceedings of the National Academy of Sciences, 110*(24), 9728-9733.

van de Geer, S., Bühlmann, P., Ritov, Y. and Dezeure, R. (2014). On asymptotically optimal confidence regions and tests for high dimensional models. *The Annals of Statistics, 42*(3), 1166-1202.

Vershynin, R. (2010). Introduction to the non-asymptotic analysis of random matrices. *arXiv preprint arXiv:1011.3027.*

Vershynin, R. (2012). How close is the sample covariance matrix to the actual covariance matrix? *Journal of Theoretical Probability, 25*(3), 655-686.

Wang, J., Zhao, Q., Hastie, T. and Owen, A. B. (2017). Confounder adjustment in multiple hypothesis testing. *The Annals of Statistics, 45*(5), 1863-1894.

Wasserman, L. and Roeder, K. (2009). High dimensional variable selection. *The Annals of Statistics, 37*(5A), 2178-2201.

Zhang, C. H. (2009). Generalized maximum likelihood estimation of normal mixture densities. *Statistica Sinica*, 1297-1318.

Zhang, C. H. and Zhang, S. S. (2014). Confidence intervals for low-dimensional parameters with high-dimensional data. *Journal of the Royal Statistical Society: Series B (Statistical Methodology), 76*(1), 217-242.

Zhang, X. and Cheng, G. (2017). Simultaneous inference for high-dimensional linear models. *Journal of the American Statistical Association, 112*(518), 757-768.

Zhu, Y. and Bradic, J. (2018a). Significance testing in non-sparse high-dimensional linear models. *Electronic Journal of Statistics, 12*(2), 3312-3364.

Zhu, Y. and Bradic, J. (2018b). Linear hypothesis testing in dense high-dimensional linear models. *Journal of the American Statistical Association, 113*(524), 1583-1600.

APPENDIX A

SUPPLEMENTARY MATERIAL TO CHAPTER 2

A.1 Technical Details

A.1.1 Concentration Inequalities

We first define several quantities which will appear throughout the supplementary material. Let $\theta_j = X_j - \mathbf{X}_{-j} b_{-j}$ and

$$b_{-j} = \underset{\tilde{b} \in \mathbb{R}^{p-1}}{\operatorname{argmin}} E||X_j - \mathbf{X}_{-j}\tilde{b}||_2^2 = \mathbf{\Sigma}^{-1}_{-j,-j}\mathbf{\Sigma}_{-j,j}.$$

Define $\kappa_1 = 2\kappa^2$, $\kappa_{2j} = 2\kappa^2\sqrt{\Lambda^{-1}_{\min}\mathbf{\Sigma}_{j,j}}$ and $\kappa_{3j} = 2\kappa^2\Lambda^{-1}_{\min}\mathbf{\Sigma}_{j,j}$.

The following lemmas shows the concentration inequalities for sub-exponential and sub-gaussian random variables which are motivated by Lemmas 5.5, 5.15 and Propositions 5.10, 5.16 in Vershynin (2010).

Lemma A.1. *Let $X_1, \cdots, X_N$ be i.i.d. mean-zero sub-exponential random variables with $\|X_i\|_{\psi_1} = K_1$. Then, for every $a = (a_1, \cdots, a_N)^\top \in \mathbb{R}^{N\times 1}$ and any $t \geq 0$, we have*

$$\mathbb{P}\left(\left|\sum_{i=1}^N a_i X_i\right| \geq t\right) \leq 2\exp\left\{-\min\left(\frac{t^2}{8e^2\|a\|^2K_1^2}, \frac{t}{4eK_1\|a\|_\infty}\right)\right\}.$$

Proof of Lemma A.1. We first derive an upper bound of the moment generating function of X_i. By expanding the exponential function in the Taylor series, we have

$$\begin{aligned} E[\exp(\lambda X_i)] &= E\left[1 + \lambda X_i + \sum_{p=2}^\infty \frac{(\lambda X_i)^p}{p!}\right] = 1 + \sum_{p=2}^\infty \frac{\lambda^p E[X_i^p]}{p!} \\ &\leq 1 + \sum_{p=2}^\infty \frac{\lambda^p (K_1 p)^p}{(p/e)^p} = 1 + \sum_{p=2}^\infty (e\lambda K_1)^p = 1 + \frac{(e\lambda K_1)^2}{1 - (e\lambda K_1)} \end{aligned}$$

provided that $|e\lambda K_1| < 1$. The inequality follows by the definition of sub-exponential norm

$$E[X_i^p] \leq (K_1 p)^p$$

and Stirling's approximation $p! \geq (p/e)^p$. In addition, if $|e\lambda K_1| < 0.5$, the quantity on the right hand side can be bounded above by

$$1 + 2(e\lambda K_1)^2 \leq \exp(2(e\lambda K_1)^2).$$

Thus, combining all of the above implies

$$E[\exp(\lambda X_i)] \leq \exp(2(e\lambda K_1)^2) \quad \text{for} \quad |\lambda| < \frac{1}{2eK_1}. \tag{A.1}$$

Next, for $\lambda > 0$, we have

$$\begin{aligned}\mathbb{P}\left(\sum_{i=1}^N a_i X_i \geq t\right) &= \mathbb{P}\left(\exp\left(\lambda \sum_{i=1}^N a_i X_i\right) \geq \exp(\lambda t)\right) \\ &\leq \exp(-\lambda t) E\left[\exp\left(\lambda \sum_{i=1}^N a_i X_i\right)\right] = \exp(-\lambda t) \prod_{i=1}^N E[\exp(\lambda a_i X_i)]\end{aligned}$$

by the exponential Markov inequality for $\sum_{i=1}^N a_i X_i$. If λ is small enough so that $|\lambda| < (2eK_1\|a\|_\infty)^{-1}$, (A.1) gives

$$\mathbb{P}\left(\sum_{i=1}^N a_i X_i \geq t\right) \leq \exp(-\lambda t) \prod_{i=1}^N \exp(2(e\lambda a_i K_1)^2) = \exp(-\lambda t + 2e^2\lambda^2\|a\|^2 K_1^2).$$

By choosing $\lambda = \min\left(t(4e^2\|a\|^2 K_1^2)^{-1}, (2eK_1\|a\|_\infty)^{-1}\right)$, we obtain

$$\mathbb{P}\left(\sum_{i=1}^N a_i X_i \geq t\right) \leq \exp\left\{-\min\left(\frac{t^2}{8e^2\|a\|^2 K_1^2}, \frac{t}{4eK_1\|a\|_\infty}\right)\right\}.$$

The second term in $\min$ can be obtained as follows. When $\lambda = (2eK_1\|a\|_\infty)^{-1}$, we have

$$-\lambda t + 2e^2\lambda^2\|a\|^2K_1^2 = -\frac{t}{2eK_1\|a\|_\infty} + \frac{\|a\|^2}{2\|a\|_\infty^2} \leq -\frac{t}{4eK_1\|a\|_\infty}$$

where the last inequality follows as

$$\lambda = \frac{1}{2eK_1\|a\|_\infty} \leq \frac{t}{(4e^2\|a\|^2K_1^2)}$$

which implies

$$\frac{\|a\|^2}{\|a\|_\infty} \leq \frac{t}{2eK_1}.$$

By repeating the same argument for $-X_i$, we get the same bound for $\mathbb{P}(-\sum_{i=1}^N a_iX_i \geq t)$, which completes the proof. ♢

Lemma A.2. *Let $X_1, \cdots, X_N$ be i.i.d. mean-zero sub-gaussian random variables with $\|X_i\|_{\psi_2} = K_2$. Then, we have the following results.*

1. *For any $|\omega_1| \leq 1$,*

$$E\left[\exp\left(\omega_1^2\frac{X_i^2}{4eK_2^2}\right)\right] \leq \exp(\omega_1^2). \tag{A.2}$$

2. *For $\omega_2 \in \mathbb{R}$,*

$$E[\exp(\omega_2X_i)] \leq \exp(8eK_2^2\omega_2^2). \tag{A.3}$$

3. *For every $a = (a_1, \cdots, a_N) \in \mathbb{R}^N$ and any $t \geq 0$,*

$$\mathbb{P}\left(\left|\sum_{i=1}^N a_iX_i\right| \geq t\right) \leq 2\exp\left(-\frac{t^2}{32eK_2^2\|a\|^2}\right). \tag{A.4}$$

Proof of Lemma A.2. Let $Y_i = X_i/(2\sqrt{e}K_2)$. We note that, for $|\omega_1^2/2| < 1$,

$$\begin{aligned} E[\exp(\omega_1^2 Y_i^2)] &= 1 + \sum_{k=1}^{\infty} \frac{\omega_1^{2k} E[Y_i^{2k}]}{k!} \\ &\leq 1 + \sum_{k=1}^{\infty} \frac{1}{(4e)^k} \frac{(2\omega_1^2 k)^k}{(k/e)^k} = \sum_{k=0}^{\infty} \left(\frac{\omega_1^2}{2}\right)^k = \left(1 - \frac{\omega_1^2}{2}\right)^{-1} \end{aligned}$$

by the Taylor series expansion of the exponential function and Stirling's approximation. We can further bound

$$E[\exp(\omega_1^2 Y_i^2)] \leq \exp(\omega_1^2) \quad \text{for} \quad |\omega_1| \leq 1$$

by using the inequality $(1-x)^{-1} \leq \exp(2x)$ for $0 \leq x \leq 0.5$, which completes (A.2).

For (A.3), we notice that

$$E[\exp(\omega Y_i)] \leq E[\omega Y_i + \exp(\omega^2 Y_i^2)] \leq \exp(\omega^2) \tag{A.5}$$

for $|\omega| \leq 1$ where the first inequality follows by $e^x \leq x + e^{x^2}$ for any $x \in \mathbb{R}$ and the second one does by (A.2). If $|\omega| \geq 1$, we have

$$E[\exp(\omega Y_i)] \leq \exp(\omega^2) E[\exp(Y_i^2)] \leq \exp(\omega^2 + 1) \leq \exp(2\omega^2) \tag{A.6}$$

due to $\omega Y_i \leq \omega^2 + Y_i^2$ for any ω, Y_i and (A.2). Thus, combining (A.5) with (A.6) gives

$$E[\exp(\omega Y_i)] \leq \exp(2\omega^2).$$

for any $\omega \in \mathbb{R}$. Letting $\omega_2 = \omega/(2\sqrt{e}K_2)$ completes (A.3).

For (A.4), notice that

$$E\left[\exp(\omega_2 \sum_{i=1}^{N} a_i X_i)\right] = \prod_{i=1}^{N} E\left[\exp(\omega_2 a_i X_i)\right]$$
$$\leq \prod_{i=1}^{N} \exp(8eK_2^2\omega_2^2 a_i^2) = \exp(8eK_2^2\omega_2^2\|a\|^2).$$

For $\omega_2 \geq 0$, we have

$$\mathbb{P}\left(\sum_{i=1}^{N} a_i X_i \geq t\right) = \mathbb{P}\left(\exp\left(\omega_2 \sum_{i=1}^{N} a_i X_i\right) \geq \exp(\omega_2 t)\right)$$
$$\leq \exp(-\omega_2 t) E\left[\exp\left(\omega_2 \sum_{i=1}^{N} a_i X_i\right)\right]$$
$$\leq \exp(-\omega_2 t + 8e\omega_2^2 K_2^2\|a\|^2)$$
$$\leq \exp\left(-\frac{t^2}{32eK_2^2\|a\|^2}\right)$$

and the same bound can be obtained for $\mathbb{P}\left(-\sum_{i=1}^{N} a_i X_i \geq t\right)$. Thus, combining those bounds gives (A.4). ♢

A.1.2 Technical details in Section 2.3

Lemma A.3. *Under Assumption 2.5,*

$$\mathbb{P}\left(n^{-1}\|\theta_j^\top \mathbf{X}_{-j}\|_\infty \geq \varepsilon_{0j}\sqrt{\frac{\log p}{n}}\right) \leq 2\exp\left\{\left(1 - \frac{1}{8e^2}\frac{\varepsilon_{0j}^2}{(\kappa_{0j})^2}\right)\log p\right\}$$

for $0 < \varepsilon_{0j} \leq \kappa_{0j}\sqrt{n(\log p)^{-1}}$.

Proof of Lemma A.3. Let $Z = (Z_1 \cdots Z_{p-1}) = n^{-1}(X_j^\top \mathbf{X}_{-j} - b_{-j}^\top \mathbf{X}_{-j}{}^\top \mathbf{X}_{-j})$. Then we have

$$Z = \frac{1}{n}\sum_{i=1}^{n}(X_{i,j} - b_{-j}^\top X_{i,-j})X_{i,-j}^\top$$

where $X_{i,j}$ is the value of the jth predictor of the ith observation and

$$X_{i,-j}^\top = (X_{i,1} \cdots X_{i,j-1}, X_{i,j+1} \cdots X_{i,p}).$$

Fix some $k \in \{1, 2, \ldots, p\} \setminus \{j\}$ and let $Z_{i,j}^{(k)} = (X_{i,j} - b_{-j}^\top X_{i,-j}) X_{i,-j}^{(k)}$, where $X_{i,-j}^{(k)}$ denotes the kth element of $X_{i,-j}$. Then $Z_k = n^{-1} \sum_{i=1}^n Z_{ij}^{(k)}$, where $E[Z_{i,j}^{(k)}] = 0$ and $Z_{i,j}^{(k)}$'s are independent across $1 \le i \le n$.

We derive an upper bound for $\|Z_{i,j}^{(k)}\|_{\psi_1}$. Notice that

$$\begin{aligned}
\|Z_{i,j}^{(k)}\|_{\psi_1} = \|(X_{i,j} - b_{-j}^\top X_{i,-j}) X_{i,-j}^{(k)}\|_{\psi_1} &\le 2\|X_{i,j} - b_{-j}^\top X_{i,-j}\|_{\psi_2} \|X_{i,-j}^{(k)}\|_{\psi_2} \\
&= 2\|X_{i,\cdot}^\top \gamma_{-j}\|_{\psi_2} \|X_{i,-j}^{(k)}\|_{\psi_2} \\
&\le 2\kappa^2 \|\gamma_{-j}\|_2 \\
&\le 2(1 + \sqrt{\Lambda_{\min}^{-1} \mathbf{\Sigma}_{j,j}})\kappa^2,
\end{aligned}$$

where $X_{i,\cdot}^\top = (X_{i,j}, X_{i,-j}^\top)$ and $\gamma_{-j}^\top = (1, -b_{-j}^\top)$. Here, the first inequality holds from the fact that $\|XY\|_{\psi_1} \le 2\|X\|_{\psi_2}\|Y\|_{\psi_2}$ for any two random variables X, Y; the second inequality comes from

$$q^{-1/2}(E|X_{i,\cdot}^\top \gamma_{-j}|^q)^{1/q} = \|\gamma_{-j}\| q^{-1/2} \{E|X_{i,\cdot}^\top (\gamma_{-j}/\|\gamma_{-j}\|)|^q\}^{1/q} \le \|\gamma_{-j}\|\kappa$$

and the third inequality follows from

$$\|\gamma_{-j}\|_2 = \sqrt{1 + \|b_{-j}\|^2} \le 1 + \|b_{-j}\| \le 1 + \sqrt{\lambda_{\max}(\mathbf{\Sigma}_{-j,-j}^{-1}) \mathbf{\Sigma}_{j,j}}.$$

By Lemma A.1, for any $\varepsilon > 0$, we have

$$\mathbb{P}\left(\frac{1}{n} \left| \sum_{i=1}^n Z_{i,j}^{(k)} \right| \ge \varepsilon \right) \le 2 \exp\left\{ -n \min\left(\frac{1}{8e^2} \left(\frac{\varepsilon}{\kappa_{0j}} \right)^2, \frac{1}{4e} \frac{\varepsilon}{\kappa_{0j}} \right) \right\}.$$

Choosing $\varepsilon = \varepsilon_{0j}\sqrt{n^{-1}\log p}$ and assuming that $n \geq \varepsilon_{0j}^2(\kappa_{0j})^{-2}\log p$, then

$$\mathbb{P}\left(\frac{1}{n}\left|\sum_{i=1}^{n} Z_{i,j}^{(k)}\right| \geq \varepsilon_{0j}\sqrt{\frac{\log p}{n}}\right) \leq 2\exp\left\{-\frac{1}{8e^2}\frac{\varepsilon_{0j}^2}{(\kappa_{0j})^2}\log p\right\}.$$

The result follows from the union bound over $k \in \{1, 2, \ldots, p-1\}$. ♢

An implication of Lemma A.3 is that

$$n^{-1}\|\theta_j^\top \mathbf{X}_{-j}\|_\infty \leq \varepsilon_{0j}\sqrt{\frac{\log p}{n}} \tag{A.7}$$

with probability tending to 1 for a fixed ε_{0j} such that $\varepsilon_0^2 > (\kappa_{0j})^2 8e^2$. We introduce an additional result below for a later use.

Lemma A.4. *Under Assumption 2.5, we have*

$$\begin{aligned}\mathbb{P}\left(\left|\frac{n}{\theta_j^\top X_j} - \frac{1}{\mathbf{\Sigma}_{j\backslash -j}}\right| \leq \varepsilon_{1j}\right) \geq 1 &- 2\exp\left\{-\frac{1}{8e^2}\left(\frac{\mathbf{\Sigma}_{j\backslash -j}^2\varepsilon_{1j}}{4\kappa_1}\right)^2 n\right\} \\ &- 2\exp\left\{-\frac{1}{8e^2}\left(\frac{\mathbf{\Sigma}_{j\backslash -j}^2\varepsilon_{1j}}{4\kappa_{2j}}\right)^2 n\right\}\end{aligned}$$

for $0 < \varepsilon_{1j} \leq \min\{(\mathbf{\Sigma}_{j\backslash -j})^{-1}, 4\min(\kappa_1, \kappa_{2j})(\mathbf{\Sigma}_{j\backslash -j})^{-2}\}$ *and*

$$\begin{aligned}\mathbb{P}\left(\left|\frac{\|\theta_j\|^2}{n} - \mathbf{\Sigma}_{j\backslash -j}\right| \leq \varepsilon_{2j}\right) \geq 1 &- 2\exp\left\{-\frac{1}{8e^2}\left(\frac{\varepsilon_{2j}}{3\kappa_1}\right)^2 n\right\} - 2\exp\left\{-\frac{1}{8e^2}\left(\frac{\varepsilon_{2j}}{6\kappa_{2j}}\right)^2 n\right\} \\ &- 2\exp\left\{-\frac{1}{8e^2}\left(\frac{\varepsilon_{2j}}{3\kappa_{3j}}\right)^2 n\right\}\end{aligned}$$

for $0 < \varepsilon_{2j} \leq 3\min(\kappa_1, 2\kappa_{2j}, \kappa_{3j})$.

Proof of Lemma A.4. We notice that

$$\theta_j^\top X_j = X_j^\top X_j - \sum_{i=1}^{n}\sum_{k=1}^{p-1} b_{-j,k} X_{i,-j}^{(k)} X_{i,j},$$

where $b_{-j,k}$ is the kth element of b_{-j} and $X_{i,-j}^{(k)}$ is the kth element of $\mathbf{X}_{-j}$. Then, we see that

$$\frac{\theta_j^\top X_j}{n} - \mathbf{\Sigma}_{j\backslash -j} = \frac{1}{n}\sum_{i=1}^{n}(X_{i,j}^2 - \mathbf{\Sigma}_{j,j}) - \frac{1}{n}\sum_{i=1}^{n}\left(\sum_{k=1}^{p-1} b_{-j,k}X_{i,-j}^{(k)}X_{i,j} - \mathbf{\Sigma}_{j,-j}\mathbf{\Sigma}_{-j,-j}^{-1}\mathbf{\Sigma}_{-j,j}\right).$$

By Lemma A.1,

$$\mathbb{P}\left(\left|\frac{1}{n}\sum_{i=1}^{n}(X_{i,j}^2 - \mathbf{\Sigma}_{j,j})\right| \le \delta_j\right) \ge 1 - 2\exp\left\{-\frac{1}{8e^2}\left(\frac{\delta_j}{\kappa_1}\right)^2 n\right\}$$
$$\mathbb{P}\left(\left|\frac{1}{n}\sum_{i=1}^{n}\left(\sum_{k=1}^{p-1} b_{-j,k}X_{i,-j}^{(k)}X_{i,j} - \mathbf{\Sigma}_{j,-j}\mathbf{\Sigma}_{-j,-j}^{-1}\mathbf{\Sigma}_{-j,j}\right)\right| \le \delta_j\right) \ge 1 - 2\exp\left\{-\frac{1}{8e^2}\left(\frac{\delta_j}{\kappa_{2j}}\right)^2 n\right\}$$

for $0 < \delta_j \le \min(\kappa_1, \kappa_{2j})$. Also, for $\varepsilon_{1j} \le (\mathbf{\Sigma}_{j\backslash -j})^{-1}$, we have

$$\begin{aligned}
&\left\{\left|\frac{n}{\theta_j^\top X_j} - \frac{1}{\mathbf{\Sigma}_{j\backslash -j}}\right| \ge \varepsilon_{1j}\right\} \\
\subset &\left[\left\{\left|\frac{1}{n}\sum_{i=1}^{n}(X_{i,j}^2 - \mathbf{\Sigma}_{j,j})\right| \ge \frac{\mathbf{\Sigma}_{j\backslash -j}^2}{4}\varepsilon_{1j}\right\}\right. \\
&\left.\bigcup\left\{\left|\frac{1}{n}\sum_{i=1}^{n}\left(\sum_{k=1}^{p-1} b_{-j,k}X_{i,-j}^{(k)}X_{i,j} - \mathbf{\Sigma}_{j,-j}\mathbf{\Sigma}_{-j,-j}^{-1}\mathbf{\Sigma}_{-j,j}\right)\right| \ge \frac{\mathbf{\Sigma}_{j\backslash -j}^2}{4}\varepsilon_{1j}\right\}\right].
\end{aligned}$$

Thus, for $\varepsilon_{1j} \le \min\{(\mathbf{\Sigma}_{j\backslash -j})^{-1}, 4\min(\kappa_1, \kappa_{2j})(\mathbf{\Sigma}_{j\backslash -j})^{-2}\}$, we have

$$\begin{aligned}
\mathbb{P}\left(\left|\frac{n}{\theta_j^\top X_j} - \frac{1}{\mathbf{\Sigma}_{j\backslash -j}}\right| \le \varepsilon_{1j}\right) \ge\ & 1 - 2\exp\left\{-\frac{1}{8e^2}\left(\frac{\mathbf{\Sigma}_{j\backslash -j}^2\varepsilon_{1j}}{4\kappa_1}\right)^2 n\right\} \\
& - 2\exp\left\{-\frac{1}{8e^2}\left(\frac{\mathbf{\Sigma}_{j\backslash -j}^2\varepsilon_{1j}}{4\kappa_{2j}}\right)^2 n\right\}
\end{aligned}$$

which proves the first inequality. Next, we note that

$$\frac{\|\theta_j\|^2}{n} - \mathbf{\Sigma}_{j\backslash -j} = \underbrace{\left(\frac{X_j^\top X_j}{n} - \mathbf{\Sigma}_{j,j}\right)}_{(*)} - 2\underbrace{\left(\frac{X_j^\top \mathbf{X}_{-j}}{n} - \mathbf{\Sigma}_{j,-j}\right)\mathbf{\Sigma}_{-j,-j}^{-1}\mathbf{\Sigma}_{-j,j}}_{(**)} + \underbrace{\mathbf{\Sigma}_{j,-j}\mathbf{\Sigma}_{-j,-j}^{-1}\left(\frac{\mathbf{X}_{-j}{}^\top \mathbf{X}_{-j}}{n} - \mathbf{\Sigma}_{-j,-j}\right)\mathbf{\Sigma}_{-j,-j}^{-1}\mathbf{\Sigma}_{-j,j}}_{(***)}.$$

The concentration inequalities for $(*)$ and $(**)$ are given respectively as

$$\mathbb{P}\left(\left|\frac{1}{n}\sum_{i=1}^{n}(X_{i,j}^2 - \mathbf{\Sigma}_{j,j})\right| \leq \frac{\varepsilon_{2j}}{3}\right) \geq 1 - 2\exp\left\{-\frac{1}{8e^2}\left(\frac{\varepsilon_{2j}}{3\kappa_1}\right)^2 n\right\}, \tag{A.8}$$

and

$$\begin{aligned}&\mathbb{P}\left(\left|\frac{1}{n}\sum_{i=1}^{n}\left(\sum_{k=1}^{p-1} b_{-j,k}X_{i,-j}^{(k)}X_{i,j} - \mathbf{\Sigma}_{j,-j}\mathbf{\Sigma}_{-j,-j}^{-1}\mathbf{\Sigma}_{-j,j}\right)\right| \leq \frac{\varepsilon_{2j}}{6}\right)\\ \geq& 1 - 2\exp\left\{-\frac{1}{8e^2}\left(\frac{\varepsilon_{2j}}{6\kappa_{2j}}\right)^2 n\right\},\end{aligned} \tag{A.9}$$

for $0 < \varepsilon_{2j} \leq \min(3\kappa_1, 6\kappa_{2j})$. Also, we notice that

$$(***) = \frac{1}{n}\sum_{i=1}^{n}\left(\sum_{k=1}^{p-1} X_{i,-j}^{(k)} b_{-j,k}\right)^2 - \mathbf{\Sigma}_{j,-j}\mathbf{\Sigma}_{-j,-j}^{-1}\mathbf{\Sigma}_{-j,j}.$$

Lemma A.1 gives us

$$\begin{aligned}&\mathbb{P}\left(\left|\frac{1}{n}\sum_{i=1}^{n}\left(\left(\sum_{k=1}^{p-1} X_{i,-j}^{(k)} b_{-j,k}\right)^2 - \mathbf{\Sigma}_{j,-j}\mathbf{\Sigma}_{-j,-j}^{-1}\mathbf{\Sigma}_{-j,j}\right)\right| \leq \frac{\varepsilon_{2j}}{3}\right)\\ \geq& 1 - 2\exp\left\{-\frac{1}{8e^2}\left(\frac{\varepsilon_{2j}}{3\kappa_{3j}}\right)^2 n\right\}\end{aligned} \tag{A.10}$$

for $0 < \varepsilon_{2j} \leq 3\kappa_{3j}$. Combining (A.8), (A.9) and (A.10) finishes the proof. $\diamondsuit$

The following result directly follows by Lemmas A.3 and A.4.

Corollary A.1. *Let* $\breve{v}_j = n\theta_j/(\theta_j^\top X_j)$ *and* $\breve{u}_j = n^{-1}\|\breve{v}_j^\top \mathbf{X}_{-j}\|_\infty$. *Under Assumption 2.5,* $\breve{v}_j$ *satisfies* $\breve{v}_j^\top X_j = n$,

$$\begin{aligned}
&\mathbb{P}\left(n^{-1}\|\breve{v}_j\|^2 \le \left(\frac{1}{\boldsymbol{\Sigma}_{j\backslash -j}} + \varepsilon_{1j}\right)^2 (\boldsymbol{\Sigma}_{j\backslash -j} + \varepsilon_{2j})\right) \\
\ge\ & 1 - 2\exp\left\{-\frac{1}{8e^2}\left(\frac{\varepsilon_{2j}}{3\kappa_{1j}}\right)^2 n\right\} - 2\exp\left\{-\frac{1}{8e^2}\left(\frac{\varepsilon_{2j}}{6\kappa_{2j}}\right)^2 n\right\} - 2\exp\left\{-\frac{1}{8e^2}\left(\frac{\varepsilon_{2j}}{3\kappa_{3j}}\right)^2 n\right\} \\
& - 2\exp\left\{-\frac{1}{8e^2}\left(\frac{\boldsymbol{\Sigma}^2_{j\backslash -j}\varepsilon_{1j}}{4\kappa_{1j}}\right)^2 n\right\} - 2\exp\left\{-\frac{1}{8e^2}\left(\frac{\boldsymbol{\Sigma}^2_{j\backslash -j}\varepsilon_{1j}}{4\kappa_{2j}}\right)^2 n\right\},
\end{aligned}$$

and

$$\begin{aligned}
&\mathbb{P}\left(\breve{u}_j \le \varepsilon_{0j}\sqrt{\frac{\log p}{n}}\left(\frac{1}{\boldsymbol{\Sigma}_{j\backslash -j}} + \varepsilon_{1j}\right)\right) \\
\ge\ & 1 - 2\exp\left\{\left(1 - \frac{1}{8e^2}\frac{\varepsilon_{0j}^2}{(\kappa_{0j})^2}\right)\log p\right\} - 2\exp\left\{-\frac{1}{8e^2}\left(\frac{\boldsymbol{\Sigma}^2_{j\backslash -j}\varepsilon_{1j}}{4\kappa_1}\right)^2 n\right\} \\
& - 2\exp\left\{-\frac{1}{8e^2}\left(\frac{\boldsymbol{\Sigma}^2_{j\backslash -j}\varepsilon_{1j}}{4\kappa_{2j}}\right)^2 n\right\},
\end{aligned}$$

for $\varepsilon_{0j}, \varepsilon_{1j}, \varepsilon_{2j}$ *given in Lemmas A.3 and A.4.*

Lemma A.5. *Let* $R_l = n^{-1}\hat{v}_l^\top \mathbf{X}_{-l}(\beta_{-l} - \hat{\beta}_{-l})$ *where* $\hat{v}_l$ *and* $\hat{u}_l$ *denote the solution to (2.10). Then,*

$$\max_l R_l = o_p(1).$$

Proof of Lemma A.5. According to the definition of $\hat{v}_l$,

$$C_2\frac{n}{\log p}\hat{u}_l^2 + n^{-1}\|\hat{v}_l\|^2 \le C_2\frac{n}{\log p}\breve{u}_l^2 + n^{-1}\|\breve{v}_l\|^2$$

where $\hat{u}_l = n^{-1}\|\hat{v}_l^\top \mathbf{X}_{-l}\|_\infty$, $\breve{v}_l = n\theta_l/\theta_l^\top X_l$ and $\breve{u}_l = n^{-1}\|\breve{v}_l \mathbf{X}_{-l}\|_\infty$. Then, we have

$$\sqrt{C_2\frac{n}{\log p}}\hat{u}_l \le C_2\frac{n}{\log p}\breve{u}_l^2 + n^{-1}\|\breve{v}_l\|^2$$

which implies

$$\sqrt{C_2\frac{n}{\log p}}\max_l n^{-1}\|\hat{v}_l^\top \mathbf{X}_{-l}\|_\infty \leq \left(\max_l(\mathbf{\Sigma}_{l\setminus -l})^{-1}+\varepsilon_1'\right)^2\left(C_2(\varepsilon_0')^2+\max_l \mathbf{\Sigma}_{l\setminus -l}+\varepsilon_2'\right)$$

with probability tending to 1 by (A.12). Therefore,

$$\max_l R_l \leq \max_l n^{-1}\|\hat{v}_l^\top \mathbf{X}_{-l}\|_\infty\sqrt{n}\|\hat{\beta}-\beta\|_1 = o_p(1)$$

by Assumptions 2.3 and 2.6. ♢

The following inequalities are direct consequences of Lemmas A.3-A.4 and the definition of $\hat{v}_l$.

Corollary A.2. *Let $\hat{v}_l$ be the solution to (2.10). Then, we have*

$$\begin{aligned}
\mathbb{P}\left(\max_l n^{-1}\|\theta_l^\top \mathbf{X}_{-l}\|_\infty \geq \varepsilon_0'\sqrt{\frac{\log p}{n}}\right) &\leq 2\exp\left\{-\frac{1}{8e^2}\left(\min_l \frac{1}{\kappa_{0l}^2}\right)(\varepsilon_0')^2\log p + 2\log p\right\},\\
\mathbb{P}\left(\max_l \frac{n}{|\theta_l^\top X_l|} \leq \max_l(\mathbf{\Sigma}_{l\setminus -l})^{-1}+\varepsilon_1'\right) &\geq 1-2\exp\left\{-\frac{1}{8e^2}\left(\min_l \frac{(\mathbf{\Sigma}_{l\setminus -l})^4}{(4\kappa_1)^2}\right)(\varepsilon_1')^2 n+\log p\right\}\\
&\quad -2\exp\left\{-\frac{1}{8e^2}\left(\min_l \frac{(\mathbf{\Sigma}_{l\setminus -l})^4}{(4\kappa_{2l})^2}\right)(\varepsilon_1')^2 n+\log p\right\},\\
\mathbb{P}\left(\max_l \frac{\|\theta_l\|^2}{n} \leq \max_l \mathbf{\Sigma}_{l\setminus -l}+\varepsilon_2'\right) &\geq 1-2\exp\left\{-\frac{1}{8e^2(3\kappa_1)^2}(\varepsilon_2')^2 n+\log p\right\}\\
&\quad -2\exp\left\{-\frac{1}{8e^2}\left(\min_l \frac{1}{(6\kappa_{2l})^2}\right)(\varepsilon_2')^2 n+\log p\right\}\\
&\quad -2\exp\left\{-\frac{1}{8e^2}\left(\min_l \frac{1}{(3\kappa_{3l})^2}\right)(\varepsilon_2')^2 n+\log p\right\},
\end{aligned}$$

and

$$\begin{aligned}\mathbb{P}\left(\max_l n^{-1}\|\hat{v}_l\|^2 \le M'\right) \ge 1 &- 2\exp\left\{-\frac{1}{8e^2}\left(\min_l \frac{1}{(\kappa_{0l})^2}\right)(\varepsilon_0')^2\log p + 2\log p\right\} \\ &- 2\exp\left\{-\frac{1}{8e^2}\left(\min_l \frac{(\mathbf{\Sigma}_{l\setminus -l})^4}{(4\kappa_1)^2}\right)(\varepsilon_1')^2 n + \log p\right\} \\ &- 2\exp\left\{-\frac{1}{8e^2}\left(\min_l \frac{(\mathbf{\Sigma}_{l\setminus -l})^4}{(4\kappa_{2l})^2}\right)(\varepsilon_1')^2 n + \log p\right\} \\ &- 2\exp\left\{-\frac{1}{8e^2(3\kappa_1)^2}(\varepsilon_2')^2 n + \log p\right\} \\ &- 2\exp\left\{-\frac{1}{8e^2}\left(\min_l \frac{1}{(6\kappa_{2l})^2}\right)(\varepsilon_2')^2 n + \log p\right\} \\ &- 2\exp\left\{-\frac{1}{8e^2}\left(\min_l \frac{1}{(3\kappa_{3l})^2}\right)(\varepsilon_2')^2 n + \log p\right\},\end{aligned}$$

where

$$M' = (\max_l(\mathbf{\Sigma}_{l\setminus -l})^{-1} + \varepsilon_1')^2(C_2\varepsilon_0'^2 + \max_l \mathbf{\Sigma}_{l\setminus -l} + \varepsilon_2') \tag{A.11}$$

for $0 < \varepsilon_0' \le (\min_l \kappa_{0l})\sqrt{n(\log p)^{-1}}, 0 < \varepsilon_1' \le \min_l \{\min((\mathbf{\Sigma}_{l\setminus -l})^{-1}, 4\min(\kappa_1, \kappa_{2l})(\mathbf{\Sigma}_{l\setminus -l})^{-2})\}$ *and* $0 < \varepsilon_2' \le \min_l(\min(3\kappa_1, 6\kappa_{2l}, 3\kappa_{3l}))$.

Under Assumption 2.6, Corollary A.2 implies that

$$\begin{aligned}&\max_l n^{-1}\|\theta_l^\top \mathbf{X}_{-l}\|_\infty \le \varepsilon_0'\sqrt{\frac{\log p}{n}}, \\ &\max_l \frac{n}{|\theta_l^\top X_l|} \le \max_l(\mathbf{\Sigma}_{l\setminus -l})^{-1} + \varepsilon_1', \\ &\max_l n^{-1}\|\theta_l\|^2 \le \max_l \mathbf{\Sigma}_{l\setminus -l} + \varepsilon_2', \\ &\max_l n^{-1}\|\hat{v}_l\|^2 \le M',\end{aligned} \tag{A.12}$$

with probability tending to 1 for a fixed $(\varepsilon_0')^2 \min_l(\kappa_{0l})^{-2} > 16e^2$ and fixed $\varepsilon_1', \varepsilon_2'$ as in Corollary A.2.

Proof of Proposition 2.1. Noting that $(n^{-1/2}\|\hat{v}_l\|)^{-1} \leq \|X_l\|/\sqrt{n}$, we have

$$\begin{aligned}
|T_l| &= \frac{\sigma}{\hat{\sigma}} \left| \frac{\sqrt{n}(\tilde{\beta}_l(\hat{v}_l) - \beta_l)}{\sigma n^{-1/2}\|\hat{v}_l\|} + \frac{\sqrt{n}\beta_l}{\sigma n^{-1/2}\|\hat{v}_l\|} \right| \\
&= \frac{\sigma}{\hat{\sigma}} \left| \frac{1}{\sigma n^{-1/2}\|\hat{v}_l\|} \left(\frac{1}{\sqrt{n}} \hat{v}_l^\top \epsilon + \sqrt{n} R_l \right) + \frac{\sqrt{n}\beta_l}{\sigma n^{-1/2}\|\hat{v}_l\|} \right| \\
&\leq \frac{\sigma}{\hat{\sigma}} \left(|Z_l| + \left| \frac{\sqrt{n} R_l}{\sigma n^{-1/2}\|\hat{v}_l\|} \right| + \left| \frac{\sqrt{n}\beta_l}{\sigma n^{-1/2}\|\hat{v}_l\|} \right| \right) \\
&\leq \frac{\sigma}{\hat{\sigma}} \left(|Z_l| + \frac{\|X_l\|}{\sqrt{n}} \left| \frac{\sqrt{n} R_l}{\sigma} \right| + \frac{\|X_l\|}{\sqrt{n}} \left| \frac{\sqrt{n}\beta_l}{\sigma} \right| \right),
\end{aligned}$$

and

$$\begin{aligned}
|T_l| &\geq \frac{\sigma}{\hat{\sigma}} \left(\left| \frac{\sqrt{n}\beta_l}{\sigma n^{-1/2}\|\hat{v}_l\|} \right| - |Z_l| - \left| \frac{\sqrt{n} R_l}{\sigma n^{-1/2}\|\hat{v}_l\|} \right| \right) \\
&\geq \frac{\sigma}{\hat{\sigma}} \left(\left| \frac{\sqrt{n}\beta_l}{\sigma n^{-1/2}\|\hat{v}_l\|} \right| - |Z_l| - \frac{\|X_l\|}{\sqrt{n}} \left| \frac{\sqrt{n} R_l}{\sigma} \right| \right),
\end{aligned}$$

where $R_l = n^{-1}\hat{v}_l^\top \mathbf{X}_{-l}(\beta_{-l} - \hat{\beta}_{-l})$. We also observe that

$$\begin{aligned}
&\left[\left\{ \left| \frac{\hat{\sigma}}{\sigma} - 1 \right| \leq \varepsilon \right\} \bigcap \left\{ \max_{l \in \mathcal{B}_j^{(2)}} |Z_l| + D' \max_{l \in \mathcal{B}_j^{(2)}} \left| \frac{\sqrt{n} R_l}{\sigma} \right| + D' \max_{l \in \mathcal{B}_j^{(2)}} \left| \frac{\sqrt{n}\beta_l}{\sigma} \right| \leq \sqrt{\tau \log p} \right\} \right. \\
&\qquad \left. \bigcap \left\{ \max_l \frac{\|X_l\|}{\sqrt{n}} \leq D' \right\} \right] \subset \left\{ \max_{l \in \mathcal{B}_j^{(2)}} |T_l| \leq \sqrt{\tau \log p} \right\},
\end{aligned}$$

and

$$\begin{aligned}
&\left[\left\{ \min_{l \in \mathcal{B}_j^{(1)}} \left| \frac{\sqrt{n}\beta_l}{\sigma n^{-1/2}\|\hat{v}_l\|} \right| - \max_{l \in \mathcal{B}_j^{(1)}} |Z_l| - D' \max_{l \in \mathcal{B}_j^{(1)}} \left| \frac{\sqrt{n} R_l}{\sigma} \right| > \sqrt{\tau \log p} \right\} \right. \\
&\left. \bigcap \left\{ \left| \frac{\hat{\sigma}}{\sigma} - 1 \right| \leq \varepsilon \right\} \bigcap \left\{ \max_l \frac{\|X_l\|}{\sqrt{n}} \leq D' \right\} \right] \subset \left\{ \min_{l \in \mathcal{B}_j^{(1)}} |T_l| > \sqrt{\tau \log p} \right\}
\end{aligned}$$

and where $D' = \sqrt{\max_l \mathbf{\Sigma}_{l,l} + \varepsilon'}$ for $0 < \varepsilon' \leq 2\kappa^2$. Note that

$$\mathbb{P}\left\{ \max_l \frac{\|X_l\|}{\sqrt{n}} \leq D' \right\} \geq 1 - 2\exp\left\{ -\frac{1}{8e^2} \frac{(\varepsilon')^2}{4\kappa^4} n + \log p \right\}. \tag{A.13}$$

We prove Proposition 2.1 in the following two steps.

1. Under Assumption 2.1, it suffices to show that

$$\mathbb{P}\left(\max_{l\in\mathcal{B}_j^{(2)}}|Z_l|+\frac{D'}{\sigma}\max_{l\in\mathcal{B}_j^{(2)}}|\sqrt{n}R_l|\le c_1\sqrt{\log p}\right)\to 1,$$

where $c_1=\sqrt{\tau}-D'\sqrt{d_0}$. We have, for $\varepsilon''>0$,

$$\begin{aligned}
&\mathbb{P}\left(\max_{l\in\mathcal{B}_j^{(2)}}|Z_l|+\frac{D'}{\sigma}\max_{l\in\mathcal{B}_j^{(2)}}|\sqrt{n}R_l|\le c_1\sqrt{\log p}\right)\\
\ge&\mathbb{P}\left(\left\{\max_{l\in\mathcal{B}_j^{(2)}}|Z_l|\le c_1\sqrt{\log p}-\varepsilon''\right\}\bigcap\left\{\frac{D'}{\sigma}\max_{k\in\mathcal{B}_j^{(2)}}|\sqrt{n}R_l|\le\varepsilon''\right\}\right)\\
\ge&\mathbb{P}\left(\max_{l\in\mathcal{B}_j^{(2)}}|Z_l|\le c_1\sqrt{\log p}-\varepsilon''\right)+\mathbb{P}\left(\frac{D'}{\sigma}\max_{l\in\mathcal{B}_j^{(2)}}|\sqrt{n}R_l|\le\varepsilon''\right)-1\\
\ge&\mathbb{P}\left(\frac{D'}{\sigma}\max_{k\in\mathcal{B}_j^{(2)}}|\sqrt{n}R_k|\le\varepsilon''\right)-2p\exp\left\{-\frac{\sigma^2(c_1\sqrt{\log p}-\varepsilon'')^2}{32e\kappa_\epsilon^2}\right\}.
\end{aligned}$$

Here the last inequality follows by Lemma A.2 under Assumption 2.2, i.e.,

$$\begin{aligned}
&\mathbb{P}\left(\max_{l\in\mathcal{B}_j^{(2)}}|Z_l|\ge c_1\sqrt{\log p}-\varepsilon''\right)\\
\le&\mathbb{P}\left(\bigcup_{l\in\mathcal{B}_j^{(2)}}\left\{|Z_l|\ge c_1\sqrt{\log p}-\varepsilon''\right\}\right)\\
\le&|\mathcal{B}_j^{(2)}|\times\mathbb{P}\left(\left|\frac{1}{\sigma\|\hat{v}_l\|}\sum_{i=1}^n\hat{v}_{li}\epsilon_i\right|\ge c_1\sqrt{\log p}-\varepsilon''\right)\\
\le&|\mathcal{B}_j^{(2)}|\times 2\times\exp\left\{-\frac{\sigma^2(c_1\sqrt{\log p}-\varepsilon'')^2}{32e\kappa_\epsilon^2}\right\}
\end{aligned}\tag{A.14}$$

conditional on $\hat{v}_l$. By the assumption

$$\frac{\sigma^2}{32e\kappa_\epsilon^2}(\sqrt{\tau}-\sqrt{d_0\max_l\mathbf{\Sigma}_{l,l}})^2>1,$$

we have

$$\frac{\sigma^2}{32e\kappa_\epsilon^2}c_1^2>1$$

for small enough ε'. Together with (A.13), Lemma A.5 and Assumption 2.4, we obtain

$$\mathbb{P}\left(\max_{l\in\mathcal{B}_j^{(2)}}|T_l|\le\sqrt{\tau\log p}\right)\to 1.$$

2. We define $c_2=\sqrt{d_1/M''}-\sqrt{\tau}$, where

$$M''=\left(\min_l \mathbf{\Sigma}_{l\backslash -l}+\varepsilon_1'\right)^2\left(\frac{2C_2}{8e^2}\left(\min_l\frac{1}{(\kappa_{0l})^2}\right)^{-1}+\max_l\mathbf{\Sigma}_{l\backslash -l}+2\varepsilon_2'\right)$$

by letting $(\varepsilon_0')^2=2\left((8e^2)^{-1}\min_l(\kappa_{0l})^{-2}\right)^{-1}+\varepsilon_2'$ in (A.11). We have, for $\varepsilon''>0$,

$$\begin{aligned}
&\mathbb{P}\left(\min_{l\in\mathcal{B}_j^{(1)}}\left|\frac{\sqrt{n}\beta_l}{\sigma n^{-1/2}\|\hat{v}_l\|}\right|-\max_{l\in\mathcal{B}_j^{(1)}}|Z_l|-D'\max_{l\in\mathcal{B}_j^{(1)}}\left|\frac{\sqrt{n}R_l}{\sigma}\right|>\sqrt{\tau\log p}\right)\\
\ge&\mathbb{P}\left(\left\{\min_{l\in\mathcal{B}_j^{(1)}}\left|\frac{\sqrt{n}\beta_l}{\sigma n^{-1/2}\|\hat{v}_l\|}\right|-\max_{l\in\mathcal{B}_j^{(1)}}|Z_l|>\sqrt{\tau\log p}+\varepsilon''\right\}\bigcap\left\{\frac{D'}{\sigma}\max_{l\in\mathcal{B}_j^{(1)}}\left|\sqrt{n}R_l\right|\le\varepsilon''\right\}\right)\\
\ge&\mathbb{P}\left(\left\{\min_{l\in\mathcal{B}_j^{(1)}}\left|\frac{\sqrt{n}\beta_l}{\sigma\sqrt{M''}}\right|-\max_{l\in\mathcal{B}_j^{(1)}}|Z_l|>\sqrt{\tau\log p}+\varepsilon''\right\}\bigcap\left\{\min_{l\in\mathcal{B}_j^{(1)}}\frac{1}{n^{-1/2}\|\hat{v}_l\|}\ge\frac{1}{\sqrt{M''}}\right\}\right)\\
&+\mathbb{P}\left(\frac{D'}{\sigma}\max_{l\in\mathcal{B}_j^{(1)}}|\sqrt{n}R_l|\le\varepsilon''\right)-1\\
\ge&\mathbb{P}\left(\min_{l\in\mathcal{B}_j^{(1)}}\left|\frac{\sqrt{n}\beta_l}{\sigma\sqrt{M''}}\right|-\max_{l\in\mathcal{B}_j^{(1)}}|Z_l|>\sqrt{\tau\log p}+\varepsilon''\right)+\mathbb{P}\left(\max_{l\in\mathcal{B}_j^{(1)}}n^{-1}\|\hat{v}_l\|^2\le M''\right)\\
&+\mathbb{P}\left(\frac{D'}{\sigma}\max_{l\in\mathcal{B}_j^{(1)}}|\sqrt{n}R_l|\le\varepsilon''\right)-2\\
\ge&\mathbb{P}\left(\max_{l\in\mathcal{B}_j^{(1)}}|Z_l|<c_2\sqrt{\log p}-\varepsilon''\right)+\mathbb{P}\left(\max_{l\in\mathcal{B}_j^{(1)}}n^{-1}\|\hat{v}_l\|^2\le M''\right)\\
&+\mathbb{P}\left(\frac{D'}{\sigma}\max_{l\in\mathcal{B}_j^{(1)}}|\sqrt{n}R_l|\le\varepsilon''\right)-2\\
\ge&1-2\left|\mathcal{B}_j^{(1)}\right|\exp\left\{-\frac{\sigma^2}{32e\kappa_\epsilon^2}(b\sqrt{\log p}-\varepsilon'')^2\right\}+\mathbb{P}\left(\max_{k\in\mathcal{B}_j^{(1)}}n^{-1}\|\check{v}_k\|^2\le M''\right)\\
&+\mathbb{P}\left(\frac{D'}{\sigma}\max_{k\in\mathcal{B}_j^{(1)}}|\sqrt{n}R_k|\le\varepsilon''\right)-2
\end{aligned}$$

where the last inequality follows from (A.14). By the assumption $\sqrt{d_1/M} - \sqrt{\tau} > 0$, we have $c_2 = \sqrt{d_1/M''} - \sqrt{\tau} > 0$ for small enough $\varepsilon_1', \varepsilon_2'$. Since $\left|\mathcal{B}_j^{(1)}\right| \leq s_0 \ll p$, by (A.12), (A.13), Lemma A.5 and Assumption 2.4, we get $\mathbb{P}\left(\min_{l \in \mathcal{B}_j^{(1)}} |T_l| > \sqrt{\tau \log p}\right) \to 1$.

$\diamondsuit$

Proof of Theorem 2.1. The argument below is conditional on the event $\{\mathcal{A}_j^{(k)}(\tau) = \mathcal{B}_j^{(k)}$ for $k = 1, 2\}$ which occurs almost surely by Proposition 2.1. Let $\breve{u}_{j1} = \max_{k \in \mathcal{A}_j^{(1)}(\tau)} n^{-1} |\breve{v}_j^\top X_k|$ and $\breve{u}_{j1} = \max_{k \in \mathcal{A}_j^{(2)}(\tau)} n^{-1} |\breve{v}_j^\top X_k|$ where $\breve{v}_j$ is as in Corollary A.1. Then, $(\breve{u}_{j1}, \breve{u}_{j1}, \breve{v}_j)$ is a feasible point to problem (2.8). By the definition of $\tilde{v}_j$,

$$C_1 \frac{n}{\log p} \tilde{u}_{j1}^2 + C_2 \frac{n}{\log p} \tilde{u}_{j2}^2 + n^{-1} \|\tilde{v}_j\|^2 \leq C_1 \frac{n}{\log p} \breve{u}_{j1}^2 + C_2 \frac{n}{\log p} \breve{u}_{j2}^2 + n^{-1} \|\breve{v}_j\|^2,$$

where $\tilde{u}_{j1} = \max_{k \in \mathcal{A}_j^{(1)}} n^{-1} |\tilde{v}_j^\top X_k|$ and $\tilde{u}_{j2} = \max_{k \in \mathcal{A}_j^{(2)}} n^{-1} |\tilde{v}_j^\top X_k|$. Then, for $i = 1, 2$, we must have

$$\sqrt{C_i \frac{n}{\log p}} \tilde{u}_{ji} \leq \max\{C_1, C_2\} \varepsilon_{0j}^2 \left(\frac{1}{\boldsymbol{\Sigma}_{j \backslash -j}} + \varepsilon_{1j}\right)^2 + \left(\frac{1}{\boldsymbol{\Sigma}_{j \backslash -j}} + \varepsilon_{1j}\right)^2 (\boldsymbol{\Sigma}_{j \backslash -j} + \varepsilon_{2j}),$$

with probability tending to 1 by Corollary A.1. Then, by Assumptions 2.3 and 2.6,

$$|\sqrt{n} R(\tilde{v}_j, \beta_{-j})| = n^{-1/2} |\tilde{v}_j^\top \mathbf{X}_{-j} (\beta_{-j} - \hat{\beta}_{-j})| \leq n^{-1} \max_{k \neq j} |\tilde{v}_j^\top X_k| \sqrt{n} \|\hat{\beta}_{-j} - \beta_{-j}\|_1 = o_p(1).$$

Hence, we obtain

$$\sqrt{n}(\tilde{\beta}_j(\tilde{v}_j) - \beta_j) = \frac{1}{\sqrt{n}} \tilde{v}_j^\top \epsilon + o_p(1). \tag{A.15}$$

Note that

$$\frac{\sum_{i=1}^n E[(\tilde{v}_{j,i} \epsilon_i)^{2+\delta} | \tilde{v}_j]}{\sigma^{2+\delta} \|\tilde{v}_j\|^{2+\delta}} = \frac{E\epsilon_1^{2+\delta}}{\sigma^{2+\delta}} \frac{\|\tilde{v}_j\|_{2+\delta}^{2+\delta}}{\|\tilde{v}_j\|^{2+\delta}} = o_{a.s.}(1).$$

Conditional on the event that $\{\|\tilde{v}_j\|_{2+\delta}/\|\tilde{v}_j\| \to 0\}$, the Lyapunov condition is satisfied and thus $\tilde{v}_j^\top \epsilon/\{\sigma\|\tilde{v}_j\|\}$ converges to $N(0,1)$. If $\epsilon \sim N(0, \sigma^2\mathbf{I})$, $\tilde{v}_j^\top \epsilon/\{\sigma\|\tilde{v}_j\|\} \sim N(0,1)$ conditional on $\tilde{v}_j$. The conclusion thus follows from (A.15) and Assumption 2.4 by the Slutsky's theorem. $\diamondsuit$

Proof of Proposition 2.2. All the arguments below are conditional on the event $\{\mathcal{A}_j^{(2)} = \mathcal{B}_j^{(2)}\}$ which occurs almost surely by Proposition 2.1. With the projection direction $\bar{v}_j$ from (2.16) and the refitted least square estimator $\check{\beta}$, the bias (2.6) reduces to

$$\begin{aligned}
\sqrt{n}R(\bar{v}_j, \beta_{-j}) &= \frac{1}{\sqrt{n}} \sum_{k \neq j} \bar{v}_j^\top X_k(\beta_k - \check{\beta}_k) \\
&= \frac{1}{\sqrt{n}} \sum_{k \in \mathcal{B}_j^{(1)}} \bar{v}_j^\top X_k(\beta_k - \check{\beta}_k) + \frac{1}{\sqrt{n}} \sum_{k \in \mathcal{B}_j^{(2)}} \bar{v}_j^\top X_k(\beta_k - \check{\beta}_k) \\
&= \frac{1}{\sqrt{n}} \sum_{k \in \mathcal{A}_j^{(1)}} \bar{v}_j^\top X_k(\beta_k - \check{\beta}_k) + \frac{1}{\sqrt{n}} \sum_{k \in \mathcal{A}_j^{(2)}} \bar{v}_j^\top X_k(\beta_k - \check{\beta}_k) \\
&= \frac{1}{\sqrt{n}} \sum_{k \in \mathcal{A}_j^{(2)}} \bar{v}_j^\top X_k \beta_k,
\end{aligned}$$

where we have used the fact that $\bar{v}_j^\top X_k = 0$ for $k \in \mathcal{A}_j^{(1)}$ from (2.16) and $\check{\beta}_{\mathcal{A}_j^{(2)}} = 0$ by (2.17). Thus, we have

$$\begin{aligned}
|\sqrt{n}R(\bar{v}_j, \beta_{-j})| &\leq \|n^{-1}\bar{v}_j^\top \mathbf{X}_{-j}\|_\infty \sqrt{n} \|\beta_{\mathcal{A}_j^{(2)}}\|_1 \\
&\leq \|n^{-1}\bar{v}_j^\top \mathbf{X}_{-j}\|_\infty \sigma \sqrt{d_0 \log p} \|\beta_{\mathcal{B}_j^{(2)}}\|_0 \\
&\leq O_p\left(\sqrt{\frac{\log p}{n}}\right) \sigma \sqrt{d_0 \log p} \|\beta_{\mathcal{B}_j^{(2)}}\|_0
\end{aligned}$$

where the second inequality holds by Assumption 2.1 under the event $\{\mathcal{A}_j^{(2)} = \mathcal{B}_j^{(2)}\}$. The last inequality follows from the fact that $\|n^{-1}\bar{v}_j^\top \mathbf{X}_{-j}\|_\infty = O_p(\sqrt{\log p/n})$, which can be verified by using similar arguments as in the proof of Corollary 1 together with the definition of $\bar{v}_j$ under Assumption 2.5. The last statement follows immediately from condition (2.20). $\diamondsuit$

A.1.3 Technical details in Section 2.4

We first state the following results which are parallel to Lemma A.3 and the first inequality in Corollary A.2. As the proof is similar to the one in Lemma A.3, we omit the details.

Corollary A.3. *Let* $\theta_l = X_l - \mathbf{X}_{-S} b_l$ *with* $b_l = \mathit{argmin}_{\tilde{b}} E\|X_l - \mathbf{X}_{-S}\tilde{b}\|^2$ *for* $l \in S$. *Under Assumption 2.5,*

$$\mathbb{P}\left(n^{-1}\|\theta_l^\top \mathbf{X}_{-S}\|_\infty \geq \xi_{0l}\sqrt{\frac{\log p}{sn}} \right) \leq 2\exp\left\{ \left(1 - c_{l,S}\frac{\delta_{0l}^2}{s(\xi_{0l})^2} \right) \log p \right\}$$

for $0 < \xi_{0l} \leq \kappa_{0l}\sqrt{sn(\log p)^{-1}}$ *where* $c_{l,S} > 0$ *is an absolute constant and* $\kappa_{0l} = 2\left(1 + \sqrt{\Lambda_{\min}^{-1}\mathbf{\Sigma}_{l,l}}\right)\kappa^2$. *As a consequence, we have*

$$\mathbb{P}\left(\max_{l\in S} n^{-1}\|\theta_l^\top \mathbf{X}_{-S}\|_\infty \geq \xi_0'\sqrt{\frac{\log p}{sn}} \right) \leq 2\exp\left\{ -\left(\min_l \frac{c_{l,S}}{s(\kappa_{0l})^2} \right)(\xi_0')^2 \log p + 2\log p \right\}.$$

for $0 < \xi_0' \leq \min_l \kappa_{0l}\sqrt{sn(\log p)^{-1}}$.

The following results are introduced for the proof of Theorem 2.2 which follows from a direct application of Proposition 2.1 in Vershynin (2012) .

Lemma A.6. *For every* $\delta > 0$, *we have*

$$\mathbb{P}\left(\|n^{-1}\mathbf{X}_S^\top \mathbf{X}_S - \mathbf{\Sigma}_{S,S}\| \leq \sqrt{\frac{4}{C_\kappa}\frac{s}{n}\log\frac{2}{\delta}} \right) \geq 1 - \delta,$$

where $C_\kappa > 0$ *is an absolute constant which only depends on* δ *and* κ.

We next introduce the following lemma which provides an upper bound for the operator norm of a matrix.

Lemma A.7. *Let* $\mathbf{B}$ *be a* $m \times m$ *matrix and* $\mathcal{N}_\varepsilon$ *be an* ε*-net of the unit sphere* $\mathcal{S}^{m-1}$ *for some* $\varepsilon \in (0, 1/2)$. *Then*

$$\|\mathbf{B}\| \leq (1 - 2\varepsilon)^{-1} \sup_{c,d\in\mathcal{N}_\varepsilon} \left| c^\top \mathbf{B} d \right|.$$

Proof of Lemma A.7. For any $c, d \in \mathcal{S}^{m-1}$, we can choose $c_{\mathcal{N}}, d_{\mathcal{N}} \in \mathcal{N}_\varepsilon$ such that $\max\{\|c - c_{\mathcal{N}}\|, \|d - d_{\mathcal{N}}\|\} \leq \varepsilon$. Some algebra gives us

$$c^\top \mathbf{B} d = c_{\mathcal{N}}^\top \mathbf{B} d_{\mathcal{N}} + (c - c_{\mathcal{N}})^\top \mathbf{B} d + c_{\mathcal{N}}^\top \mathbf{B}(d - d_{\mathcal{N}}),$$

which implies that

$$\left|c^\top \mathbf{B} d\right| \leq 2\varepsilon \|\mathbf{B}\| + \sup_{c_{\mathcal{N}}, d_{\mathcal{N}} \in \mathcal{N}_\varepsilon} \left|c_{\mathcal{N}}^\top \mathbf{B} d_{\mathcal{N}}\right|.$$

Taking supremum over all $c, d \in \mathcal{S}^{m-1}$ and rearranging terms give us the desired result. $\diamondsuit$

Lemma A.8. *For every $\delta > 0$, we have*

$$\mathbb{P}\left(\|(n^{-1}\mathbf{X}_S^\top \mathbf{X}_{-S} - \mathbf{\Sigma}_{S,-S})\mathbf{\Sigma}_{-S,-S}^{-1}\mathbf{\Sigma}_{-S,S}\| \leq 3\sqrt{\frac{8}{C_{\kappa'}} \log \frac{2}{\delta} \frac{s}{n}}\right) \geq 1 - \delta$$

where $C_{\kappa'} > 0$ denotes an absolute constant which only depends on $\kappa' = 2\kappa^2\sqrt{\Lambda_{\min}^{-1} D^2}$.

Proof of Lemma A.8. We prove the result in several steps. First, we bound the operator norm by using the so-called ε-net argument. Then we apply the concentration inequality for sub-exponential random variables and finally use the union bound to finish the proof. For two vectors $a, b \in \mathbb{R}^{q \times 1}$, write $\langle a, b \rangle = a^\top b$. By Lemma A.7 and Lemma 5.2 in Vershynin (2012), we have

$$\begin{aligned}
&\|(n^{-1}\mathbf{X}_S^\top \mathbf{X}_{-S} - \mathbf{\Sigma}_{S,-S})\mathbf{\Sigma}_{-S,-S}^{-1}\mathbf{\Sigma}_{-S,S}\| \\
=& \sup_{c,d \in \mathcal{S}^{s-1}} \left|\frac{1}{n}\sum_{i=1}^n \left(\langle X_{i,S}, c\rangle \langle \mathbf{\Sigma}_{S,-S}\mathbf{\Sigma}_{-S,-S}^{-1} X_{i,-S}, d\rangle - c^\top \mathbf{\Sigma}_{S,-S}\mathbf{\Sigma}_{-S,-S}^{-1}\mathbf{\Sigma}_{-S,S} d\right)\right| \\
\leq& 3 \sup_{c,d \in \mathcal{N}_{1/3}} \left|\frac{1}{n}\sum_{i=1}^n \left(\langle X_{i,S}, c\rangle \langle \mathbf{\Sigma}_{S,-S}\mathbf{\Sigma}_{-S,-S}^{-1} X_{i,-S}, d\rangle - c^\top \mathbf{\Sigma}_{S,-S}\mathbf{\Sigma}_{-S,-S}^{-1}\mathbf{\Sigma}_{-S,S} d\right)\right|
\end{aligned}$$

where $\mathcal{N}_{1/3}$ denotes a $1/3$-net of $\mathcal{S}^{s-1}$ with the covering number $|\mathcal{N}_{1/3}| \leq 7^s$.

Let us fix $c, d \in \mathcal{N}_{1/3}$. Because each row of $\mathbf{X}_S$ and $\mathbf{X}_{-S}$ is independent sub-gaussian random vector, we can apply the concentration inequality in Corollary 5.17 of Vershynin (2010). Specifi-

cally, we have

$$\begin{aligned}&\mathbb{P}\left(\left|\frac{1}{n}\sum_{i=1}^{n}\left(\langle X_{i,S},c\rangle\langle\boldsymbol{\Sigma}_{S,-S}\boldsymbol{\Sigma}_{-S,-S}^{-1}X_{i,-S},d\rangle-c^{\top}\boldsymbol{\Sigma}_{S,-S}\boldsymbol{\Sigma}_{-S,-S}^{-1}\boldsymbol{\Sigma}_{-S,S}d\right)\right|\geq\epsilon\right)\\ \leq&2\exp\left(-cn\frac{\epsilon^2}{(\kappa')^2}\right)\end{aligned}$$

provided that $\epsilon^2 \leq (\kappa')^2$, where $\|\langle X_{i,S},c\rangle\langle\boldsymbol{\Sigma}_{S,-S}\boldsymbol{\Sigma}_{-S,-S}^{-1}X_{i,-S},d\rangle\|_{\psi_1}\leq\kappa'$ and $c>0$ is an absolute constant. Applying the union bound over $c,d\in\mathcal{N}_{1/3}$, we have

$$\sup_{c,d\in\mathcal{N}_{1/3}}\left|\frac{1}{n}\sum_{i=1}^{n}\left(\langle X_{i,S},c\rangle\langle\boldsymbol{\Sigma}_{S,-S}\boldsymbol{\Sigma}_{-S,-S}^{-1}X_{i,-S},d\rangle-c^{\top}(\boldsymbol{\Sigma}_{S,-S}\boldsymbol{\Sigma}_{-S,-S}^{-1}\boldsymbol{\Sigma}_{-S,S})d\right)\right|\geq\epsilon$$

with probabiliity at most $2|\mathcal{N}_{1/3}|^2\exp\left[-cn\epsilon^2/(\kappa')^2\right]$, which implies

$$\begin{aligned}\mathbb{P}\left(\|(n^{-1}\mathbf{X}_S^{\top}\mathbf{X}_{-S}-\boldsymbol{\Sigma}_{S,-S})\boldsymbol{\Sigma}_{-S,-S}^{-1}\boldsymbol{\Sigma}_{-S,S}\|<3\epsilon\right)&\geq1-2|\mathcal{N}_{1/3}|^2\exp\left[-cn\left(\frac{\epsilon}{\kappa'}\right)^2\right]\\&\geq1-2\exp\left[4s-n\epsilon^2C_{\kappa'}\right]\end{aligned}$$

where $C_{\kappa'}=c/(\kappa')^2$. Then by letting $\epsilon^2=(8/C_{\kappa'})\log(2/\delta)(s/n)$, we have

$$\mathbb{P}\left(\|(n^{-1}\mathbf{X}_S^{\top}\mathbf{X}_{-S}-\boldsymbol{\Sigma}_{S,-S})\boldsymbol{\Sigma}_{-S,-S}^{-1}\boldsymbol{\Sigma}_{-S,S}\|\leq3\sqrt{\frac{8}{C_{\kappa'}}\log\frac{2}{\delta}\frac{s}{n}}\right)\geq1-\delta$$

which completes the proof. ♢

Lemma A.9. *Let* $\hat{\mathbf{A}}=n^{-1}\mathbf{X}_S^{\top}\boldsymbol{\Theta}$ *and* $\mathbf{A}=\boldsymbol{\Sigma}_{S,S}-\boldsymbol{\Sigma}_{S,-S}\boldsymbol{\Sigma}_{-S,-S}^{-1}\boldsymbol{\Sigma}_{-S,S}$*. Under the assumption that* $s/n=o(1)$ *and* $\|\mathbf{A}^{-1}\|\leq B$ *for some constant* $B>0$*, we have* $\|w\|=O_p(\|a_S\|)$*.*

Proof of Lemma A.9. Note that

$$\|w\|=\|(n^{-1}\mathbf{X}_S^{\top}\boldsymbol{\Theta})^{-1}a_S\|\leq\|\hat{\mathbf{A}}^{-1}\|\|a_S\|.$$

We want to bound $\|\hat{\mathbf{A}}^{-1}\|$. Using the properties of operator norm, we have

$$\|\hat{\mathbf{A}}^{-1}\| \leq \|\hat{\mathbf{A}}^{-1} - \mathbf{A}^{-1}\| + \|\mathbf{A}^{-1}\| \leq \|\hat{\mathbf{A}}^{-1}\|\|\mathbf{A}^{-1}\|\|\mathbf{A} - \hat{\mathbf{A}}\| + \|\mathbf{A}^{-1}\|.$$

Rearranging the terms, we obtain

$$\|\hat{\mathbf{A}}^{-1}\|(1 - \|\mathbf{A}^{-1}\|\|\mathbf{A} - \hat{\mathbf{A}}\|) \leq \|\mathbf{A}^{-1}\|.$$

With the assumption $\|\mathbf{A}^{-1}\| \leq B$, we have

$$1 - \|\mathbf{A}^{-1}\|\|\mathbf{A} - \hat{\mathbf{A}}\| \geq 1 - B\|\mathbf{A} - \hat{\mathbf{A}}\|.$$

Under the assumption $s/n = o(1)$, by Lemmas A.6 and A.8, we have $\|\mathbf{A} - \hat{\mathbf{A}}\| = o_p(1)$. Thus $1 - \|\mathbf{A}^{-1}\|\|\mathbf{A} - \hat{\mathbf{A}}\|$ is bounded from below by a positive constant with probability tending to one. Thus

$$\|\hat{\mathbf{A}}^{-1}\| \leq (1 - \|\mathbf{A}^{-1}\|\|\mathbf{A} - \hat{\mathbf{A}}\|)^{-1}\|\mathbf{A}^{-1}\| \leq (1 - B\|\mathbf{A} - \hat{\mathbf{A}}\|)^{-1}\|\mathbf{A}^{-1}\|$$

which implies that $\|\hat{\mathbf{A}}^{-1}\| = O_p(1)$. The conclusion follows directly. ♢

Lemma A.10. *Let $\mathbf{\Theta} \in \mathbb{R}^{n\times s}$ where the l-th column vector is θ_l for $l \in S$ as in Corollary A.3 and $\breve{v}_a = \mathbf{\Theta}w$ where $w = (n^{-1}\mathbf{X}_S^\top\mathbf{\Theta})^{-1}a_S$. Then, under Assumption 2.5 and $\|a_S\| = O(1)$, we have $n^{-1}\|\breve{v}_a\|^2 = O_p(1)$.*

Proof of Lemma A.10. We note that

$$\|\mathbf{\Theta}w\|^2 \leq \|\mathbf{X}_S - \mathbf{X}_{-S}\mathbf{\Sigma}_{-S,-S}^{-1}\mathbf{\Sigma}_{-S,S}\|^2\|w\|_2^2 \leq 2\underbrace{\{\|\mathbf{X}_S\|^2 + \|\mathbf{X}_{-S}\mathbf{\Sigma}_{-S,-S}^{-1}\mathbf{\Sigma}_{-S,S}\|^2\}}_{I}\|w\|_2^2.$$

We shall control I below. Lemma 5.3 in Vershynin (2012) gives us

$$\|\mathbf{X}_S\|^2 \leq 4 \max_{c\in\mathcal{N}_{1/2}} c^\top \mathbf{X}_S' \mathbf{X}_S c,$$

$$\|\mathbf{X}_{-S}\boldsymbol{\Sigma}_{-S,-S}^{-1}\boldsymbol{\Sigma}_{-S,S}\|^2 \leq 4 \max_{d\in\mathcal{N}_{1/2}} d^\top \boldsymbol{\Sigma}_{S,-S}\boldsymbol{\Sigma}_{-S,-S}^{-1}\mathbf{X}_{-S}'\mathbf{X}_{-S}\boldsymbol{\Sigma}_{-S,-S}^{-1}\boldsymbol{\Sigma}_{-S,S} d.$$

Let $\mathbf{Q} = \boldsymbol{\Sigma}_{S,-S}\boldsymbol{\Sigma}_{-S,-S}^{-1}\left(n^{-1}\mathbf{X}_{-S}^\top\mathbf{X}_{-S} - \boldsymbol{\Sigma}_{-S,-S}\right)\boldsymbol{\Sigma}_{-S,-S}^{-1}\boldsymbol{\Sigma}_{-S,S}$. Since the elements of the terms inside the maximization can be expressed as a sum of independent sub-exponential random variables, we can use similar arguments as in the proof of Lemma A.3 to show that for every $\delta > 0$,

$$\mathbb{P}\left(\|\mathbf{Q}\| \leq \sqrt{\frac{4}{C_{\kappa'}}\frac{s}{n}\log\frac{2}{\delta}}\right) \leq 1-\delta$$

where $C_{\kappa'} > 0$ is an absolute constant which only depends on $\kappa' = 2\kappa^2\sqrt{\Lambda_{\min}^{-1}D^2}$. Together with Lemma A.6, we have

$$\begin{aligned} n^{-1}\{\|\mathbf{X}_S\|^2 + \|\mathbf{X}_{-S}\boldsymbol{\Sigma}_{-S,-S}^{-1}\boldsymbol{\Sigma}_{-S,S}\|^2\} \leq & C_0\left\{o_p(1) + \lambda_{\max}(\boldsymbol{\Sigma}_{S,S}) + \lambda_{\max}(\boldsymbol{\Sigma}_{S,-S}\boldsymbol{\Sigma}_{-S,-S}^{-1}\boldsymbol{\Sigma}_{-S,S})\right\} \\ \leq & C_0\left\{o_p(1) + 2\lambda_{\max}(\boldsymbol{\Sigma}_{S,S})\right\}, \end{aligned}$$

for some constant C_0. Therefore, we have

$$n^{-1}\|\boldsymbol{\Theta}w\|_2^2 \leq 2C_0(o_p(1) + 2\Lambda_{\min}^{-2})O_p(\|a_S\|^2) = O_p(1).$$

♢

Proof of Theorem 2.2. The arguments below are conditional on the sets $\mathcal{A}_S^{(1)}$ and $\mathcal{A}_S^{(2)}$ which have nonrandom limits by Proposition 2.1. Let $\breve{u}_{a1} = \max_{k\in\mathcal{A}_j^{(1)}} n^{-1}|\breve{v}_a^\top X_k|$ and $\breve{u}_{a2} = \max_{k\in\mathcal{A}_j^{(2)}} n^{-1}|\breve{v}_a^\top X_k|$, where $\breve{v}_a$ is as in Lemma A.10. Then, $(\breve{u}_{a1}, \breve{u}_{a2}, \breve{v}_a)$ is a feasible point to problem (2.22). By the definition of $\tilde{v}_a$,

$$C_1\frac{n}{\log p}\tilde{u}_{a1}^2 + C_2\frac{n}{\log p}\tilde{u}_{a2}^2 + n^{-1}\|\tilde{v}_a\|^2 \leq C_1\frac{n}{\log p}\breve{u}_{a1}^2 + C_2\frac{n}{\log p}\breve{u}_{a2}^2 + n^{-1}\|\breve{v}_a\|^2.$$

Then, for $i = 1, 2$, we must have

$$\begin{aligned}\sqrt{C_i \frac{n}{\log p}} \tilde{u}_{ai} &\leq \max\{C_1, C_2\} \frac{n}{\log p} \max_{k \notin S} n^{-1} |w^\top \mathbf{\Theta}^\top X_k| + n^{-1} \|\breve{v}_a\|^2 \\ &\leq \max\{C_1, C_2\} \|w\| (\xi_0')^2 + M_a\end{aligned}$$

with probability tending to 1 for $0 < \xi_0' \leq \min_l \kappa_{0l} \sqrt{sn(\log p)^{-1}}$ and some constant M_a according to Corollary A.3 and Lemma A.10. Then, by Assumptions 2.3 and 2.6,

$$|\sqrt{n} R(\tilde{v}_a, \beta_{-S})| = n^{-1/2} |\tilde{v}_a^\top \mathbf{X}_{-S} (\beta_{-S} - \hat{\beta}_{-S})| \leq n^{-1} \max_{k \notin S} |\tilde{v}_a^\top X_k| \sqrt{n} \|\hat{\beta}_{-S} - \beta_{-S}\|_1 = o_p(1).$$

Hence, we obtain

$$\sqrt{n}(\tilde{\beta}_S(\tilde{v}_a) - a_S^\top \beta_S) = \frac{1}{\sqrt{n}} \tilde{v}_a^\top \epsilon + o_p(1). \tag{S1}$$

Finally we can apply the central limit theorem as in the proof of Theorem 2.1, which completes the proof. $\diamondsuit$

A.2 Additional numerical results

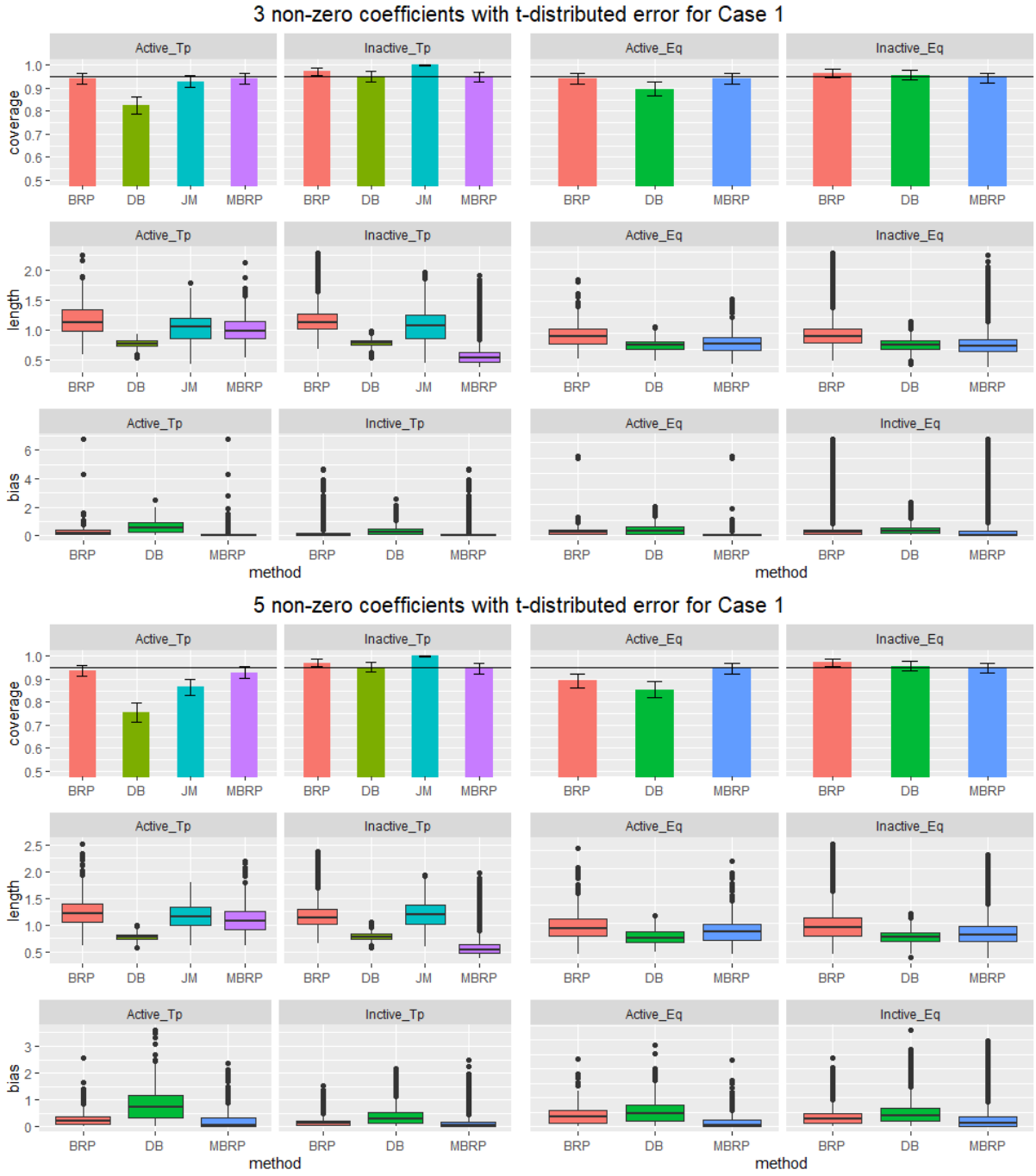

Figure A.1: Simulation results for Case 1 with $s_0 = 3, 5$ and t-distributed random error. Barplots for the empirical coverage and boxplots for the length and bias of the 95% confidence intervals. The horizontal line in the barplots indicates the nominal level. Error bars in the barplots represent the interval within one standard deviation of the empirical coverage.

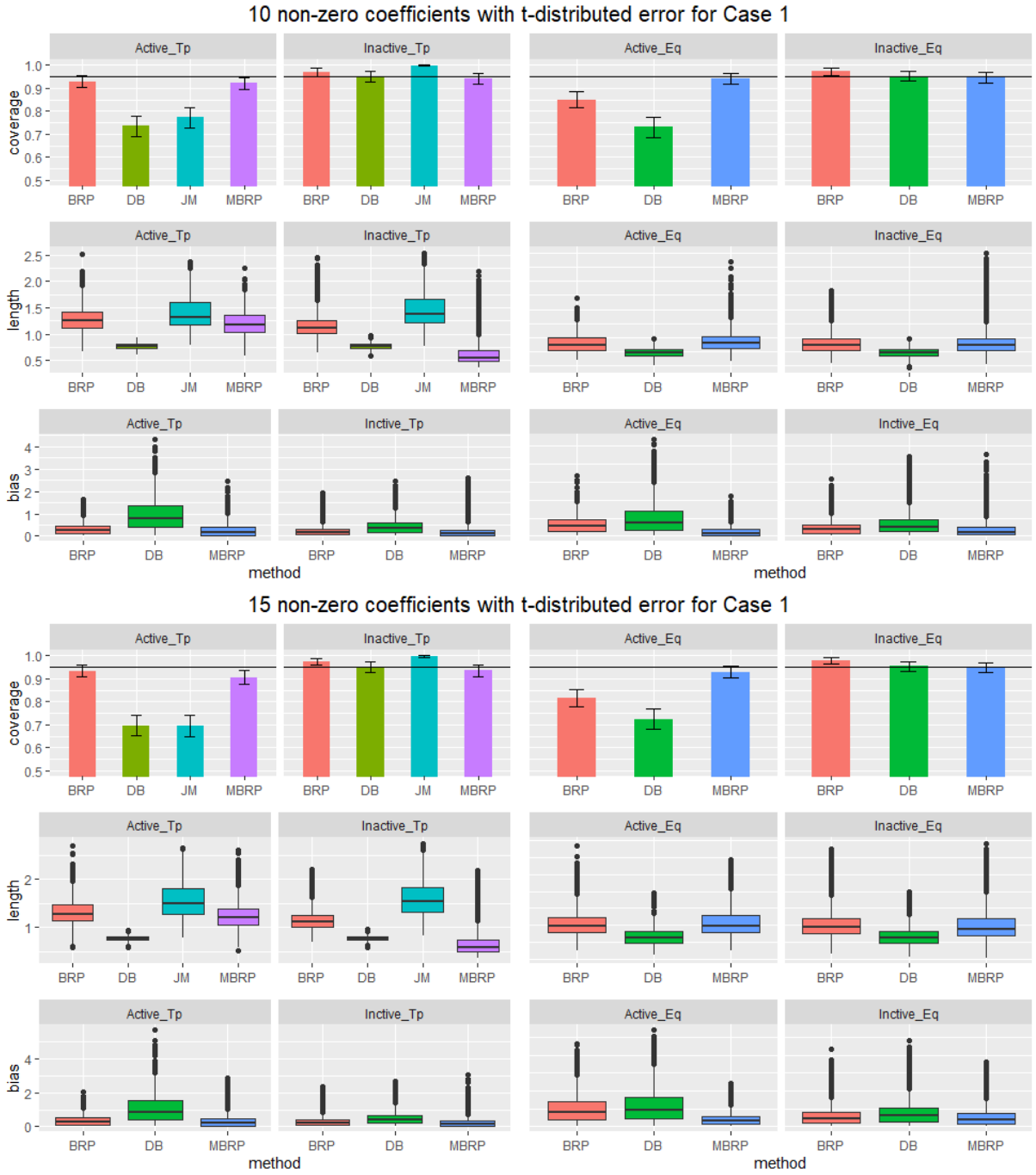

Figure A.2: Simulation results for Case 1 with $s_0 = 10, 15$ and t-distributed random error. Barplots for the empirical coverage and boxplots for the length and bias of the 95% confidence intervals. The horizontal line in the barplots indicates the nominal level. Error bars in the barplots represent the interval within one standard deviation of the empirical coverage.

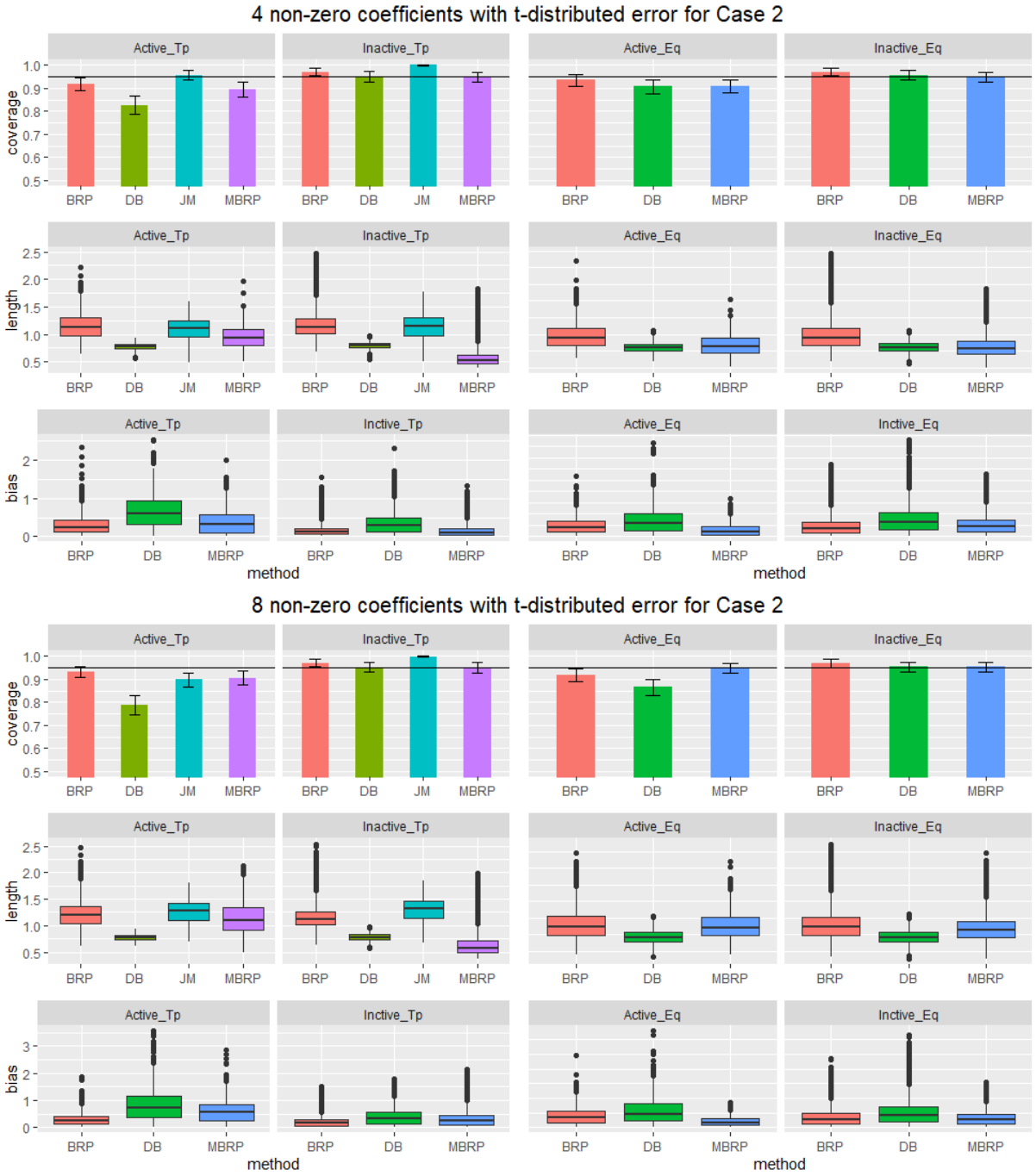

Figure A.3: Simulation results for Case 1 with $s_0 = 4, 8$ and t-distributed random error. Barplots for the empirical coverage and boxplots for the length and bias of the 95% confidence intervals. The horizontal line in the barplots indicates the nominal level. Error bars in the barplots represent the interval within one standard deviation of the empirical coverage.

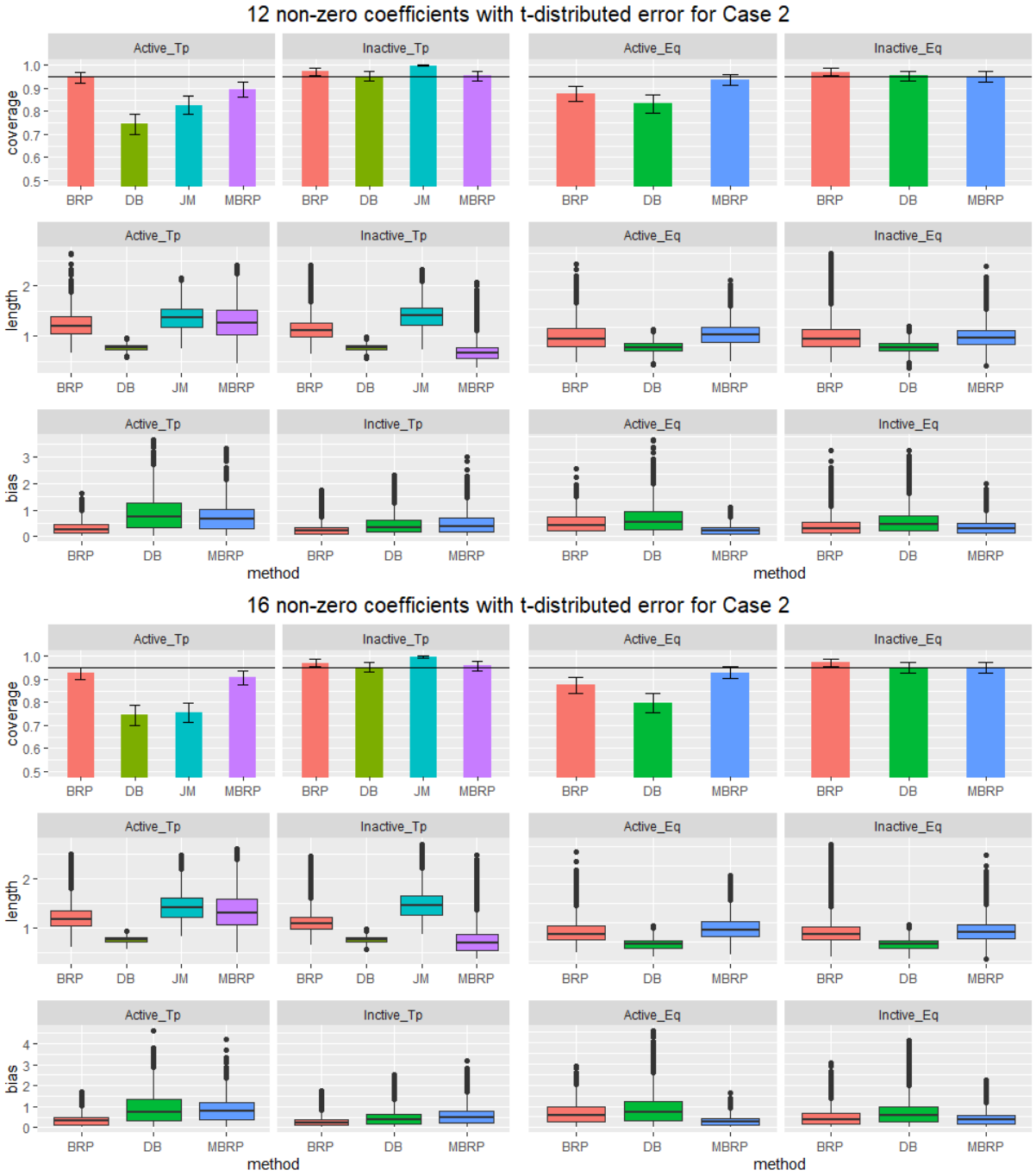

Figure A.4: Simulation results for Case 1 with $s_0 = 12, 16$ and t-distributed random error. Barplots for the empirical coverage and boxplots for the length and bias of the 95% confidence intervals. The horizontal line in the barplots indicates the nominal level. Error bars in the barplots represent the interval within one standard deviation of the empirical coverage.

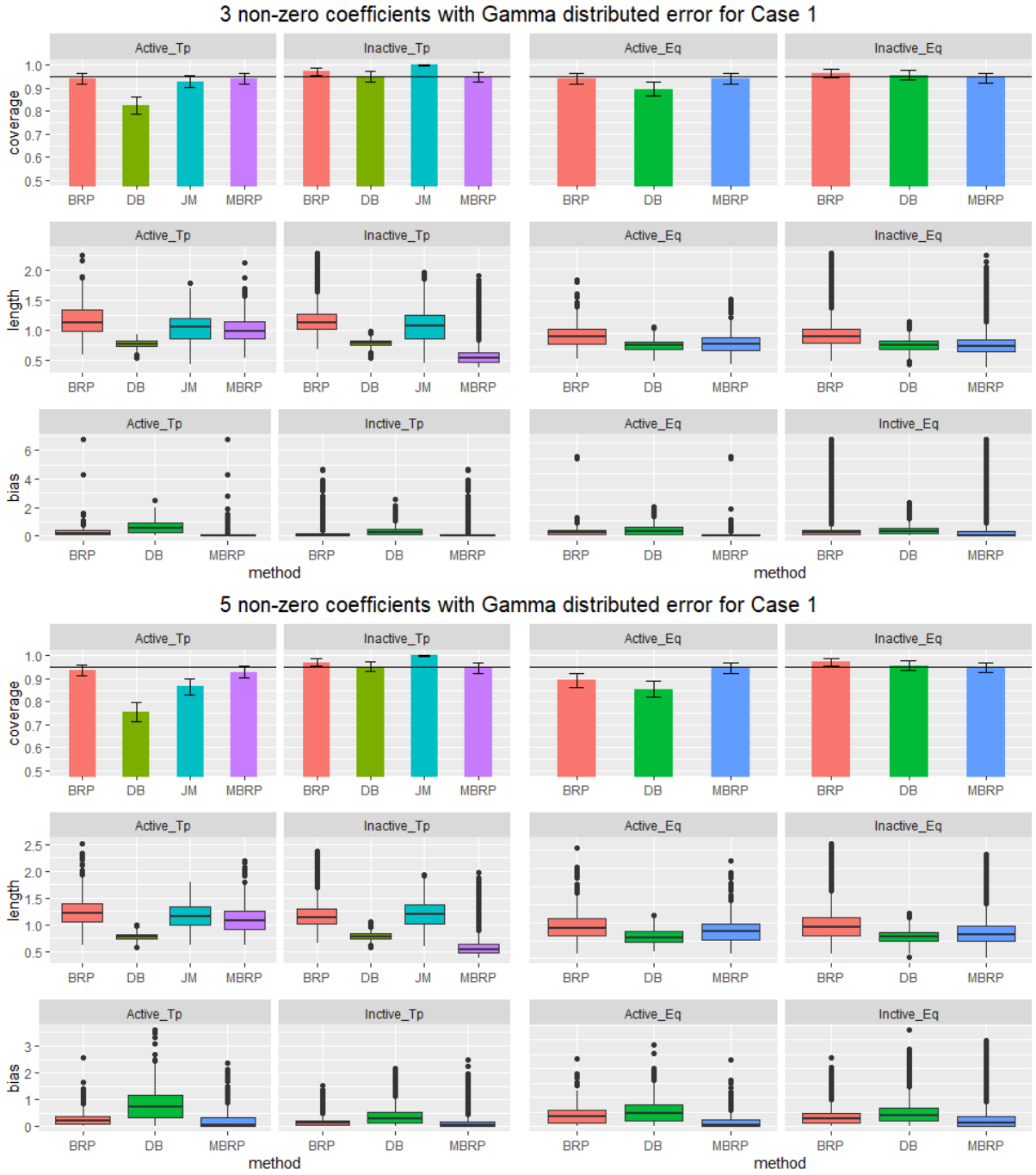

Figure A.5: Simulation results for Case 1 with $s_0 = 3, 5$ and Gamma-distributed random error. Barplots for the empirical coverage and boxplots for the length and bias of the 95% confidence intervals. The horizontal line in the barplots indicates the nominal level. Error bars in the barplots represent the interval within one standard deviation of the empirical coverage.

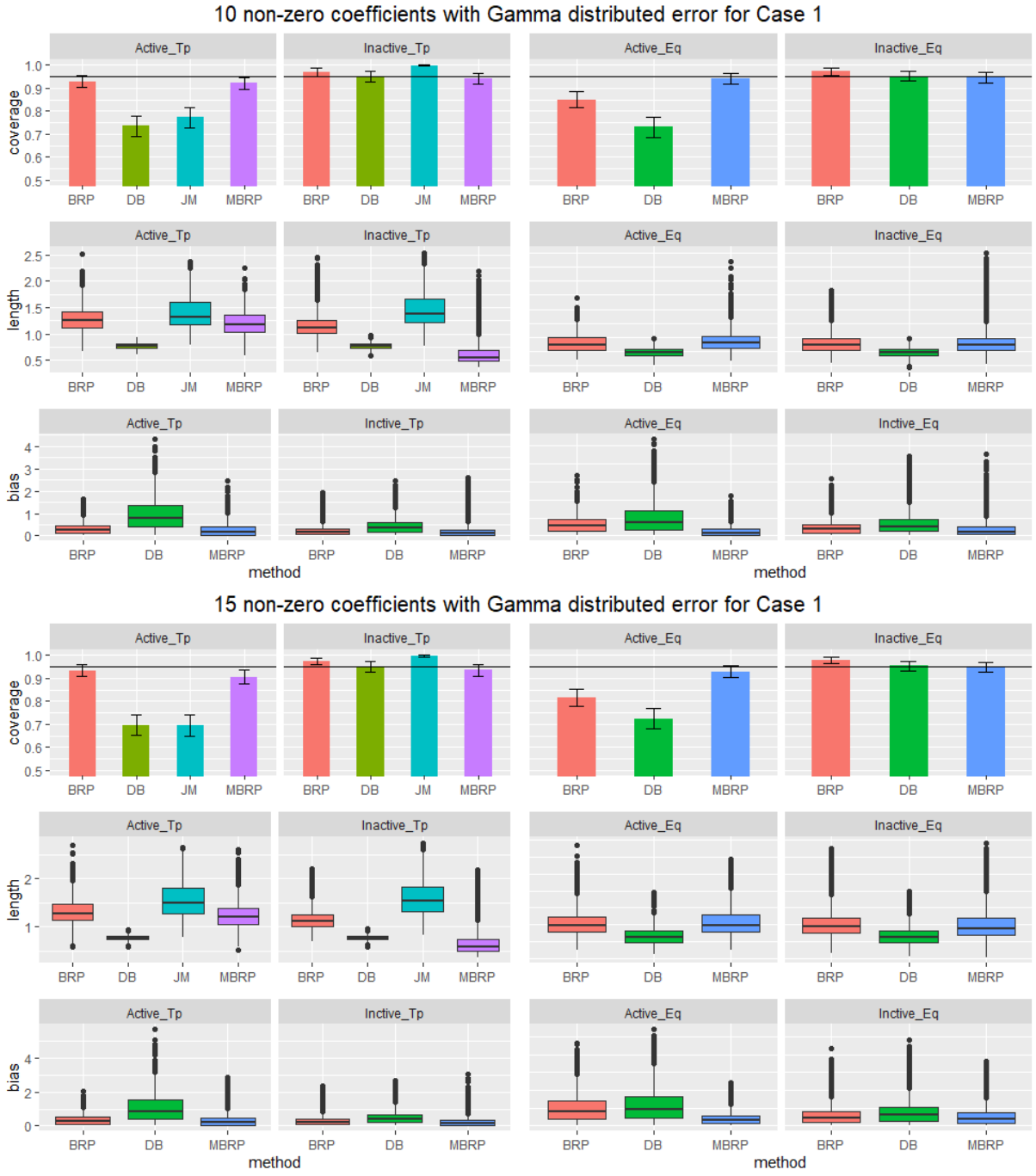

Figure A.6: Simulation results for Case 1 with $s_0 = 10, 15$ and Gamma-distributed random error. Barplots for the empirical coverage and boxplots for the length and bias of the 95% confidence intervals. The horizontal line in the barplots indicates the nominal level. Error bars in the barplots represent the interval within one standard deviation of the empirical coverage.

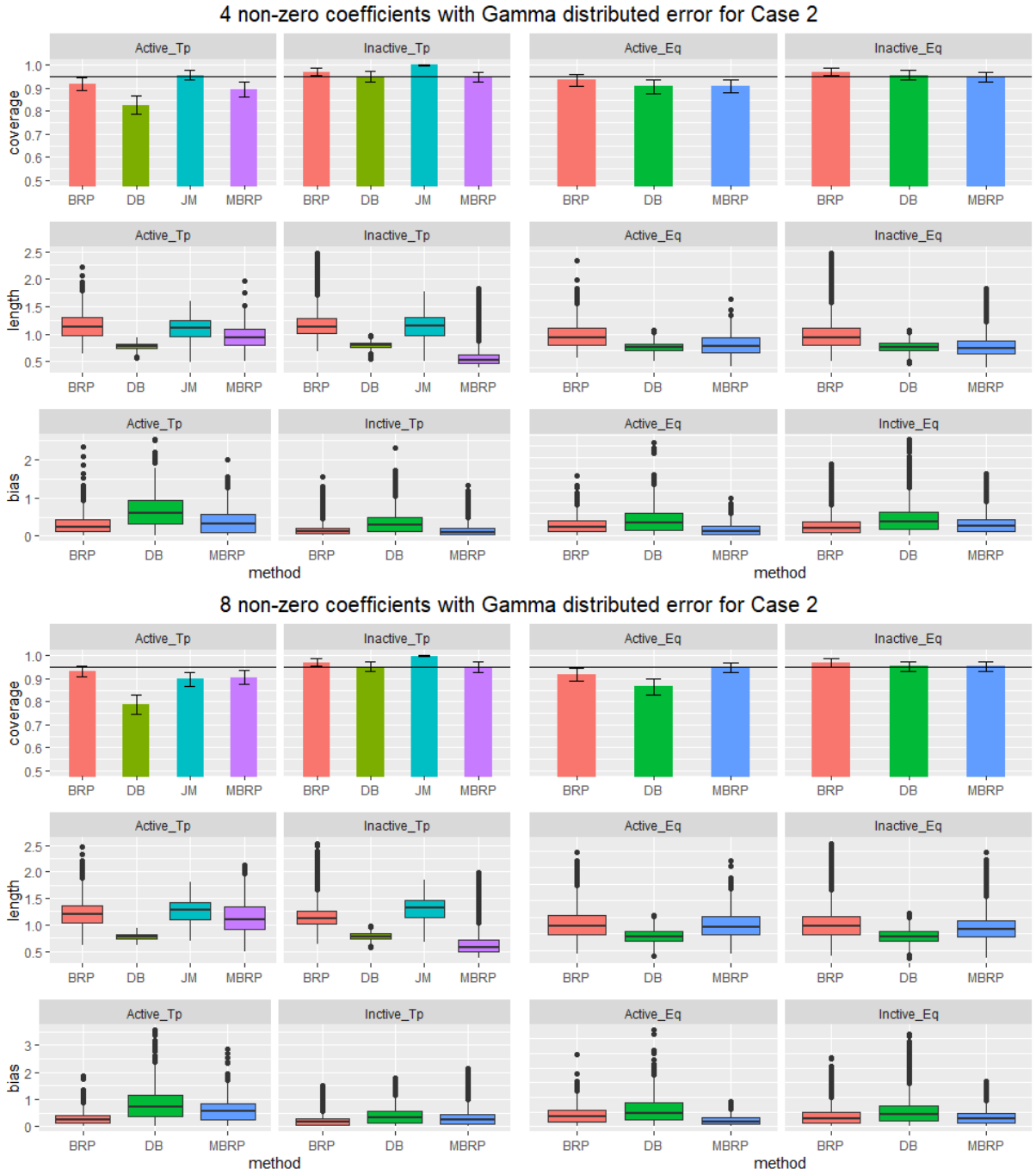

Figure A.7: Simulation results for Case 2 with $s_0 = 4, 8$ and Gamma-distributed random error. Barplots for the empirical coverage and boxplots for the length and bias of the 95% confidence intervals. The horizontal line in the barplots indicates the nominal level. Error bars in the barplots represent the interval within one standard deviation of the empirical coverage.

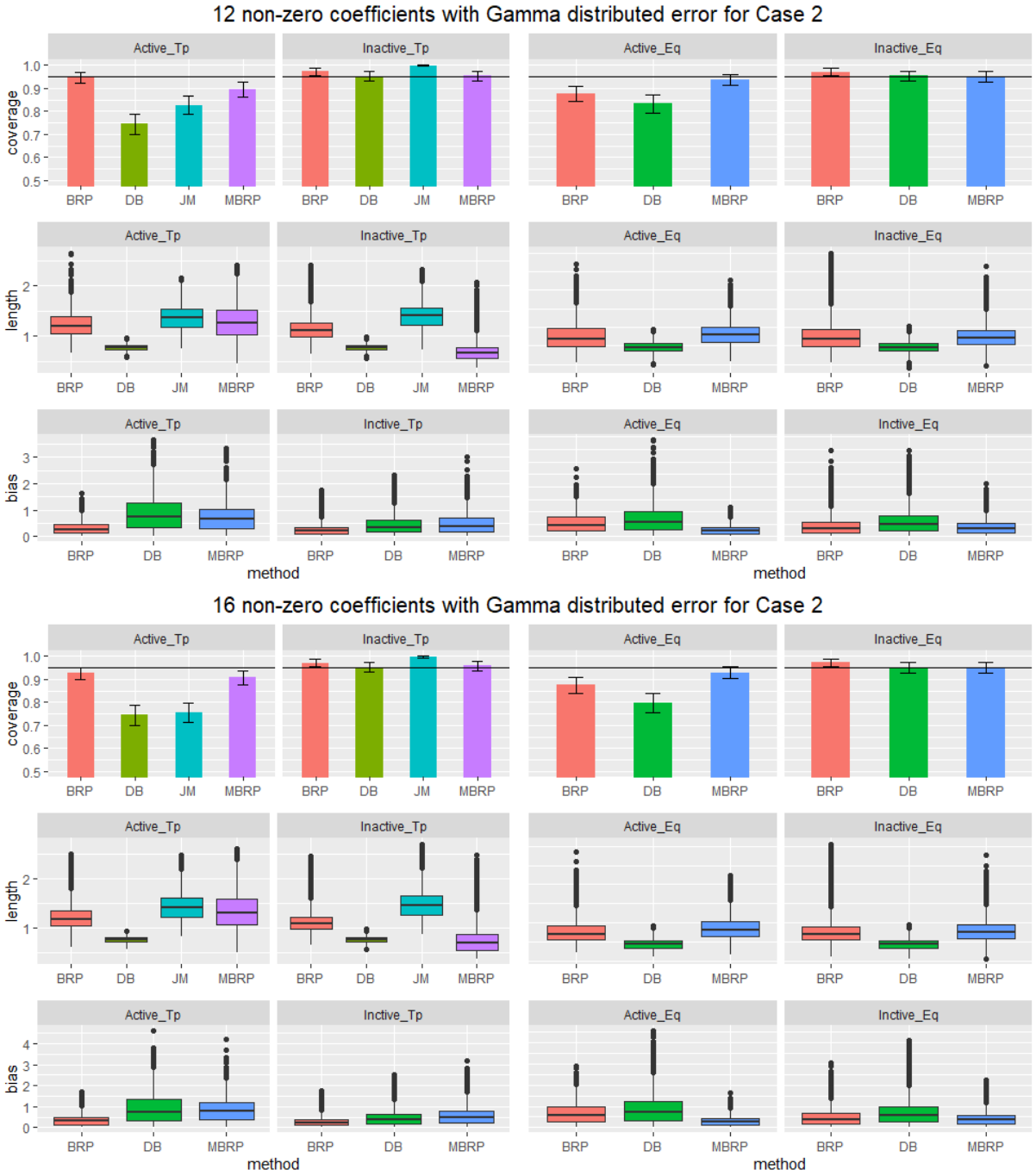

Figure A.8: Simulation results for Case 2 with $s_0 = 12, 16$ and Gamma-distributed random error. Barplots for the empirical coverage and boxplots for the length and bias of the 95% confidence intervals. The horizontal line in the barplots indicates the nominal level. Error bars in the barplots represent the interval within one standard deviation of the empirical coverage.

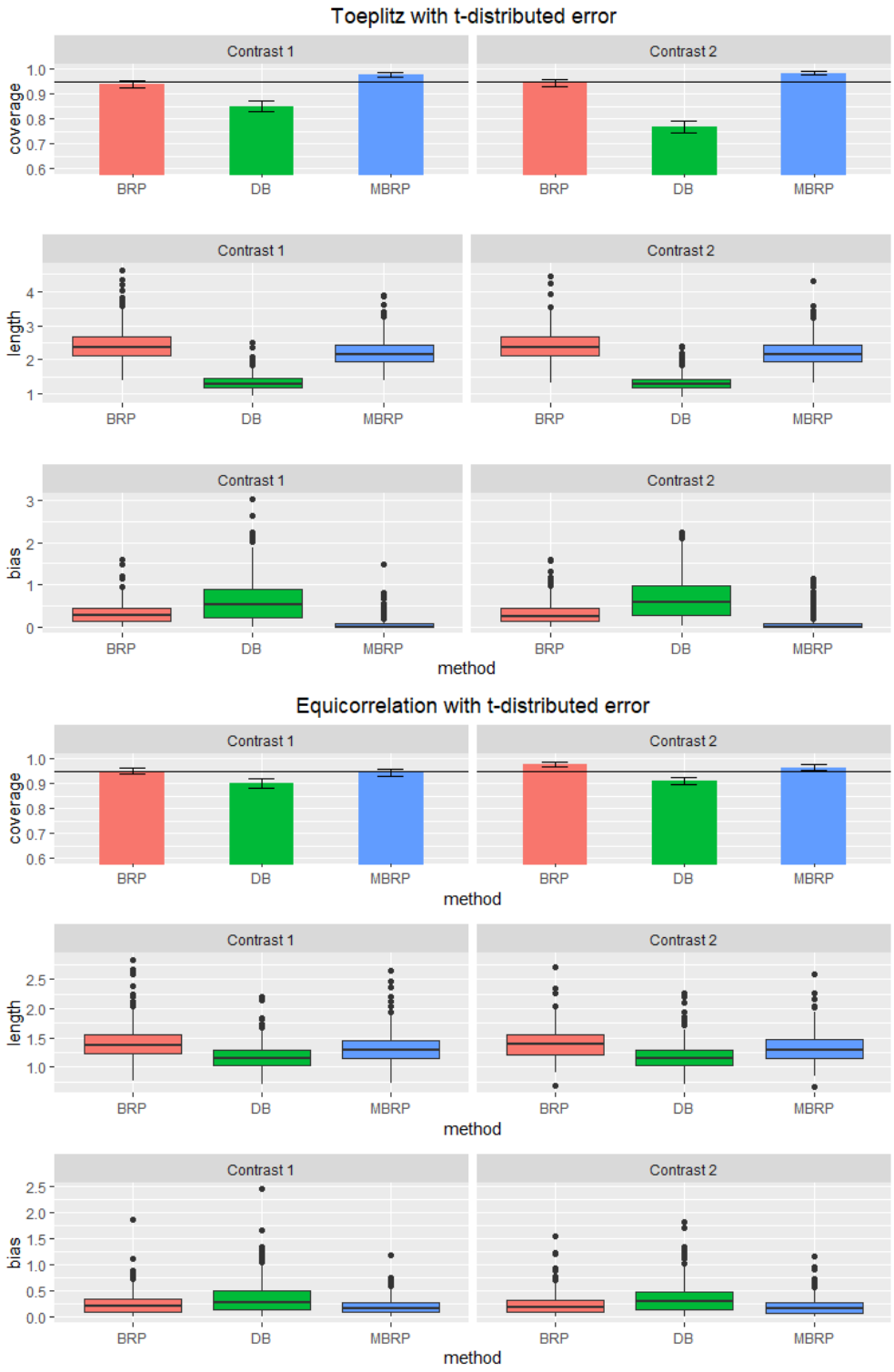

Figure A.9: Simulation results for a sparse linear combination of β and t-distributed random error. Barplots for the empirical coverage and boxplots for the length and bias of the 95% confidence intervals for each contrast. The horizontal line in the barplots indicates the nominal level. Error bars in the barplots represent the interval within one standard deviation of the empirical coverage.

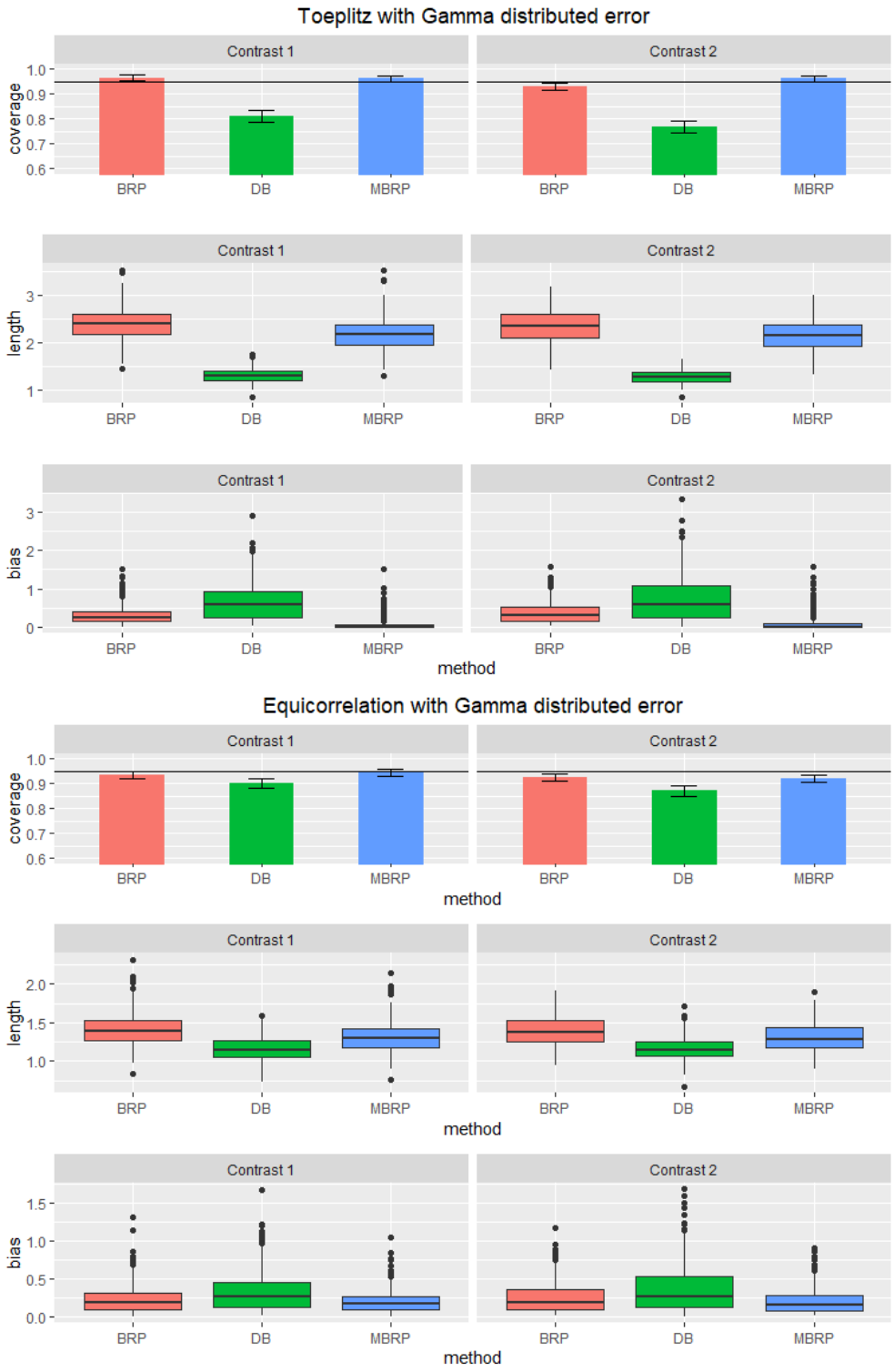

Figure A.10: Simulation results for a sparse linear combination of β and Gamma-distributed random error. Barplots for the empirical coverage and boxplots for the length and bias of the 95% confidence intervals for each contrast. The horizontal line in the barplots indicates the nominal level. Error bars in the barplots represent the interval within one standard deviation of the empirical coverage.

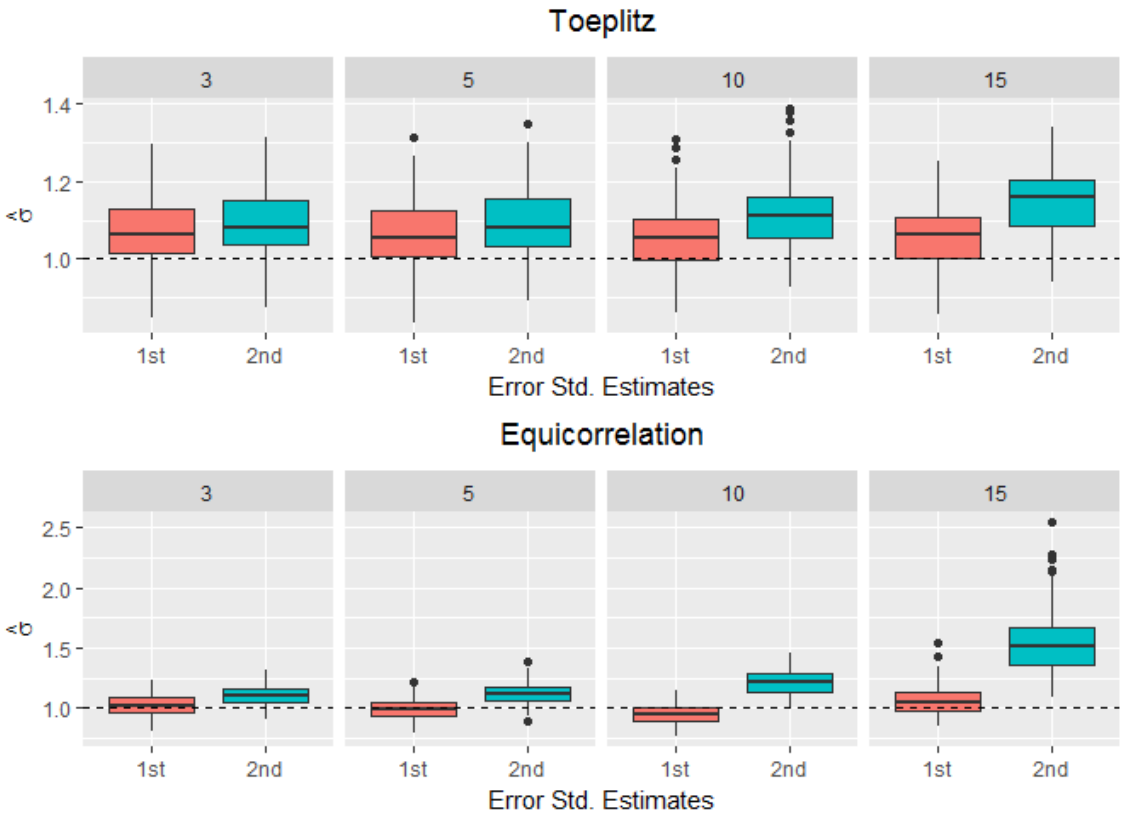

Figure A.11: Boxplots of the two different error variance estimators. Data i s generated by Case 1 with $s_0 = 3, 5, 10$ and 15. "1st" denotes the estimator $\|Y - X\hat{\beta}\|^2/n$ and "2nd" denotes the estimator $\|Y - X\hat{\beta}\|^2/(n - \|\hat{\beta}\|_0)$. The number on the top of each panel denotes the number of non-zero coefficients. The horizontal dashed line corresponds to the true error variance.

APPENDIX B

SUPPLEMENTARY MATERIAL TO CHAPTER 3

B.1 Data generation for Figures 3.1-3.2

To generate Figures 3.1-3.2, 300 independent simulation runs are conducted with $n = 100$, $m = 2000$ and $d = 1$. We simulate $X = (X_1, \cdots, X_{100})^\top, Z = (Z_1, \cdots, Z_{100})^\top$ by

$$X_k \sim N(r\varepsilon_k^*, 1), \quad Z_k \sim N(r\varepsilon_k^*, 1) \tag{B.1}$$

where $r = 1.0, 1.5, 2.0$ and $\varepsilon_k^* \overset{i.i.d.}{\sim} N(0,1)$. We generate $Y_i \in \mathbb{R}^{100\times 1}$ under (3.1) with $\alpha = (\alpha_1, \ldots, \alpha_m)^\top$ and $\beta = (\beta_1, \ldots, \beta_m)^\top$ such that

$$\text{Category A} : \alpha_{I_A} = 0.5 \times \mathbf{1}_{|I_A|}, \quad \beta_{I_A} = \mathbf{0}_{|I_A|}, \quad \text{Category B} : \alpha_{I_B} = \mathbf{0}_{|I_B|}, \quad \beta_{I_B} = 0.5 \times \mathbf{1}_{|I_B|},$$
$$\text{Category C} : \alpha_{I_C} = \beta_{I_C} = 0.5 \times \mathbf{1}_{|I_C|}, \quad \text{Category D} : \alpha_{I_D} = \beta_{I_D} = \mathbf{0}_{|I_D|},$$

where $I_A, I_B, I_C, I_D \subset \{1, \ldots, M\}$ denote some mutually disjoint index sets. We fix $|I_A| = 67, |I_B| = 66, |I_C| = 66$ and randomly generate these index sets for each simulation run. And the following `R` command is used to generate the grids for thresholds t_1, t_2 are used:

$$\text{for } t_1 : \texttt{seq}(\min|Z_i^U|, \max|Z_i^U|, \texttt{len} = 250), \quad \text{for } t_2 : \texttt{seq}(\min|Z_i^A|, \max|Z_i^A|, \texttt{len} = 250).$$

B.2 Extension of the two-step procedure to GLM

Our goal here is to extend the idea of the two-step procedure under the model (3.1) to the generalized linear model (GLM) setup.

B.2.1 Setup

Assume we have the response vector $Y_i = (Y_{i1}, \ldots, Y_{in})^\top \in \mathbb{R}^{n\times 1}$ for $i = 1, \ldots, m$ and let $X = (X_1, \ldots, X_n)^\top \in \mathbb{R}^{n\times 1}$ and $\mathbf{Z} = (Z_1, \ldots, Z_n)^\top \in \mathbb{R}^{n\times d}$ be the covariate of interest and the

design matrix associated with the confounding factors, respectively. Under the GLM framework, the response is often modeled by the exponential family with the probability density such that

$$f(Y_{ij};\theta_{ij},\phi)=\exp\left\{\frac{Y_{ij}\theta_{ij}-\kappa(\theta_{ij})}{a(\phi)}+c(Y_{ij},\phi)\right\} \tag{B.2}$$

where θ_{ij} is called the natural parameter and ϕ is the fixed dispersion parameter and $\kappa(\cdot), a(\cdot), c(\cdot)$ are the known function. Recall that the GLM relates the linear predictor $\eta_{ij}=X_j\alpha_{0i}+Z_j^\top\beta_{0i}$ to the mean of the response μ_{ij} by using the link function g such that

$$\mathrm{E}[Y_{ij}]=\kappa'(\theta_{ij})=\mu_{ij}=g^{-1}(\eta_{ij})$$

where $\alpha_{0i}\in\mathbb{R}$ and $\beta_{0i}\in\mathbb{R}^{d\times 1}$ denote the true parameters associated with the covariate and confounding factors, respectively. If g is chosen to be the so-called canonical link function[1] such that $\theta_{ij}=\eta_{ij}$, the log-likelihood is

$$\ell_n(\alpha_i,\beta_i)=\sum_{j=1}^{n}\left\{\frac{Y_{ij}(X_j\alpha_i+Z_j^\top\beta_i)-\kappa(X_j\alpha_i+Z_j^\top\beta_i)}{a(\phi)}+c(Y_{ij},\phi)\right\} \tag{B.3}$$

under (B.2). Recall that our main interest is to conduct multiple testing for the set of the null hypotheses $\{H_{0i}:\alpha_{0i}=0\}_{i=1}^m$ by using both the unadjusted and adjusted z-statistics which will be defined in the following section.

B.2.2 Unadjusted and Adjusted z-statistics in GLM with the canonical link

Let $\hat{\alpha}_i^A$ be the estimator of α_{0i} after adjusting for the confounding effect and $\hat{\alpha}_i^U$ be the unadjusted version without taking into account the confounding factors. Then, $\hat{\alpha}_i^U$ and $\hat{\alpha}_i^A$ are defined as

$$\begin{aligned}\hat{\alpha}_i^U&=\operatorname*{argmax}_{\tau_i}\ell_n^U(\tau_i)=\operatorname*{argmax}_{\tau_i}\ell_n(\tau_i,0),\\(\hat{\alpha}_i^A,\hat{\beta}_i^A)^\top&=\operatorname*{argmax}_{\alpha_i,\beta_i}\ell_n(\alpha_i,\beta_i).\end{aligned} \tag{B.4}$$

[1]We consider the canonical link for g just to simplify the notation. The similar arguments in the next section can be also used to define the unadjusted and adjusted z-statistics for the other choice of g.

Recall that the asymptotic joint distribution of $\hat{\alpha}_i^U$ and $\hat{\alpha}_i^A$ needs to be derived to define the adjusted and unadjusted z-statistics. To do so, we follow the same idea in the classical MLE theory: applying the Taylor expansion and Central Limit Theorem (CLT).

According to Fahrmexr (1990)[2], under suitable conditions, the quasi-MLE $\hat{\alpha}_i^U$ is weakly consistent for $\tau_{0i} := \tau_{0i}(n)$ such that τ_{0i} is the root of the following equation:

$$s_n(\tau_i) = \mathbb{E}\left[\frac{\partial \ell_n^U(\tau_i)}{\partial \tau_i}\right] = 0. \tag{B.5}$$

Let $f : \mathbb{R}^{d+2} \to \mathbb{R}^{d+2}$ be the function such that

$$\begin{aligned} f(\tau_{0i}, \alpha_{0i}, \beta_{0i}) &= \left(\left.\frac{\partial \ell_n^U(\tau_i)}{\partial \tau_i}\right|_{\tau_i=\tau_{0i}} \quad \nabla \ell_n(\alpha_{0i}, \beta_{0i})\right)^\top \\ &= \sum_{j=1}^n a(\phi)^{-1} \begin{pmatrix} X_j \left\{Y_{ij} - \kappa'(X_j\tau_{0i})\right\} \\ X_j \left\{Y_{ij} - \kappa'(X_j\alpha_{0i} + Z_j^\top \beta_{0i})\right\} \\ Z_{j1} \left\{Y_{ij} - \kappa'(X_j\alpha_{0i} + Z_j^\top \beta_{0i})\right\} \\ \vdots \\ Z_{jd} \left\{Y_{ij} - \kappa'(X_j\alpha_{0i} + Z_j^\top \beta_{0i})\right\} \end{pmatrix} \end{aligned}$$

where $\nabla \ell_n(\alpha_{0i}, \beta_{0i})$ denotes the gradient of ℓ_n evaluated at $(\alpha_{0i}, \beta_{0i})$ and $Z_j^\top = (Z_{j1}, \ldots, Z_{jd})$. By using the Taylor expansion for the vector-valued function, it follows that

$$f(\hat{\alpha}_i^U, \hat{\alpha}_i^A, \hat{\beta}_i^A) \approx f(\tau_{0i}, \alpha_{0i}, \beta_{0i}) + \{Df(\tau_{0i}, \alpha_{0i}, \beta_{0i})\} (\hat{\alpha}_i^U - \tau_{0i}, \hat{\alpha}_i^A - \alpha_{0i}, \hat{\beta}_i^A - \beta_{0i})^\top$$

[2]For more details about the misspecified GLM, see Fahrmexr (1990).

where

$$Df(\tau_{0i}, \alpha_{0i}, \beta_{0i}) = \begin{pmatrix} \left.\frac{\partial^2 \ell_n^U(\tau_i)}{\partial \tau_i^2}\right|_{\tau_i=\tau_{0i}} & \mathbf{0}_{1\times(d+1)} \\ \mathbf{0}_{(d+1)\times 1} & \nabla^2 \ell_n(\alpha_{0i}, \beta_{0i}) \end{pmatrix}$$
$$= \begin{pmatrix} -X^\top \mathbf{Q}_1 X & 0 & \mathbf{0}_{1\times d} \\ 0 & -X^\top \mathbf{Q}_2 X & -X^\top \mathbf{Q}_2 Z \\ \mathbf{0}_{d\times 1} & -Z^\top \mathbf{Q}_2 X & -Z^\top \mathbf{Q}_2 Z \end{pmatrix}$$

for

$$\mathbf{Q}_1 = \text{diag}\left\{\kappa''(X_j\tau_{0i})/a(\phi)\right\}_{j=1}^n, \quad \mathbf{Q}_2 = \text{diag}\left\{\kappa''(X_j\alpha_{0i} + Z_j^\top\beta_{0i})/a(\phi)\right\}_{j=1}^n.$$

Let $b_k^\top$ be the k-th row vector of $\{-\nabla^2\ell_n(\alpha_{0i}, \beta_{0i})\}^{-1}$ and $\mathbf{W} = (W_1, \ldots, W_n)^\top = (X, \mathbf{Z})$. By the first-order condition such that $f(\hat{\alpha}_i^U, \hat{\alpha}_i^A, \hat{\beta}_i^A) = \mathbf{0}_{3\times 1}$ from (B.4), it follows that

$$\begin{pmatrix} \hat{\alpha}_i^U - \tau_{0i} \\ \hat{\alpha}_i^A - \alpha_{0i} \\ \hat{\beta}_i^A - \beta_{0i} \end{pmatrix} \approx \{-Df(\tau_{0i}, \alpha_{0i}, \beta_{0i})\}^{-1} f(\tau_{0i}, \alpha_{0i}, \beta_{0i}) = \sum_{j=1}^n V_j$$

where

$$V_j = a(\phi)^{-1} \begin{pmatrix} (X^\top \mathbf{Q}_1 X)^{-1} X_j \left\{Y_{ij} - \kappa'(X_j\tau_{0i})\right\} \\ b_1^\top W_j \left\{Y_{ij} - \kappa'(X_j\alpha_{0i} + Z_j^\top\beta_{0i})\right\} \\ \vdots \\ b_{d+1}^\top W_j \left\{Y_{ij} - \kappa'(X_j\alpha_{0i} + Z_j^\top\beta_{0i})\right\} \end{pmatrix}.$$

Since V_j's are the independent (but not identically distributed) random vectors, the multivariate version of the Lindeberg-Feller CLT can be used. Thus, we have the following asymptotic normality such that

$$\frac{1}{n}\sum_{j=1}^n V_j \approx N_{d+2}\left(\mathbf{0}_{(d+2)\times 1}, \frac{\bar{\mathbf{S}}}{n}\right) \tag{B.6}$$

by (B.5) and the fact that $\mathbb{E}[Y_{ij}] = \kappa'(X_j\alpha_{0i} + Z_j^\top\beta_{0i})$ where $\bar{\mathbf{S}} = n^{-1}\sum_{j=1}^n \mathbb{E}[(V_j - \mathbb{E}[V_j])(V_j -$

$\mathbb{E}[V_j])^\top]$. By some algebra, $\sum_{j=1}^n \mathbb{E}[(V_j - \mathbb{E}[V_j])(V_j - \mathbb{E}[V_j])^\top]$ can be calculated as

$$a(\phi)^{-2} \begin{pmatrix} (X^\top \mathbf{Q}_1 X)^{-2}(X^\top \mathbf{M} X) & M_1 \\ M_1^\top & \mathbf{M}_2 \end{pmatrix}$$

where

$$\begin{aligned}
\mathbf{M} &= \text{diag}\left\{\mathbb{E}((Y_{ij} - \kappa'(X_j\alpha_{0i} + Z_j^\top \beta_{0i}))^2)\right\}_{j=1}^n = \text{diag}\left\{\kappa''(X_j\alpha_{0i} + Z_j^\top \beta_{0i})a(\phi)\right\}_{j=1}^n, \\
M_1 &= \begin{pmatrix} (X^\top \mathbf{Q}_1 X)^{-1}(X^\top \mathbf{M}\mathbf{W} b_1) & \dots & (X^\top \mathbf{Q}_1 X)^{-1}(X^\top \mathbf{M}\mathbf{W} b_{d+1}) \end{pmatrix}, \\
\mathbf{M}_2 &= \begin{pmatrix} (b_1^\top \mathbf{W}^\top \mathbf{M}\mathbf{W} b_1) & \dots & (b_1^\top \mathbf{W}^\top \mathbf{M}\mathbf{W} b_{d+1}) \\ \vdots & \ddots & \vdots \\ (b_{d+1}^\top \mathbf{W}^\top \mathbf{M}\mathbf{W} b_1) & \dots & (b_{d+1}^\top \mathbf{W}^\top \mathbf{M}\mathbf{W} b_{d+1}) \end{pmatrix}.
\end{aligned}$$

Thus, (B.6) implies that the asymptotic joint distribution of $\hat{\alpha}_i^U$ and $\hat{\alpha}_i^A$ is

$$\begin{pmatrix} \hat{\alpha}_i^U \\ \hat{\alpha}_i^A \end{pmatrix} \approx N_2 \left(\begin{pmatrix} \tau_{0i} \\ \alpha_{0i} \end{pmatrix}, \begin{pmatrix} \sigma_{i1}^2 & \rho_i \sigma_{i1}\sigma_{i2} \\ \rho_i \sigma_{i1}\sigma_{i2} & \sigma_{i2}^2 \end{pmatrix} \right) \tag{B.7}$$

where $\sigma_{i1}^2 = a(\phi)^{-2}(X^\top \mathbf{Q}_1 X)^{-2}(X^\top \mathbf{M} X), \sigma_{i2}^2 = a(\phi)^{-2} b_1^\top \mathbf{W}^\top \mathbf{M}\mathbf{W} b_1$ and

$$\rho_i = \frac{X^\top \mathbf{M}\mathbf{W} b_1}{\sqrt{X^\top \mathbf{M} X}\sqrt{b_1^\top \mathbf{W}^\top \mathbf{M}\mathbf{W} b_1}}.$$

Note that $\mathbf{Q}_1, \mathbf{M}$ and b_1 depend on the unknown parameters τ_{0i}, α_{0i} and β_{0i}. Thus, we consider their estimated versions $\widehat{\mathbf{Q}}_1, \widehat{\mathbf{M}}$ and $\hat{b}_1$ by replacing those with $\hat{\alpha}_i^U, \hat{\alpha}_i^A, \hat{\beta}_i^A$. Then, σ_{i1}^2 and σ_{i2}^2 can be estimated by

$$\hat{\sigma}_{i1}^2 = a(\phi)^{-2}(X^\top \widehat{\mathbf{Q}}_1 X)^{-2}(X^\top \widehat{\mathbf{M}} X), \quad \hat{\sigma}_{i2}^2 = a(\phi)^{-2} \hat{b}_1^\top \mathbf{W}^\top \widehat{\mathbf{M}}\mathbf{W} \hat{b}_1$$

and the unadjusted and adjusted z-statistics are defined as

$$Z_i^U = \frac{\hat{\alpha}_i^U}{\hat{\sigma}_{i1}}, \quad Z_i^A = \frac{\hat{\alpha}_i^A}{\hat{\sigma}_{i2}}$$

and we have

$$\begin{pmatrix} Z_i^U \\ Z_i^A \end{pmatrix} \approx N_2 \left(\begin{pmatrix} \sigma_{i1}^{-1}\tau_{0i} \\ \sigma_{i2}^{-1}\alpha_{0i} \end{pmatrix}, \begin{pmatrix} 1 & \rho_i \\ \rho_i & 1 \end{pmatrix} \right) \tag{B.8}$$

from from (B.7).

B.2.3 Two-stage procedure for GLM with the canonical link

Recall that the two-stage procedure rejects the null hypothesis $H_{0i} : \alpha_{0i} = 0$ when

$$|Z_i^U| \geq t_1, |Z_i^A| \geq t_2$$

for some thresholds $t_1, t_2 \in \mathbb{R}^+$. The false discovery proportion (FDP) can be written as

$$\begin{aligned} \text{FDP}(t_1, t_2) &\approx \frac{\sum_{i:H_{0i} \text{ is true}} L(\sigma_{i1}^{-1}\tau_{0i}, \rho_i; t_1, t_2)}{1 \vee \sum_{i=1}^M \mathbf{1}\{|Z_i^U| \geq t_1, |Z_i^A| \geq t_2\}} \\ &\leq \frac{\sum_{i=1}^m L(\sigma_{i1}^{-1}\tau_{0i}, \rho_i; t_1, t_2)}{1 \vee \sum_{i=1}^M \mathbf{1}\{|Z_i^U| \geq t_1, |Z_i^A| \geq t_2\}} \end{aligned}$$

where $L(\sigma_{i1}^{-1}\tau_{0i}, \rho_i; t_1, t_2) = \mathbb{P}(|\sigma_{i1}^{-1}\tau_{0i} + B_1| \geq t_1, |B_2| \geq t_2 | \sigma_{i1}^{-1}\tau_{0i}, \rho_i)$ for the bivariate normal random variables (B_1, B_2) such that

$$\begin{pmatrix} B_1 \\ B_2 \end{pmatrix} \sim N_2 \left(\begin{pmatrix} 0 \\ 0 \end{pmatrix}, \begin{pmatrix} 1 & \rho_i \\ \rho_i & 1 \end{pmatrix} \right)$$

where ρ_i is the same as (B.7). Recall that our goal at this point is to estimate the numerator of the upper bound of FDP.

We again use the nonparametric empirical Bayes approach to estimate the prior distribution of the location parameter $\sigma_{i1}^{-1}\tau_{0i}$ of Z_i^U. One additional thing to deal with is for ρ_i: though it is to be

known conditional on $X, \mathbf{Z}$ in the linear model, that is not the case in the GLM setup. Thus, we use the plug-in estimates $\hat{\rho}_i$ for ρ_i calculated by using $\hat{\alpha}_i^U, \hat{\alpha}_i^A, \hat{\beta}_i^A$. Note that we have the following approximate Gaussian location model such that

$$Z_i^U \approx \sigma_{i1}^{-1}\tau_{0i} + \varepsilon_i, \quad \varepsilon_i \sim N(0,1)$$

from (B.8). Suppose that $\sigma_{i1}^{-1}\tau_{0i} \overset{i.i.d.}{\sim} G_n$ where the dependence on n is due to τ_{0i} from (B.5). Then, we estimate it by using the general maximum likelihood estimator (GMLE) $\widetilde{G}_{m,n}$ such that

$$\widetilde{G}_{n,m} = \underset{G \in \mathcal{G}}{\operatorname{argmax}} \sum_{i=1}^{m} \log f_G(Z_i^U)$$

where $\mathcal{G}$ denotes the set of all probability distributions on $\mathbb{R}$ and $f_G(x) = \int \phi(x-u)dG(u)$ is the convolution between G and ϕ. Based on this, we approximate $\sum_{i=1}^m L(\sigma_{i1}^{-1}\tau_{0i}, \rho_i; t_1, t_2)$ by $\sum_{i=1}^m \int L(x, \hat{\rho}_i; t_1, t_2) d\widetilde{G}_{m,n}(x)$. With a modification of John Storey's approach, we consider the FDR estimate given by

$$\widetilde{\text{FDP}}_\lambda^{\text{GLM}}(t_1, t_2) = \frac{\sum_{i=1}^m \int L(x, \hat{\rho}_i; t_1, t_2) d\widetilde{G}_{m,n}(x) \mathbf{1}\left\{|Z_i^A| \le \lambda\right\}}{(1-2\Phi(-\lambda)) \sum_{i=1}^m \mathbf{1}\left\{|Z_i^U| \ge t_1, |Z_i^A| \ge t_2\right\}},$$

where λ is a prespecified number as in John Storey's approach. Thus, for a desired FDR level $q \in (0,1)$, we choose the optimal threshold such that

$$(\widetilde{T}_1^{\text{GLM}}, \widetilde{T}_2^{\text{GLM}}) = \underset{(t_1,t_2) \in \mathcal{F}_{q,\lambda}^{\text{GLM}}}{\operatorname{argmax}} \sum_{i=1}^{m} \mathbf{1}\left\{|Z_i^U| \ge t_1, |Z_i^A| \ge t_2\right\},$$

where

$$\mathcal{F}_{q,\lambda}^{\text{GLM}} := \left\{(t_1, t_2) \in \mathbb{R}^+ \times \mathbb{R}^+ : \widetilde{\text{FDP}}_\lambda^{\text{GLM}}(t_1, t_2) \le q\right\}.$$

B.3 Technical Details

We first introduce some concentration inequalities for a later use.

Lemma B.1. *Under Assumptions 3.3-3.4, for $x_0 > 0$, we have*

$$\mathbb{P}\left(|\Omega - \mathbb{E}[\Omega]| > x_0\right) \leq C_0 \exp\left\{-c_0 n(x_0^2/c_0' \wedge x_0/c_0'')\right\},$$
$$\mathbb{P}\left(\|\Psi - \mathbb{E}[\Psi]\|_{\max} > x_0\right) \leq C_1 \exp\left\{-c_1 n(x_0^2/c_1' \wedge x_0/c_1'')\right\},$$
$$\mathbb{P}\left(\|\Gamma - \mathbb{E}[\Gamma]\|_{\max} > x_0\right) \leq C_2 \exp\left\{-c_2 n(x_0^2/c_2' \wedge x_0/c_2'')\right\},$$

and, for $0 < x_1 < 3\left(1 \wedge D_0^2/D_2 \wedge D_0^2 E[\Omega]^{-1}\right)$,

$$\mathbb{P}\left(\|\Omega_{\mathbf{Z}|X} - C_{\mathbf{Z}|X}\|_{\max} > x_1\right) \leq C_3 \exp\left\{-c_3 n(x_1^2/c_3' \wedge x_1/c_3'')\right\}, \tag{B.9}$$

and, for $0 < x_2 < L^{-1}\left(3 \wedge 3D_0^2/D_2 \wedge 3D_0^2 E[\Omega]^{-1}\right) \wedge \left(1 \wedge \frac{3w_0^{-1/2}}{(1 \wedge D_0^{-1})} \wedge (D_1 d)^{-1}\right) := L'$,

$$\mathbb{P}\left(\|\hat{\boldsymbol{a}} - \boldsymbol{a}\|_{\max} > x_2\right) \leq C_4 \exp\left\{-c_4 n(x_2^2/c_4' \wedge x_2/c_4'')\right\}, \tag{B.10}$$

where $C_l, c_l, c_l', c_l'' > 0$ denote some absolute constants for $l = 0, \cdots, 4$ and, for $w_0 = \mathbb{E}[\Gamma] C_{\mathbf{Z}|X}^{-1} \mathbb{E}[\Gamma]^\top$,

$$L = \left(\frac{w_0^{3/2}\left(1 \wedge D_0^{-1}\right)}{6\left\{d^2(1+2D_0)D_1 + D_0^2 D_1^2 d^3\right\} + D_1 d w_0^{3/2}\left(1 \wedge D_0^{-1}\right)} \wedge 1\right)$$

and $D_0, D_1, D_2 > 0$ are some constants such that $\|\mathbb{E}[\Gamma]\|_{\max} \leq D_0$, $\|C_{\mathbf{Z}|X}^{-1}\|_2 \leq D_1$ and $\mathbb{E}[X_1^2] \geq D_2$. As a consequence of the above concentration inequalities, we have

$$\Omega_{\mathbf{Z}|X}^{-1} \xrightarrow{a.s.} C_{\mathbf{Z}|X}^{-1}, \quad \Omega_{X|\mathbf{Z}} \xrightarrow{a.s.} C_{X|\mathbf{Z}}, \quad A \xrightarrow{a.s.} A_0.$$

Proof of Lemma B.1. Each element of $\Psi - \mathbb{E}[\Psi]$, $\Gamma - \mathbb{E}[\Gamma]$ and $\Omega - \mathbb{E}[\Omega]$ is sub-exponential. The first three inequalities thus follow from the union bound and the tail bound for sum of sub-exponential random variables, see e.g. Corollary 5.17 of Vershynin (2010). For (B.9), some algebra gives us

$$\|\Omega_{\mathbf{z}|X} - C_{\mathbf{z}|X}\|_{\max} \leq \|\Psi - \mathbb{E}[\Psi]\|_{\max} + D_0^2|\Omega^{-1} - \mathbb{E}[\Omega]^{-1}| \tag{B.11}$$
$$+ \left\{|\Omega^{-1} - \mathbb{E}[\Omega]^{-1}| + D_2^{-1}\right\}\left\{\|\Gamma - \mathbb{E}[\Gamma]\|_{\max}^2 + 2D_0\|\Gamma - \mathbb{E}[\Gamma]\|_{\max}\right\}.$$

Then, for $0 < x_1 < 3\left(1 \wedge D_0^2/D_2 \wedge D_0^2 E[\Omega]^{-1}\right)$, the following inclusion of events can be verified

$$\begin{aligned}\left\{\|\Omega_{\mathbf{z}|X} - C_{\mathbf{z}|X}\|_{\max} > x_1\right\} \subset &\left[\left\{\|\Psi - \mathbb{E}[\Psi]\|_{\max} > \frac{x_1}{3}\right\} \bigcup \left\{|\Omega^{-1} - \mathbb{E}[\Omega]^{-1}| > \frac{x_1}{3D_0^2}\right\}\right. \\ &\left. \bigcup \left\{\|\Gamma - \mathbb{E}[\Gamma]\|_{\max} > \left(\frac{D_2}{2(1+2D_0)} \wedge 1\right)\frac{x_1}{3}\right\}\right] \\ \subset &\left[\left\{\|\Psi - \mathbb{E}[\Psi]\|_{\max} > \frac{x_1}{3}\right\} \bigcup \left\{|\Omega - \mathbb{E}[\Omega]| > \frac{D_2^2 x_1}{6D_0^2}\right\}\right. \\ &\left. \bigcup \left\{\|\Gamma - \mathbb{E}[\Gamma]\|_{\max} > \left(\frac{D_2}{2(1+2D_0)} \wedge 1\right)\frac{x_1}{3}\right\}\right].\end{aligned}$$

The first inclusion follows because, conditional on the events such that

$$\begin{aligned}&\left[\left\{\|\Psi - \mathbb{E}[\Psi]\|_{\max} \leq \frac{x_1}{3}\right\} \bigcap \left\{|\Omega^{-1} - \mathbb{E}[\Omega]^{-1}| \leq \frac{x_1}{3D_0^2}\right\}\right. \\ &\qquad\left. \bigcap \left\{\|\Gamma - \mathbb{E}[\Gamma]\|_{\max} \leq \left(\frac{D_2}{2(1+2D_0)} \wedge 1\right)\frac{x_1}{3}\right\}\right],\end{aligned}$$

(B.11) implies that

$$\begin{aligned}&\|\Omega_{\mathbf{z}|X} - C_{\mathbf{z}|X}\|_{\max} \\ \leq &\frac{x_1}{3} + \left(\frac{x_1}{3D_0^2} + D_2^{-1}\right)\left\{\left(\frac{D_2}{2(1+2D_0)} \wedge 1\right)^2 \frac{x_1^2}{3^2} + 2D_0\left(\frac{D_2}{2(1+2D_0)} \wedge 1\right)\frac{x_1}{3}\right\} + D_0^2\frac{x_1}{3D_0^2} \\ \leq &\frac{x_1}{3} + 2D_2^{-1}(1+2D_0)\left(\frac{D_2}{2(1+2D_0)} \wedge 1\right)\frac{x_1}{3} + \frac{x_1}{3} \leq x_1.\end{aligned}$$

The second inclusion holds by noticing that

$$\begin{aligned}
&\left\{|\Omega^{-1} - \mathbb{E}[\Omega]^{-1}| > \frac{x_1}{3D_0^2}\right\} = \left\{|\Omega - \mathbb{E}[\Omega]| > |\Omega\mathbb{E}[\Omega]|\frac{x_1}{3D_0^2}\right\} \\
\subset &\left[\left\{|\Omega - \mathbb{E}[\Omega]| > |\Omega\mathbb{E}[\Omega]|\frac{x_1}{3D_0^2}, |\Omega\mathbb{E}[\Omega]| > \frac{\mathbb{E}[\Omega]^2}{2}\right\} \bigcup \left\{|\Omega\mathbb{E}[\Omega]| \leq \frac{\mathbb{E}[\Omega]^2}{2}\right\}\right] \\
\subset &\left[\left\{|\Omega - \mathbb{E}[\Omega]| > \frac{\mathbb{E}[\Omega]^2 x_1}{6D_0^2}\right\} \bigcup \left\{|\Omega - \mathbb{E}[\Omega]| > \frac{\mathbb{E}[\Omega]}{2}\right\}\right] \subset \left\{|\Omega - \mathbb{E}[\Omega]| > \frac{D_2^2 x_1}{6D_0^2}\right\}
\end{aligned} \tag{B.12}$$

when $x_1 < 3D_0^2\mathbb{E}[\Omega]^{-1}$ and $\mathbb{E}[\Omega] = \mathbb{E}[X_1^2] \geq D_2$.

As for the last inequality, we first observe that

$$\begin{aligned}
\|\hat{\boldsymbol{a}} - \boldsymbol{a}\|_{\max} &= \left\|\frac{\Gamma}{\sqrt{w}} - \frac{\mathbb{E}[\Gamma]}{\sqrt{w_0}}\right\|_{\max} \\
&\leq \left|\frac{1}{\sqrt{w}} - \frac{1}{\sqrt{w_0}}\right| \{\|\Gamma - \mathbb{E}[\Gamma]\|_{\max} + \|\mathbb{E}[\Gamma]\|_{\max}\} + \frac{1}{\sqrt{w_0}} \|\Gamma - \mathbb{E}[\Gamma]\|_{\max}
\end{aligned} \tag{B.13}$$

where $w = \Gamma\Omega_{\mathbf{Z}|X}^{-1}\Gamma^\top$ and $w_0 = \mathbb{E}[\Gamma]C_{\mathbf{Z}|X}^{-1}\mathbb{E}[\Gamma]^\top$. It also follows that, for $0 < x'' < w_0^{-1/2}$,

$$\begin{aligned}
\left\{\left|\frac{1}{\sqrt{w}} - \frac{1}{\sqrt{w_0}}\right| > x''\right\} &\subset \left\{\left|\sqrt{w} - \sqrt{w_0}\right| > \frac{w_0}{2}x''\right\} \\
&= \left\{\left|\frac{\sqrt{w}}{\sqrt{w_0}} - 1\right| > \frac{\sqrt{w_0}}{2}x''\right\} \\
&\subset \left\{\left|\frac{w}{w_0} - 1\right| > \frac{\sqrt{w_0}}{2}x''\right\} = \left\{|w - w_0| > \frac{w_0^{3/2}}{2}x''\right\}.
\end{aligned} \tag{B.14}$$

Combining (B.13) with (B.14) implies that, for $0 < x' < \left(3 \wedge \frac{3w_0^{-1/2}}{(1 \wedge D_0^{-1})}\right)$,

$$
\begin{aligned}
&\{\|\hat{\boldsymbol{a}} - \boldsymbol{a}\|_{\max} > x'\} \\
\subset &\left[\left\{\left|\frac{1}{\sqrt{w}} - \frac{1}{\sqrt{w_0}}\right| > \frac{\sqrt{x'}}{\sqrt{3}}\right\} \bigcup \left\{\|\Gamma - \mathbb{E}[\Gamma]\|_{\max} > \frac{\sqrt{x'}}{\sqrt{3}}\right\}\right. \\
&\left. \bigcup \left\{\left|\frac{1}{\sqrt{w}} - \frac{1}{\sqrt{w_0}}\right| \|\mathbb{E}[\Gamma]\|_{\max} > \frac{x'}{3}\right\} \bigcup \left\{\frac{1}{\sqrt{w_0}} \|\Gamma - \mathbb{E}[\Gamma]\|_{\max} > \frac{x'}{3}\right\}\right] \\
\subset &\left[\left\{\left|\frac{1}{\sqrt{w}} - \frac{1}{\sqrt{w_0}}\right| > \frac{x'}{3}\left(1 \wedge D_0^{-1}\right)\right\} \bigcup \left\{\|\Gamma - \mathbb{E}[\Gamma]\|_{\max} > \frac{x'}{3}\left(1 \wedge \sqrt{w_0}\right)\right\}\right] \\
\subset &\left[\left\{|w - w_0| > \frac{x'}{6} w_0^{3/2}\left(1 \wedge D_0^{-1}\right)\right\} \bigcup \left\{\|\Gamma - \mathbb{E}[\Gamma]\|_{\max} > \frac{x'}{3}\left(1 \wedge \sqrt{w_0}\right)\right\}\right].
\end{aligned} \tag{B.15}
$$

Thus, we need to derive the tail bound of $|w - w_0|$. Note that

$$
\begin{aligned}
|w - w_0| &\leq \left|\Gamma \Omega_{\mathbf{Z}|X}^{-1} \Gamma^\top - \mathbb{E}[\Gamma] \Omega_{\mathbf{Z}|X}^{-1} \mathbb{E}[\Gamma]^\top + \mathbb{E}[\Gamma] \Omega_{\mathbf{Z}|X}^{-1} \mathbb{E}[\Gamma]^\top - \mathbb{E}[\Gamma] C_{\mathbf{Z}|X}^{-1} \mathbb{E}[\Gamma]^\top\right| \\
&\leq \underbrace{\left|\Gamma \Omega_{\mathbf{Z}|X}^{-1} \Gamma^\top - \mathbb{E}[\Gamma] \Omega_{\mathbf{Z}|X}^{-1} \mathbb{E}[\Gamma]^\top\right|}_{(*)} + \|\mathbb{E}[\Gamma]\|_2^2 \|\Omega_{\mathbf{Z}|X}^{-1} - C_{\mathbf{Z}|X}^{-1}\|_2
\end{aligned}
$$

and

$$
\begin{aligned}
(*) &= \left|(\Gamma - \mathbb{E}[\Gamma]) \left(\Omega_{\mathbf{Z}|X}^{-1} - C_{\mathbf{Z}|X}^{-1} + C_{\mathbf{Z}|X}^{-1}\right) (\Gamma - \mathbb{E}[\Gamma] + 2\mathbb{E}[\Gamma])^\top\right| \\
&\leq \left\{\|\Gamma - \mathbb{E}[\Gamma]\|_2^2 + 2\|\Gamma - \mathbb{E}[\Gamma]\|_2 \|\mathbb{E}[\Gamma]\|_2\right\} \left\{\|\Omega_{\mathbf{Z}|X}^{-1} - C_{\mathbf{Z}|X}^{-1}\|_2 + \|C_{\mathbf{Z}|X}^{-1}\|_2\right\},
\end{aligned}
$$

which implies that

$$
\begin{aligned}
&|w - w_0| \\
\leq &d^2 \left\{\|\Gamma - \mathbb{E}[\Gamma]\|_{\max}^2 + 2D_0 \|\Gamma - \mathbb{E}[\Gamma]\|_{\max}\right\} \left\{\|\Omega_{\mathbf{Z}|X}^{-1} - C_{\mathbf{Z}|X}^{-1}\|_2 + D_1\right\} + D_0^2 d^2 \|\Omega_{\mathbf{Z}|X}^{-1} - C_{\mathbf{Z}|X}^{-1}\|_2.
\end{aligned} \tag{B.16}
$$

We have

$$\begin{aligned}\|\Omega_{\mathbf{Z}|X}^{-1} - C_{\mathbf{Z}|X}^{-1}\|_2 &= \|\Omega_{\mathbf{Z}|X}^{-1}(C_{\mathbf{Z}|X} - \Omega_{\mathbf{Z}|X})C_{\mathbf{Z}|X}^{-1}\|_2 \\ &\leq d\|\Omega_{\mathbf{Z}|X} - C_{\mathbf{Z}|X}\|_{\max}\|\Omega_{\mathbf{Z}|X}^{-1}\|_2\|C_{\mathbf{Z}|X}^{-1}\|_2 \\ &\leq D_1^2 d\|\Omega_{\mathbf{Z}|X} - C_{\mathbf{Z}|X}\|_{\max}\left\{1 - D_1 d\|\Omega_{\mathbf{Z}|X} - C_{\mathbf{Z}|X}\|_{\max}\right\}^{-1}.\end{aligned} \tag{B.17}$$

The last inequality holds when $\|\Omega_{\mathbf{Z}|X} - C_{\mathbf{Z}|X}\|_{\max} < (D_1 d)^{-1}$ due to the fact that

$$\begin{aligned}\|\Omega_{\mathbf{Z}|X}^{-1}\|_2 &\leq \|\Omega_{\mathbf{Z}|X}^{-1} - C_{\mathbf{Z}|X}^{-1}\|_2 + \|C_{\mathbf{Z}|X}^{-1}\|_2 \\ &\leq \|\Omega_{\mathbf{Z}|X}^{-1}\|_2\|C_{\mathbf{Z}|X}^{-1}\|_2\|C_{\mathbf{Z}|X} - \Omega_{\mathbf{Z}|X}\|_2 + \|C_{\mathbf{Z}|X}^{-1}\|_2 \\ &\leq D_1 d\|\Omega_{\mathbf{Z}|X}^{-1}\|_2\|\Omega_{\mathbf{Z}|X} - C_{\mathbf{Z}|X}\|_{\max} + \|C_{\mathbf{Z}|X}^{-1}\|_2\end{aligned}$$

which is equivalent to $\|\Omega_{\mathbf{Z}|X}^{-1}\|_2\left\{1 - D_1 d\|\Omega_{\mathbf{Z}|X} - C_{\mathbf{Z}|X}\|_{\max}\right\} \leq \|C_{\mathbf{Z}|X}^{-1}\|_2$.

For $0 < x < (1 \wedge (D_1 d)^{-1})$ where $\kappa = d^2(1 + 2D_0)D_1 + D_0^2 D_1^2 d^3$ and

$$L = \left\{\frac{w_0^{3/2}\left(1 \wedge D_0^{-1}\right)}{6\kappa + D_1 d w_0^{3/2}\left(1 \wedge D_0^{-1}\right)} \wedge 1\right\},$$

we have

$$\begin{aligned}&\left[\left\{\|\Omega_{\mathbf{Z}|X} - C_{\mathbf{Z}|X}\|_{\max} \leq Lx\right\} \cap \left\{\|\Gamma - \mathbb{E}[\Gamma]\|_{\max} \leq Lx\right\}\right] \\ &\subset \left\{|w - w_0| \leq \frac{w_0^{3/2}\left(1 \wedge D_0^{-1}\right)}{6}x\right\}\end{aligned} \tag{B.18}$$

because, conditional on the two events $\left\{\|\Omega_{\mathbf{Z}|X} - C_{\mathbf{Z}|X}\|_{\max} \leq Lx\right\}$ and $\{\|\Gamma - \mathbb{E}[\Gamma]\|_{\max} \leq Lx\}$, (B.16) and (B.17) provide

$$\begin{aligned}|w - w_0| &\leq d^2\left(L^2x^2 + 2D_0Lx\right)\left(\frac{D_1^2 dLx}{1 - D_1 dLx} + D_1\right) + D_0^2 d^2\frac{D_1^2 dLx}{1 - D_1 dLx} \\ &\leq d^2(1 + 2D_0)Lx\left(\frac{D_1}{1 - D_1 dLx}\right) + \frac{D_0^2 D_1^2 d^3 Lx}{1 - D_1 dLx} = \frac{\kappa Lx}{1 - D_1 dLx} \\ &\leq \frac{\kappa w_0^{3/2}\left(1 \wedge D_0^{-1}\right)x}{6\kappa + D_1 d w_0^{3/2}\left(1 \wedge D_0^{-1}\right) - D_1 d w_0^{3/2}\left(1 \wedge D_0^{-1}\right)x} \leq \frac{w_0^{3/2}\left(1 \wedge D_0^{-1}\right)}{6}x.\end{aligned}$$

For $0 < x_2 < L^{-1}\left(3 \wedge 3D_0^2/D_2 \wedge 3D_0^2 E[\Omega]^{-1}\right) \wedge \left(1 \wedge \frac{3w_0^{-1/2}}{(1 \wedge D_0^{-1})} \wedge (D_1 d)^{-1}\right)$, by (B.15) and (B.18), we have

$$\begin{aligned}
&\{\|\hat{\boldsymbol{a}} - \boldsymbol{a}\|_{\max} > x_2\} \\
&\subset \left[\left\{\|\Omega_{\mathbf{Z}|X} - C_{\mathbf{Z}|X}\|_{\max} > L x_2\right\} \bigcup \left\{\|\Gamma - \mathbb{E}[\Gamma]\|_{\max} > \left(\frac{\left(1 \wedge \sqrt{w_0}\right)}{3} \wedge L\right) x_2\right\}\right],
\end{aligned}$$

which completes the proof by applying the union bound and together the tail bounds of $\|\Omega_{\mathbf{Z}|X} - C_{\mathbf{Z}|X}\|_{\max}$ and $\|\Gamma - \mathbb{E}[\Gamma]\|_{\max}$.

A direct implication of the exponential tail bounds is

$$\Omega \xrightarrow{a.s.} \mathbb{E}[\Omega], \quad \Gamma \xrightarrow{a.s.} \mathbb{E}[\Gamma], \quad \Omega_{\mathbf{Z}|X} \xrightarrow{a.s.} C_{\mathbf{Z}|X} \tag{B.19}$$

by the Borel-Cantelli lemma. We next show

$$\Omega_{\mathbf{Z}|X}^{-1} \xrightarrow{a.s.} C_{\mathbf{Z}|X}^{-1}, \quad \Omega_{X|\mathbf{Z}} \xrightarrow{a.s.} C_{X|\mathbf{Z}}. \tag{B.20}$$

Since $\Omega_{\mathbf{Z}|X} \xrightarrow{a.s.} C_{\mathbf{Z}|X}$, we have $\Omega_{\mathbf{Z}|X}^{-1} \xrightarrow{a.s.} C_{\mathbf{Z}|X}^{-1}$ by (B.17). Similarly, it can be shown that $\Omega_{X|\mathbf{Z}} \xrightarrow{a.s.} C_{X|\mathbf{Z}}$ under the assumption that $\lambda_{\min}(\mathbb{E}[\Psi]) > 0$. Thus, by the continuous mapping theorem together with (B.19) and (B.20), we conclude that $A \xrightarrow{a.s.} A_0$. ♢

The following lemma shows the strong uniform consistency of $\hat{\sigma}_i^2$ and the tail bound for $\hat{\sigma}_i^2/\sigma_i^2$.

Lemma B.2. *Under Assumptions 3.3 and 3.6,*

$$\max_{1 \le i \le m} \left|\frac{\hat{\sigma}_i^2}{\sigma_i^2} - 1\right| \xrightarrow{a.s.} 0 \tag{B.21}$$

and, for $0 < \delta_1 < (n - d - 1)/\log m$,

$$\mathbb{P}\left(\max_{1 \le i \le m} \left|\frac{\hat{\sigma}_i^2}{\sigma_i^2} - 1\right| > \nu_1 \sqrt{\delta_1} \middle| \mathbf{W}\right) \le 2m \exp\left\{-\delta_1 (\log m)\right\} \tag{B.22}$$

where $\nu_1 = 4\sqrt{\log m/(n-d-1)}$.

Proof of Lemma B.2. Since $\hat{\sigma}_i^2/\sigma_i^2|\mathbf{W} \sim \chi^2_{n-d-1}/(n-d-1)$, by the tail bound for chi-square random variable as in Lemma 1 of Laurent and Massart (2000), we have

$$\mathbb{P}\left(\left|\frac{\hat{\sigma}_i^2}{\sigma_i^2} - 1\right| > 2\sqrt{\frac{\delta_0}{n-d-1}} + 2\frac{\delta_0}{n-d-1}\Big|\mathbf{W}\right) \leq 2\exp(-\delta_0)$$

for $\delta_0 > 0$. By the union bound, we have

$$\mathbb{P}\left(\max_{1\leq i\leq m}\left|\frac{\hat{\sigma}_i^2}{\sigma_i^2} - 1\right| > 2\sqrt{\frac{\delta_0}{n-d-1}} + 2\frac{\delta_0}{n-d-1}\Big|\mathbf{W}\right) \leq 2m\exp(-\delta_0).$$

Letting $\delta_0 = (n-d-1)\delta_0'$ for $0 < \delta_0' < 1$,

$$\begin{aligned}\mathbb{P}\left(\max_{1\leq i\leq m}\left|\frac{\hat{\sigma}_i^2}{\sigma_i^2} - 1\right| > 2\sqrt{\delta_0'} + 2\delta_0'\Big|\mathbf{W}\right) &\leq \mathbb{P}\left(\max_{1\leq i\leq m}\left|\frac{\hat{\sigma}_i^2}{\sigma_i^2} - 1\right| > 4\delta_0'\Big|\mathbf{W}\right) \\ &\leq 2m\exp(-(n-d-1)\delta_0').\end{aligned}$$

Thus, under Assumptions 3.3 and 3.6, (B.21) follows by the Borel-Cantelli Lemma because

$$\mathbb{P}\left(\max_{1\leq i\leq m}\left|\frac{\hat{\sigma}_i^2}{\sigma_i^2} - 1\right| > 4\delta_0'\right) = \mathbb{E}_{\mathbf{W}}\left[\mathbb{P}\left(\max_{1\leq i\leq m}\left|\frac{\hat{\sigma}_i^2}{\sigma_i^2} - 1\right| > 4\delta_0'\Big|\mathbf{W}\right)\right] \leq 2m\exp(-(n-d-1)\delta_0').$$

Choosing $\delta_0 = \delta_1(\log m)$ for $0 < \delta_1 < (n-d-1)/\log m$, we have

$$\begin{aligned}\mathbb{P}\left(\max_{1\leq i\leq m}\left|\frac{\hat{\sigma}_i^2}{\sigma_i^2} - 1\right| \leq \nu_1\sqrt{\delta_1}\Big|\mathbf{W}\right) &\geq \mathbb{P}\left(\max_{1\leq i\leq m}\left|\frac{\hat{\sigma}_i^2}{\sigma_i^2} - 1\right| \leq 2\left(\frac{\delta_1(\log m)}{n-d-1} + \sqrt{\frac{\delta_1(\log m)}{n-d-1}}\right)\Big|\mathbf{W}\right) \\ &> 1 - 2m\exp\left\{-\delta_1(\log m)\right\}.\end{aligned}$$

♢

We next derive the tail bounds for $\max_{1\leq i\leq m}|\hat{\eta}_i|$ and $\max_{1\leq i\leq m}|\tilde{\eta}_i|$.

Lemma B.3. *Under Assumptions 3.3-3.5, for* $0 < \delta_1 < (n-d-1)/(16\log m), \delta_2 > 0$ *and* x_2 *as*

in Lemma B.1, we have

$$\begin{aligned}
&\mathbb{P}\left(\max_{1\le i\le m}|\hat{\eta}_i|>\nu_2(1+\delta_2)\right)\le C_4 m\exp\left\{-c_4 n(x_2^2/c_4'\wedge x_2/c_4'')\right\}+2m\exp\left\{-\nu_2^2\delta_2^2\right\},\\
&\mathbb{P}\left(\max_{1\le i\le m}|\tilde{\eta}_i|>\nu_2\left(1-\nu_1\sqrt{\delta_1}\right)^{-1}(1+\delta_2)\right)\\
\le& 2m\exp\left\{-\delta_1(\log m)\right\}+C_4 m\exp\left\{-c_4 n(x_2^2/c_4'\wedge x_2/c_4'')\right\}+2m\exp\left\{-\nu_2^2\delta_2^2\right\},
\end{aligned}$$

where $\nu_1=4\sqrt{\log m/(n-d-1)}$ *and* $\nu_2=(d+\|\boldsymbol{a}\|_1)B(\log m)^{b\vee\frac{1}{2}}$.

Proof of Lemma B.3. Note that

$$\mathbb{P}(|\epsilon_i|\le x)\ge 1-2\exp(-x^2) \tag{B.23}$$

for any $x>0$ by the well known result about the tail bound of a standard normal random variable. Under model (3.4), we have

$$\begin{aligned}
\mathbb{P}\left(|\hat{\eta}_i|\le\nu_2(1+\delta_2)\right)&\ge\mathbb{P}\left(\{|\eta_i|\le\nu_2\}\cap\{|\epsilon_i|\le\nu_2\delta_2\}\right)\\
&\ge\mathbb{P}\left(|\eta_i|\le\nu_2\right)+\mathbb{P}\left(|\epsilon_i|\le\nu_2\delta_2\right)-1\\
&\ge\mathbb{P}\left(|\eta_i|\le\nu_2,\|\hat{\boldsymbol{a}}-\boldsymbol{a}\|_{\max}\le x_2\right)-2\exp\left\{-\nu_2^2\delta_2^2\right\}\\
&=\mathbb{P}\left(\|\hat{\boldsymbol{a}}-\boldsymbol{a}\|_{\max}\le x_2\right)-2\exp\left\{-\nu_2^2\delta_2^2\right\}\\
&\ge 1-C_4\exp\left\{-c_4 n(x_2^2/c_4'\wedge x_2/c_4'')\right\}-2\exp\left\{-\nu_2^2\delta_2^2\right\}
\end{aligned}$$

where the third inequality follows by choosing $x=\nu_2\delta_2$ for $\delta_2>0$ in (B.23) and the equality holds by Lemma B.1 because

$$\begin{aligned}
|\eta_i|=|\hat{\boldsymbol{a}}^\top\boldsymbol{\xi}_i|\le\|\hat{\boldsymbol{a}}\|_1\|\boldsymbol{\xi}_i\|_{\max}&\le(\|\hat{\boldsymbol{a}}-\boldsymbol{a}\|_1+\|\boldsymbol{a}\|_1)B(\log m)^b\\
&\le(d\|\hat{\boldsymbol{a}}-\boldsymbol{a}\|_{\max}+\|\boldsymbol{a}\|_1)B(\log m)^b\\
&\le(dx_2+\|\boldsymbol{a}\|_1)B(\log m)^b\le(d+\|\boldsymbol{a}\|_1)B(\log m)^b=\nu_2
\end{aligned} \tag{B.24}$$

conditional on the event $\{\|\hat{\boldsymbol{a}}-\boldsymbol{a}\|_{\max}\le x_2\}$ for x_2 as in Lemma B.1 which is smaller than 1.

Thus, it follows that

$$\mathbb{P}\left(\max_{1\le i\le m}|\hat{\eta}_i|\le \nu_2(1+\delta_2)\right)=\mathbb{P}\left(\bigcap_{i=1}^{m}\{|\hat{\eta}_i|\le \nu_2(1+\delta_2)\}\right)$$
$$\ge 1-C_4 m\exp\left\{-c_4 n(x_2^2/c_4'\wedge x_2/c_4'')\right\}-2m\exp\left\{-\nu_2^2\delta_2^2\right\}.$$

For the second inequality, we first observe that

$$\left|\frac{\hat{\sigma}_i}{\sigma_i}-1\right|\le\left|\frac{\hat{\sigma}_i^2}{\sigma_i^2}-1\right| \tag{B.25}$$

and, provided that $|\hat{\sigma}_i/\sigma_i-1|<1$,

$$|\tilde{\eta}_i|=\left|\frac{\sigma_i}{\hat{\sigma}_i}-1+1\right||\hat{\eta}_i|\le\left(\frac{|\hat{\sigma}_i/\sigma_i-1|}{1-|\hat{\sigma}_i/\sigma_i-1|}\right)|\hat{\eta}_i|+|\hat{\eta}_i|=\frac{|\hat{\eta}_i|}{1-|\hat{\sigma}_i/\sigma_i-1|}.$$

Thus, we have

$$\begin{aligned}
&\mathbb{P}\left(\max_{1\le i\le m}|\tilde{\eta}_i|\le\nu_2\left(1-\nu_1\sqrt{\delta_1}\right)^{-1}(1+\delta_2)\right)\\
\ge&\mathbb{P}\left(\left\{\max_{1\le i\le m}\left|\frac{\hat{\sigma}_i}{\sigma_i}-1\right|\le\nu_1\sqrt{\delta_1}\right\}\bigcap\left\{\max_{1\le i\le m}|\hat{\eta}_i|\le\nu_2(1+\delta_2)\right\}\right)\\
\ge&\mathbb{P}\left(\left\{\max_{1\le i\le m}\left|\frac{\hat{\sigma}_i^2}{\sigma_i^2}-1\right|\le\nu_1\sqrt{\delta_1}\right\}\bigcap\left\{\max_{1\le i\le m}|\hat{\eta}_i|\le\nu_2(1+\delta_2)\right\}\right)\\
\ge&1-2m\exp\{-\delta_1(\log m)\}-C_4 m\exp\left\{-c_4 n(x_2^2/c_4'\wedge x_2/c_4'')\right\}-2m\exp\left\{-\nu_2^2\delta_2^2\right\}
\end{aligned}$$

where the last inequality follows due to

$$\begin{aligned}
\mathbb{P}\left(\max_{1\le i\le m}\left|\frac{\hat{\sigma}_i^2}{\sigma_i^2}-1\right|\le\nu_1\sqrt{\delta_1}\right)&=\mathbb{E}_{\mathbf{W}}\left[\mathbb{P}\left(\max_{1\le i\le m}\left|\frac{\hat{\sigma}_i^2}{\sigma_i^2}-1\right|\le\nu_1\sqrt{\delta_1}\middle|\mathbf{W}\right)\right]\\
&\ge 1-2m\exp\{-\delta_1(\log m)\}
\end{aligned} \tag{B.26}$$

by (B.22). ♢

We derive the concentration inequalities for $m^{-1}\sum_{i=1}^m\hat{\eta}_i$ and $m^{-1}\sum_{i=1}^m\hat{\eta}_i^2$ in the following lemma.

Lemma B.4. *Under Assumptions 3.3-3.5, for $\delta_3 > 0, 0 < \delta_4 < 2^5\nu_3$ and x_2 as in Lemma B.1, we have*

$$\mathbb{P}\left(\left|\frac{1}{m}\sum_{i=1}^{m}\hat{\eta}_i - \mathbb{E}\left[\eta_1\right]\right| > \delta_3\right) \leq 2\exp\left\{-\frac{m\delta_3^2}{2\nu_3}\right\} + C_4\exp\left\{-c_4 n(x_2^2/c_4' \wedge x_2/c_4'')\right\}, \quad \text{(B.27)}$$

and

$$\begin{aligned}
&\mathbb{P}\left(\left|\frac{1}{m}\sum_{i=1}^{m}\hat{\eta}_i^2 - \mathbb{E}\left[\eta_1^2\right] - 1\right| > \delta_4\right) \\
\leq& 2\exp\left\{-\frac{m\delta_4^2}{2^{11}\nu_3^2}\right\} + 2\exp\left\{-\frac{m\delta_4^2}{32(d+\|\boldsymbol{a}\|_1)^2B^2(\log m)^{2b}\nu_3}\right\} \\
&+3C_4\exp\left\{-c_4 n(x_2^2/c_4' \wedge x_2/c_4'')\right\},
\end{aligned}$$

where $\nu_3 = 4(d+\|\boldsymbol{a}\|_1)^2B^2(\log m)^{2b} + 1$.

Proof of Lemma B.4. We have

$$\begin{aligned}
&\mathbb{P}\left(\left|\frac{1}{m}\sum_{i=1}^{m}\hat{\eta}_i - \mathbb{E}\left[\eta_1\right]\right| > \delta_3\right) \\
\leq&\mathbb{P}\left(\left|\frac{1}{m}\sum_{i=1}^{m}\hat{\eta}_i - \mathbb{E}\left[\eta_1\right]\right| > \delta_3, \|\hat{\boldsymbol{a}} - \boldsymbol{a}\|_{\max} \leq x_2\right) + \mathbb{P}\left(\|\hat{\boldsymbol{a}} - \boldsymbol{a}\|_{\max} > x_2\right).
\end{aligned}$$

Since the model (3.4) can be rewritten as

$$\hat{\eta}_i - \mathbb{E}[\eta_1] = \eta_i - \mathbb{E}[\eta_1] + \epsilon_i$$

and, by (B.24), $|\eta_i - \mathbb{E}[\eta_1]| \leq 2(d+\|\boldsymbol{a}\|_1)B(\log m)^b$ conditional on the event $\{\|\hat{\boldsymbol{a}} - \boldsymbol{a}\|_{\max} \leq x_2\}$, $(\eta_i - \mathbb{E}[\eta_1])$'s can be shown to be sub-gaussian with the variance proxy $4(d+\|\boldsymbol{a}\|_1)^2B^2(\log m)^{2b}$. Thus, $(\hat{\eta}_i - \mathbb{E}[\eta_1])$'s are also sub-gaussian with the variance proxy ν_3 as ϵ_i's are sub-gaussian with the variance proxy one and η_i's and ϵ_i's are independent. Then, the first inequality follows from Lemma 4 and Corollary 1.7 in Rigollet and Hütter (2015).

For the second inequality, we observe that

$$\begin{aligned}(\hat{\eta}_i - \mathbb{E}[\eta_1])^2 - \mathbb{E}[(\hat{\eta}_i - \mathbb{E}[\eta_1])^2] &= \hat{\eta}_i^2 - \mathbb{E}[\hat{\eta}_1^2] - 2\mathbb{E}[\eta_1](\hat{\eta}_i - \mathbb{E}[\hat{\eta}_1]) \\ &= \hat{\eta}_i^2 - \mathbb{E}[\eta_1^2] - 1 - 2\mathbb{E}[\eta_1](\hat{\eta}_i - \mathbb{E}[\eta_1])\end{aligned}$$

under model (3.4). By Lemma 1.12 in Rigollet and Hütter (2015), conditional on the event $\{\|\hat{\boldsymbol{a}} - \boldsymbol{a}\|_{\max} \leq x_2\}$, it follows that

$$\hat{\eta}_i^2 - \mathbb{E}[\eta_1^2] - 1 - 2\mathbb{E}[\eta_1](\hat{\eta}_i - \mathbb{E}[\eta_1])$$

is sub-exponential with the parameter $16\nu_3$. According to Theorem 1.13 in Rigollet and Hütter (2015),

$$\begin{aligned}&\mathbb{P}\left(\left|\frac{1}{m}\sum_{i=1}^m \hat{\eta}_i^2 - \mathbb{E}[\eta_1^2] - 1 - 2\mathbb{E}[\eta_1]\left(\frac{1}{m}\sum_{i=1}^m \hat{\eta}_i - \mathbb{E}[\eta_1]\right)\right| > \frac{\delta_4}{2}\right) \\ \leq &\mathbb{P}\left(\left|\frac{1}{m}\sum_{i=1}^m \hat{\eta}_i^2 - \mathbb{E}[\eta_1^2] - 1 - 2\mathbb{E}[\eta_1]\left(\frac{1}{m}\sum_{i=1}^m \hat{\eta}_i - \mathbb{E}[\eta_1]\right)\right| > \frac{\delta_4}{2}, \|\hat{\boldsymbol{a}} - \boldsymbol{a}\|_{\max} \leq x_2\right) \\ &+ \mathbb{P}\left(\|\hat{\boldsymbol{a}} - \boldsymbol{a}\|_{\max} > x_2\right) \\ \leq &2\exp\left\{-\frac{m}{2}\left(\frac{\delta_4^2}{2^{10}\nu_3^2} \wedge \frac{\delta_4}{2^5\nu_3}\right)\right\} + C_4\exp\left\{-c_4 n(x_2^2/c_4' \wedge x_2/c_4'')\right\}\end{aligned}$$

for any $\delta_4 > 0$. Since we have

$$\begin{aligned}&\mathbb{P}\left(\left|\frac{1}{m}\sum_{i=1}^m \hat{\eta}_i^2 - \mathbb{E}[\eta_1^2] - 1 - 2\mathbb{E}[\eta_1]\left(\frac{1}{m}\sum_{i=1}^m \hat{\eta}_i - \mathbb{E}[\eta_1]\right)\right| > \frac{\delta_4}{2}\right) \\ \geq &\mathbb{P}\left(\left|\frac{1}{m}\sum_{i=1}^m \hat{\eta}_i^2 - \mathbb{E}[\eta_1^2] - 1\right| > \delta_4\right) + \mathbb{P}\left(\left|2\mathbb{E}[\eta_1]\left(\frac{1}{m}\sum_{i=1}^m \hat{\eta}_i - \mathbb{E}[\eta_1]\right)\right| \leq \frac{\delta_4}{2}\right) - 1 \\ \geq &\mathbb{P}\left(\left|\frac{1}{m}\sum_{i=1}^m \hat{\eta}_i^2 - \mathbb{E}[\eta_1^2] - 1\right| > \delta_4\right) \\ &+ \mathbb{P}\left(\left|\left(\frac{1}{m}\sum_{i=1}^m \hat{\eta}_i - \mathbb{E}[\eta_1]\right)\right| \leq \frac{\delta_4}{4|\mathbb{E}[\eta_1]|}, \|\hat{\boldsymbol{a}} - \boldsymbol{a}\|_{\max} \leq x_2\right) - 1\end{aligned}$$

and

$$\begin{aligned}
&\mathbb{P}\left(\left|\left(\frac{1}{m}\sum_{i=1}^{m}\hat{\eta}_i - \mathbb{E}[\eta_1]\right)\right| \le \frac{\delta_4}{4|\mathbb{E}[\eta_1]|}, \|\hat{\boldsymbol{a}}-\boldsymbol{a}\|_{\max} \le x_2\right)\\
\ge&\mathbb{P}\left(\left|\left(\frac{1}{m}\sum_{i=1}^{m}\hat{\eta}_i - \mathbb{E}[\eta_1]\right)\right| \le \frac{\delta_4}{4(d+\|\boldsymbol{a}\|_1)B(\log m)^b}, \|\hat{\boldsymbol{a}}-\boldsymbol{a}\|_{\max} \le x_2\right) \quad (\because (B.24))\\
\ge&1-2\exp\left\{-\frac{m\delta_4^2}{32(d+\|\boldsymbol{a}\|_1)^2B^2(\log m)^{2b}\nu_3}\right\} - 2C_4\exp\left\{-c_4 n(x_2^2/c_4' \wedge x_2/c_4'')\right\}
\end{aligned}$$

by letting $\delta_3 = \delta_4/(4(d+\|\boldsymbol{a}\|_1)B(\log m)^b)$ in (B.27), the proof can be completed. ♢

Lemma B.5. *For $0 < \delta_1 < (n-d-1)/(16\log m), \delta_2, \delta_3 > 0$ and $0 < \delta_4 \le 2^5\nu_3$ and x_2 as in Lemma B.1, under Assumptions 3.3-3.5, we have*

$$\begin{aligned}
&\mathbb{P}\left(\left|\frac{1}{m}\sum_{i=1}^{m}\log\frac{f_{\widehat{G}_{m,n}}(\hat{\eta}_i)}{f_{\widehat{G}_{m,n}}(\tilde{\eta}_i)}\right| > \frac{\nu_1\sqrt{\delta_1}}{1-\nu_1\sqrt{\delta_1}}\left(\frac{\mathbb{E}[\eta_1^2]+1+\delta_4}{2} + \nu_2(1+\delta_2)\{|\mathbb{E}[\eta_1]|+\delta_3\}\right)\right)\\
\le&2m\exp\left\{-\nu_2^2\delta_2^2\right\} + 2m\exp\left\{-\delta_1(\log m)\right\} + 2\exp\left\{-\frac{m\delta_3^2}{2\nu_3}\right\} + 2\exp\left\{-\frac{m\delta_4^2}{2^{11}\nu_3^2}\right\}\\
&+2\exp\left\{-\frac{m\delta_4^2}{32(d+\|\boldsymbol{a}\|_1)^2B^2(\log m)^{2b}\nu_3}\right\} + (m+4)C_4\exp\left\{-c_4 n(x_2^2/c_4' \wedge x_2/c_4'')\right\}
\end{aligned}$$

and

$$\begin{aligned}
&\mathbb{P}\left(\left|\frac{1}{m}\sum_{i=1}^{m}\log\frac{f_{\widetilde{G}_{m,n}}(\hat{\eta}_i)}{f_{\widetilde{G}_{m,n}}(\tilde{\eta}_i)}\right| > \frac{\nu_1\sqrt{\delta_1}}{1-\nu_1\sqrt{\delta_1}}\left(\frac{\mathbb{E}[\eta_1^2]+1+\delta_4}{2} + \frac{\nu_2(1+\delta_2)}{1-\nu_1\sqrt{\delta_1}}\{|\mathbb{E}[\eta_1]|+\delta_3\}\right)\right)\\
\le&2m\exp\left\{-\nu_2^2\delta_2^2\right\} + 4m\exp\left\{-\delta_1(\log m)\right\} + 2\exp\left\{-\frac{m\delta_3^2}{2\nu_3}\right\} + 2\exp\left\{-\frac{m\delta_4^2}{2^{11}\nu_3^2}\right\}\\
&+2\exp\left\{-\frac{m\delta_4^2}{32(d+\|\boldsymbol{a}\|_1)^2B^2(\log m)^{2b}\nu_3}\right\} + (m+4)C_4\exp\left\{-c_4 n(x_2^2/c_4' \wedge x_2/c_4'')\right\}
\end{aligned}$$

where $\nu_1 = 4\sqrt{\log m/(n-d-1)}$, $\nu_2 = (d+\|\boldsymbol{a}\|_1)B(\log m)^{b\vee\frac{1}{2}}$ and $\nu_3 = B^2(\log m)^{2b}+1$.

Proof of Lemma B.5. When $|\hat{\sigma}_i/\sigma_i - 1| < 1$, by (B.25), we have

$$\left|\sum_{i=1}^m (\tilde{\eta}_i^2 - \hat{\eta}_i^2)\right| \leq \max_{1\leq i\leq m}\left|\frac{\sigma_i^2}{\hat{\sigma}_i^2} - 1\right| \left|\sum_{i=1}^m \hat{\eta}_i^2\right| \leq \frac{\max_{1\leq i\leq m}\left|\frac{\hat{\sigma}_i^2}{\sigma_i^2} - 1\right|}{1 - \max_{1\leq i\leq m}\left|\frac{\hat{\sigma}_i^2}{\sigma_i^2} - 1\right|} \left|\sum_{i=1}^m \hat{\eta}_i^2\right|,$$

$$\left|\sum_{i=1}^m (\hat{\eta}_i - \tilde{\eta}_i)\right| \leq \frac{\max_{1\leq i\leq m}\left|\frac{\hat{\sigma}_i}{\sigma_i} - 1\right|}{1 - \max_{1\leq i\leq m}\left|\frac{\hat{\sigma}_i}{\sigma_i} - 1\right|} \left|\sum_{i=1}^m \hat{\eta}_i\right| \leq \frac{\max_{1\leq i\leq m}\left|\frac{\hat{\sigma}_i^2}{\sigma_i^2} - 1\right|}{1 - \max_{1\leq i\leq m}\left|\frac{\hat{\sigma}_i^2}{\sigma_i^2} - 1\right|} \left|\sum_{i=1}^m \hat{\eta}_i\right|.$$

Recall that $\widehat{G}_{m,n}(u) = \sum_{j=1}^m \hat{\pi}_j \mathbf{1}\{\hat{s}_j \leq u\}$ denotes the solution of (3.5), where $\hat{\pi}_j \geq 0$ with $\sum_{j=1}^m \hat{\pi}_j = 1$ and $\{\hat{s}_1, \cdots, \hat{s}_m\}$ is the set of support points for $\widehat{G}_{m,n}$. It follows that

$$\begin{aligned}
&\left|\frac{1}{m}\sum_{i=1}^m \log f_{\widehat{G}_{m,n}}(\hat{\eta}_i) - \frac{1}{m}\sum_{i=1}^m \log f_{\widehat{G}_{m,n}}(\tilde{\eta}_i)\right| = \left|\frac{1}{m}\sum_{i=1}^m \log\left[\frac{\sum_{j=1}^m \phi(\hat{\eta}_i - \hat{s}_j)\hat{\pi}_j}{\sum_{j=1}^m \phi(\tilde{\eta}_i - \hat{s}_j)\hat{\pi}_j}\right]\right| \\
=&\left|\frac{1}{m}\sum_{i=1}^m \log\left[\exp\left\{-(\hat{\eta}_i^2 - \tilde{\eta}_i^2)/2\right\}\frac{\sum_{j=1}^m \exp\left\{\tilde{\eta}_i\hat{s}_j + (\hat{\eta}_i - \tilde{\eta}_i)\hat{s}_j - \hat{s}_j^2/2\right\}\hat{\pi}_j}{\sum_{j=1}^m \exp\left\{\tilde{\eta}_i\hat{s}_j - \hat{s}_j^2/2\right\}\hat{\pi}_j}\right]\right| \qquad \text{(B.28)} \\
\leq&\left|\frac{1}{m}\sum_{i=1}^m \left(\frac{|\tilde{\eta}_i^2 - \hat{\eta}_i^2|}{2} + |\hat{\eta}_i - \tilde{\eta}_i| \max_{1\leq j\leq m}|\hat{s}_j|\right)\right| \leq \left|\frac{1}{m}\sum_{i=1}^m \left(\frac{|\tilde{\eta}_i^2 - \hat{\eta}_i^2|}{2} + |\hat{\eta}_i - \tilde{\eta}_i| \max_{1\leq i\leq m}|\hat{\eta}_i|\right)\right| \\
\leq&\frac{\max_{1\leq i\leq m}\left|\frac{\hat{\sigma}_i^2}{\sigma_i^2} - 1\right|}{2\left(1 - \max_{1\leq i\leq m}\left|\frac{\hat{\sigma}_i^2}{\sigma_i^2} - 1\right|\right)}\left|\frac{1}{m}\sum_{i=1}^m \hat{\eta}_i^2\right| + \max_{1\leq i\leq m}|\hat{\eta}_i|\frac{\max_{1\leq i\leq m}\left|\frac{\hat{\sigma}_i^2}{\sigma_i^2} - 1\right|}{1 - \max_{1\leq i\leq m}\left|\frac{\hat{\sigma}_i^2}{\sigma_i^2} - 1\right|}\left|\frac{1}{m}\sum_{i=1}^m \hat{\eta}_i\right|,
\end{aligned}$$

where the second inequality follows from the fact that the support of $\widehat{G}_{m,n}(u)$ is always within the range of $\hat{\eta}_i$ as noticed in Section 3.2.3. Let

$$\begin{aligned}
U :=& \frac{\max_{1\leq i\leq m}\left|\frac{\hat{\sigma}_i^2}{\sigma_i^2} - 1\right|}{2\left(1 - \max_{1\leq i\leq m}\left|\frac{\hat{\sigma}_i^2}{\sigma_i^2} - 1\right|\right)}\left|\frac{1}{m}\sum_{i=1}^m \hat{\eta}_i^2\right| + \max_{1\leq i\leq m}|\hat{\eta}_i|\frac{\max_{1\leq i\leq m}\left|\frac{\hat{\sigma}_i^2}{\sigma_i^2} - 1\right|}{1 - \max_{1\leq i\leq m}\left|\frac{\hat{\sigma}_i^2}{\sigma_i^2} - 1\right|}\left|\frac{1}{m}\sum_{i=1}^m \hat{\eta}_i\right|, \\
u_{m,n} :=& \frac{\nu_1\sqrt{\delta_1}}{1 - \nu_1\sqrt{\delta_1}}\left(\frac{\mathbb{E}[\eta_1^2] + 1 + \delta_4}{2} + \nu_2(1 + \delta_2)(|\mathbb{E}[\eta_1]| + \delta_3)\right).
\end{aligned}$$

We have the following inclusions of the events

$$\begin{aligned}
&\left[\left\{\max_{1\le i\le m}|\hat{\eta}_i|\le \nu_2(1+\delta_2)\right\}\bigcap\left\{\max_{1\le i\le m}\left|\frac{\hat{\sigma}_i^2}{\sigma_i^2}-1\right|\le \nu_1\sqrt{\delta_1}\right\}\right. \\
&\left.\bigcap\left\{\left|\frac{1}{m}\sum_{i=1}^m\hat{\eta}_i-\mathbb{E}\left[\eta_1\right]\right|\le\delta_3\right\}\bigcap\left\{\left|\frac{1}{m}\sum_{i=1}^m\hat{\eta}_i^2-\mathbb{E}\left[\eta_1^2\right]-1\right|\le\delta_4\right\}\right] \qquad \text{(B.29)}\\
\subset&\left[\left\{\max_{1\le j\le m}|\hat{\eta}_i|\le \nu_2(1+\delta_2)\right\}\bigcap\left\{\max_{1\le i\le m}\left|\frac{\hat{\sigma}_i^2}{\sigma_i^2}-1\right|\le \nu_1\sqrt{\delta_1}\right\}\right. \\
&\left.\bigcap\left\{\left|\frac{1}{m}\sum_{i=1}^m\hat{\eta}_i\right|\le|\mathbb{E}[\eta_1]|+\delta_3\right\}\bigcap\left\{\left|\frac{1}{m}\sum_{i=1}^m\hat{\eta}_i^2\right|\le\mathbb{E}[\eta_1^2]+1+\delta_4\right\}\right]\subset\left\{U\le u_{m,n}\right\}.
\end{aligned}$$

Thus, by (B.28)-(B.29), we have

$$\begin{aligned}
&\mathbb{P}\left(\left|\frac{1}{m}\sum_{i=1}^m\log\frac{f_{\widehat{G}_{m,n}}(\hat{\eta}_i)}{f_{\widehat{G}_{m,n}}(\tilde{\eta}_i)}\right|\le u_{m,n}\right)\ge\mathbb{P}\left(U\le u_{m,n}\right)\\
\ge&\mathbb{P}\left(\max_{1\le i\le m}|\hat{\eta}_i|\le\nu_2(1+\delta_2)\right)+\mathbb{P}\left(\max_{1\le i\le m}\left|\frac{\hat{\sigma}_i^2}{\sigma_i^2}-1\right|\le\nu_1\sqrt{\delta_1}\right)\\
&+\mathbb{P}\left(\left|\frac{1}{m}\sum_{i=1}^m\hat{\eta}_i-\mathbb{E}\left[\eta_1\right]\right|\le\delta_3\right)+\mathbb{P}\left(\left|\frac{1}{m}\sum_{i=1}^m\hat{\eta}_i^2-\mathbb{E}[\eta_1^2]-1\right|\le\delta_4\right)-3,
\end{aligned}$$

which completes the proof of the first inequality by Lemmas B.3-B.4 and (B.26). Similar argument can be used to verify the second inequality. ♢

In the following lemma, we introduce the large deviation inequality for $d_H\left(f_{\widetilde{G}_{m,n}},f_{G_n}\right)$ which can be proved by using the similar argument in Theorem 1 in Zhang (2009) with the fact (B.24).

Lemma B.6. *Under Assumptions 3.3-3.5 and the event* $\{\|\hat{\boldsymbol{a}}-\boldsymbol{a}\|_{\max}\le x_2\}$ *for* x_2 *as in Lemma B.1, if* $\widetilde{G}_{m,n}$ *satisfies*

$$\prod_{i=1}^m\left\{\frac{f_{\widetilde{G}_{m,n}}(\hat{\eta}_i)}{f_{G_n}(\hat{\eta}_i)}\right\}\ge e^{-2t^2mc_m^2/15} \qquad \text{(B.30)}$$

where

$$c_m=\frac{\sqrt{2}(\log m)^{b+\frac{1}{2}+(b\vee\frac{1}{2})}}{\sqrt{m}}\left[m^{1/p}\sqrt{\log m}\left\{(d+\|\boldsymbol{a}\|_1)B\vee 1\right\}(\log m)^b\right]^{p/(2+2p)},$$

then there exists an universal constant t^* such that for all $t \geq t^*$ and $\log m \geq 4/p$,

$$\mathbb{P}\left(d_H\left(f_{\widetilde{G}_{m,n}}, f_{G_n}\right) \geq tc_m | \mathbf{W}\right) \leq \exp\left\{-\frac{t^2 m c_m^2}{2\log m}\right\} \leq e^{-t^2 \log m}.$$

The following lemma shows that $d_H\left(f_{\widetilde{G}_{m,n}}, f_{G_n}\right) = o_{a.s.}(1)$.

Lemma B.7. *Under Assumptions 3.3-3.6, $d_H\left(f_{\widetilde{G}_{m,n}}, f_{G_n}\right) = o_{a.s.}(1)$.*

Proof of Lemma B.7. Define $d_H := d_H\left(f_{\widetilde{G}_{m,n}}, f_{G_n}\right)$ and note that d_H is indexed by both n and m. Since d_H is indexed by only n under Assumption 3.6, for any $\varepsilon > 0$, it suffices to show that $\sum_{n=1}^{\infty} \mathbb{P}(d_H \geq \varepsilon) < \infty$ by the Borel-Cantelli Lemma.

For the same x_2 in Lemma B.1 and large enough n, it follows that

$$\begin{aligned} \mathbb{P}(d_H \geq \varepsilon) &\leq \mathbb{P}(d_H \geq tc_m) \\ &\leq \mathbb{P}(d_H \geq tc_m, \|\hat{\boldsymbol{a}} - \boldsymbol{a}\|_{\max} \leq x_2) + \mathbb{P}(\|\hat{\boldsymbol{a}} - \boldsymbol{a}\|_{\max} > x_2) \end{aligned} \tag{B.31}$$

where the first inequality follows because c_m can be made arbitrary small for large enough n under Assumption 3.6. By noticing that

$$\begin{aligned} &\mathbb{P}(d_H \geq tc_m, \|\hat{\boldsymbol{a}} - \boldsymbol{a}\|_{\max} \leq x_2) \\ \leq &\mathbb{P}\left(d_H \geq tc_m, \|\hat{\boldsymbol{a}} - \boldsymbol{a}\|_{\max} \leq x_2, \frac{1}{m}\sum_{i=1}^{m} \log \frac{f_{\widetilde{G}_{m,n}}(\hat{\eta}_i)}{f_{G_n}(\hat{\eta}_i)} \geq -\frac{2t^2 c_m^2}{15}\right) \\ &+ \mathbb{P}\left(\|\hat{\boldsymbol{a}} - \boldsymbol{a}\|_{\max} \leq x_2, \frac{1}{m}\sum_{i=1}^{m} \log \frac{f_{\widetilde{G}_{m,n}}(\hat{\eta}_i)}{f_{G_n}(\hat{\eta}_i)} < -\frac{2t^2 c_m^2}{15}\right), \end{aligned}$$

we aim to get an upper bound for each term on the right hand side. Lemma B.6 provides

$$\begin{aligned} &\mathbb{P}\left(d_H \geq tc_m, \|\hat{\boldsymbol{a}} - \boldsymbol{a}\|_{\max} \leq x_2, \frac{1}{m}\sum_{i=1}^{m} \log \frac{f_{\widetilde{G}_{m,n}}(\hat{\eta}_i)}{f_{G_n}(\hat{\eta}_i)} \geq -\frac{2t^2 c_m^2}{15}\right) \\ =&\mathbb{E}_{\mathbf{W}}\left[\mathbb{P}\left(d_H \geq tc_m, \frac{1}{m}\sum_{i=1}^{m} \log \frac{f_{\widetilde{G}_{m,n}}(\hat{\eta}_i)}{f_{G_n}(\hat{\eta}_i)} \geq -\frac{2t^2 c_m^2}{15} \Big| \mathbf{W}\right) \mathbf{1}\left\{\|\hat{\boldsymbol{a}} - \boldsymbol{a}\|_{\max} \leq x_2\right\}\right] \leq D_3 m^{-2} \end{aligned} \tag{B.32}$$

for some constant $D_3 > 0$ and large enough t.

Also,

$$
\begin{aligned}
&\mathbb{P}\left(\frac{1}{m}\sum_{i=1}^{m}\log\frac{f_{\widetilde{G}_{m,n}}(\hat{\eta}_i)}{f_{G_n}(\hat{\eta}_i)} < -\frac{2t^2c_m^2}{15}, \|\hat{\boldsymbol{a}}-\boldsymbol{a}\|_{\max}\le x_2\right)\\
=&\mathbb{P}\Bigg(\frac{1}{m}\sum_{i=1}^{m}\log\frac{f_{\widehat{G}_{m,n}}(\hat{\eta}_i)}{f_{G_n}(\hat{\eta}_i)} - \frac{1}{m}\sum_{i=1}^{m}\log\frac{f_{\widehat{G}_{m,n}}(\hat{\eta}_i)}{f_{\widehat{G}_{m,n}}(\tilde{\eta}_i)} - \frac{1}{m}\sum_{i=1}^{m}\log\frac{f_{\widetilde{G}_{m,n}}(\tilde{\eta}_i)}{f_{\widetilde{G}_{m,n}}(\hat{\eta}_i)}\\
&+\frac{1}{m}\sum_{i=1}^{m}\log\frac{f_{\widetilde{G}_{m,n}}(\tilde{\eta}_i)}{f_{\widehat{G}_{m,n}}(\tilde{\eta}_i)} < -\frac{2t^2c_m^2}{15}, \|\hat{\boldsymbol{a}}-\boldsymbol{a}\|_{\max}\le x_2\Bigg) \qquad \text{(B.33)}\\
\le&\mathbb{P}\left(\frac{2t^2c_m^2}{15} < \left|\frac{1}{m}\sum_{i=1}^{m}\log\frac{f_{\widehat{G}_{m,n}}(\hat{\eta}_i)}{f_{\widehat{G}_{m,n}}(\tilde{\eta}_i)}\right| + \left|\frac{1}{m}\sum_{i=1}^{m}\log\frac{f_{\widetilde{G}_{m,n}}(\tilde{\eta}_i)}{f_{\widetilde{G}_{m,n}}(\hat{\eta}_i)}\right|, \|\hat{\boldsymbol{a}}-\boldsymbol{a}\|_{\max}\le x_2\right)\\
\le&\mathbb{P}\left(2u_{m,n} < \left|\frac{1}{m}\sum_{i=1}^{m}\log\frac{f_{\widehat{G}_{m,n}}(\hat{\eta}_i)}{f_{\widehat{G}_{m,n}}(\tilde{\eta}_i)}\right| + \left|\frac{1}{m}\sum_{i=1}^{m}\log\frac{f_{\widetilde{G}_{m,n}}(\tilde{\eta}_i)}{f_{\widetilde{G}_{m,n}}(\hat{\eta}_i)}\right|, \|\hat{\boldsymbol{a}}-\boldsymbol{a}\|_{\max}\le x_2\right)\\
\le&\mathbb{P}\left(u_{m,n} < \left|\frac{1}{m}\sum_{i=1}^{m}\log\frac{f_{\widehat{G}_{m,n}}(\hat{\eta}_i)}{f_{\widehat{G}_{m,n}}(\tilde{\eta}_i)}\right|\right) + \mathbb{P}\left(u_{m,n} < \left|\frac{1}{m}\sum_{i=1}^{m}\log\frac{f_{\widehat{G}_{m,n}}(\hat{\eta}_i)}{f_{\widehat{G}_{m,n}}(\tilde{\eta}_i)}\right|\right)
\end{aligned}
$$

where the second inequality follows due to the fact that, conditional on the event $\{\|\hat{\boldsymbol{a}}-\boldsymbol{a}\|_{\max}\le x_2\}$,

$$
u_{m,n} = \frac{\nu_1\sqrt{\delta_1}}{1-\nu_1\sqrt{\delta_1}}\left(\frac{\mathbb{E}[\eta_1^2]+1+\delta_4}{2} + \nu_2(1+\delta_2)(|\mathbb{E}[\eta_1]|+\delta_3)\right) = O\left(\frac{(\log m)^{b+\frac{1}{2}+(b\vee\frac{1}{2})}}{\sqrt{n}}\right)
$$

by (B.24) and

$$
\frac{2t^2c_m^2}{15} \ge \frac{2t^2}{15}\frac{(\log m)^{b+\frac{1}{2}+(b\vee\frac{1}{2})}}{m^{p/(1+p)}} \ge \frac{2t^2}{15D_5}\frac{(\log m)^{b+\frac{1}{2}+(b\vee\frac{1}{2})}}{\sqrt{n}} \ge \frac{2t^2}{15D_4D_5}u_{m,n} \ge 2u_{m,n} \qquad \text{(B.34)}
$$

for large enough n and $t \ge (t^* \vee \sqrt{15D_4D_5})$ where $D_4, D_5 \ge 0$ denote some constants such that $u_{m,n} \le D_4\frac{(\log m)^{b+\frac{1}{2}+(b\vee\frac{1}{2})}}{\sqrt{n}}$ and $m^{p/(1+p)} \le D_5\sqrt{n}$ under Assumptions 3.5-3.6.

Thus, for large enough n, combining (B.31) together with (B.32) and (B.33) implies that

$$\begin{aligned}
&\mathbb{P}\left(d_H \geq \varepsilon\right) \\
\leq & D_3 m^{-2} + 4m \exp\left\{-\nu_2^2 \delta_2^2\right\} + 6m \exp\left\{-\delta_1 (\log m)\right\} + 4 \exp\left\{-\frac{m\delta_3^2}{2\nu_3}\right\} + 4 \exp\left\{-\frac{m\delta_4^2}{2^{11}\nu_3^2}\right\} \\
&+ 4 \exp\left\{-\frac{m\delta_4^2}{32(d+\|\boldsymbol{a}\|_1)^2 B^2 (\log m)^{2b} \nu_3}\right\} + (2m+9) C_4 \exp\left\{-c_4 n (x_2^2/c_4' \wedge x_2/c_4'')\right\}
\end{aligned}$$

by Lemma B.5. Then, under Assumption 3.6, each infinite series with respect to n on the right hand side can be shown to be finite with the choice of $\delta_1 > 2$ and $\delta_2 > \sqrt{2}/((d+\|\boldsymbol{a}\|_1)B)$. This implies $\sum_{n=1}^{\infty} \mathbb{P}\left(d_H \geq \varepsilon\right) < \infty$, which completes the proof. ♢

We next show $d_H\left(f_{G_n}, f_{G_0}\right) = o_{a.s.}(1)$ in the following lemma.

Lemma B.8. *Under Assumptions 3.3-3.6, we have* $d_H\left(f_{G_n}, f_{G_0}\right) = o_{a.s.}(1)$.

Proof of Lemma B.8. We first note that $d_H^2\left(f_{G_n}, f_{G_0}\right) \leq d_{TV}\left(f_{G_n}, f_{G_0}\right)$ where d_{TV} denotes the total variation distance such that

$$d_{TV}\left(f_{G_n}, f_{G_0}\right) = \frac{1}{2} \int \left| \int \phi(x-y) \left\{ dP(\hat{\mathbf{a}}^\top \boldsymbol{\xi}_i \leq y | \mathbf{W}) - dP(\mathbf{a}^\top \boldsymbol{\xi}_i \leq y) \right\} \right| dx.$$

The main idea of the proof is to find an upper bound of $d_{TV}\left(f_{G_n}, f_{G_0}\right)$ in terms of $\|\hat{\mathbf{a}} - \mathbf{a}\|_{\max}$.

Let $\boldsymbol{\xi} = (\xi_1, \cdots, \xi_d)^\top$ be a random vector with a density h and $\mathbf{a} = (a_1, \cdots, a_d)^\top$. Without loss of generality, we suppose the first l elements of $\boldsymbol{a}$ are zero and the rest is non-zero for some $0 \leq l \leq d$. Then, the density of $\mathbf{a}^\top \boldsymbol{\xi}$ can be written as

$$f_{\mathbf{a}^\top \boldsymbol{\xi}}(y) = \begin{cases} \frac{1}{|a_d|} \int h\left(z_1, \cdots, z_{d-1}, \frac{y - \sum_{i=l+1}^{d-1} a_i z_i}{a_d}\right) dz_1 \cdots dz_{d-1} & \text{for } l < d, \\ \delta_{y=0} & \text{for } l = d \end{cases}$$

where $\sum_{i=l+1}^{d-1} a_i z_i$ is defined to be 0 if $l = d-1$. We show this when $l < d$ because it is

straightforward if $l = d$. When $l < d$, the joint density of $(a_1\xi_1, \cdots, a_d\xi_d)$ is

$$g_{\boldsymbol{a}}(\boldsymbol{z}) = \left(\prod_{i=1}^{l} \delta_{z_i=0}\right) \frac{1}{\prod_{i=l+1}^{d} |a_i|} h_{-l}\left(\frac{z_{l+1}}{a_{l+1}}, \cdots, \frac{z_d}{a_d}\right)$$

where $\prod_{i=1}^{l} \delta_{z_i=0}$ is defined to be 1 if $l = 0$ and h_{-l} denotes the density of $(\xi_{l+1}, \cdots, \xi_d)$. Then, the density of $\boldsymbol{a}^\top \boldsymbol{\xi}$ is

$$\begin{aligned} f_{\boldsymbol{a}^\top \boldsymbol{\xi}}(y) &= \frac{1}{\prod_{i=l+1}^{d} |a_i|} \int h_{-l}\left(\frac{z_{l+1}}{a_{l+1}}, \cdots, \frac{y - \sum_{i=l+1}^{d-1} z_i}{a_d}\right) dz_{l+1} \cdots dz_{d-1} \\ &= \frac{1}{|a_d|} \int h_{-l}\left(z_{l+1}, \cdots, z_{d-1}, \frac{y - \sum_{i=l+1}^{d-1} a_i z_i}{a_d}\right) dz_{l+1} \cdots dz_{d-1} \\ &= \frac{1}{|a_d|} \int h\left(z_1, \cdots, z_{d-1}, \frac{y - \sum_{i=l+1}^{d-1} a_i z_i}{a_d}\right) dz_1 \cdots dz_{d-1}. \end{aligned}$$

Without loss of generality, we also consider the first k elements of $\hat{\boldsymbol{a}}$ are zero and the rest is non-zero for some $0 \leq k \leq d$. Similarly, the density of $\hat{\mathbf{a}}^\top \boldsymbol{\xi}$ is

$$f_{\hat{\boldsymbol{a}}^\top \boldsymbol{\xi}}(y) = \begin{cases} \frac{1}{|\hat{a}_d|} \int h\left(z_1, \cdots, z_{d-1}, \frac{y - \sum_{i=k+1}^{d-1} \hat{a}_i z_i}{\hat{a}_d}\right) dz_1 \cdots dz_{d-1} & \text{for } k < d, \\ \delta_{y=0} \quad \text{for } k = d. \end{cases}$$

Though we only show the case $l < d$ and $k < d$ below, it can be verified that $d_{TV}\left(f_{G_n}, f_{G_0}\right)$ is

upper bounded by $\frac{1}{2}\int\left|\int\left\{\phi(x-\hat{\mathbf{a}}^\top\mathbf{z})-\phi(x-\mathbf{a}^\top\mathbf{z})\right\}h(\mathbf{z})d\mathbf{z}\right|dx$ for the other cases. Note that

$$\begin{aligned}
d_{TV}\left(f_{G_n},f_{G_0}\right) &= \frac{1}{2}\int\left|\int\frac{\phi(x-y)}{|\hat{a}_d|}\int h\left(z_1,\cdots,z_{d-1},\frac{y-\sum_{i=k+1}^{d-1}\hat{a}_i z_i}{\hat{a}_d}\right)dz_1\cdots dz_{d-1}dy\right. \\
&\quad\left.-\int\frac{\phi(x-y)}{|a_d|}\int h\left(z_1,\cdots,z_{d-1},\frac{y-\sum_{i=l+1}^{d-1}a_i z_i}{a_d}\right)dz_1\cdots dz_{d-1}dy\right|dx \\
&\leq \frac{1}{2}\int\left|\int\phi(x-\hat{\mathbf{a}}^\top\mathbf{z})h(\mathbf{z})d\mathbf{z}-\phi(x-\mathbf{a}^\top\mathbf{z})h(\mathbf{z})d\mathbf{z}\right|dx \\
&\leq \frac{1}{2}\int\int\left|\phi(x-\hat{\mathbf{a}}^\top\mathbf{z})-\phi(x-\mathbf{a}^\top\mathbf{z})\right|dx h(\mathbf{z})d\mathbf{z} \\
&\leq \frac{1}{2}\int\left\{\exp\left\{|(\hat{\mathbf{a}}-\mathbf{a})^\top\mathbf{z}|^2\right\}-1\right\}^{1/2}h(\mathbf{z})d\mathbf{z} \\
&\leq \frac{1}{\sqrt{2}}\int\sqrt{|(\hat{\mathbf{a}}-\mathbf{a})^\top\mathbf{z}|^2}h(\mathbf{z})d\mathbf{z} \leq \frac{dB(\log m)^b\|\hat{\mathbf{a}}-\mathbf{a}\|_{\max}}{\sqrt{2}}
\end{aligned}$$

under the event that $\|\hat{\mathbf{a}}-\mathbf{a}\|_{\max}\leq(dB(\log m)^b)^{-1}\varepsilon$ for $0<\varepsilon<1$ because $e^x\leq 1+2x$ for any $0<x<1$ and

$$|(\hat{\mathbf{a}}-\mathbf{a})^\top\mathbf{z}|^2\leq\|\hat{\mathbf{a}}-\mathbf{a}\|_{\max}^2\|\mathbf{z}\|_1^2\leq(dB(\log m)^b)^2\|\hat{\mathbf{a}}-\mathbf{a}\|_{\max}^2.$$

under Assumption 3.5. Then, for $0<\varepsilon<\sqrt{2}dB(\log m)^b L'$ where L' is the same as in Lemma B.1, it follows that

$$\begin{aligned}
\left\{d_H^2(f_{G_n},f_{G_0})>\varepsilon/2\right\} &\subset \left[\left\{d_{TV}(f_{G_n},f_{G_0})>\varepsilon/2,\|\hat{\mathbf{a}}-\mathbf{a}\|_{\max}\leq(dB(\log m)^b)^{-1}\varepsilon\right\}\right. \\
&\qquad\left.\bigcup\left\{\|\hat{\mathbf{a}}-\mathbf{a}\|_{\max}>(dB(\log m)^b)^{-1}\varepsilon\right\}\right] \\
&\subset \left[\left\{\frac{dB(\log m)^b\|\hat{\mathbf{a}}-\mathbf{a}\|_{\max}}{\sqrt{2}}>\varepsilon/2,\|\hat{\mathbf{a}}-\mathbf{a}\|_{\max}\leq(dB(\log m)^b)^{-1}\varepsilon\right\}\right. \\
&\qquad\left.\bigcup\left\{\|\hat{\mathbf{a}}-\mathbf{a}\|_{\max}>(dB(\log m)^b)^{-1}\varepsilon\right\}\right] \\
&\subset \left\{\|\hat{\mathbf{a}}-\mathbf{a}\|_{\max}>(dB(\log m)^b)^{-1}\varepsilon/\sqrt{2}\right\}
\end{aligned}$$

Under Assumption 3.6, for large enough n and any fixed $0 < r < 1$, we have

$$\begin{aligned}\mathbb{P}\left(d_H^2(f_{G_n}, f_{G_0}) > \varepsilon/2\right) &\leq \mathbb{P}\left(\|\hat{\mathbf{a}} - \mathbf{a}\|_{\max} > (dB(\log m)^b)^{-1}\varepsilon/\sqrt{2}\right) \\ &\leq \mathbb{P}\left(\|\hat{\mathbf{a}} - \mathbf{a}\|_{\max} > \frac{\varepsilon}{\sqrt{2}dB(\log n)^b}\right) \\ &\leq \mathbb{P}\left(\|\hat{\mathbf{a}} - \mathbf{a}\|_{\max} > \frac{\varepsilon'}{\sqrt{2}dBn^{r/2}}\right)\end{aligned}$$

where $D_6 > 0$ is some constant such that $(\log m)^b \leq D_6(\log n)^b$ for large enough n which must exist under Assumption 3.6. The last inequality follows by the fact that $\log n \leq n^{r/2b}$ for large enough n. Thus, we can conclude that $d_H\left(f_{G_n}, f_{G_0}\right) = o_{a.s.}(1)$ by the Borel-Cantelli lemma with Lemma B.1. ♢

Now we introduce the proofs of Lemmas 3.1 and 3.2, respectively.

Proof of Lemma 3.1. Note that

$$\begin{aligned}&\left|\int L(Ax, t_1, t_2)d\widetilde{G}_{m,n}(x) - \int L_0(A_0x, t_1, t_2)dG_0(x)\right| \\ \leq &\left|\int \left\{L(Ax, t_1, t_2) - L_0(A_0x, t_1, t_2)\right\} d\widetilde{G}_{m,n}(x)\right| + \left|\int L_0(A_0x, t_1, t_2)(d\widetilde{G}_{m,n}(x) - dG_0(x))\right|.\end{aligned}$$

It thus suffices to show that

$$\sup_{t_1 \leq t_1', t_2 \leq t_2', x \in \mathbb{R}} |L(Ax, t_1, t_2) - L_0(A_0x, t_1, t_2)| \xrightarrow{a.s.} 0, \tag{B.35}$$

$$\sup_{t_1 \leq t_1', t_2 \leq t_2'} \left|\int L_0(A_0x, t_1, t_2)(d\widetilde{G}_{m,n}(x) - dG_0(x))\right| \xrightarrow{a.s.} 0. \tag{B.36}$$

We first verify the pointwise convergence in (B.35), (B.36) and proceed to show the uniform convergence as stated. As $\widetilde{G}_{m,n} = \widetilde{G}_{m(n),n}$ under Assumption 3.6, throughout the proof, we denote $\widetilde{G}_{m,n}$ by $\widetilde{G}_n$ for the notational simplicity.

1. **Pointwise convergence**

   Let $a_n = a_n(t_1, t_2) = \left|\int L_0(A_0x, t_1, t_2)(d\widetilde{G}_n(x) - dG_0(x))\right|$ under Assumption 3.6. By

Lemmas B.7 and B.8,

$$d_H(f_{\widetilde{G}_n}(x), f_{G_0}(x)) \leq d_H(f_{\widetilde{G}_n}(x), f_{G_n}(x)) + d_H(f_{G_n}(x), f_{G_0}(x)) = o_{a.s.}(1). \quad \text{(B.37)}$$

Since $\int |f(x) - g(x)|dx \leq 2d_H(f,g)\sqrt{2 - d_H^2(f,g)}$ and $f_G(x) \leq 1/\sqrt{2\pi}$ for any G, we have

$$\int |f_{\widetilde{G}_n}(x) - f_{G_0}(x)|^2 dx \leq \frac{2}{\sqrt{2\pi}} \int |f_{\widetilde{G}_n}(x) - f_{G_0}(x)|dx = o_{a.s.}(1).$$

For a density function or distribution function f, denote by f^* its Fourier transformation. By the Parseval's identity, we have

$$\begin{aligned}\int |f_{\widetilde{G}_n}(x) - f_{G_0}(x)|^2 dx &= \int \left|\phi^*(t)\widetilde{G}_n^*(t) - \phi^*(t)G_0^*(t)\right|^2 dt \\ &= \int \phi^*(t)^2 \left|\widetilde{G}_n^*(t) - G_0^*(t)\right|^2 dt = o_{a.s.}(1).\end{aligned}$$

Consider any convergent subsequence of a_n, say a_{n_j}. As $\int \phi^*(t)^2 \left|\widehat{G}_{n_j}^*(t) - G_0^*(t)\right|^2 dt = o_{a.s.}(1)$, there exists a further subsequence $\widehat{G}_{n_{j_k}}^*(t)$ such that

$$\widehat{G}_{n_{j_k}}^*(t) \overset{a.s.}{\to} G_0^*(t)$$

for almost every t with respect to the measure $\phi^*(t)dt$ (and thus also with respect to the Lebesgue measure). By the continuity theorem, $\widehat{G}_{n_{j_k}}(t) \overset{a.s.}{\to} G_0(t)$ for any continuous point t of $G_0(t)$. Then, we have $a_{n_{j_k}} \to 0$ by the Portmanteau theorem. As a_{n_j} is convergent, it must converge to zero as well. Since a_{n_j} is an arbitrary convergent subsequence, we have

$$a_n = \left|\int L_0(A_0 x, t_1, t_2)(d\widetilde{G}_n(x) - dG_0(x))\right| \overset{a.s.}{\to} 0 \quad \text{(B.38)}$$

for any t_1, t_2. To show that $|L(Ax, t_1, t_2) - L_0(A_0 x, t_1, t_2)| \overset{a.s.}{\to} 0$ for given x, t_1 and t_2, we note that the covariance matrix of (V_1, V_2) converges almost surely to the covariance matrix

of $(\breve{V}_1, \breve{V}_2)$ by Lemma B.1. It follows from the continuous mapping theorem that

$$|L(Ax, t_1, t_2) - L_0(A_0 x, t_1, t_2)| \xrightarrow{a.s.} 0.$$

2. **Uniform convergence**

We first show (B.35). For any $\delta > 0$, we can choose a large enough $M' = M'(\delta)$ such that

$$\int_{|x|>M'} dG_0(x) < \delta. \tag{B.39}$$

For such M', using similar argument as above, we can verify that

$$\left| \int_{|x|>M'} (d\widetilde{G}_n(x) - dG_0(x)) \right| \xrightarrow{a.s.} 0. \tag{B.40}$$

We partition the rectangular region $[0, t_1'] \times [0, t_2']$ into finite disjoint sets $\cup_{1 \le j \le B_1} \mathcal{V}_j$ such that uniformly over j,

$$\sup_{(t_1,t_2),(\tilde{t}_1,\tilde{t}_2) \in \mathcal{V}_j} \left| \int (L_0(A_0 x, t_1, t_2) - L_0(A_0 x, \tilde{t}_1, \tilde{t}_2)) dG_0(x) \right| < \delta, \tag{B.41}$$

and also for $|x| \le M'$

$$\sup_{(t_1,t_2),(\tilde{t}_1,\tilde{t}_2) \in \mathcal{V}_j} \left| L_0(A_0 x, t_1, t_2) - L_0(A_0 x, \tilde{t}_1, \tilde{t}_2) \right| < \delta. \tag{B.42}$$

We have for large enough m and uniformly over j,

$$\begin{aligned}
&\sup_{(t_1,t_2),(\tilde{t}_1,\tilde{t}_2)\in\mathcal{V}_j}\left|\int (L_0(A_0x,t_1,t_2)-L_0(A_0x,\tilde{t}_1,\tilde{t}_2))d\widetilde{G}_n(x)\right| \\
\le &\sup_{(t_1,t_2),(\tilde{t}_1,\tilde{t}_2)\in\mathcal{V}_j}\left|\int_{|x|\le M'} (L_0(A_0x,t_1,t_2)-L_0(A_0x,\tilde{t}_1,\tilde{t}_2))d\widetilde{G}_n(x)\right| \\
&+\sup_{(t_1,t_2),(\tilde{t}_1,\tilde{t}_2)\in\mathcal{V}_j}\left|\int_{|x|> M'} (L_0(A_0x,t_1,t_2)-L_0(A_0x,\tilde{t}_1,\tilde{t}_2))d\widetilde{G}_n(x)\right| \qquad \text{(B.43)} \\
\le &\sup_{(t_1,t_2),(\tilde{t}_1,\tilde{t}_2)\in\mathcal{V}_j}\left|\int_{|x|\le M'} (L_0(A_0x,t_1,t_2)-L_0(A_0x,\tilde{t}_1,\tilde{t}_2))d\widetilde{G}_n(x)\right| \\
&+2\left|\int_{|x|> M'} (d\widetilde{G}_n(x)-dG_0(x)+dG_0(x))\right| \le 5\delta
\end{aligned}$$

almost surely from (B.39),(B.40) and (B.42). Choosing $(t_1^j,t_2^j)\in\mathcal{V}_j$ for $1\le j\le B_1$, we have

$$\begin{aligned}
&\sup_{t_1\le t_1',t_2\le t_2'}\left|\int L_0(A_0x,t_1,t_2)(d\widetilde{G}_n(x)-dG_0(x))\right| \\
=&\sup_{(t_1,t_2)\in\cup_{1\le j\le B}\mathcal{V}_j}\left|\int L_0(A_0x,t_1,t_2)(d\widetilde{G}_n(x)-dG_0(x))\right| \\
=&\max_{1\le j\le B}\sup_{(t_1,t_2)\in\mathcal{V}_j}\Bigg|\int \left\{L_0(A_0x,t_1,t_2)-L_0(A_0x,t_1^j,t_2^j)+L_0(A_0x,t_1^j,t_2^j)\right\} \\
&(d\widetilde{G}_n(x)-dG_0(x))\Bigg| \le 6\delta+\max_{1\le j\le B_1}\left|\int L_0(A_0x,t_1^j,t_2^j)(d\widetilde{G}_n(x)-dG_0(x))\right|
\end{aligned}$$

by (B.41) and (B.43). The proof for (B.35) is completed in view of (B.38).

To show (B.36), by the triangle inequality, it suffices to show that

$$\sup_{t_1\le t_1',t_2\le t_2',x\in\mathbb{R}}|L(Ax,t_1,t_2)-L_0(Ax,t_1,t_2)|\xrightarrow{a.s.}0, \qquad \text{(B.44)}$$

$$\sup_{t_1\le t_1',t_2\le t_2',x\in\mathbb{R}}|L_0(Ax,t_1,t_2)-L_0(A_0x,t_1,t_2)|\xrightarrow{a.s.}0. \qquad \text{(B.45)}$$

Then, (B.44) follows by applying the Scheffe's Lemma with the pointwise almost sure convergence of the probability density of (V_1,V_2) to that of $(\breve{V}_1,\breve{V}_2)$ by Lemma B.1. We next

show (B.45). We first observe that, for any $a, t_1, t_2 \in \mathbb{R}$,

$$\begin{aligned} L_0(a, t_1, t_2) &= \mathbb{P}(a + \breve{V}_1 \geq t_1, \breve{V}_2 \geq t_2) + \mathbb{P}(a + \breve{V}_1 \leq -t_1, \breve{V}_2 \geq t_2) \\ &\quad + \mathbb{P}(a + \breve{V}_1 \geq t_1, \breve{V}_2 \leq -t_2) + \mathbb{P}(a + \breve{V}_1 \leq -t_1, \breve{V}_2 \leq -t_2) \\ &= \{\Phi(-t_2) - \Phi(t_1 - a) + \Psi_1(t_1 - a, t_2)\} \\ &\quad + \{\Phi(-t_1 - a) - \Psi_1(-t_1 - a, t_2)\} + \{\Phi(-t_2) - \Psi_1(t_1 - a, -t_2)\} \\ &\quad + \Psi_1(-t_1 - a, -t_2), \end{aligned} \tag{B.46}$$

where $\Psi_1(t_1, t_2) = \mathbb{P}(\breve{V}_1 \leq t_1, \breve{V}_2 \leq t_2)$. For any $\delta > 0$, we can choose some large enough $M''(\delta, t_1', t_2', A_0) > 0$ such that

$$\begin{aligned} &\{\Phi(t_1' - A_0 M'') \vee \Psi_1(t_1' - A_0 M'', t_2')\} \leq \delta, \\ &\{\Phi(-t_1' + A_0 M'') \wedge \Psi_1(-t_1' + A_0 M'', -t_2')\} \geq 1 - \delta \end{aligned} \tag{B.47}$$

which implies, for any $x \geq M'', t_1 \leq t_1', t_2 \leq t_2'$,

$$\begin{aligned} &\Phi(-t_1 - A_0 x) \leq \delta, \\ &\Psi_1(-t_1 - A_0 x, -t_2) \leq \delta, \\ &\Psi_1(t_1 - A_0 x, -t_2) \leq \delta, \end{aligned} \tag{B.48}$$

and, for any $x \leq -M''$,

$$\begin{aligned} &1 - \delta \leq \Phi(t_1 - A_0 x), \\ &1 - \delta \leq \Psi_1(-t_1 - A_0 x, t_2), \\ &1 - \delta \leq \Psi_1(t_1 - A_0 x, t_2). \end{aligned} \tag{B.49}$$

Here we use the fact that Φ and Ψ_1 are non-decreasing continuous function. Thus, to show (B.45), it suffices to show that

$$\sup_{t_1 \leq t_1', t_2 \leq t_2', |x| \geq M''} |L_0(Ax, t_1, t_2) - L_0(A_0 x, t_1, t_2)| \xrightarrow{a.s.} 0, \tag{B.50}$$

$$\sup_{t_1\le t_1',t_2\le t_2',|x|<M''} |L_0(Ax,t_1,t_2)-L_0(A_0x,t_1,t_2)| \overset{a.s.}{\to} 0. \tag{B.51}$$

By (B.46),

$$\begin{aligned}
&\sup_{t_1\le t_1',t_2\le t_2',|x|\ge M''} |L_0(Ax,t_1,t_2)-L_0(A_0x,t_1,t_2)| \\
\le &\sup_{t_1\le t_1',t_2\le t_2',|x|\ge M''} |\Phi(-t_1-Ax)-\Phi(-t_1-A_0x)| \\
&+\sup_{t_1\le t_1',t_2\le t_2',|x|\ge M''} |\Phi(t_1-Ax)-\Phi(t_1-A_0x)| \\
&+\sup_{t_1\le t_1',t_2\le t_2',|x|\ge M''} |\Psi_1(-t_1-Ax,-t_2)-\Psi_1(-t_1-A_0x,-t_2)| \\
&+\sup_{t_1\le t_1',t_2\le t_2',|x|\ge M''} |\Psi_1(-t_1-Ax,t_2)-\Psi_1(-t_1-A_0x,t_2)| \\
&+\sup_{t_1\le t_1',t_2\le t_2',|x|\ge M''} |\Psi_1(t_1-Ax,-t_2)-\Psi_1(t_1-A_0x,-t_2)| \\
&+\sup_{t_1\le t_1',t_2\le t_2',|x|\ge M''} |\Psi_1(t_1-Ax,t_2)-\Psi_1(t_1-A_0x,t_2)|.
\end{aligned}$$

Since $A \overset{a.s.}{\to} A_0$, by (B.47), there exists some $N(M''(\delta,t_1',t_2',A_0,\omega)) > 0$ such that $n \ge N(M''(\delta,t_1',t_2',A_0,\omega))$ implies that

$$\begin{aligned}
&\{\Phi(t_1'-AM'')\vee\Psi_1(t_1'-AM'',t_2')\}\le\delta, \\
&\{\Phi(-t_1'+AM'')\wedge\Psi_1(-t_1'+AM'',-t_2')\}\ge 1-\delta
\end{aligned}$$

Since Φ and Ψ_1 are non-decreasing continuous function, for $|x|\ge M''$,

$$\begin{aligned}
&\Phi(-t_1-Ax)\le\delta, \\
&\Psi_1(-t_1-Ax,-t_2)\le\delta, \\
&\Psi_1(t_1-Ax,-t_2)\le\delta,
\end{aligned} \tag{B.52}$$

or

$$\begin{aligned} 1-\delta &\leq \Phi(t_1 - Ax), \\ 1-\delta &\leq \Psi_1(-t_1 - Ax, t_2), \\ 1-\delta &\leq \Psi_1(t_1 - Ax, t_2). \end{aligned} \tag{B.53}$$

Therefore, (B.50) can be verified by (B.48)-(B.49) and (B.52)-(B.53) as δ can be arbitrary. For (B.51), since L_0 is Lipschitz with respect to the first argument, it follows that

$$|L_0(Ax, t_1, t_2) - L_0(A_0x, t_1, t_2)| \leq \frac{6}{\sqrt{2\pi}}|Ax - A_0x| < \frac{6M''}{\sqrt{2\pi}}|A - A_0| \tag{B.54}$$

which completes the proof because $A \xrightarrow{a.s.} A_0$.

$\diamondsuit$

Proof of Lemma 3.2. We first note that

$$V_m(t_1, t_2) = \sum_{i:\alpha_i=0} \mathbf{1}\left\{|\breve{Z}_i^U| \geq \hat{r}_i t_1, |\breve{Z}_i^A| \geq \hat{r}_i t_2\right\} = \breve{V}_m(\hat{r}_i t_1, \hat{r}_i t_2)$$

where $\hat{r}_i = \hat{\sigma}_i/\sigma_i$. Define an event

$$\begin{aligned} \mathcal{A} = &\left\{\max_{1\leq i\leq m} |\hat{\sigma}_i^2/\sigma_i^2 - 1| \to 0\right\} \\ &\bigcap \left\{\sup_{t_1\leq t_1', t_2\leq t_2'} \left| m_0^{-1} \sum_{i:\alpha_i=0} \mathbf{1}\left\{|\breve{Z}_i^U| \geq t_1, |\breve{Z}_i^A| \geq t_2\right\} - K_0(t_1, t_2)\right| \to 0\right\}. \end{aligned}$$

Then, $\mathbb{P}(\mathcal{A}) = 1$ by Assumption 3.2 and Lemma B.2. For any $\omega \in \mathcal{A}$ and $\delta > 0$, we have $1 - \delta < \hat{r}_i < 1 + \delta$ for any i when m is large enough. For this ω, we have

$$\breve{V}_m((1+\delta)t_1, (1+\delta)t_2) \leq V_m(t_1, t_2) \leq \breve{V}_m((1-\delta)t_1, (1-\delta)t_2)$$

for large enough m. By Assumption 3.2, we get

$$K_0((1+\delta)t_1,(1+\delta)t_2) \le \liminf_m \frac{1}{m_0}V_m(t_1,t_2) \le \limsup_m \frac{1}{m_0}V_m(t_1,t_2) \le K_0((1-\delta)t_1,(1-\delta)t_2).$$

As K_0 is continuous and δ is arbitrary, we have $V_m(t_1,t_2)/m_0 \to K_0(t_1,t_2)$ for any $\omega \in \mathcal{A}$. Similar arguments can be used to show the rest. $\diamondsuit$

Theorem 3.1 is proved as follows.

Proof of Theorem 3.1. By the Glivenko-Cantelli lemma, we can show that the convergence in Lemma 3.2 holds uniformly, i.e.,

$$\sup_{t_1\le t_1^*,t_2\le t_2^*}\left|\frac{V_m(t_1,t_2)}{m_0} - K_0(t_1,t_2)\right| \overset{a.s.}{\to} 0 \quad \text{and} \quad \sup_{t_1\le t_1^*,t_2\le t_2^*}\left|\frac{S_m(t_1,t_2)}{m_1} - K_1(t_1,t_2)\right| \overset{a.s.}{\to} 0.$$

This implies, under Assumption 3.1,

$$\sup_{t_1\le t_1^*,t_2\le t_2^*}|\mathcal{K}_m(t_1,t_2) - K(t_1,t_2)| \overset{a.s.}{\to} 0 \tag{B.55}$$

where $\mathcal{K}_m(t_1,t_2) = m^{-1}\{V_m(t_1,t_2)+S_m(t_1,t_2)\}$. We next show that

$$\sup_{t_1\le t_1^*,t_2\le t_2^*}|\widetilde{\text{FDP}}_\lambda(t_1,t_2) - \text{FDP}_\lambda^\infty(t_1,t_2)| \overset{a.s.}{\to} 0, \tag{B.56}$$

$$\sup_{t_1\le t_1^*,t_2\le t_2^*}\left|\frac{V_m(t_1,t_2)}{V_m(t_1,t_2)+S_m(t_1,t_2)} - \frac{\pi_0 K_0(t_1,t_2)}{K(t_1,t_2)}\right| \overset{a.s.}{\to} 0. \tag{B.57}$$

To show (B.56), we first observe that, for large enough m,

$$|\mathcal{K}_m(t_1,t_2) - K(t_1,t_2)| \le \frac{|K(t_1,t_2)|}{2}$$

which implies

$$|\mathcal{K}_m(t_1,t_2)| \ge \frac{|K(t_1,t_2)|}{2} \ge \frac{K(t_1^*,t_2^*)}{2} > 0$$

because $\inf_{t_1\le t_1^*,t_2\le t_2^*}|K(t_1,t_2)|\ge K(t_1^*,t_2^*)>0$. For large enough m, it follows that

$$
\begin{aligned}
&|\widetilde{\text{FDP}}_\lambda(t_1,t_2)-\text{FDP}^\infty_\lambda(t_1,t_2)|\\
=&\frac{1}{(1-2\Phi(-\lambda))|\mathcal{K}_m(t_1,t_2)K(t_1,t_2)|}\bigg|\int L(Ax,t_1,t_2)d\widetilde{G}_{m,n}(x)F_m(\lambda)K(t_1,t_2)\\
&-\mathbb{E}_{\boldsymbol{a}^\top\boldsymbol{\xi}}[L_0(A_0\boldsymbol{a}^\top\boldsymbol{\xi},t_1,t_2)]F(\lambda)\mathcal{K}_m(t_1,t_2)\bigg|\\
\le&\frac{2}{(1-2\Phi(-\lambda))K(t_1^*,t_2^*)^2}\bigg|\int L(Ax,t_1,t_2)d\widehat{G}_m(x)F_m(\lambda)K(t_1,t_2)\\
&-\mathbb{E}_{\boldsymbol{a}^\top\boldsymbol{\xi}}[L_0(A_0\boldsymbol{a}^\top\boldsymbol{\xi},t_1,t_2)]F(\lambda)\mathcal{K}_m(t_1,t_2)\bigg|.
\end{aligned}
$$

Thus, for (B.56), it suffices to verify that

$$
\begin{aligned}
\sup_{t_1\le t_1^*,t_2\le t_2^*}\bigg|\int L(Ax,t_1,t_2)d\widehat{G}_m(x)F_m(\lambda)K(t_1,t_2)\\
-\mathbb{E}_{\boldsymbol{a}^\top\boldsymbol{\xi}}[L_0(A_0\boldsymbol{a}^\top\boldsymbol{\xi},t_1,t_2)]F(\lambda)\mathcal{K}_m(t_1,t_2)\bigg|\overset{a.s.}{\to}0,
\end{aligned}
$$

which can be shown by (B.55) and Lemmas 3.1-3.2. We can also show (B.57) by using similar argument.

As $\text{FDP}^\infty_\lambda(t_1^*,0)<q$ and $\text{FDP}^\infty_\lambda(0,t_2^*)<q$, we have for large enough m,

$$
\widetilde{\text{FDP}}_\lambda(t_1^*,0)<q\quad\text{ and }\quad\widetilde{\text{FDP}}_\lambda(0,t_2^*)<q,
$$

which implies that $\widetilde{T}_1^* \le t_1^*$ and $\widetilde{T}_2^* \le t_2^*$. Thus we have

$$\begin{aligned}
&\liminf_m \left\{ \widetilde{\text{FDP}}_\lambda(\widetilde{T}_1^*, \widetilde{T}_2^*) - \frac{V_m(\widetilde{T}_1^*, \widetilde{T}_2^*)}{V_m(\widetilde{T}_1^*, \widetilde{T}_2^*) + S_m(\widetilde{T}_1^*, \widetilde{T}_2^*)} \right\} \\
\ge &\lim_m \inf_{t_1 \le t_1^*, t_2 \le t_2^*} \left\{ \widetilde{\text{FDP}}_\lambda(t_1, t_2) - \frac{V_m(t_1, t_2)}{V_m(t_1, t_2) + S_m(t_1, t_2)} \right\} \\
= &\lim_m \inf_{t_1 \le t_1^*, t_2 \le t_2^*} \left\{ \widetilde{\text{FDP}}_\lambda(t_1, t_2) - \text{FDP}_\lambda^\infty(t_1, t_2) + \frac{\pi_0 K_0(t_1, t_2)}{K(t_1, t_2)} - \frac{V_m(t_1, t_2)}{V_m(t_1, t_2) + S_m(t_1, t_2)} \right. \\
&\left. + \text{FDP}_\lambda^\infty(t_1, t_2) - \frac{\pi_0 K_0(t_1, t_2)}{K(t_1, t_2)} \right\} \ge 0
\end{aligned}$$

by (B.56), (B.57) and the fact that

$$\text{FDP}_\lambda^\infty(t_1, t_2) - \frac{\pi_0 K_0(t_1, t_2)}{K(t_1, t_2)} \ge 0$$

from (3.10). As $\widetilde{\text{FDP}}_\lambda(\widetilde{T}_1^*, \widetilde{T}_2^*) \le q$, we obtain

$$\limsup_m \frac{V_m(\widetilde{T}_1^*, \widetilde{T}_2^*)}{V_m(\widetilde{T}_1^*, \widetilde{T}_2^*) + S_m(\widetilde{T}_1^*, \widetilde{T}_2^*)} \le q.$$

Finally by Fatou's lemma, we get

$$\limsup_m \widetilde{\text{FDR}}_m \le \mathbb{E}\left[\limsup_m \frac{V_m(\widetilde{T}_1^*, \widetilde{T}_2^*)}{V_m(\widetilde{T}_1^*, \widetilde{T}_2^*) + S_m(\widetilde{T}_1^*, \widetilde{T}_2^*)} \right] \le q.$$

♢

We justify (3.10) as follows.

Corollary B.1. *Under Assumptions 2.3-2.6, for every $t_1, t_2 > 0$, we have*

$$\left| \int L(Ax, t_1, t_2) dG_n(x) - \int L_0(A_0 x, t_1, t_2) dG_0(x) \right| \xrightarrow{a.s.} 0.$$

Proof of Corollary B.1. Note that

$$\begin{aligned}
&\left|\int L(Ax,t_1,t_2)dG_n(x) - \int L_0(A_0x,t_1,t_2)dG_0(x)\right| \\
=&\left|\int L(Ax,t_1,t_2)dG_n(x) - \int L_0(A_0x,t_1,t_2)dG_n(x)\right| \\
&+\left|\int L_0(A_0x,t_1,t_2)dG_n(x) - \int L_0(A_0x,t_1,t_2)dG_0(x)\right|.
\end{aligned}$$

Thus, it suffices to show that

$$\begin{aligned}
&|L(Ax,t_1,t_2) - L_0(A_0x,t_1,t_2)| \xrightarrow{a.s.} 0, \\
&\left|\int L_0(A_0x,t_1,t_2)(dG_n(x) - dG_0(x))\right| \xrightarrow{a.s.} 0,
\end{aligned}$$

both of which can be verified by using the similar arguments as in Lemma 3.1. ♢